SOLID STATE ABSTRACTS

an abstract journal devoted to the theory, production and use of solid state materials and devices

VOLUME 1 NUMBERS 8 - 9

PHYSICS

METALLURGY

ELECTRONICS

SEMICONDUCTORS

PHOSPHORS

MAGNETICS

DIELECTRICS

SUPERCONDUCTORS

METALS

SOLID STATE ABSTRACTS

VOLUME 1, NUMBERS 8 - 9

May/June 1961

Abstracts 8155-8579

TABLE OF CONTENTS

Abstracts of the Solid State Literature

Metallurgy and Chemistry of Solids

General . . . 375
Thermodynamic Properties . . . 375
Crystal Structure (Including Imperfections and Impurities) . . . 377
Crystal Growth . . . 382
Crystal Surfaces . . . 385
Environmental Effects . . . 386

Solid State Physics

Crystal Physics (Including Energy Band Structure) . . . 386
Electrical Properties . . . 388
Dielectric Properties . . . 388
Carrier Properties . . . 390
Conductivity . . . 391
Superconductivity . . . 393
Magnetoelectric (Galvanomagnetic) Properties . . . 395
Electrical Properties of Surfaces . . . 396
Magnetic Properties . . . 396
General . . . 396
Ferro- and Ferrimagnetism . . . 397
Paramagnetism . . . 401
Optical Properties . . . 405
Absorption (Transmission) . . . 405
Radiation . . . 406
Luminescence . . . 406
Photoelectronic Properties . . . 408
Electromagnetic Properties . . . 409
Thermal Properties . . . 410
Mechanical Properties . . . 411

Solid State Devices

Resistors . . . 412
Diodes . . . 412
Transistors . . . 414
Functional Units . . . 416
Magnetoelectric Devices . . . 417
Photodevices . . . 417
Thermal Devices . . . 418
Ferrite Devices . . . 418
Masers and Lasers . . . 419
Superconductive Devices . . . 420
Electromechanical Devices . . . 420

Basic Solid State Device Circuits

General . . . 421
Amplifiers . . . 422
Oscillators . . . 423
Switching Circuits . . . 424
Signal Converters . . . 424
Wave Generators (See also Oscillators) . . . 425
Pulse Circuits . . . 425
Other Circuits . . . 426

Applications of Solid State Devices

Radio and Television . . . 426
Microwave and Telemetry . . . 427
Other Communication-Type Applications . . . 427
Computers . . . 427
Power Applications . . . 430
Control Applications . . . 431
Instrumentation . . . 431
Other Applications . . . 434

Subject Index . . . 434

Author Index . . . 442

Editor: GEOFFREY KNIGHT, JR., Ph.D.

Assistant Editor: JOHN A. MURPHY

PUBLISHED MONTHLY BY

Cambridge Communications Corporation, 238 Main Street, Cambridge 42, Massachusetts, Tel. 491-0710

Subscription Rate: $25.00 per year. Single Copies and Back Issues: $2.50. Advertising Rates on Request.

Cambridge Communications Corp. is not prepared to furnish copies of the articles abstracted. However, there are many libraries throughout the country which maintain photocopying services.

SYMBOLS USED IN THE ABSTRACTS

L: Letter to the Editor. A: Only an abstract is given in the reference. R: Only a review is given in the reference. E: Erratum.

The reference numbers in the indices are the abstract numbers, not the page numbers.

Copyright 1962 by Cambridge Communications Corp. Printed in the U.S.A. by the University Press, Inc.

ABSTRACTS OF THE SOLID STATE LITERATURE

METALLURGY AND CHEMISTRY OF SOLIDS

GENERAL

8155 VOLUMETRIC DETERMINATION OF GERMANIUM by G. J. Abel, Jr. (Am. Smelting and Refining); Analyt. Chem., Vol. 32, pp. 1886-1887, Dec. 1960

The method for the iodimetric titration of Ge is described. By simple distillation from a hydrochloric acid solution, macro amounts of Ge are separated from interfering elements. The Ge distillate is reduced by hypophosphite to divalent Ge and titrated iodimetrically. The method is simple and the results are precise and accurate.

THERMODYNAMIC PROPERTIES

8156 X-RAY FLUORESCENCE METHOD FOR DETERMINATION OF THE TRANSITION-METAL CONTENT IN VERY SMALL SPECIMENS OF ALLOYS by P. J. Brown (Cavendish Lab.); J. Sci. Instr., Vol. 37, pp. 394-397, Oct. 1960

A method for the quantitative determination of the transition metal content in very small quantities of alloys containing transition metals of the first long period is described. The method depends upon measurement of the intensity of the fluorescent x-rays emitted by the specimen, and the results are evaluated by comparison with a series of standards. An accuracy of better than one per cent can be achieved in specimens containing as little as 0.2 mg of the transition metals.

8157 PHASE EQUILIBRIA IN THE SYSTEM La_2O_3 – IRON OXIDE IN AIR by V. L. Moruzzi and M. W. Shafer (IBM); J. Am. Ceram. Soc., Vol. 43, pp. 367-372, July 1960

Phase equilibria data for compositions in the system La_2O_3 – iron oxide in air are presented. Liquidus and solidus curves were obtained by the quenching method in the iron-rich portion of the system. The remainder of the diagram was determined using a strip-furnace technique. Two compounds have been found, the orthorhombic perovskite $LaFeO_3$ and a compound with the magnetoplumbite structure corresponding to a composition $LaFe_{12}O_{19}$. $LaFeO_3$ was determined to melt congruently at about 1890°C while $LaFe_{12}O_{19}$ has both a stability minimum and maximum at 1380° and 1421°C, respectively. The iron-rich portion of the system is essentially ternary while the remainder can be considered to be a simple binary. Liquid compositions have been determined and are plotted in terms of the ternary system La_2O_3–Fe_2O_3–FeO.

Phase Diagram of the BaF_2–$BaTiO_3$ System - See 8224

8158 DETERMINATION OF THE STANDARD FREE ENERGY OF FORMATION OF LEAD SELENIDE by C. B. Finch and J. B. Wagner, Jr. (Yale U.); J. Electrochem. Soc., Vol. 107, pp. 932-933, Nov. 1960

Measurements of the standard free energy of formation of PbSe are reported. A galvanic cell was assembled by placing a 99.999 per cent lead pellet in a graphite crucible. A crucible of the solid ionic electrolyte, $PbCl_2$ + 1 per cent KCl, containing a PbSe pellet with excess selenium was placed on top of the lead pellet. Glass wool or asbestos was packed between the walls of the graphite and electrolyte crucibles to prevent vapor transport of selenium to the pure lead. A graphite electrode was placed in contact with the PbSe pellet and the entire cell was placed in a glass tube under argon. Electromotive force measurements were made over the temperature range 200° - 300°C. Over this range the standard free energy of formation of PbSe can be expressed by the equation $\Delta G° = -nFE = [-23,352 + 3.8(t-250)]$ cal, where F is the Faraday constant, E is the electromotive force, and t is the temperature in °C. The total estimated accuracy is better than ±80 cal in $\Delta G°$ under the experimental conditions.

8159 THE DISSOCIATION PRESSURE OF CdSb by V. J. Silvestri (IBM); J. Phys. Chem., Vol. 64, pp. 826-827, June 1960

Measurement of the dissociation pressure of CdSb by a dew point technique in the temperature range 287° to 448°C is discussed. In this temperature range the data may be represented by the equation $\log P = -7200/T + 10$. The heat of dissociation calculated from the slope of the equation is 33 kcal/mole. CdSb thermally dissociates according to the following reaction: $CdSb(s) \rightleftharpoons Cd(g) + Sb(s)$.

Pressure Dependence of Melting Point of InSb - See 8271

8160 THE TEMPERATURE DEPENDENCE OF THE SURFACE TENSION OF GERMANIUM by V. B. Lazarev and P. P. Pugachevich (Kurnakov Inst. Genl. Inorg. Chem.); Proc. Acad. Sci. USSR, Phys.-Chem., Vol. 134, pp. 823-825, Sept.-Oct. 1960

Measurements of the temperature dependence of the surface tension Γ of germanium by the maximum gas bubble pressure technique are reported. The procedure of Sugden was employed with two infinitesimally thin-walled capillaries made of spectrally pure graphite. The end of the capillary introduced in the

melt was ground so as to eliminate the effect of the wetting angle on the measurements. The measurements were carried out on single crystal germanium heated in a graphite crucible in a special vacuum furnace. Purified argon was used to produce the gas bubbles. The experimental results can be described by the expression $\Gamma = 621.4 - 0.261\,(t° - 936°)$, where t° is the temperature in degrees Centigrade and 936° is the melting point of germanium. The equation indicates that the surface tension of germanium at the melting point is 621.4 dyne/cm.

8161 SOME OBSERVATIONS ON THE SYSTEM ZnS-AlP by A. Addamiano (GE); J. Electrochem. Soc., Vol. 107, pp. 1006-1007, Dec. 1960

An investigation of the solid solubility of AlP in ZnS is described. Intimate mixtures of fine powders of ZnS and AlP with the molar content of AlP ranging from 0.5 per cent to 80 per cent were fired in sealed fused silica tubes in an argon atmosphere for 24 hr at 900°C. X-ray diffraction of the products indicated that the solubility of AlP in ZnS is very small, probably about 1 mole per cent or less. The solubility was also studied by reacting a mixture of Zn_3P_2 and Al_2S_3 in a sealed quartz tube in an argon atmosphere at 900°C for 24 hr. A bright yellow emission was observed at liquid air temperature under 36.50A irradiation in all the fired mixtures for AlP concentrations up to 80 per cent and at room temperature in samples containing up to ~10 per cent AlP. The emission is similar to emission observed in ZnS:P, Cl phosphors. This similarity supports the theory of charge compensation and shows that in ZnS:P, Al phosphors, P is the activator and Al the coactivator atom.

8162 GERMANIUM HEAVILY DOPED WITH III-V COMPOUNDS by J. O. McCaldin (Hughes Semicon.); Bull. Am. Phys. Soc., Ser. II, Vol. 5, p. 105(A), Mar. 4, 1960

The preparation of Ge heavily doped with III-V compounds was discussed. Specimens of Ge saturated with a III-V compound (InSb, InAs, InP, GaSb, or GaAs) were prepared by fusing the compound into a large Ge die in an evacuated quartz capsule. On cooling, the saturated material first regrows on the undissolved portion of the Ge die, and is followed by the formation of a quasi-binary eutectic. Thus, information about eutectic compositions and temperatures was also obtained; the eutectic is composed typically of ~50 per cent III-V compound and the eutectic temperature is ~50°C to ~150°C lower than the melting point of either component. The "regrowth" Ge solid solution, on the other hand, contains on the order of 1 per cent III-V compound. Large mutual solubility effects have been observed between the III and V impurities. In the system GeGaSb, Ge single crystal specimens containing 10^{20}/cc or more of both dopants have been prepared for Hall mobility measurement. Solubilities and carrier mobilities in this system were discussed.

8163 CRYSTAL CHEMICAL AND MAGNETIC STUDIES OF GARNET SYSTEMS $\{YCa_2\}\,[M_2^{4+}]\,(Fe_3)\,O_{12} - \{Y_3\}\,[Fe_2]\,(Fe_3)\,O_{12}$, M = Zr or Hf by S. Geller, R. M. Bozorth, C. E. Miller and D. D. Davis (Bell Labs.); J. Phys. Chem. Solids, Vol. 13, pp. 28-32, May 1960

The existence of a complete solid-solution range in the system $\{YCa_2\}\,[Zr_2]\,(Fe_3)\,O_{12} - \{Y_3\}\,[Fe_2]\,(Fe_3)\,O_{12}$ is reported. The Zr^{4+} ion is even larger than the Sn^{4+} ion and in this system apparently prefers only the octhadral sites. The behavior of the plot of $n_B(\infty, 0)$ vs composition is similar to that of the $Ca_3Fe_2Sn_3O_{12}$–$Y_3Fe_2Fe_3O_{12}$ system and corroborates the interaction model for garnets recently derived by Gilleo. A small spontaneous magnetization is observed in the garnets $\{YCa_2\}\,[Zr_2]\,(Fe_3)\,O_{12}$ and $\{YCa_2\}\,[Zr_2]\,(Me_{0.5}Fe_{2.5})\,O_{12}$, Me = Al and Ga, indicating the establishment of magnetic sublattices among the tetrahedral sites. The garnet $\{YCa_2\}\,[Hf_2]\,(Fe_3)\,O_{12}$ is readily formed. The Hf^{4+} ion, which is very nearly the same size as that of Zr^{4+}, also prefers the octahedral site.

8164 IONIZATION POTENTIAL OF ATOMS AND MUTUAL SOLUBILITY OF METALS [in Russian] by A. A. Vorob'ev, P.A. Savintsev, and B. F. Ufimtsev (Tomsk Polytech. Inst.); Izv. VUZ Fiz., No. 3, pp. 233-234, 1960

The conditions governing mutual solubility of metals are analyzed. It can be assumed that intermetallic compounds are formed if the ionization potentials of the metal atoms differ significantly. Conversely, the ionization potentials for atoms of components of eutectic alloys must be approximately the same. Atoms of metals forming solid solutions should be characterized by average values of the potential difference.

8165 VARIATION WITH TEMPERATURE OF THE DISTRIBUTION COEFFICIENT OF INDIUM IN GERMANIUM by M. A. Lee (GE, Ltd.); Solid-State Electronics, Vol. 1, pp. 194-201, July 1960

A relationship for an alloyed-junction transistor giving the solid solubility of the emitter material (indium) in the base crystal (germanium) in terms of the slope of a plot of reciprocal current gain versus emitter current is derived. Measurements were made on batches of transistors alloyed at temperatures in the range 350°-805°C. The temperature dependence of the distribution coefficient agrees with that predicted by Hall, down to about 550°C; below that temperature, the observed values are higher than predicted. The possible causes of this divergence are discussed.

8166 DISTRIBUTION COEFFICIENT OF ZINC IN GALLIUM ARSENIDE by A. Shibata (Sony); J. Phys. Soc. Japan, Vol. 15, p. 2107(L), Nov. 1960

A determination of the distribution coefficient of Zn in GaAs is reported. A vacuum sealed quartz tube containing about 15 gm of Zn-doped GaAs was held in a horizontal furnace at about 1280°C for several hours and then pulled out at a speed of 25 mm/hr. The direction of growth was not determined. The Zn concentration was determined by polarography. The distribution coefficient of Zn in GaAs was then determined by plotting log $C^s(g)$ vs log (1-g), where C^s is the impurity concentration of the solid as a function of g, the fraction of the melt which has solidified. The slope, δ, of the line is related to the distribution coefficient k by $k = (1 + \delta)$. The distribution coefficient of Zn in GaAs was found to be 0.31.

8167 VOLUME CHANGES IN Ni_3Mn ALLOY ON ORDERING by V. I. Mel'nikova and I. N. Bogachev (Urals Polytech. Inst.); Phys. Metals Metallog., Vol. 10, No. 2, pp. 44-49, 1960

The nature of the volume changes in Ni_3Mn alloy on ordering and disordering is discussed. The relationship between the rate of volumetric changes and the temperature of isothermal soaking below T_c is determined. Data for the temperature dependence of the coefficient of linear expansion of the alloy both in the ordered and disordered states are given.

THERMODYNAMIC PROPERTIES (Cont'd)

8168 COMPOSITION STABILITY LIMITS OF BINARY SEMICONDUCTOR-COMPOUNDS by R. F. Brebrick (U.S. Naval Ord. Labs.); Bull. Am. Phys. Soc., Ser. II, Vol. 5, pp. 263-264(A), Apr. 25, 1960

The composition stability limits of an essentially ordered, nondegenerate, semiconductor crystal MN showing small deviations from the stoichiometric composition, were discussed. The assumptions were made that: (1) clustering of atomic point defects is unimportant; (2) the predominant atomic point defects are M vacancies and N vacancies; (3) each M vacancy is associated with one acceptor level and each N vacancy with one donor level; and (4) the coexisting condensed phase is one or the other of the pure elements M or N. Expressions for the chemical potentials of the crystal components provide the starting point. Characterizing a limit of stability by the corresponding value of the net relative electron concentration, $(n-p)/2n$, analytical expressions were obtained for the stability limits. The magnitude of the stability range was larger the more negative the standard free energy of formation of the compound and the larger the intrinsic disorder ratio. The latter is the square root of the Schottky constant for ionized vacancies divided by the intrinsic carrier concentration. The effects of electrically active impurities were considered in the approximation that the molar Gibbs free energy of the compound and its coexisting phase are not significantly altered. The result was a generalization of that obtained for the solubility of an electrically active impurity in a doped elemental semiconductor.

CRYSTAL STRUCTURE
(Including Imperfections and Impurities)

8169 BONDING AND SEMICONDUCTIVITY RELATIONSHIPS IN Bi_2Te_3 AND CdI_2 TYPE STRUCTURES by C. H. L. Goodman (GE Ltd.); J. Electrochem. Soc., Vol. 107, pp. 564-565, June 1960

A bonding scheme for the 3 layer CdI_2 structure which is similar to the bonding scheme proposed for Bi_2Te_3 is suggested. I atoms, with the same coordination as the outer Te atoms in 5 layered Bi_2Te_3, would employ p^3 (plus s^2, lone pair) bonding orbitals while the metal atom, with 6-coordination like Bi in Bi_2Te_3, would employ sp^3d^2 hybridized bonding orbitals. The 16 valence electrons of CdI_2 form 2 electron covalent-ionic bonds within the triple I-Cd-I layer structure, I-I interlayer bonding being of van der Waal's type. The scheme indicates that $A^{II}X_2^{VII}$ and $A^{IV}X_2^{VI}$ compounds with CdI_2 structure (e.g., CdI_2, $ZrSe_2$) should be semiconductors or insulators, while compounds such as $NiTe_2$ should be metallic. The greater electronegativity differences for $A^{II}X_2^{VII}$ compared with $A^{IV}X_2^{VI}$ compounds should result in considerably lower energy gaps for the latter, which should also have higher energy gaps than related $A_2^{V}X_3^{VI}$ compounds with Bi_2Te_3 type structure. Not all CdI_2 type compounds can be described by this scheme.

8170 PRECISION LATTICE DETERMINATION by W. L. Bond (Bell Labs.); Acta Cryst., Vol. 13, pp. 814-818, Oct. 1960

A method for determining the lattice constants of single crystals in which several errors are minimized or corrections computed and an apparatus employing the method are described. The apparatus measures the angle between two reflecting positions of the crystal. With nearly perfect crystals the lattice constants can be measured to a few parts in a million.

8171 THE STRUCTURE OF BISMUTH AT LOW TEMPERATURES by C. S. Barrett (U. Chicago); Austl. J. Phys., Vol. 13, pp. 209-222, July 1960

A precision determination of the displacement parameter of zone-refined Bi containing less than 0.3 parts per million of spectroscopically detectable impurity has been carried out as a function of temperature. Procedures were used that minimize uncertainties in integrated intensities due to extinction, absorption, temperature factor, dispersion and f-curve errors, and statistical errors. The parameter b/d (where d is the spacing of the (111) rhombohedral planes of one sublattice and b is the displacement of the other sublattice (111) planes) is 0.40437 ± 0.00008 at 4.2°K, 0.4043 ± 0.00008 at 78°K, and 0.4041 ± 0.0005 at 296 ± 2°K; the rhombohedral parameter, u, corresponding to these values is, respectively, 0.23406, 0.23400, and 0.23401. The small but presumably significant dependence on temperature at low temperatures is in disagreement with predictions of a theory of Blount and Cohen and may signify a lessening of resistance to the atom displacement from simple cubic, due to thermal expansion of the structure. Powder patterns yielded 57.31_4, 57.28_6, and 57.23_6° for the rhombohedral angle at 4.2°, 78°, and 304°K, respectively.

8172 AN X-RAY STUDY ON THE STRUCTURE OF COBALT DICHLORIDE HEXAHYDRATE by J. Mizuno (Tohoku U.); J. Phys. Soc. Japan, Vol. 15, pp. 1412-1420, Aug. 1960

A determination of the crystal structure of $CoCl_2 \cdot 6H_2O$ by the x-ray single crystal method is presented. The unit cell is monoclinic with $a = 10.34$ A, $b = 7.06$ A and $\beta = 122°20'$. The space group is C_{2h}^3 – C2/m and the unit cell contains two molecules. Two Cl-ions and four water molecules are octahedrally coordinated to Co^{2+} ion to form the group $[CoCl_2 \cdot 4H_2O]$. These groups are held together parallel to the b axis by O···H–O type hydrogen bonds. The other two water molecules of the formula unit are far from Co^{2+} ion. The crystal has the layer structure parallel to (001), and this causes the perfect cleavage. The structure proposed for this salt by Stroganov et al. seems to be incorrect.

8173 CRYSTAL STRUCTURE OF FERROELECTRIC $LiH_3(SeO_3)_2$ by K. Vedam, Y. Okaya, and R. Pepinsky (Pennsylvania State U.); Phys. Rev., Vol. 119, pp. 1252-1255, Aug. 15, 1960

The structure of the room-temperature ferroelectric $LiH_3(SeO_3)_2$, determined by x rays, using the heavy-atom method, and refined on the IBM 704, is discussed. The crystals are monoclinic, with space group Pn and $a = 6.25_8$ A, $b = 7.88_6$ A, $c = 5.43_3$ A, $\beta = 105.2°$. Fairly strong O–H···O bonds with distances 2.52, 2.56, and 2.57 A are found, nearly perpendicular to the polar direction. The O–Se–O angles in one of the two selenite ions are rather similar; in the other ion these angles are unequal, as in the structure of H_2SeO_3. Possible positions for the Li ions based on crystal-chemical considerations are given.

8174 X-RAY STUDY OF LATTICE DEFECTS IN Si SINGLE CRYSTALS BY TRANSMISSION BERG-BARRETT TECHNIQUE by M. Yoshimatsu (Rigaku Denki) and K. Kohra (U. Tokyo); J. Phys. Soc. Japan, Vol. 15, pp. 2367-2368(L), Dec. 1960

The use of the transmission Berg-Barrett technique for studying lattice defects in very thin Si single crystals is discussed. In comparison with the Lang technique, no special apparatus is

required, the exposure time is much shorter, and, although the resolution is poorer, individual dislocations can be resolved under favorable conditions. The experimental arrangement is described. The extinction effect is used rather than anomalous transmission to obtain image contrast. Two x-ray micrographs showing individual dislocations and lattice defects in the neighborhood of a twin boundary in Si single crystals are presented.

8175 A THEORETICAL STUDY OF POINT DEFECTS IN THE ROCKSALT STRUCTURE SUBSTITUTIONAL K^+ IN NaCl by J. R. Hardy (U. Bristol); J. Phys. Chem. Solids, Vol. 15, pp. 39-49, Aug. 1960

A method based on lattice statics for studying the ionic displacements about a substitutional K ion in NaCl is described. These are evaluated for certain ions close to the defect and for certain specific directions at large distances from the defect. These last results are used to calculate the interaction energy between a widely separated pair of defects. The correspondence with the predictions of elastic-continuum theory is demonstrated, and a method for calculating the macroscopic volume changes produced by defects is presented.

8176 VACANCY INTERACTIONS IN SILICON by H. H. Woodbury and G. W. Ludwig (GE); Phys. Rev. Lett., Vol. 5, pp. 96-97(L), Aug. 1, 1960

Experiments which indicate that an interaction occurs between a vacancy and a chemical impurity in Si are discussed. Electron spin resonance spectra were observed in Si samples which were cooled slowly after alloying and had diffusing Mn and Cu introduced into the samples. A different spectra was observed after rapidly cooling Si containing only Mn. It is suggested that vacancies formed by the precipitation of Cu are annihilated by the interstitial Mn to form substitutional Mn. The Mn in the rapidly-cooled Si containing only Mn occupies interstitial sites. In n-type Si containing an excess of P, the substitutional Mn is $Mn^=$ and in p-type Si containing an excess of B, the substitutional Mn is Mn^+. A striking difference in the stability of the resonance center was observed between the Cu-doped and Cu-free samples. Similar experiments in Cr-doped Si containing vacancies produced by Cu and by electron irradiation are also discussed.

8177 MECHANISM FOR THE PRODUCTION OF F CENTERS IN NaCl BY IRRADIATION WITH GAMMA RAYS by J. N. Crawford, Jr. and F. W. Young, Jr. (Oak Ridge Natl. Lab.); J. Appl. Phys., Vol. 31, pp. 1688-1689(L), Sept. 1960

An experimental investigation of the mechanism suggested by Seitz for the production of F centers by gamma ray irradiation of ionic crystals is discussed. According to this mechanism, excitons created during irradiation recombine at crystalline imperfections such as dislocations, thus causing cation-anion vacancy pairs to evaporate from the imperfections. These vacancies are than ionized to form color centers. It is shown that if such evaporation takes place and gamma irradiation produces 4×10^{17} F centers, then each dislocation should climb 3μ. NaCl plates were irradiated to produce greater than 4×10^{17} F centers/cm^3 and the etch pits at the dislocations were observed by an optical microscope before and after irradiation. No measurable amount of climb was observed.

8178 ON THE COLOR DEPTH IN ALKALI HALIDE CRYSTALS SUBJECTED TO BOMBARDMENT UNDER DIFFERENT ANGLES BY ELECTRONS WITH ENERGIES FROM 6 TO 15 KV by A. R. Shul'man and E. P. Gel' (M. I. Kalinin Polytech. Inst.); Soviet Phys.-Solid State, Vol. 2, pp. 489-494, Sept. 1960

Color depth as an indication of electron penetration depth in alkali halides is discussed. For single crystals of NaF, NaCl, KCl, and KBr, the mean color depth is an exponential function of the primary energy of the bombarding electrons. Empirical formulas show this relationship. Color depth, however, has no linear dependence on the cosine of the angle of incidence of the bombarding electrons. The possibility that penetrating electrons take non-rectilinear paths within the crystal is suggested.

8179 SPECIFIC IONIZATION MEASUREMENTS AND ENERGY REQUIREMENTS FOR F-CENTER FORMATION by R. D. Jordan and R. S. Alger (U.S. Naval Radiological Def. Lab.); J. Appl. Phys., Vol. 31, pp. 747-752, May 1960

Measurements made of the energy required to produce F centers in pure and sensitized alkali halide crystals by bombardment with electrons and deuterons accelerated in a Van de Graaff generator are discussed. In KBr+KH exposed to 1.2-Mev electrons, 35 ev were required per F center. This value is in agreement with other published data. A value of approximately 100 ev was required with deuterons and KBr+KH. Slightly lower yields were found for several other salts. The specific ionizations of electrons, deuterons, and gamma rays were investigated and used to determine the accelerator beam size and penetration. The ranges of electrons in KBr, KCl, and NaCl were measured as a function of accelerator voltage and found to agree well with ranges predicted by the Feather rule. Energy transport and features of the specific ionization pattern are discussed in terms of the Seitz synthesis of crystal imperfections.

8180 MANIFESTATION OF EDGE AND SCREW DISLOCATIONS IN SILVER [in Russian] by V. N. Danilov and G. F. Slavikovskii (Kiev Polytech. Inst.); Izv. VUZ Fiz., No. 4, pp. 122-125, 1960

Experimental results on the manifestation of edge and screw dislocations in Ag are presented. A simple method of thermal etching is reported. It is shown that edge dislocations appear as etch pits during evaporation of the atoms, while screw dislocations are detected as growth or etch spirals. The dislocation density in Ag under thermal etching is computed and agrees with the density under chemical etching.

8181 REVEALING OF DISLOCATIONS AND SOME ETCH PATTERNS IN SILICON SINGLE CRYSTALS by N. N. Sirota and A. A. Tonoyan (S.S.P., Acad. Sci. Belorussian SSR); Proc. Acad. Sci. USSR, Phys.-Chem., Vol. 134, pp. 987-989, Sept.-Oct. 1960

Etch patterns observed in Si single crystals along planes close to the (111) plane are discussed. After cutting, the crystals were polished with abrasive powders of various sizes and chemically polished and etched. The chemical polishing was done at 30°-35°C for 2-3 minutes in a solution consisting of 10 cc (37-38%) hydrofluoric acid, 10 cc nitric acid, and 10 cc glacial acetic acid. The etching was performed at the same temperature for 1.5-2 minutes following the addition of 15 cc of double distilled water to the solution. Etch patterns having a helical shape were observed. Often the etch patterns included both a helix and a terrace structure. Etch patterns

consisting only of nonintersecting terraces one above the other were also observed. Low resistivity single crystals ($\rho = 0.1$ ohm-cm) were also etched for 10 minutes in a boiling 20 per cent KOH solution. Etch patterns consisting of sharply outlined closed polygons, one above another with their sides practically parallel were observed. The measurements indicate that the etch pits are connected with the dislocations and faults which originate from the growth structure.

8182 THE DISLOCATION ETCH PITS OF CdS CRYSTALS by J. Nishimura (Iwate U.); J. Phys. Soc. Japan, Vol. 15, p. 732(L), Apr. 1960

Etch pits revealed by etching the (0001) plane of CdS single crystals grown under different conditions are discussed. The etch pits were revealed by etching with a thiourea-HCl solution at 60°C for 5 min. Crystals grown by sublimation and recrystallization at 930°C for 48 hrs in H_2S exhibited subgrain boundaries (type 1) along the $[10\bar{1}0]$ direction in almost the whole region of the etched surface except near the intersections of the subboundaries. In crystals grown at 1050°C for 72 hrs in H_2S, arrays of pits (type 2) occur along the [1210] directions. When the crystals grow at 950°-1000°C for 72 hrs, both types of boundaries occur. The type 1 and type 2 boundaries are arrays of edge dislocations with Burgers vector $a\langle 1\bar{2}10\rangle$ and slip plane $\{10\bar{1}0\}$ and Burgers vector $\sqrt{3}\, a\langle 10\bar{1}0\rangle$ and slip plane $\{1\bar{2}10\}$ respectively, where a is the magnitude of the lattice vector in the $[1\bar{2}10]$ direction and $\sqrt{3}\, a$ is the magnitude of the lattice vector in the $[10\bar{1}0]$ direction.

8183 SURFACE STRUCTURE IN CORUNDUM: Part I, ETCHING OF DISLOCATIONS by R. Scheuplein and P. Gibbs (U. Utah); J. Am. Ceram. Soc., Vol. 43, pp. 458-472, Sept. 1960

Triangular etch pits, corresponding to the intersection of individual edge dislocations with the surface, observed in corundum single crystals after about 5 minutes of immersion in boiling phosphoric acid are discussed. Dislocations of both the (0001), $\langle 11\bar{2}0\rangle$ and $\{1\bar{2}10\}$, $\langle\bar{1}010\rangle$ slip systems (where reference is made to the slip plane and slip direction, respectively) have been detected by this method. Edge dislocations of the (0001), $\langle 11\bar{2}0\rangle$ system etched on surfaces close to and including the $\{10\bar{1}1\}$ and $\{20\bar{2}1\}$ planes. Dislocations of the $\{1\bar{2}10\}$, $\langle\bar{1}010\rangle$ systems etched on the basal (0001) plane. The orientation dependence and technique of etching are described. The agreement with the Nye formula and with some of the expected properties of dislocations is cited as evidence that individual edge dislocations are actually detected. Typical photomicrographs of the etched surface in as-received, deformed, flame-polished, and polygonized crystals are shown.

Dislocation Content in Epitaxially Vapor-Grown Crystals – See 8215

Effect of Crystal Polarity on the Generation of Dislocations During Growth - See 8209

Generation of Dislocations in Ge Single Crystals by Change of Pulling Speed – See 8208

8184 CIRCULAR EDGE DISLOCATION LOOP by F. Kroupa (Czech. Acad. Sci.); Czech. J. Phys., Vol. 10B, No. 4, p. 284-293, 1960

A solution of the stress, deformation and deformation energy for an edge dislocation with its dislocation line having the shape of a circle in an unlimited isotropic medium is discussed. The possibility of using this solution in studying the dislocation loop in a crystal is cited.

8185 BEHAVIOR OF INDIVIDUAL DISLOCATIONS IN STRAIN-HARDENED LiF CRYSTALS by J. J. Gilman and W. G. Johnston (GE Res. Labs.); J. Appl. Phys., Vol. 31, pp. 687-692, Apr. 1960

Measurement of the velocities of dislocations as a function of stress for both undeformed and deformed crystals is discussed. The motion is slower at a given stress in a strained crystal, and extra stress is needed to give the same velocity in a strained crystal as in one that is unstrained. It has been found that the extra stress is just equal to the difference in macroscopic flow stresses for the two states of a crystal. Existing theories of strain-hardening do not correctly predict the behavior of LiF. Barrier-type theories are ruled out because the distance that a dislocation can move in a strain-hardened crystal does not seem to be limited. Theories of Taylor hardening or of cutting of a dislocation forest do not give the observed dependence of strain-hardening on dislocation density. It is observed that the strain-hardening increment is proportional to the dislocation density (also to the plastic strain), and the proportionality constant is 3-5 dynes/disl. The data are consistent with the idea that the hardening is due to defects left in the wakes of moving dislocations. These defects would interfere with the movement of subsequent dislocations on the same or nearby glide planes.

8186 THE PLASTIC RESISTANCE OF CRYSTALS by J. J. Gilman (GE Res. Labs.); J. Phys. Austl., Vol. 13, pp. 327-346, July 1960

The plastic resistance of crystals to dislocation motion is described. This plastic resistance is almost independent of dislocation velocity except at very high velocities, but is strongly influenced by temperature, impurities, and radiation damage. In LiF crystals, the plastic resistance is much higher for glide on {100} planes than on {110} planes. It is shown that the yield stresses and indentation hardnesses of many crystals can be correlated with their elastic moduli, provided the crystal structure type is held constant. For example, for fcc metals the yield stress is equal to $1.6 \times 10^{-3} G$ (shear modulus) at −200°C. This is taken to mean that one important factor that determines the plastic resistance is the elastic modulus of a crystal. Crystal structure type also has a big effect, so the detailed structure of the core of a dislocation also influences the plastic resistance. The temperature dependence of the plastic resistance is discussed. A sharp drop in the plastic resistance of covalent crystals is observed at a temperature that is roughly equal to two-thirds of the melting temperature. It is suggested that this is because the cores of dislocations in covalent crystals "melt" at this temperature.

8187 DISLOCATION VELOCITIES IN GERMANIUM AND SILICON by J. R. Patel, A. R. Chaudhuri, and L. G. Rubin (Raytheon); Bull. Am. Phys. Soc., Ser. II, Vol. 5, p. 375(A), June 15, 1960

Stein-Low method measurements on the average dislocation velocities under various stress conditions in initially dislocation-free Ge and Si were discussed. The effects of stress, temperature, and impurities have been determined. This method also permitted a very sensitive determination of the delay time; its dependence on stress and temperature also have been measured. Dislocation velocities are strikingly different in Si and

Ge from those found in LiF and in Si-Fe, in that the velocities become more or less independent of stress at velocities of 10^{-2} to 10^{-5} cm/sec in the temperature range 400° to 600°C. Average dislocation velocities also were determined from measured values of dislocation density after deforming to the upper yield point, assuming that all dislocations were mobile. Velocities thus measured were lower than those obtained by stress pulsing. This indicates that all the dislocations are not mobile. In fact, for certain orientations only 5 per cent may be mobile. The temperature and strain rate dependence of the strength of Ge and Si was discussed in terms of the numbers and velocities of dislocations.

8188 A COMPARISON OF ETCHING AND FRACTURING TECHNIQUES FOR STUDYING TWIN STRUCTURES IN Ge, Si, AND III-V INTERMETALLIC COMPOUNDS by J. W. Faust, Jr. and H. F. John (Westinghouse); J. Electrochem. Soc., Vol. 107, pp. 562-564, June 1960

Three etching techniques and a fracturing technique for revealing twins in Ge, Si, and the III-V intermetallic compounds are discussed. The etching techniques are as follows: (1) Preferentially etch a lapped surface. The twin boundary is revealed by the change in the characteristic etch pits as a result of the orientation difference across the boundary. If the orientations of the faces across the twin plane are not equivalent, a step is also produced at the boundary. (2) Chemically or electrolytically polish a lapped surface. The twin is revealed as a groove (if the orientations of the faces across the twin plane are equivalent) or as a step (if the orientations are not equivalent). (3) Immerse a mechanically-polished surface in a chemical polish or a preferential etch for a very short time. The twin line is revealed as a groove. The interpretation of the results obtained by method 3 is discussed. When Ge and Si are carefully fractured along their {111} cleavage planes, each twin plane changes the direction of the {111} cleavage planes. A line is then observed for each twin boundary. This technique is more rapid and more easily interpreted than the etching methods. The number of twins revealed by the fracture technique was the same as that revealed by electron micrographic examination.

8189 "FLASH ETCHING" OF Al_2O_3 GRAIN BOUNDARIES by E. K. Beauchamp (U. Utah); J. Am. Ceram. Soc., Vol. 43, p. 552(L), Oct. 1960

The flash etching technique for etching grain boundaries in polycrystalline Al_2O_3 is described. The specimen surface is polished with abrasives and then raised quickly to flame-polish temperatures (about 1900°C) with a slightly reducing oxyacetylene flame and held at that temperature for 2 to 5 seconds. The flash etched boundaries are more clearly defined than chemically etched boundaries. The flash etching technique removes scratches produced during polishing while chemical etching accentuates these scratches.

8190 TOPOGRAPHY AND ETCH PATTERNS OF SYNTHETIC QUARTZ by F. Augustine and D. R. Hale (Clevite); J. Phys. Chem. Solids, Vol. 13, pp. 344-346, June 1960

Surface details of growth patterns of synthetic quartz crystals are discussed. Growth hillocks with spiral ramps are often found on rhombohedral faces and on the irregular surface of growing basal pinacoids. In some instances small hillocks are replaced through etching by pits in a substantially one-to-one relationship.

8191 DETECTION OF GROWTH STRIATIONS IN GERMANIUM CRYSTALS by A. C. English (GE); J. Appl. Phys., Vol. 31, pp. 1498-1500(L), Aug. 1960

Two methods for detecting growth striations in Ge crystals grown by the Czochralski technique are discussed. The crystals were grown with one rotation of the seed per minute and a growth rate of 7.5 cm/hr. Both methods utilize wafers cut parallel to the axis of the crystal in order to intersect the growth face. In one method the wafer is heated in contact with a sheet of iron, nickel, copper, or some other metal to a temperature of about 700°C in hydrogen for a few minutes. A film of Ge is formed on the sheet of iron and a film of iron on the surface of the Ge wafer. The iron sheet is the negative of the matching Ge wafer. The periodicity of the film deposit matches the pitch of the elevating screw on the crystal growing apparatus. In the second method a layer of In is melted on the Ge wafer at about 550°C in hydrogen or an inert gas with a cover plate of iron to spread the In layer. After cooling the In is dissolved in HCl to reveal the structure of the Ge surface. Uniformly spaced, parallel curved lines consisting of walls of crystals extending out of the base Ge, with the same orientation of the base Ge, have been found in the region attacked by the In in a wafer alloyed under helium. In a wafer alloyed in argon, unsymmetrical grooves in the Ge are produced by the In alloying. Both methods indicate the presence in the crystal of periodic regions of high activity with a periodicity matching the distance of elevation per rotation during crystal growing.

8192 PHOTOMETRIC DETERMINATION OF ANTIMONY AND THALLIUM IN LEAD by C. L. Luke (Bell Labs.); Analyt. Chem., Vol. 31, pp. 1680-1682, Oct. 1959

The determination of traces of Sb and Tl in Pb is discussed. The metals are separated from the bulk of the Pb by co-precipitation with MnO_2 and then determined by photometric rhodamine B methods.

8193 THE PURIFICATION OF SILICON AND THE PRODUCTION OF HOMOGENEOUS MONOCRYSTALS [in French] by J. Goorissen and B. Okkerse (Philips); Acta Electronica, Vol. 4, No. 4, pp. 479-491, 1960

Impurity concentrations in the solid and liquid phases of Si purification processes are discussed. The role of the solidification surface is emphasized and the effect of crystal imperfections on the electrical properties of the Si is described. Several zone refining processes are mentioned outlining pulling, floating zone and co-precipitation techniques for achieving uniform impurity distribution in Si monocrystals.

8194 TECHNIQUES AND RESULTS OF ZONE REFINING SOME METALS by J. H. Wernick, D. Dorsi, and J. J. Byrnes (Bell Labs.); J. Electrochem. Soc., Vol. 106, pp. 245-248, Mar. 1959

Techniques and results for the floating zone refining of Ni, Ti, V and for the boat zone refining of Al and Au are discussed. These elements have been purified by zone melting. A considerable amount of purification was obtained by volatilization during floating zone melting.

Purification of Ge by Distillation - See 8155

8195 STATISTICAL DYNAMICS OF CRYSTALLINE DIFFUSION. Part I. EXCHANGE MECHANISM by R. Kikuchi

(Hughes); Ann. Phys., Vol. 11, pp. 306-327, Nov. 1960

Application of the path probability method for irreversible cooperative phenomena to atomic diffusion in crystals is discussed. A binary alloy of bcc structure with the concentration gradient along a [100] direction, with the direct exchange mechanism for atomic migration assumed, is considered. The path probability $\mathcal{G}$ for change of state during a short time interval is written in terms of the path parameters $\{Y_{ij}\}$ using the pair approximation of the cluster-variation method. The most probable path is determined by maximizing $\mathcal{G}$ with respect to $\{Y_{ij}\}$. The system is isothermal and a flow of atoms is maintained by two particle reservoirs of different chemical potentials placed at the two ends of the system. When there is no chemical potential gradient, the system is in an equilibrium state identical to that obtained by the pair approximation, which is equivalent to Bethe's approximation or the quasi-chemical approximation. The diffusion coefficient is obtained from the stationary state by expanding the state parameters in terms of the concentration gradient. The expression of the diffusion coefficient is given for an arbitrary value of the concentration and is written in terms of a probability parameter for a unit interchange of atoms.

8196 A METHOD OF EVALUATING DIFFUSION COEFFICIENTS IN CRYSTALS by O. P. Manley (MIT); J. Phys. Chem. Solids, Vol. 13, pp. 244-250, June 1960

The mechanism of diffusion proposed by Rice is reconsidered. The analysis, with the aid of an extension of Kac's theorem, yields an activation energy which is simply related to the minimal local deformation energy. It is also found that in contrast with Rice's treatment, the activation energy may be calculated directly from the atomic force constants without resorting to normal mode analysis.

8197 INFLUENCE OF ARSENIC PRESSURE ON THE DOPING OF GALLIUM ARSENIDE WITH GERMANIUM by J. O. McCaldin and R. Harada (Hughes Semicon.); J. Appl. Phys., Vol. 31, pp. 2065-2066(L), Nov. 1960

Equilibrium relationships which indicate the influence of the vapor pressure of the Group V element on the doping of III-V compounds with a Group IV element are derived. It is found that a tenfold increase or decrease in pressure from a reference pressure should make the Group IV impurity an effective donor or acceptor dopant, respectively. The relationships were investigated by diffusion treatments of Ge-doped GaAs. Slices from an ingot which was predominantly p-type were heated 70 hrs at 900°C at 5 mm arsenic pressure. These slices were found to be p-type everywhere at the surface after diffusion. Slices treated for 70 hrs at 5 atm arsenic pressure were found to be n-type everywhere at the surface. A p-n junction was found at a depth of 30μ to 70μ at most places and at a greater depth at the grain boundaries. The experimental conditions allowed only the surface and some grain boundaries to be at equilibrium.

8198 ON THE DIFFUSION OF MERCURY ATOMS IN SELENIUM [in Russian] by M. V. Reznik and M. I. Korsunskii (Khar'kov Polytech. Inst.); Izv. VUZ Fiz., No. 3, pp. 107-111, 1960

The diffusion rate of Hg atoms in a layer of amorphous and crystalline Se $10^{-4}-10^{-5}$ cm thick is analyzed. It is shown that the order of magnitude of the diffusion coefficient can be estimated by means of the change in the electrical conductivity of the Se. It is found that the lower value of the diffusion coefficient D in amorphous Se is 10^{-11} cm^2/sec; D = 10^{-13} cm^2/sec in crystalline Se. The method used can be applied to determine the diffusion rate of impurities in dielectrics and semiconductors.

8199 DIFFUSION OF LITHIUM IN SILICON by Yu. M. Shashkov and I. P. Akimchencko (Baikov Inst. Metall., USSR); Soviet Phys.-Doklady, Vol. 4, pp. 1115-1117, Mar.-Apr. 1960

Measurements of the diffusion of Li in Si are discussed. Single crystals and crystals containing a large number of twins and dislocations were used. A thin layer of the diffusant was deposited on the polished surface of one sample and the other sample was placed above the Li layer. The diffusion was carried out in a quartz tube with a stream of helium or argon passing through it and the samples resting on a special quartz holder. The samples were rapidly cooled after the diffusion. In samples containing twins and dislocations, the diffusion took place both parallel and perpendicular to the propagation of the twins and dislocations. Experimental data obtained for diffusions in the temperature range 400° to 800°C indicate that the diffusion rate of Li in Si is independent of the structural perfection of the crystals. The data points conform to the equation $D = 2.2 \times 10^{-3} \exp\left(\frac{-16,200}{RT}\right)$ cm^2/sec.

8200 SOLVENT EVAPORATION TECHNIQUE FOR THE GROWTH OF ARSENIC-DOPED GERMANIUM SINGLE CRYSTALS FOR ESAKI DIODES by F. A. Trumbore and E. M. Porbansky (Bell Labs.); J. Appl. Phys., Vol. 31, p. 2068(L), Nov. 1960

A solvent evaporation technique which utilizes the relatively high volatility of As to grow low resistivity As doped Ge is described. A rotating Ge seed is dipped into an arsenic-germanium melt and allowed to puddle at a constant temperature. The seed is not pulled. As arsenic evaporates from the melt, arsenic-doped germanium is grown on the seed. Uniformly homogeneous material can be obtained by the isothermal process. The technique requires no elaborate pulling mechanism, little attention on the part of the operator, and can be applied to any system where there is a volatile component or solvent. A crystal with a total variation in resistivity from 0.00069 to 0.00080 ohm-cm, with three-quarters of the crystal exhibiting a uniform resistivity of 0.00071 ohm-cm to within ±3 per cent, was grown. Esaki diodes with 20-25 ma peak currents, rc products of $5-10 \times 10^{-11}$ sec and peak current to valley current ratios of 4 to 1 have been fabricated from the material.

8201 IMPURITY INTRODUCTION DURING EPITAXIAL GROWTH OF SILICON by R. Glang and B. W. Kippenhan (IBM); IBM J. Res. and Dev., Vol. 4, pp. 299-301(L), July 1960

The growth of doped epitaxial Si layers on Si substrates is discussed. A small weighed quantity of the impurity or a Si master alloy containing a known impurity concentration was used as the impurity source. Deposits produced by means of the free impurity have impurity concentrations which are proportional to the amount of impurity put in the source region, while those produced using master alloys contain roughly the same impurity concentration as the source material. Experiments were also conducted using sources consisting of a master alloy and pure Si in predetermined weight ratios up to a dilution ratio of 100:1. These mixed sources act like one uniform alloy which

has been "diluted" corresponding to the weight ratio. Various steps in the epitaxial growth process are discussed.

Dielectric Absorption Measurements of Divalent Cation Impurities in NaCl and KCl - See 8244

8202 PRECIPITATION IN SILICON CRYSTALS CONTAINING ALUMINUM by R. Bullough, R. C. Newman, J. Wakefield, and J. B. Willis (Assoc. Elect. Ind.); J. Appl. Phys., Vol. 31, pp. 707-714, Apr. 1960

Annealing of Si crystals containing Al at various temperatures within the range 700° to 1350°C is discussed. Particular emphasis is given to the range 1200° to 1300°C. Precipitation, which occurs during the heat treatment in the bulk crystal and on various structural defects, has been detected by transmission optical microscopy. A lowering of the Al concentration in the neighborhood of the precipitate particles after heating at 1250°C has been revealed at the surface by a novel technique involving the etching of crystals which also contain phosphorus, where internal cylindrical and planar p-n junctions are formed around individual dislocations and grain boundaries, respectively. At this temperature, no precipitation is observed on dislocations in plastically deformed crystals. The precipitation of Al is interpreted in terms of a chemical reaction involving the co-precipitation of oxygen and possibly carbon.

8203 CHLORINE AND IODINE AS IMPURITIES IN InAs AND GaP by G. R. Antell (Assoc. Elect. Ind.); J. Appl. Phys., Vol. 31, p. 1686(L), Sept. 1960

Mass spectrometric studies of InAs which had been zone leveled under an atmosphere containing 1.2×10^{19} atoms of chlorine/cm^3 and GaP crystals grown from a vapor phase at 950°C in an atmosphere which contained 7×10^{18} atoms of Iodine/cm^3 are discussed. The InAs was found to contain about 10^{19} atoms of chlorine/cm^3 and the GaP was found to contain less than 10^{15} atoms of Iodine/cm^3. The low observed solubility of I in GaP and the high observed solubility of Cl in InAs can be explained on the basis of the covalent radii of the impurities and the space available in each compound to take interstitial impurities.

8204 DEFECTS IN THE CRYSTAL AND MAGNETIC STRUCTURES OF FERROUS OXIDE by W. L. Roth (GE Res. Labs.); Acta Cryst., Vol. 13, pp. 140-149, Feb. 1960

Investigation of the defect structure of non-stoichiometric FeO by measuring the neutron scattering of powders quenched from the high temperature equilibrium state is reported. The nuclear scattering shows the defects to consist of both cation vacancies in octahedral sites and interstitial cations in tetrahedral sites. The defects give rise to diffuse scattering which suggests the atomic arrangement in the vicinity of the defect is similar to that in magnetite. The average magnetic moment of iron atoms in normal positions, obtained by measuring the scattering of neutrons by the periodic arrangement of spins in the antiferromagnetic state, indicates the magnetic structure in the vicinity of the defect is paramagnetic. The model is supported by magnetic studies which demonstrated the existence at low temperature of a magnetic remanence in exchange contact with the antiferromagnetic structure.

8205 DETERMINATION OF SURFACE STRUCTURE USING ULTRA-HIGH VACUUM REPLICATION by L. Bachmann, W. H. Orr, T. N. Rhodin, and B. M. Siegel (Cornell U.); J. Appl. Phys., Vol. 31, pp. 1458-1462, Aug. 1960

The application of electron microscopy to the problem of characterizing the distribution of preferred sites for nucleation and growth on clean surfaces of evaporated films of Mg metal is discussed. The films were deposited, platinum-shadowed, and carbon-backed in the same system under ultra-high vacuum conditions to minimize surface contamination and to improve the fidelity of surface replication. Upon examination of both clean and oxidized films in the electron microscope, the distribution of the Pt deposit was observed to be markedly influenced by the vacuum conditions used in the replication procedure. In addition, the particle size and separation of the Pt grains and their distribution with relation to the substrate indicated an enhanced surface mobility on cleaved mica and an apparent reaction on Mg. These observations may have bearing on both the surface properties of metal deposits and on the development of high-resolution replication techniques.

8206 CLEAVAGE WHISKERS by J. D. Venables (Union Carbide); J. Appl. Phys., Vol. 31, pp. 1503-1504(L), Aug. 1960

Elongated fragments, or cleavage whiskers, formed on cleavage steps in Si, Ge, InSb, HgSe, Mg_2Ge, MgO, and Sb are discussed. The whiskers lie completely in the cleavage step, have a free end running out of the step, or lie, debris-like, loose on the surface. Electron microscopic examination has shown that the Si and InSb whiskers are single crystals, range in size from 5000 to <500 A, are of the same composition as the parent material, and are quite uniform in cross section from end to end. A mechanism for the formation of the whiskers is discussed.

CRYSTAL GROWTH

8207 ON THE OBSERVATION OF MACROSCOPIC SPIRALS ON GALLIUM ARSENIDE SURFACES by W. J. Little and K. A. McCarthy (Tufts U.); J. Appl. Phys., Vol. 31, pp. 1298-1299(L), July 1960

Spirals observed on the (111) surfaces of GaAs crystals are discussed. Previously proposed mechanisms for the formation of such spirals required many atomic steps to congregate. It is suggested that in a GaAs crystal grown by a seed with a (111) surface many atomic steps crowd together because the Ga atoms added to the As layer are not tetrahedrally bonded. A crystal was examined and found to agree with many features of the growth mechanism theories.

8208 DISLOCATIONS GENERATED BY CHANGE OF PULLING VELOCITY OF GERMANIUM MONOCRYSTALS [in Polish] by A. Kobus and A. Brochocki; Arch. Elektrotech., Vol. 9, No. 4, pp. 717-720, 1960

The generation of dislocations in germanium single crystals pulled with varying velocity is discussed. The influence of the pulling velocity changes on the shape of the interface and on the dislocation density was investigated. It was found that a greater change of interface shape and dislocation density takes place on the outer edges of the crystal than inside the crystal.

8209 GROWTH OF GaAs CRYSTALS IN THE <111> POLAR DIRECTION by P. L. Moody, H. C. Gatos, and M. C. Lavine (Lincoln Lab.); J. Appl. Phys., Vol. 31, pp. 1696-1697(L), Sept. 1960

The effect of crystallographic polarity in the <111> direction on the perfection of GaAs crystals grown in that direction is

iscussed. The crystals were pulled vertically in a syringe-ype furnace. Single crystals were grown when the end of the <111> seed terminating in As atoms (B {111} surface) was used, nd crystals in which twinning or large grain formation ccurred were grown when the end terminating with Ga atoms (A {111} surface) was used. The dislocation density in a B crystal was found to be smaller than the dislocation density in an A crystal grown from the same seed. In the A crystals the dislocation density increased with increasing distance from the seed. It is believed that the effect of the <111> crystallographic polarity on crystal growth is related to the bonding characteristics of the A and B surface atoms.

8210 GERMANIUM CRYSTALS GROWN FROM HOLLOW CYLINDRICAL SEEDS by R. C. Frank (GM) and J. E. Thomas, Jr. (Wayne State U.); J. Appl. Phys., Vol. 31, pp. 1689-1690 (L), Sept. 1960

ome observations made on crystals grown with hollow single rystal and polycrystalline Ge seeds are discussed. The new rystal grew both inward and outward from the hollow seed, he growth inward being extremely rapid. A small hump formed n the center, probably as the result of the reduction in gas ressure inside the closed cylinder and expansion of the Ge on olidification. Growth rings concentric with the center of rotation were observed. In the single crystals (grown from the single crystal seed) the growth rings were very circular and uniform and in polycrystalline materials they had a tendency to be circular but were considerably warped by the individual grains. In the single crystals the growth continues upward with each succeeding ring toward the center until a plateau is reached. There is then no further growth upward until the crystal grows together and an additional small step is formed. In the polycrystals, no plateau is formed and the growth continues steadily upward until the center is reached. A very high dislocation density was found at the very center of the single crystal.

8211 IMPROVEMENTS ON THE PEDESTAL METHOD OF GROWING SILICON AND GERMANIUM CRYSTALS by W. C. Dash (GE); J. Appl. Phys., Vol. 31, pp. 736-737 (L), Apr. 1960

The growth of large dislocation-free Si and Ge crystals by a modification of the pedestal method which does not require a slotted Si pedestal is described. A stable melt is held in good thermal contact with the top of an unslotted Si rod if the rod diameter is about 5/16 in at the top. For use with Ge the technique requires a rod diameter of 1/2 in which tapers down to 1/4 in at the top. Larger crystals can be grown by the modified technique than with the pedestal method utilizing slotted pedestals. Si crystals up to ~12 mm in diameter weighing ~20 gms and Ge crystals up to ~6 mm in diameter weighing 10 to 12 gms have been grown.

8212 METHOD OF MANUFACTURING SEMI-CONDUCTOR MATERIALS by J. M. N. Hanlet (Soc. d'Electronique et d'Automatisme); U.S. Pat. 2,880,117, Issued Mar. 31, 1959

The preparation of boron-free high resistivity Si single crystals by the thermal decomposition of $SiCl_4$ is described. The crystals are grown with their [111] axis along the axis of a tantalum tape that is stretched down the middle of a water cooled reaction chamber. Dry purified hydrogen, at 0.5 liter per minute (lpm), is fed into the chamber while the tape is electrically heated to 1300°C. A 1.5-2.0 lpm flow of $SiCl_4$ is started and continued until the deposited film is as thick as desired. An RF coil is then passed down the crystal.

8213 SYNTHESIS OF LARGE CdS AND ZnS CRYSTALS by J. Nishimura (Iwate U.) and Y. Tanabe (Tohoku U.); J. Phys. Soc. Japan, Vol. 14, pp. 850-851 (L), June 1959

A technique for growing large single crystals of CdS and ZnS from a charge of the sulfide powder is described. Polycrystals of easy grain growth are first prepared from the powder by sublimation and recrystallization. The c-axis of the grains in the polycrystals are parallel with the normal to the substrate in CdS and make an angle of 25° with the normal to the substrate in ZnS. Single crystals are then grown from the polycrystals by heat treatment under saturated vapor. The whole process can be carried out in a single run. Crystal growing furnaces are described and some photographs of grown crystals are presented.

8214 CRYSTAL GROWING PROCEDURES by L. E. Ravich (Hupp); U.S. Pat. 2,890,939, Issued June 16, 1959

A two stage process for growing crystals of PbS, ZnS, or CdS is described. The process is illustrated by the growth of CdS crystals. A crucible containing CdS powder is heated in a tube to 650°C and then more slowly (e.g., at 10°C/min) up to 900°C. Hydrogen gas flowing over the crucible carries the vapors to a region where they react with H_2S gas, causing seed crystals to precipitate. Initially the flow of H_2S is much greater than the flow of H_2. A short time after the 900°C temperature is reached, the H_2 gas flow is greatly increased and the tube in which the crystals are grown is moved so that the crucible is in a cooler region of the furnace and the crystal growing region is now in a hotter region. The change in temperature at the crystal growing region results in an optimum temperature for crystal growth on the seeds.

Growth of Low Resistivity Ge - See 8200

Growth of Ge-III-V Compounds - See 8162

8215 DISLOCATION CONTENT IN EPITAXIALLY VAPOR-GROWN CRYSTALS by H. S. Ingham, Jr. and P. J. McDade (IBM); IBM J. Res. and Dev., Vol. 4, pp. 302-304 (L), July 1960

The perfection of epitaxial Ge layers grown on Ge by the disproportionation of GeI_2 is discussed. It was found that the perfection of the grown crystals is principally controlled by the condition of the surface of the seed crystal and that the perfection of the seed significantly affects the dislocation content of the deposit only in certain cases. Doping and growth rate have no effect on the crystalline perfection. It has been found that a very thin oxide layer can be removed by treating the surfaces with H_2.

8216 GROWTH OF SINGLE CRYSTAL SILICON OVER-GROWTHS ON SILICON SUBSTRATES by A. Mark (USASRDL); J. Electrochem. Soc., Vol. 107, pp. 568-569, June 1960; p. 1026, Dec. 1960

The production of epitaxial Si layers on Si substrates by the reduction of $SiCl_4$ by hydrogen is discussed. The deposit growth assumes the growth pattern of the substrate and the mechanical quality of the grown surface depends on the geometrical configuration of the substrate. It is difficult to distinguish the overgrown layer from the substrate. Electron diffraction studies

have indicated that the deposits were single crystals of fair quality. Several device applications of the layers are pointed out.

Epitaxial Growth of Doped Si Layers - See 8201

Preparation of CdS Phosphors - See 8388

8217 MODIFICATION IN TECHNIQUE FOR GROWING SINGLE CRYSTALS OF ZnF_2:Mn by L. M. Matarrese and F. L. Hughes (U.S. Naval Res. Lab.); J. Appl. Phys., Vol. 31, p. 2063 (L), Nov. 1960

A modification of the moving-crucible technique which permits the growth of clear, bubble-free crystals of single crystals of ZnF_2 with small additions of MnF_2 is described. A grooved and slotted graphite insert is placed in the crucible along with the starting powder. The proper critical temperature distribution within the crucible is achieved by the insert which provides a sink for the heat of crystallization. A thermal gradient large enough to eliminate such imperfections as bubbles then occurs at the liquid-solid interface. Details of the crystal growing apparatus and procedures are given, and impurity segregation in a typical boule is discussed.

8218 THE GROWTH OF LARGE SINGLE CRYSTALS OF ZINC OXIDE by J. W. Nielsen and E. F. Dearborn (Bell Labs.); J. Phys. Chem., Vol. 64, pp. 1762-1763, Nov. 1960

The growth of large single crystals of ZnO from molten PbF_2 is discussed. Crystal growth was begun at 1150°C. The samples were held at this temperature for 2 to 4 hours and then cooled at a constant rate of 1° to 10° per hour. Both air and oxygen atmospheres were employed. The samples were withdrawn near 800°C and allowed to cool in air. The ZnO crystals were mechanically separated from the PbF_2 since no chemical separation method is known. The habit of the ZnO crystals on the melt surface was platey. Crystals nucleated at temperatures below 1050°C tended to be more drum shaped and crystals grown by the evaporation of PbF_2 at 1150°C were always very thin plates and exhibited the largest ratio of growth rate in the a-direction to the growth rate in the c-direction. The large crystals grown from PbF_2 have been used as seeds in hydrothermal crystal growth experiments. The ZnO-PbF_2 system was found to have a eutectic at 8.8 mole per cent ZnO at 733°C.

8219 GROWTH OF SINGLE CRYSTALS OF ANTHRACENE by J. N. Sherwood and S. J. Thomson (U. Glasgow); J. Sci. Instr., Vol. 37, pp. 242-245, July 1960

The growth of single crystals of anthracene from melts of zone-purified material, in an all-glass oven, is described. The important factors which govern the successful growth of single crystals by the moving-vessel technique have been investigated. These factors include the purity of the anthracene, the temperature gradient, the shape of the growth vessel, and the growth rate.

Vacuum Deposited Metallic Films - See 8415

8220 THE PREPARATION OF FINE POWDER HEXAGONAL Fe_2C AND ITS COERCIVE FORCE by W. D. Johnston, R. R. Heikes, and J. Petrolo (Westinghouse); J. Phys. Chem., Vol. 64, pp. 1720-1722, Nov. 1960

The preparation of the relatively rare hexagonal form of Fe_2C in fine powder form by the reaction of a gaseous mixture of H_2 and CO with Raney iron at 240°C is discussed. The occurrence of the hexagonal form appears to require the exclusion of Fe_3O_4. If Fe_3O_4 is present, the carbide is found in the more common Hägg form. The coercive force of the fine powder hexagonal Fe_2C prepared by this method is approximately 800 oe.

8221 SOME PROBLEMS IN THE PREPARATION OF FERRITES FOR VARIOUS MICROWAVE DEVICES by D. H. Pringle and W. D. Hepburn (Ferranti); Solid State Phys. Electronics and Telecommun., Academic Press, 1960, Vol. 3, pp. 252-269

The preparation of ferrites with predetermined specific properties is discussed. The application of such ferrites is described. A detailed description of the preparation of a magnesium manganese ferrite ($Mg_{0.9}Mn_{0.1}Fe_{1.6}O_{3.4\pm}$), which has been developed for low field use at K-band and higher frequencies, is given. The dielectric and magnetic loss mechanisms of ferrites are also discussed.

Preparation of High Permeability Garnets - See 8330

8222 PREPARATION OF LARGE CALCIUM-TUNGSTATE CRYSTALS CONTAINING PARAMAGNETIC IONS FOR MASER APPLICATIONS by K. Nassau and L. G. G. van Uitert (Bell Labs.); J. Appl. Phys., Vol. 31, p. 1508 (L), Aug. 1960

The growth of pure $CaWO_4$ single crystals containing rare earths by the Czochralski technique is discussed. No flux was used and crystals up to 7 in. in length and 1/2 in. in diameter have been grown. Single crystals were grown at temperatures near 1600°C from a melt consisting of calcium tungstate (both flux-grown material and commercial luminescent material were used) alone or in combination with flux-grown $Na_{0.5}re_{0.5}WO_4$, where re is an element such as cerium, europium, gadolinium, terbium, dysprosium, and erbium. The crystals were rotated during growth at 12 rpm and pulled at rates of up to 3 in/hr. Seed crystals were not required since growth initiated readily on a platinum wire. Larger crystals could be grown by tying to a platinum rod the small pieces grown on the platinum wire. Crystals with rare earth concentrations as high as 4 formula per cent can be grown.

8223 METHOD OF GROWING QUARTZ SINGLE CRYSTALS by M. Jaffe and T. J. Turobinski (Clevite); U.S. Pat. 2,923,605, Issued Feb. 2, 1960

The growth of quartz single crystals which have a large proportion of material useful for oscillator plates is described. A y-bar seed whose length is perpendicular to one of the x-axes and at 30° to the other x-axis is used. Rapid growth occurs along the z-axis and along the x-axis when the bar is exposed to the proper chemical and physical environment. Slow growth takes place on the major rhombohedral faces and no significant growth occurs on the primary prism faces. Crystal growth is stopped before the crystal has fully grown, in particular before the crystal has grown in any direction greater than the length of the original seed.

8224 THE GROWTH OF BARIUM TITANATE SINGLE CRYSTALS FROM MOLTEN BARIUM FLUORIDE by R. C. Linares (Bell Labs.); J. Phys. Chem., Vol. 64, pp. 941-942, July 1960

An investigation of the BaF_2-$BaTiO_3$ phase diagram and the growth of $BaTiO_3$ crystals from BaF_2 solutions is discussed. A eutectic was found at 1260°C and 16.5 mole per cent $BaTiO_3$. The solubility of $BaTiO_3$ is 49.2 mole per cent at 1393°C.

CRYSTAL GROWTH (Cont'd)

Butterfly twin and cube crystals were grown by the following process: a mixture of 50 gm of $BaTiO_3$ and 50 gm of BaF_2 was heated at 1350°C for 4 hours in a Pt crucible. At the end of this time a crucible containing 5 gm of $BaTiO_3$ powder was placed in the furnace and allowed to reach the furnace temperature. The molten solution was then poured on the powder. The temperature was held constant from 0 to 2.5 hours and then decreased at rates from 1°to 25°C per hour. At the end of the cooling cycle (1270° to 1300°C) the crucible was removed from the furnace and the melt poured off. The crystals were in the bottom of the crucible. Since BaF_2 is very difficult to remove from the crystal and crucible, the possibility of pulling $BaTiO_3$ from a BaF_2 melt while slowly cooling the melt was also investigated.

8225 STUDY OF SOLID-SOLUTION SINGLE CRYSTALS CONTAINING $BaTiO_3$ by T. Sakudo (Electrotech. Lab., Tokyo); J. Phys. Soc. Japan, Vol. 15, pp. 2112-2113(L), Nov. 1960

The growth and properties of $BaTiO_3$-$SrTiO_3$ and $BaTiO_3$-$PbTiO_3$ solid solution single crystals are discussed. The crystals were grown by a modification of Remeika's method using KF as flux. The maximum soaking temperature was higher in the case of (Ba-Sr) TiO_3 and lower in the case of (Ba-Pb) TiO_3 than in the case of $BaTiO_3$. The butterfly-wing habit of pure $BaTiO_3$ disappeared gradually and the crystal size became smaller with increasing mole ratio of Sr and Pb to Ba. The compositions of the grown crystals were found to differ from those of the starting materials. Data on the variation of dielectric constant with temperature and on the Curie temperature, spontaneous polarization, coercive field, and birefringence of (Ba-Pb) TiO_3 crystals with various mole per cents of $PbTiO_3$ are given.

8226 ELECTROLYTIC PRODUCTION OF BORON by G. T. Miller (Hooker Chem.); J. Electrochem. Soc., Vol. 106, pp. 815-819, Sept. 1959

The preparation of elemental B by the fused salt electrolysis of potassium fluoborate is discussed. A study of anode and cathode materials is included, particularly the effect of various grades of graphite as anode material. The effect of various additives to the electrolyte on B yield and purity is evaluated. A method of passivating elemental B is described.

CRYSTAL SURFACES

8227 THE MECHANISMS FOR SILICON OXIDATION IN STEAM AND OXYGEN by J. R. Ligenza and W. G. Spitzer (Bell Labs.); J. Phys. Chem. Solids, Vol. 14, pp. 131-136, July 1960

Some of the mechanisms which are important in the growth of SiO_2 films on high purity Si surfaces are discussed. Films have been prepared by using O^{16} and O^{18} sources and their optical properties investigated by the use of infrared absorption measurements. Two of the fundamental infrared absorption bands show considerable isotopic shifts when films of $SiO_2{}^{16}$ and $SiO_2{}^{18}$ are compared. The SiO_2 films studied here were prepared either by oxidizing Si in oxygen at high temperature or by oxidation in high pressure steam at a somewhat lower temperature. Measurements of films prepared by successive isotopic oxidation show that in both the steam and oxygen cases considerable oxygen isotopic exchange has taken place; this indicates that mobile oxygen species diffuse into the film from the silica-gas interface. In the steam oxidation the mobile species is responsible for the growth of the film and the rate limiting step for the growth is at the silica-silicon interface. The results of the oxygen oxidation are not completely understood and while oxygen exchange is also observed in this case, further work is necessary to determine whether a diffusing oxygen species is responsible for the growth of the oxide film.

8228 THE OXIDATION OF INTERMETALLIC COMPOUNDS. Part I. HIGH TEMPERATURE OXIDATION OF InSb by A. J. Rosenberg and M. C. Lavine (Lincoln Lab.); J. Phys. Chem., Vol. 64, pp. 1135-1142, Sept. 1960

The oxidation of single crystal InSb in the range 212°-494°C is discussed. Initially, Sb is preferentially attacked and evaporates from the surface as $(Sb_2O_3)_2$. In_2O_3 is simultaneously formed and produces a compact crystalline film. Further reaction is then confined to the formation of In_2O_3 and elemental Sb. The latter accumulates at the In_2O_3–InSb interface. Associated with the crystallization of the In_2O_3 film, there is a singularity in the kinetics; the rate drops precipitously and comes under diffusion control. The rates increase slightly with oxygen pressure and vary with crystallographic orientation. Small lattice substitutions of Te (for Sb) or Cd (for In) in InSb increase the rate. The maximum oxide film thickness which is attainable in reasonable times is less than one micron. The rate constant for diffusion-limited oxide growth is four orders of magnitude less than that for Sb alone, but only a factor of two less than In alone.

8229 OXIDATION OF INTERMETALLIC COMPOUNDS. Part II. INTERRUPTED OXIDATION OF InSb by A. J. Rosenberg (Lincoln Lab.); J. Phys. Chem., Vol. 64, pp. 1143-1150, Sept. 1960

The later stages of the oxidation of InSb above 300° are discussed. These stages are limited by the migration of atomic defects through the growing film of In_2O_3. By utilizing a new kinetic procedure it has been shown that the concentration of defects is sufficient to confine any space charge to negligibly thin regions at the boundaries of the oxide film. The experimental method is based on rate measurements following interruptions of the reaction, and permits the simultaneous determination of D, the diffusion coefficient, and C_0, the solubility, of the mobile defect in In_2O_3. The necessary mathematical formulation has a simple analytical form and contains a rigorous internal check. In the temperature range 308° to 407°, the quantities D and C_0 are given by $D = 0.0078 \exp(-31200/RT)\ cm^2/sec$, and $C_0 = 9.4 \times 10^{22} \exp(-5400/RT)$ defects/cm^3. The values of D and C_0 decrease gradually with increasing film thickness in the range 600 – 1500 A. Evidence that Sb can also penetrate In_2O_3 during the interruptions is also presented.

8230 THE ADSORPTION OF OXYGEN ON CLEAN SILICON SURFACES by M. Green and K. H. Maxwell (Zenith); J. Phys. Chem. Solids, Vol. 13, pp. 145-150, May 1960

The adsorption of oxygen in the pressure range 30 –200μ Hg of oxygen at room temperature on clean Si surfaces produced by crushing in vacuo is discussed. The initial adsorption to the extent of about a monolayer was very rapid but kinetic data were obtained for the subsequent slow adsorption. The results were complex and probably sensitive to the crystal faces exposed during crushing. The adsorption process was found to

terminate at an oxygen take-up equivalent to about 1.5 oxygen atoms per surface Si atom. A unique configuration, with an inherent termination at a coverage of 1.5, can be constructed for oxygen adsorbed on the {111} and {110} faces of silicon. Prolonged crushing of the Si led to an enhanced take-up of oxygen which may result from the heating of very small particles during the fast adsorption stage. The surface areas of the powders were determined by the B.E.T. method, using krypton at liquid nitrogen temperature.

8231 DISPLACEMENT PROCESSES ON GERMANIUM SURFACES by K. H. Maxwell and M. Green (Zenith); J. Phys. Chem. Solids, Vol. 14, pp. 94-103, July 1960

Displacement experiments on Ge surfaces produced by crushing are described. A monolayer of either water, methanol, n-butanol, isopropanol or atomic hydrogen was first adsorbed, the excess gas removed from the gaseous phase, and then a known amount of oxygen admitted to the system. The results show that oxygen reacted with the Ge surface in spite of the material already adsorbed thereon. For those surfaces covered with a monolayer of water it was found that oxygen displaced most of the water from the surface. The take-up of oxygen was retarded in the early stages of the reaction, compared with a clean germanium surface, but was greater at longer times. The logarithmic rate law was not obeyed. The results with alcohols were qualitatively very similar to water but the retarding effect at the beginning of oxygen adsorption was greater for the large molecules. Oxygen adsorbed to a considerable extent on surfaces covered with a monolayer of hydrogen and, as with the other materials, the initial take-up of oxygen was less than with a clean surface. The oxygen take-up after long times was approximately the same as that on a clean Ge surface. Only a small fraction, if any, of the hydrogen was desorbed during the adsorption of oxygen. This certainly suggests that the binding of the hydrogen atoms to the Ge surface is not of the simple covalent type that might have been expected.

8232 CHEMICAL TECHNIQUES FOR THE INVESTIGATION OF SURFACES by R. J. Kokes (Johns Hopkins U.); J. Phys. Chem. Solids, Vol. 14, pp. 51-55, July 1960

A microcatalytic technique in which studies are made with very small amounts of reactant and catalyst is discussed. Applications of this technique to studies of catalytic activity, both steady and non-steady state, are reviewed and some obvious extensions are noted. Tracer investigations aimed at the study of the nature of the surface itself are also discussed.

8233 SOME ASPECTS OF THE CHEMISTRY OF GERMANIUM AND SILICON SURFACES by M. Green (Zenith); J. Phys. Chem. Solids, Vol. 14, pp. 77-86, July 1960

Some recent aspects of the chemistry of Ge and Si surfaces are reviewed and discussed. The topics covered are clean surfaces, adsorption from the gaseous phase, and electrochemistry.

8234 DAMAGED LAYERS AND CRYSTALLINE PERFECTION IN THE {111} SURFACES OF III-V INTERMETALLIC COMPOUNDS by E. P. Warekois, M. C. Lavine, and H. C. Gatos (Lincoln Lab.); J. Appl. Phys., Vol. 31, pp. 1302-1303(L), July 1960

Experiments indicating that the same cold-working treatment (abrasion or sandblasting) introduces an appreciably greater depth of damage in the GaAs and InSb {111} surfaces terminating with group V atoms (B surfaces) than in the {111} surfaces terminating with group III atoms (A surfaces) are discussed. After the cold work introduced by abrasion was removed by chemical etching, it was found that the B surfaces are more perfect than the A surfaces. This is consistent with the bond model proposed for the A and B surfaces of the III-V compounds and the observation that single crystals of InSb grown in the B <111> direction possess a greater degree of perfection than those grown in the A <111> direction. The differences in depth of damage between the A and B surfaces are also believed to be related to the difference in the bonding characteristics of the A and B surface atoms.

Surface Treatments for Ge - See 8299

Dislocation Etch Patterns in Si - See 8180

Dislocation Etch Patterns in Ag - See 8181

Dislocation Etch Pits in Corundum - See 8183

Dislocation Etch Pits in CdS - See 8182

Flash Etching of Al_2O_3 Grain Boundaries - See 8189

Etching of Twin Structures in Ge, Si and III-V Compounds - See 8188

8235 OHMIC CONTACTS TO SEMICONDUCTING CERAMICS by D. R. Turner and H. A. Sauer (Bell Labs.); J. Electrochem. Soc., Vol. 107, pp. 250-251, Mar. 1960

A technique for fabrication of ohmic contacts to $BaTiO_3$ and compound semiconductors such as GaAs and Bi_2Te_3 is described. The area to be contacted is dipped in stannous and then palladium chloride solutions, to deposit a thin palladium layer that catalyzes the initial nickel deposition. The area is then dipped in electroless nickel for 3 min at 95°C. As deposited, the contact is non-ohmic and must be heat treated. Additionally a slow resistance increase is observed on aging. The most stable contacts are treated at 400°C for 5-10 min. Heat treatment removes the oxygen layer that is initially between the nickel and ceramic. For GaAs, the contact must be tinned with Pb-Sn solder.

ENVIRONMENTAL EFFECTS

Heat Treatment Effects on CdS Films - See 8384

Precipitation of Impurities in Si by Annealing - See 8202

Compensation of Ni Ferrite by Sintering - See 8269

Thermal Conductivity Conversion in GaAs - See 8273

Introduction of Traps in Si by γ-Irradiation - See 8237

Formation of Color Centers in NaCl by γ-Irradiation - See 817

Radiative Recombination in Electron Bombarded Ge - See 8373

SOLID STATE PHYSICS

CRYSTAL PHYSICS
(Including Energy Band Structure)

8236 THE COHESIVE ENERGY AND STABLE LATTICE OF

CESIUM CHLORIDE by J. F. Colwell (Cornel U.); Diss. Abstr., Vol. 21, pp. 1603-1604(A), Dec. 1960

The cohesive energy and stable lattice of the ionic crystal was discussed. Calculations of the cohesive CsCl energy for two different lattice structures (the simple cubic and the face centered cubic) by using the method of Löwdin were given. The sc lattice had an energy lower than the fcc lattice by about 1.4 per cent of the total cohesive energy. This was in agreement with the stability of the sc lattice at normal temperatures. The wave functions and energies were found numerically, starting with atomic orbitals found by Hartree. A comparison of KCl and CsCl showed that the repulsive energy was about the same in the two cases, but the coulomb correction was larger in the latter case. This indicated that the reason for the structure of CsCl is the size of Cs^+.

Energy Gap of CdI_2-Type Compounds - See 8169

Energy Gap of Bi_2Se_3 - See 8268

8237 GAMMA IRRADIATION OF SILICON. Part I. LEVELS IN n-TYPE MATERIAL CONTAINING OXYGEN by E. Sonder and L. C. Templeton (Oak Ridge Natl. Lab.); J. Appl. Phys., Vol. 31, pp. 1279-1286, July 1960

The measurement of the resistivity and Hall coefficient of n-type silicon containing oxygen as a function of temperature before and after a number of successive irradiations in a Co^{60} gamma-ray source is described. A net acceptor level 0.17 ev below the conduction band was observed to result from the irradiation. Its rate of introduction was 7×10^{-4} traps/cm^3 per photon/cm^2 in 50-ohm-cm material and was about twice that in more heavily doped material (~2 ohm-cm). Acceptor levels, lying deep within the forbidden gap, were also observed. Their total introduction rate was smaller than that of the 0.17-ev level by a factor of 50. A lowering of the mobility below ~100°K was also a result of the irradiations. In heavily irradiated samples this lowering of the mobility was much greater than could be explained on the basis of point-charge scattering.

Energy Levels of InSb-GaSb - See 8262

8238 SURFACE STATES OF ONE-DIMENSIONAL CRYSTALS. Part II. by A. E. Aerts (Lab. voor Krist. en Studie van Vaste Stoffen, Ghent); Physica, Vol. 26, pp. 1057-1062, Dec. 1960

Energy levels at the surface of semi-infinite ionic and valence crystals composed of two kinds of atoms are calculated. The potential of the surface atoms is assumed to be asymmetric. It is shown that the number and the position of the localized surface states are affected by the lattice constant, by the atomic potential strength of the two different kinds of atoms, and by the step in potential energy at the surface. The position of the levels is calculated by the scattering matrix method of Saxon and Hutner for various values of these parameters. Generally only one level is found in the first forbidden energy gap, sometimes two or none. Only crystals with clean surfaces are considered.

8239 THEORY OF TAMM SURFACE STATES IN APPROXIMATION HIGHER THAN TIGHT-BINDING APPROXIMATION by M. Tomasek and J. Koutecky (Czech. Acad. Sci.); Czech. J. Phys., Vol. 10B, No. 4, pp. 268-274, 1960

The influence of the non-zero value of exchange integrals between Wannier functions, localized in non-neighboring elementary cells (higher approximation than tight-binding), on the conditions of existence of Tamm surface states and the position of the energy level corresponding to the surface state is shown.

8240 THE CHARGE AND POTENTIAL DISTRIBUTIONS AT THE ZINC OXIDE ELECTRODE by J. F. Dewald (Bell Labs.); Bell Sys. Tech. J., Vol. 39, pp. 615-639, May 1960

Capacitance measurements made on single crystal zinc oxide electrodes in contact with aqueous electrolytes are reported. Over a wide range of bias and bulk donor density, the results are in almost quantitative accord with predictions of the simple Poisson-Boltzmann (Poisson-Fermi in the degenerate case) equation. This is shown to imply the complete absence of surface-state effects in this system. A very sharp discontinuity in the flat-band potential is observed at bulk electron densities in the range from 0.6×10^{18} to 2×10^{18}cm^{-3}. This and other effects, arising under varying surface treatments, are discussed in some detail. The use of the semiconductor/electrolyte interface in studying the properties of low-lying donors is illustrated for the case of boron, which is shown to lie about 0.3 ev below the conduction band.

Formation Energies of Ions in CsBr and CsI - See 8245

8241 VIBRATIONAL MODES NEAR IMPURITIES by H. B. Rosenstock and C. C. Klick (U.S. Naval Res. Lab.); Phys. Rev., Vol. 119, pp. 1198-1203, Aug. 15, 1960

The nature of the vibrations of the lattice near an impurity in a solid is examined. In particular, two problems are considered: first, the direct absorption of light by the "localized" mode introduced by the presence of the impurity, and the relation of its frequency to that of the "reststrahlen" absorption; second, the relative importance of the "localized" modes and of the "lattice" modes in producing the observed broadening of the spectra due to electronic transitions of the impurity center. It is found that the large number of lattice modes together produce a mean displacement of the same order of magnitude as do the very few local ones. The implications for the "configuration coordinate" model for phosphors are examined; both theory and experiment suggest that if only one mode, or group of modes, are effective in producing broadening, their frequency is substantially lower than that of the localized modes which are optically active.

Lattice Wave Scattering by Point Defects - See 8403

8242 ELECTRON DENSITY DISTRIBUTION IN GERMANIUM by N. N. Sirota and A. U. Sheleg (S.S.P., Acad. Sci. Belorussian SSR); Proc. Acad. Sci. USSR, Phys. Chem., Vol. 135, pp. 1165-1167, Nov.-Dec. 1960

Measurement of the atomic scattering factor and electron density distribution of germanium is discussed. The x-ray measurements were made on n-type germanium powder at room temperature with CuK_α-radiation. The electron density distribution for the [111] and [113] directions in the (110) plane of the germanium elementary cell is shown. The germanium ion radius found from the $1.5e/A^3$ density contour is equal to 0.5 A with 6 electrons outside this volume. The ion radius determined from the $0.05e/A^3$ contour has a value 2 A with only a very

small number of electrons outside this volume. At the point 3/4 3/4 3/4 in the [111] direction the electron density is small and does not exceed 0.03 e/A^3. Between the points 0, 0, 0 and 1/4 1/4 1/4 the lowest electron density is 0.6e/A^3.

ELECTRICAL PROPERTIES

DIELECTRIC PROPERTIES

8243 EFFECT OF THE LATTICE ON DIELECTRIC PROPERTIES OF AN ELECTRON GAS by D. S. Falk (Lincoln Lab.); Phys. Rev., Vol. 118, pp. 105-109, Apr. 1, 1960

Dielectric behavior of a system of N electrons in the presence of a rigid periodic background of positive charge is considered. Following Martin and Schwinger, an inverse dielectric operator, K′, is introduced. An approximate equation which takes into account the long-range nature of the coulomb field is derived for K′. A representation is used where K′ is a matrix with rows and columns labeled by vectors of the reciprocal lattice. Poles and zeros in the dielectric operator are found to be manifestations of Bragg's law. Assuming these to be the major effect of the lattice, the equation for K′ is solved. The result is examined in the weak-binding limit and seen here, except at the Bragg reflections, to agree with that of Nozières and Pines. Finally the ground-state energy of the system is exhibited.

Dielectric Constant Tensor of Semiconductors - See 8395

8244 THE INTENSITY OF DIELECTRIC ABSORPTION IN ALKALI HALIDES AS A FUNCTION OF THE CONCENTRATION OF DIVALENT CATION IMPURITIES by J. S. Cook and J. S. Dryden (CSIRO); Austrl. J. Phys., Vol. 13, pp. 260-269, July 1960

Measurements of the dielectric absorption of sodium chloride containing calcium, and of potassium chloride containing strontium, as a function of concentration of the divalent impurity are presented. From the intensity of the absorption it is possible to estimate accurately the number of divalent impurity cations associated with positive ion vacancies so as to form dipoles. In both systems at room temperature equilibrium it is found that a large proportion of the divalent impurity ions are associated with the positive ion vacancies in a higher complex than a dipole. By quenching from different temperatures, an investigation of the equilibria between divalent impurities, vacancies, dipoles, and higher complexes is made. The kinetics of the aggregation of the dipoles are studied for the NaCl(Ca^{++}) system.

8245 DIFFUSION AND IONIC CONDUCTIVITY IN CESIUM BROMIDE AND CESIUM IODIDE by D. W. Lynch (U. Illinois); Phys. Rev., Vol. 118, pp. 468-473, Apr. 15, 1960

Measurement of the diffusion coefficients of the constituent ions in CsBr and CsI single crystals between 300° and 550°C by means of radioactive tracers is reported. The results were compared with electrical conductivity measurements. Approximate satisfaction of the Nernst-Einstein equation indicates that the conductivity is nearly completely ionic and the diffusion measurements show that the halogen ion defects are the more mobile. Attempts to identify the mechanisms for ionic transport by means of the Bardeen-Herring correlation factor are discussed. Schottky defects seem likely but the assumption of an additional mechanism for catonic transport is required. If Schottky defects are predominant their formation enthalpies are 2.0 ev and 1.9 ev in CsBr and CsI respectively, and the activation enthalpies for halogen vacancy motion are 0.27 ev and 0.3 ev respectively, while the cesium vacancy activation enthalpy is about 0.58 ev for both salts.

8246 PYROELECTRICITY, INTERNAL DOMAINS, AND INTERFACE CHARGES IN TRIGLYCINE SULFATE by A. G. Chynoweth (Bell Labs.); Phys. Rev., Vol. 117, pp. 1235-1243, Mar. 1, 1960

The determination of the spontaneous polarization of triglycine sulfate between the Curie point and −140°C by the dynamic pyroelectric technique is discussed. No evidence of any phase transitions over this temperature range was found (other than the Curie point). The polarization could still be reversed by an applied field, though slowly, at the lowest temperatures attained. In the paraelectric region above the Curie point, the pyroelectric behavior shows some deviations at low applied fields from the predictions of Devonshire's theory. The cause of these deviations is not known but they may be due to non-uniform conditions, either mechanical or electrical, in the crystal. With no field applied to the crystal, pyroelectric signals can be generated temporarily above the Curie point. These are ascribed mainly to polarizations induced by the compensation charges while they last, which accumulate around residual domains that cannot be removed by the poling field at room temperature. These residual domains have been delineated using powder pattern and etching techniques and are revealed as long thin domains, pointed at both ends and lying along the ferroelectric direction, either in the interior of the crystal or intercepting the surfaces. The cause of these persistent domains is not known. It is found that on cooling a crystal through the Curie point, there is a strong tendency for it to repolarize with the same polarity it had previously. This phenomenon is ascribed to the presence of ferroelectrically inactive surface layers giving rise to interface charges.

8247 SOME PROPERTIES OF X-RAY DAMAGED ROCHELLE SALT by K. Okada (Aichi Gakugei U.); J. Phys. Soc. Japan, Vol. 15, pp. 363-364(L), Feb. 1960

Observations made on Rochelle salt crystals following x-radiation at 10°C are discussed. Double asymmetric hysteresis loops were observed in crystals partially polarized before irradiation. Domain walls in crystals irradiated for 1 hour did not move on the application of a dc field below 200v/cm. Shifts in the Curie points observed in the irradiated samples on the application of a moderate dc field were opposite to those in unirradiated samples.

8248 JUMP PHENOMENON IN RESONANCE CURVE OF FERROELECTRIC CERAMICS by K. Negishi (Kobayasi Inst. Phys. Res.); J. Phys. Soc. Japan, Vol. 15, p. 534(L), Mar. 1960

The dependence of the mechanical Q of ferroelectric ceramics on the driving voltage is discussed. Measurements were made on a circular disk of lead zirconate-titanate ceramic 26.2 mm in diameter and 2.1 mm thick resonating in a radial mode at 93.18 kc. The amplitude of the resonance decreased to one-third of its original value and the frequency of the peak shifted to a lower frequency by about 350 cps when the applied voltage of 0.1 v was increased to 10v. A decrease in amplitude and a shift in the frequency of the peak to lower values

was also observed with an applied voltage of 1 v. A hysteresis o the resonance curve was observed with an applied voltage f 10v. Similar behavior was observed in all the lead zircon- es-titanate and barium titanate ceramics investigated but the ysteresis was observed only in samples with high mechanical Q.

8249 180° DOMAIN WALL MOTIONS IN $BaTiO_3$ CRYSTAL by K. Husimi (Elect. Commun. Lab.); J. Phys. Soc. Japan, Vol. 15, p. 731 (L), Apr. 1960

180° domain wall motions observed in $BaTiO_3$ under high and w fields are discussed. Domain growth was observed after peated application of a low field. The domain wall velocity as large along the [100] direction. Domain shrinks were ob- rved after a domain growth by the application of a low neg- ive field for about one minute followed by the application a field with the same strength but opposite polarity for about ve seconds. The domain shrinkage begins at the corners of e square. The patterns first have an octangular shape and en become square, with their diagonals along the [110] axes. uare domains with sharp 90° edges and with diagonals along e [110] direction were obtained by applying a negative kv/cm, 0.3μsec pulse four times to a crystal which had pre- iously undergone low field domain motion. Domain shrinkage high fields was also observed. The experiments indicate at with the application of a field up to about 5kv/cm, polar- ization reversal takes place by sidewise domain wall motion, s in the case of low field switching, but many additional anti- arallel domains appear. Photographs of domain growths and rinks are presented.

8250 MOTION OF 180° DOMAIN WALLS IN METAL ELEC- RODED BARIUM TITANATE CRYSTALS AS A FUNCTION OF LECTRIC FIELD AND SAMPLE THICKNESS by R. C. Miller nd A. Savage (Bell Labs.); J. Appl. Phys., Vol. 31, pp. 52-669, Apr. 1960

Quantitative measurements of the velocity of the sidewise mo- on of 180° domain-walls in $BaTiO_3$ crystals, most of which ere electroded with 200-A thick films of Au are discussed. he wall velocity has been measured as a function of several ariables including the applied electric field, the crystal hickness and the impurity content added to the crystal growth elts. The wall velocity as a function of the field E is de- ribed by $v_\infty \exp(-\delta/E)$ where δ and v_∞ are constants over veral decades of velocity. The quantities δ and v_∞ are the tivation field and extrapolated wall velocity for $E = \infty$, re- pectively. This field dependence of the wall velocity is the me as that reported previously for liquid electroded speci- ens. The thickness dependence of the wall velocity, which through δ, is very pronounced and similar to that observed in easurements of other variables under different experimental nditions. The present data are explained in terms of a sur- ce layer estimated to be of the order of 100-A thick. It is ggested that high fields within the surface layer may give rise electron field emission and the electroluminescence which is served during polarization reversal. Effects on the wall mo- on which persist for times of the order of minutes are ascribed dielectric relaxation phenomena. The observed dependence the wall motion on the impurity content of the crystal, and veral other parameters, may result from changes in the char- teristics of the surface layer.

8251 DETAILED STUDY OF SWITCHING CURRENT IN BARIUM TANATE by M. E. Drougard (IBM); J. Appl. Phys., Vol. 31, pp. 352-355, Feb. 1960

The dependence of the instantaneous value of the switching current in single crystals of $BaTiO_3$ on the applied field, the state of net polarization of the crystal, and possibly other factors is explained. The switching current density can be expressed as the product of a function of the polarization, $\phi(p)$, and a function of the electric field, $\exp(-\alpha/E)$. The form of the function $\phi(p)$ indicates a predominance of sideways expansion of 180° domains, with an exponentially increasing domain wall velocity. This last result is shown to be in agreement with a picture of domain wall motion by nucleation of new domain wall layers. This interpretation, together with some details of the switching current pattern, suggests that a crystal, although apparently single-domain, may always retain some small domains of opposite polarization.

8252 FERROELECTRIC BEHAVIOR IN BARIUM ZIRCONIUM METANIOBATE by G. Goodman (GE); J. Am. Ceram. Soc., Vol. 43, pp. 105-113, Feb. 1960

The observation of an unusual type of ferroelectric behavior in barium zirconium metaniobate, $BaNb_{1.5}Zr_{0.25}O_{5.25}$ is reported. The orthorhombic, pseudotetragonal single crystal displays dielectric properties in the a-b plane. No evidence of a first- or second-order ferroelectric-paraelectric transition has been observed up to 1400°C. The crystal melts incongruently at about 1525°C. A maximum in the dielectric constant occurs at 80°C, when measured at 10^3 cps but is not accompanied by any effect in the spontaneous polarization. The temperature of this k' maximum has the frequency dependence of a dielectric relaxation process with an average activation energy of 0.2 ev. These properties are consistent with the idea of a higher than second-order ferroelectric-paraelectric transition in this material. The dielectric behavior is explicable in terms of 180° "dipole aggregates" having a wide range of activation energies of reversal. There are suggestions in the technical literature of similar behavior in other materials.

8253 FERROELECTRICITY IN TETRAMETHYLAMMONIUM-TRICHLORO-MERCURATE by E. Fatuzzo and R. Nitsche (RCA); Phys. Rev., Vol. 117, p. 936, Feb. 15, 1960

Tetramethylammonium-trichloro-mercurate, $[N(CH_3)_4] \cdot HgCl_3$, which is ferroelectric between −80° and +200°C is discussed. Above 200° it decomposes without showing a Curie point. At room temperature the spontaneous polarization is about 1.2 $\mu coul/cm^2$, the coercive field 3kv/cm and the dielectric constant 60.

8254 ELECTRICAL PROPERTIES OF LEAD-BARIUM NIOBATES AND ASSOCIATED MATERIALS by P. Baxter and N. J. Hellicar (GE Ltd.); J. Am. Ceram. Soc., Vol. 43, pp. 578-583, Nov. 1960

The electrical properties of materials in the system lead-barium niobate are described. Particularly useful materials are obtained when between 25 and 50 mole per cent of lead niobate is replaced by barium niobate. Materials with a 40 to 45 mole per cent replacement have permittivities of more than 1500 and radial electromechanical coupling coefficients of more than 0.35, but the Curie temperature is then only about 250°C, the minimum value obtained in the system. Higher Curie temperatures are accompanied by somewhat lower values of permittivity and coupling coefficient. The effects of several other additives on the properties of lead niobate are discussed and it is shown that barium-strontium niobates are only weakly ferroelectric at room temperature.

Dielectric Properties of Ba-Sr and Ba-Pb Titanates - See 8225

8255 PIEZORESISTIVITY IN SEMICONDUCTIVE BARIUM TITANATES by O. Saburi (Murata Mfg.); J. Phys. Soc. Japan, Vol. 15, pp. 733-734(L), Apr. 1960

The temperature dependence of the longitudinal and transverse piezoresistivity of several different (Ba·Sr)TiO_3 compositions doped with 0.1 mole per cent Ce is discussed. The piezoresistivity in both cases was found to be small at a temperature well below the Curie point and to have a negative peak, depending on the Sr content, in the neighborhood of the Curie point. Above the Curie point the piezoresistivity decreases rapidly, changes sign, and tends to a positive value asymptotically. The peak at the Curie point becomes higher with decreasing Sr content and reaches $-0.135\%/K\,gm/cm^2$ ($1.38\times10^{-9}\,cm^2/dyne$) in $BaTiO_3$. For each composition the temperature-piezoresistivity curve is very similar to the temperature-temperature coefficient of resistivity curve. It is suggested that the differences between the present results and those of Sauer et al. are due to the different methods used in each case to apply the mechanical pressure.

8256 PIEZORESISTIVE EFFECT IN p-TYPE PbTe by L. E. Hollander and T. J. Diesel (Lockheed); J. Appl. Phys., Vol. 31, pp. 692-693, Apr. 1960

A large positive piezoresistive effect in p-type PbTe is reported. The following room temperature coefficients were determined: $\pi_{Hydrostatic} = +150 \pm 50$; $\pi_{11} = 80 \pm 30$; $\pi_{\ell(111)} = +220 \pm 50$, all in $10^{-12}/d$. The shear coefficient π_{44} is estimated to be $+255 \times 10^{-12} cm^2/d$. The calculated value of π_{12} was $+35 \pm 40 \times 10^{-12} cm^2/d$. These measurements were performed on single-crystal, p-type PbTe with a mobility of approximately 700 $cm^2/v\,sec$ and a carrier concentration of about 10^{18} per cm^3. Consideration of the coefficients indicates the major axes of the energy ellipsoids are oriented in the (111) direction, which is in agreement with magnetoresistance measurements.

8257 MEASUREMENT OF PIEZOELECTRIC CONSTANTS OF A CdS CRYSTAL by T. Tanaka and S. Tanaka (U. Tokyo); J. Phys. Soc. Japan, Vol. 15, p. 726(L), Apr. 1960

Measurement of the piezoelectric constants of CdS by the relative method of Fukada is discussed. The sample was clamped together with an x-cut quartz plate and a Rochelle salt pick up. An alternating voltage was applied to the quartz and the amplitude of the signal due to the piezoelectric strain was observed on an oscilloscope. An alternating voltage was then applied to the CdS sample and the piezoelectric signal was observed on the oscilloscope. The strain of the CdS sample was determined from the ratio of the two amplitudes. From the measured strain and $S = d \cdot E$, where S is the strain vector, E is the electric field, and d is the piezoelectric strain coefficient tensor, $|d_{33}| = 7.7 \times 10^{-8}$ cgs and $|d_{31}| = 4.6 \times 10^{-8}$ cgs were determined.

8258 PIEZOELECTRIC PROPERTIES OF POLYCRYSTALLINE LEAD TITANATE ZIRCONATE COMPOSITIONS by D. A. Berlincourt, H. Jaffe, and C. Cmolik (Clevite); Proc. IRE, Vol. 48, pp. 220-229, Feb. 1960

The piezoelectric, elastic, and dielectric properties of lead titanite zirconate ceramic compositions near the rhombohedral-tetragonal phase boundary are discussed. These compositions have markedly higher electromechanical coupling factors, remanent ferroelectric charge, and coercive field, than ceramic barium titanate. Another interesting feature is a pronounced change in the free permittivity ϵ_{33}^T by the poling process; this change is in opposite directions for rhombohedral and tetragonal compositions. The dielectric and elastic anisotropy ratios of poled lead titanate zirconate are much greater than those of barium titanate, indicating a greater degree of alignment of domains during poling.

CARRIER PROPERTIES

8259 THE RECOMBINATION OF ELECTRON-HOLE PAIRS IN GERMANIUM [in French] by G. Mesnard and A. Dolce; J. Phys. Radium, Vol. 21, pp. 33S-34S, Feb. 1960

A study of the hole-electron recombination mechanisms in n-type Ge at high injection levels is discussed. It has been found that 4σ is proportional to L^n where $n = \frac{1}{2}$ for high injection levels and $\frac{1}{2} < n < 1$ for average injection levels, and L is the illumination on the sample. Photoconductivity has also been studied as a function of temperature.

8260 FURTHER CONSIDERATION OF BULK LIFETIME MEASUREMENT WITH A MICROWAVE ELECTRODELESS TECHNIQUE by H. Jacobs and F. A. Brand (USASRDL) and A. P. Ramsa (Monmouth Coll.); Proc. IRE, Vol. 48, pp. 229-233, Feb. 1960

A variation of the pulsed-light microwave electrodeless technique for measuring bulk lifetime in semiconductors is described. In the new technique bulk lifetime is determined by generating excess carriers with a dc light source and measuring changes in microwave power absorption as a function of position of the sample in a waveguide. No electrodes are required and the measurements are not greatly influenced by surface recombination.

Radiative Recombination in Electron Bombarded Ge - See 8373

Radiative Recombination in Diamond - See 8372

Effective Mass of Bi_2Te_3 - See 8397

8261 THEORY OF CURRENT-CARRIER TRANSPORT AND PHOTOCONDUCTIVITY IN SEMICONDUCTORS WITH TRAPPING by W. Van Roosbroeck (Bell Labs.); Bell Sys. Tech. J., Vol. 39, pp. 515-613, May 1960

Fundamental differential equations under the unrestricted approximation of electrical neutrality that admits trapping are derived. The transport equations derived hold without explicit reference to detailed trapping and recombination statistics. Modified ambipolar diffusivity, drift velocity and lifetime functions apply in the steady state. The same diffusion length is shown to hold for both carriers, and a general "diffusion-length lifetime" is defined. Mass-action statistics are considered for cases of (one or) two energy levels. Certain "effective" (rather than physically proper) electron and hole capture and release frequencies or times that apply to concentration increments are defined. Criteria for minority-carrier trapping, recombination and majority-carrier trapping, and for "shallow" and "deep" traps are given. Applications of the formulation include: the diffusion-length lifetime for the Shockley-Read electron and hole lifetimes; linear and nonlinear steady-state and transient photoconductivity; negative photoconductivity; the photoconductive decay observed by Hornbeck and Haynes i

CARRIER PROPERTIES Cont'd)

-type silicon; the photomagnetoelectric effect; and drift of n injected pulse. Photomagnetoelectric current is found to be ecreased by minority-carrier trapping, through an increase in ffusion length. A simple general criterion for the local di- ection of drift of a concentration disturbance is given. With apping, there may be a "reverse drift," whose direction is ormally that for the opposite conductivity type, and also cal regions of carrier depletion that may extend in practice ver appreciable distances.

262 CHARGE CARRIER PRODUCTION AND MOBILITY IN NTHRACENE CRYSTALS by R. G. Kepler (du Pont); Phys. ev., Vol. 119, pp. 1226-1229, Aug. 15, 1960

easurement of the drift mobilities of electrons and holes in nthracene crystals by a pulsed photoconductivity technique is iscussed. The room temperature mobilities vary from about 0.3 m^2/volt sec to about 3 cm^2/volt sec depending on the crystal rientation, and the mobilities increase as the temperature is vered. The wave length dependence of the number of charge rriers produced by a pulse of light, as well as other experi- ental data, indicates that the charge carriers are not produced the interior of anthracene crystals, but that they are released m a surface layer of the crystal either directly by photons or excitons which migrate to the surface.

262 ELECTRICAL PROPERTIES OF AN EQUIMOLECULAR nSb-GaSb ALLOY by V. I. Ivanov-Omskii and B. T. Kolo- iets (Physicotech. Inst.); Soviet Phys.-Solid State, Vol. 2, p. 363-368, Sept. 1960

arameters of the equimolecular InSb-GaSb alloy are evaluated nd the effect of alloy formation on carrier mobility is discussed. ubstitution of In by Ga had no practical effect on the hole mo- ility, but changed the electron mobility. Values for electron obility, hole mobility, and forbidden zone width (at room tem- erature), forbidden zone width at 0°K, the change in width a function of temperature, effective electron mass, and ef- ctive hole mass are recorded for the alloy and its starting inary components.

263 MOBILITY OF AN ELECTRON IN THE DONOR IMPURI- Y BAND OF A COMPENSATED SEMICONDUCTOR by A. A. laradudin (U. Maryland) and B. S. Gourary (Johns Hopkins .); Bull. Am. Phys. Soc., Ser. II, Vol. 5, p. 264(A), Apr. 5, 1960

he motion of an electron in an aperiodic one-dimensional po- ntial consisting of a random linear array of attractive elta-function potentials of equal strength was discussed. It as shown that the ground state of this electron is nondegener- e and that its energy is separated from that of the next high- energy state by a gap. These two results imply that mobility such a system is an activated process. The relevance of the esent model to impurity band conduction in nearly compen- ted semiconductors was discussed, and its relation to the re- nt work of N. F. Mott was described.

264 MAGNETO-ELECTRICAL FIELD-EFFECT MEASUREMENTS y A. E. Aerts (Lab. for Krist., Ghent); J. Electronics Control, ol. 9, pp. 217-228, Sept. 1960

xperimental observations of the influence of combined orthog- nal transverse electric and magnetic fields on the mobility of arriers in the space charge layer at the surface of a semicon- uctor are discussed. It was found that the Hall field can change the type of surface layer and that for weak fields the mobility of the carriers is proportional to the Hall field. By combining the magnetic and electric field effects in different ambients, some of the regions of Schrieffer's curve of the influence of the surface potential on the field effect mobility was investigated. Temperature effects were also studied and it was found that it was more difficult to invert the surface type at a high temperature.

8265 GROUP THEORY OF SCATTERING PROCESSES IN CRYSTALS by R. J. Elliott and R. Loudon (Clarendon Labs.); J. Phys. Chem. Solids, Vol. 15, pp. 146-151, Aug. 1960

A general method for determining selection rules for scattering of various types in crystals by using the properties of space groups is given. The method is particularly useful for those lattices which contain screw axes or glide planes and diamond is considered in detail. Examples of particular kinds of selection rule which are of interest in silicon and germanium are examined.

8266 EXCHANGE AND CORRELATION EFFECTS IN ELECTRON-PHONON SCATTERING IN NORMAL METALS by M. Bailyn (Northwestern U.); Phys. Rev., Vol. 117, pp. 974-984, Feb. 15, 1960

An extension of the theory of Bardeen for the electron shielding of the perturbation potential arising from lattice vibrations, covering exchange and correlation effects, is presented. The method is to set up a self-consistent set of one-electron equations, and calculate the effect of the perturbation in the charge densities. The exchange term is corrected to conform to the results of the Bohm-Pines theory, but the plasma wave function is assumed not to be disturbed by the lattice. With this approximate model, a solution to the problem can be obtained. For small-angle scattering, the results do not return to the original Bardeen values. The interaction potential matrix element depends on the initial electron wave vector k as well as on the difference between initial and final state wave vectors. Hence, to use the results an average over k is made over the Fermi surface. The general effect of the exchange hole is to increase the scattering.

CONDUCTIVITY

8267 A CRYOSTAT FOR ELECTRICAL MEASUREMENTS ON SEMICONDUCTORS by B. V. Rollin, J. R. Mills, and J. P. Russel (Clarendon Labs.); Cryogenics, Vol. 1, pp. 75-76, Dec. 1960

A cryostat for making routine measurements of the resistivity and Hall coefficient of semiconductor samples is described. The design enables the cryostat to be dismantled and assembled in a very short time, so that a different specimen may be measured every day. The difficulties of siphoning liquid helium have been avoided by using the transport Dewar as the experimental Dewar.

8268 DEVICE FOR MEASUREMENT OF THE ELECTRICAL PROPERTIES OF Bi_2Se_3 AT ELEVATED TEMPERATURES by M. J. Smith, E. S. Kirk, and C. W. Spencer (Cornell U.); J. Appl. Phys., Vol. 31, pp. 1504-1505(L), Aug. 1960

A device in which the electrical properties of Bi_2Se_3 crystals can be measured at temperatures exceeding 600°C without undergoing decomposition and some measurements made with the

device are described. The specimen is mounted on baked lava stone and inserted, together with associated electrical leads, in a vacuum tight glass container. A supplementary source of Se to the vapor phase is provided by a small perforated Vycor tube, attached to the specimen mount, containing either about 10 gm of finely divided Bi_2Se_3 or a mixture of Bi_2Se_3 and about 1 gm of Se. Plots of resistivity and Hall coefficient as a function of temperature, measured in single crystals in a direction parallel to the cleavage plane, are presented. The resistivity curve indicates an energy gap of 0.36 ev in the temperature range above 480°C and an energy of 0.09 ev in the temperature range 125° to 350°C. This latter value is probably due to donor levels below the conduction band. The data indicates electron concentrations of 4×10^{17} and 5×10^{17} cm^{-3} at −80° to 25°C, respectively. The corresponding mobility values are 2600 and 1600 $cm^2/v\text{-sec}$, respectively.

8269 ELECTRICAL RESISTIVITY OF NICKEL FERRITE by H. Lord (U. Coll., North Wales); Nature, Vol. 188, pp. 929-930 (L), Dec. 10, 1960

An experimental investigation of the influence of oxygen pressure during sintering on the electrical properties of nickel ferrite is discussed. It was found that some oxygen is lost during nickel ferrite formation even at 1100°C and this loss is only slightly inhibited by application of pressures up to 6 atmospheres. By introducing excess nickel into the ferrite lattice and by suitable adjustment of the sintering pressure an approximately compensated nickel ferrite in which the intrinsic activation process comes into effect can be prepared. The systematic shift of the peak in activation energy to the higher pressure region indicates that the loss of oxygen increases with sintering temperature.

8270 THE INFLUENCE OF PRESSURE ON SOME PROPERTIES OF SEMICONDUCTORS [in French] by J. Robin (Faculté des Sciences de Dakov); J. Phys. Radium, Vol. 21, pp. 130-140, Feb. 1960

Work dealing with the pressure dependence of some properties (e.g., electrical conductivity, resistivity of the p-n junction, and the absorption edge of the fundamental band) of certain semiconductors is summarized. The influence of pressure is indicated by the variation of the width of the energy gap sometimes accompanied by the change of electron and hole mobilities. [59 references]

8271 PRESSURE DEPENDENCE OF RESISTIVITY OF INDIUM ANTIMONIDE TO 70,000 ATMOSPHERES by H. A. Gebbie, P. L. Smith, I. G. Austin, and J. H. King (Natl. Phys. Lab.); Nature, Vol. 188, pp. 1095-1096 (L), Dec. 24, 1960

Measurement of the pressure dependence of resistivity of InSb to 70,000 atmospheres is discussed. Typical data taken at 293° and 184°K are presented. At 293°K the resistivity dropped sharply at a pressure of 30,000 atmospheres. This drop is attributed to melting, with a transition from semiconduction in the crystal to metallic conduction in the liquid phase. The melting point was found to decrease linearly with pressure to about 30,000 atmospheres. The melting point exhibits a significantly different behavior at higher pressures. A latent heat of fusion of 27 cal/gm was obtained by inserting the slope of the melting curve at zero pressure in the Clausius-Clapeyron equation. The disagreement between this value and the experimentally determined value of 47.2 cal/gm is attributed to the presence of complex phases in the liquid near the melting point.

8272 ON THE ELECTRICAL RESISTIVITY OF METALLIC ALLOYS AS A FUNCTION OF ORDER [in French] by M. T. Beal (Faculté des Sciences); J. Phys. Chem. Solids, Vol. 15, pp. 72-81, Aug. 1960

A theoretical study on how the ordering of alloys and its influence on resistivity vary with temperature is presented. A molecular-field approximation has been used, with interactions between nearest neighbors only. A recurrence formula gives the ordering parameters of shells of neighbors at increasing distances from given atoms. The resistivity is then computed, taking into account nearest neighbors only, and with a model of free electrons scattered in the Born approximation. This study is quite general above the critical temperature T_c; only the simple case of β-brass has been studied below T_c. The short range order is found to have very little effect, except in the immediate neighborhood of T_c. It contributes to the resistivity a term with a finite slope just below T_c, and with a non-vanishing slope just above T_c. These conclusions are in fairly reasonable agreement with observations made on Cu_3Au, $Cu\text{-}Zn_\alpha$, $Cu\text{-}Zn_\beta$ and Au_3Cu.

Conductivity Changes in Au, Sn and In Effected by Electrostatic Charging - See 8282

8273 THERMAL CONVERSION IN n-TYPE GaAs by J. J. Wysock (RCA); J. Appl. Phys., Vol. 31, p. 1686 (L), Sept. 1960

An experimental investigation of the thermal conversion observed when n-type GaAs with carrier concentrations of $5 \times 10^{16}/cm^3$ or less is heated at approximately 800°C for short times is discussed. Evidence strongly indicates that copper is the impurity responsible for conversion. It was found that impurities such as An, Cd, Au, Ni, or S do not cause conversion. Attempts were made to reconvert both Cu-diffused and converted wafers by heating with molten In or KCN. Reconversion took place only in those regions where In at 850°-950°C dissolved the GaAs and in only one out of 5 Cu-diffused wafers and in none of the converted wafers upon heating in molten KCN. The difficulty in leaching Cu from GaAs might be due to a strong Cu-As bond. The effect of Cu contamination from the acids used to etch the GaAs was investigated. In 6 runs using wafers etched in CP grade acids all the wafers converted and in 8 runs using wafers etched with triple-distilled acids in which no copper was detected by spectroscopic analysis conversion took place in only 2 runs.

8274 ELECTRICAL RESISTIVITY OF EUROPIUM AND YTTERBIUM by M. A. Curry, S. Legvold, and F. H. Spedding (Iowa State U.); Phys. Rev., Vol. 117, pp. 953-954, Feb. 15, 196

Electrical resistivity measurements on europium and ytterbium metals from 1.3° to 300°K are reported. Europium exhibits a sharp peak in its resistivity at 90°K which must correspond to its magnetic ordering temperature. The shape of the peak indicates antiferromagnetic ordering below 90°K. Ytterbium has no sharp anomalies in its resistivity.

8275 ELECTRICAL CONDUCTIVITY OF α-Fe_2O_3 by T. Nakau (Kyoto U.); J. Phys. Soc. Japan, Vol. 15, p. 727 (L), Apr. 1960

Electrical conductivity measurements performed over the temperature range 200°-300°K on low conductivity natural single crystals of α-Fe_2O_3 containing Ca, Mg, and Sn impurities are discussed. The measurements were carried out in both the [001] and [10$\bar{1}$0] crystallographic directions. The slopes of the

logarithm of conductivity vs reciprocal temperature were quite different for the two directions in a crystal containing 3.3 atomic per cent Mg and 1.0 atomic per cent Sn and were almost equal in a sample containing 5.4 atomic per cent Mg and 2.4 atomic per cent Ca. In both cases the slope of the curve was the same above and below the transition temperature. In the [10$\bar{1}$0] direction in each sample the curve steps up at the transition temperature with increasing temperature and steps down at the transition temperature in the [0001] direction. It is suggested that Morin did not observe the step at the transition temperature since he used polycrystalline material.

8276 ON THE MECHANISM OF THE ELECTRICAL CONDUCTION IN CdSe by H. Tubota, N. Suzuki, and K. Hirakawa (Kyushu U.); J. Phys. Soc. Japan, Vol. 15, p. 1701(L), Sept. 1960

Room temperature resistivities measured in n-type CdSe single crystals following the diffusion of the group I, II, III, and VI elements into the semiconductor are discussed. The results indicate that electrical conduction in CdSe is caused by Se vacancies. The diffusion of Se causes the resistivity to increase due to the decrease of Se vacancies. The opposite occurs on the diffusion of Cd. The group III and IV elements In and Pb locate at interstitial sites and cause the resistivity to decrease. The group I elements Cu and Ag which cause a slight increase in resistivity substitute for the Cd atoms. The decrease in resistivity caused by the diffusion of Sn cannot be explained on the basis of the size of the atomic radii of Sn, Se, and Cd.

8277 AN ELECTRICAL RESISTIVITY STUDY OF THE BETA ALLOYS OF THE AgAuCd SYSTEM by F. Rothwarf (Temple U.); Diss. Abstr., Vol. 21, pp. 1607-1608(A), Dec. 1960

Measurements of electrical resistivity as a function of temperature on four sets of alloys in the beta region of the AgAuCd ternary system are reported. The four sections of the phase diagram studied were the binary alloys of AgCd and AuCd and the two sets of ternary alloys AgAuCd whose Cd concentration = 47.5 and 50 per cent, respectively. Plots of the resistivity slopes vs AgCd concentration in low and high temperature phases presented fluctuating behavior. It is suspected that these fluctuations are related to the Ag and Au ion-core potentials which vary with composition and structure in these alloys. It was assumed that a ternary ordering of Ag and Au on Au lattice sites occurred, since AgCd and AuCd possessed ordered structures. The ordering process could be thought of as stabilizing the cubic lattice against shear transformations at the higher temperatures.

Avalanche Breakdown in Transistor Junctions - See 8439

8278 OBSERVATION OF STARK SPLITTING OF ENERGY BANDS BY MEANS OF TUNNELING TRANSITIONS by A. G. Chynoweth, G. H. Wannier, R. A. Logan, and D. E. Thomas (Bell Labs.); Phys. Rev. Lett., Vol. 5, pp. 57-58(L), July 15, 1960

Measurements of conductance vs forward bias at liquid helium temperature in narrow indium antimonide p-n junctions are discussed. The junctions were formed by alloying pellets of 0.1 per cent Cd – 99.9 per cent In – into n-type InSb crystals. The donor and acceptor concentrations on the n- and p-sides were $6.7 \times 10^{17}\,cm^{-3}$ and $10^{18}\,cm^{-3}$, respectively. Although the junctions were not narrow enough to exhibit Esaki effects, at all except the very highest forward biases (>200 mv) the dominant current generation mechanism was tunneling. All junctions exhibited structure in the conductance plots which can be explained by means of phonon or multiphonon emission processes. An additional fine structure was observed at biases between 100 and 130 mv. It is shown that this structure can be explained by means of the stark effect.

Tunneling Probability in Ge Diodes - See 8418

SUPERCONDUCTIVITY

8279 SURFACE IMPEDANCE OF A SUPERCONDUCTOR IN A MAGNETIC FIELD by G. Dresselhaus and M. S. Dresselhaus (Cornell U.); Phys. Rev., Vol. 118, pp. 77-91, Apr. 1, 1960

Explicit expressions for the static magnetic field variation of the surface impedance in a superconductor are derived. Detailed consideration is given to the two limiting cases of the classical skin effect and of the extreme anomalous skin effect, with the static field either parallel or perpendicular to the r-f current. The transport calculation is carried out for a two-fluid model with the supercurrent obeying the London equation and the normal current following a nonlocal relation. It is suggested that a comparison between theory and the experimental data yields information on the energy band structure of normal electrons in the superconducting state.

X-Ray Spectra of Superconducting CuS - See 8371

8280 ALTERNATIVE SUPERCONDUCTING GROUND STATES by J. C. Fisher (GE Res. Labs.); Austl. J. Phys., Vol. 13, pp. 446-450, July 1960

A comparison between (a) the trial ground state composed of a linear combination of normal state configurations in which individual electron states of opposite momentum and equal spin projection ($k\uparrow, -k\uparrow$) and ($k\downarrow, -k\downarrow$), abbreviated ($k\sigma, -k\sigma$), are both either occupied or unoccupied, and (b) the trial ground state with ($k\uparrow, -k\downarrow$) pairing proposed by Bardeen, Cooper, and Schrieffer is developed. The two trial states lead to identical thermodynamics as long as an average matrix element $-V = -\langle V'_{kk'} \rangle_{av}$ is treated as a disposable parameter. They lead to similar coherence effects for ultrasonic attenuation and nuclear spin relaxation. They differ in that spin paramagnetism is predicted for ($k\sigma, -k\sigma$) pairing. Detailed knowledge of the electron-phonon interaction in superconductors seems at present inadequate to rule out either possibility for all superconductors.

8281 SPEED OF THE SUPERCONDUCTING-NORMAL TRANSITION IN TIN FILMS by D. J. Oliver, M. J. Rayner, and E. N. Rhoderick (Services Electronic Res. Lab.); Nature, Vol. 187, p. 492(L), Aug. 6, 1960

The rate at which resistance is restored in a superconducting tin film by the application of a magnetic field above the critical value is discussed. The experiments were performed at ~0.1°K below the transition temperature on dumbbell-shaped evaporated films, the central regions of which were approximately 1 cm long, 100-400μ wide, and 100 A thick. No delay was observed between the time at which the pulsed magnetic field became constant and the restoration of resistance. No evidence of progressive growth of resistance or of any resistance remaining after the end of the magnetic pulse was observed. It was found that the superconducting normal and

normal-superconducting transitions take place within 15 μsec and that the relaxation time for the destruction of superconductivity is less than $\sim 10^{-8}$ sec.

8282 CHANGES IN SUPERCONDUCTING CRITICAL TEMPERATURE PRODUCED BY ELECTROSTATIC CHARGING by R. E. Glover, III and M. D. Sherrill (U. North Carolina); Phys. Rev. Lett., Vol. 5, pp. 248-250(L), Sept. 15, 1960

An investigation of the effect of charging on the normal-state conductivity of Au films and on both the superconducting transition temperature and the normal-state conductivity of Sn and In films is discussed. The Au films were evaporated on mica substrates at room temperature and the Sn and In films were evaporated on mica substrates held at liquid N temperature. Au films were evaporated on the opposite sides of the substrates to form the second condenser plate. In Au at room temperature and 77°K it was found that negative charging increased the conductivity while positive charging decreased it. The relative change was of the same order of magnitude as the ratio of added or subtracted electrons to the number of atoms in the film. In Sn and In films measurements made as the films were cooled to liquid He temperature indicated that negative charging decreased the normal-state conductivity and positive charging increased it. The transition temperature decreased in In films and increased in Sn films with negative charging. The influence of piezoelectric effects in the substrate on the transition temperature shifts was investigated.

8283 THE CRITICAL FIELD OF SUPERCONDUCTING ALUMINUM UNDER PRESSURE by D. Gross and J. L. Olsen (Eidgenossische Tech. Hochsch., Zurich); Cryogenics, Vol. 1, pp. 91-95, Dec. 1960

Measurements of the effect of pressure p on the critical field H_c of aluminum between 0.3°K and the transition temperature T_c are discussed. Pressures up to about 1700 atmospheres have been achieved by the ice bomb technique. It was found that $\partial H_c/\partial_p = -[3.1 \pm 0.2 + (1.7 \pm 0.2)(T/T_c)^2] \times 10^{-9}$ gauss $dyn^{-1} cm^2$. This yields $d \ln \gamma / d \ln v = 8 \pm 4$, where γT is the electronic specific heat per mole. Results on zinc are also given. In this case $\partial H_c/\partial_p$ appears to be anisotropic.

8284 CRITICAL FIELD CURVE OF SUPERCONDUCTING MERCURY by D. K. Finnemore, D. E. Mapother, and R. W. Shaw (U. Illinois); Phys. Rev., Vol. 118, pp. 127-129, Apr. 1, 1960

Precise measurement of the critical field curve of mercury in a range of reduced temperature, $t = T/T_c$, from 1 to 0.27 is reported. The observed H_c values show an appreciable deviation from a parabolic temperature dependence, lying above the parabola which passes through the experimental values of H_0 and T_c. The general behavior is similar to that previously observed in the case of lead. Values of the temperature coefficient of the normal electronic specific heat, γ, are derived, but are somewhat uncertain since the H_c data indicate an appreciable entropy contribution from the superconducting electrons at the lowest temperature of measurement. The qualitative behavior of $H_c(T)$ for lead and mercury is in accord with recent infrared measurements which give direct indication that the energy gap value for these elements is anomalously large.

8285 DESTRUCTION OF SUPERCONDUCTIVITY IN THIN FILMS BY FIELD AND CURRENT by N. I. Ginzburg and A. I. Shal'nikov (Moscow State U.); Soviet Phys.-JETP, Vol. 10, pp. 285-289, Feb. 1960

Measurements made on the critical magnetic fields and current required to destroy superconductivity in thin cylindrical tin films are discussed. Qualitative agreement with the Ginzburg-Landau theory was obtained. The structure of the films studied is discussed.

8286 CRITICAL CURRENTS IN SUPERCONDUCTING TIN FILMS by N. E. Alekseevskii and M. N. Mikheeva (Inst. Phy Problems); Soviet Phys.-JETP, Vol. 2, pp. 211-213(L), July 1960

Critical currents measured with very short current pulses in film of superconducting tin are discussed. The films used were in the form of a flat disk with a central current lead and a radial distribution of current flow. The measurements showed that the critical current depends on the time τ, increasing as τ decreases. It was found that near the critical temperature T_c the form of the magnetic field of the critical current H_{ci} vs ΔT curve, where $\Delta T = T_c - T$, depends on the temperature of the substrate at the time of deposition of the film. Films prepared by evaporating the metal onto a substrate cooled to liquid nitrogen temperature and then warmed up to room temperature show a temperature dependence of H_{ci} which can be roughly represented by the relations $H_{ci} = a\Delta T$. Films obtained by the evaporation on a substrate at room temperature show a temperature dependence of critical current field near T_c close to that predicted by the Ginzburg-Landau theory.

8287 STUDY OF THE INTERMEDIATE STATE IN SUPERCONDUCTORS USING CERIUM PHOSPHATE GLASS by W. DeSorbo (GE); Phys. Rev. Lett., Vol. 4, pp. 406-408(L), Apr. 15, 19

The use of magneto-optic Faraday rotation in cerium phosphate glass to study the intermediate state in superconductors is discussed. The technique utilizes the diamagnetism of the superconducting state to investigate the topography of the superconducting and normal domains at the surface of the specimen. It is assumed that the local magnetic field distribution and variations at the surface indicate the amount of normal and superconducting material in the specimen. The technique is particularly useful in the study of the dynamics and time-dependent phenomena of the intermediate state as well as in the study of both the magnitude and direction of frozen-in moments, supercooling phenomena, and the critical field. Experiments performed by this technique on cold-worked and cold-rolled tantalum and on single crystal zone refined tin and on polycrystalline tin are discussed.

8288 ON THE SUPERCONDUCTIVITY OF THE COMPOUND BiPt by N. N. Zhuravlev, A. A. Stepanova, and N. I. Zyuzin (Moscow State U.); Soviet Phys.-JETP, Vol. 10, pp. 627-628(L), Mar. 1960

The transition temperature of the compound BiPt is discussed. It is suggested that the different values for T_c reported by Matthias and Alekseevskii are due to defect structures introduced during the preparation of the compound. BiPt was found to have the NiAs structure up to high temperatures, and a coefficient of thermal expansion $\alpha_{||} = 4.0 \pm 1.0 \times 10^{-6} deg^{-1}$ in the direction of the horizontal axis and $\alpha_{\perp} = 19.0 \pm 2.0 \times 10^{-6} deg^{-1}$ perpendicular to the axis. In stoichiometric BiPt and alloys containing a higher or lower Bi content which were annealed and rapidly cooled from various temperatures not exceeding the liquidus temperature for the given composition, the main phase always had the NiAs structure. When these alloys were rapidl

oled from temperatures 50°, 100°, and 200°C above the quidus point, however, defect structures were formed. A eduction in unit cell dimensions of the NiAs phase was und in these alloys. The decrease in unit cell dimension re- lts in a reduction in the minimum bismuth-bismuth inter- tomic distance which produces a change in T_c.

89 THE SUPERCONDUCTIVITY OF ELECTROLYTICALLY POSITED COPPER-BISMUTH ALLOYS by N. E. Alekseev- ii, V. V. Bondar, and Yu. M. Polukarov (Inst. Phys. oblems); Soviet Phys.-JETP, Vol. 11, pp. 213-214(L), ly 1960

perconductivity observed in electrolytically-deposited cop- r-bismuth alloys is discussed. Electrolytic deposits contain- g 25 - 90 per cent (by weight) Bi were obtained from a solu- ion consisting of 1N $Cu(ClO_4)$, 4N $Bi(ClO_4)_3$, 4N $HClO_4$ ith current densities from 80 to 250 ma/cm^2. Measurements ere made on alloys deposited on both sides of Cu plates 30 3 x 0.5 mm. When the resistivity of the samples was meas- red at low temperatures, a sudden drop was observed close to °K. When the specimens were annealed at 120°C, the de- rease in resistance was not observed on remeasuring down to .5°K. When the anneal was performed at 80°C the sharp ecrease in resistance did not disappear. It is suggested that he change in resistance occurs when a nonequilibrium phase n the alloy undergoes a transition to the superconducting tate at about 2.2°K. This phase decomposes during the an- eal at 120°C. The anneal at 80°C causes a second nonequi- ibrium phase to decompose. This second phase, however, is ot responsible for the appearance of the superconductivity.

290 THE EXISTENCE OF SUPERCONDUCTING ANTIFERRO- MAGNETICS by B. V. Karpenko (Urals State U.); Phys. Metals Metallog., Vol. 10, No. 2, pp. 140-142(L), 1960

he existence of superconductivity in antiferromagnetic metals s analyzed. It is found that increased scattering of spin waves ill reduce the energy gap (i.e., will prevent superconduc- ivity) and that if the s-d exchange is fairly intense, there ill not be any superconducting state.

MAGNETOELECTRIC (GALVANOMAGNETIC) PROPERTIES

291 MAGNETORESISTANCE AND HALL COEFFICIENT OF GRAPHITE SINGLE CRYSTAL AT 4.2°K BETWEEN ZERO ND 200 KGAUSS by W. J. Spry (Natl. Carbon); Bull. Am. hys. Soc., Ser. II, Vol. 5, p. 373(A), June 15, 1960

Measurements of the magnetoresistance and the Hall coefficient n the same single crystal of graphite to fields as large as 200 gauss were discussed. The experiment was carried out at .2°K in a pulsed magnetic field. The magnetoresistance in- reases monotonically with the magnetic field, while the Hall oefficient approaches a limiting value. The results were dis- ussed in terms of an analysis proposed by J. W. McClure.

292 OSCILLATORY MAGNETORESISTANCE IN n-TYPE bTe by Y. Kanai, R. Nii, and N. Watanabe (Elect. Com- mun. Lab., Tokyo); J. Phys. Soc. Japan, Vol. 15, p. 1717(L), ept. 1960

Hall effect and magnetoresistance measurements performed at 4.2°K in a pulsed magnetic field greater than 100 kgauss on n-type PbTe are discussed. Some oscillation was found in the magneto-resistance but no anomaly was found in the Hall effect.

8293 SURFACE MAGNETOCONDUCTIVITY EXPERIMENTS ON SILICON by R. E. Coovert (U. Illinois); Diss. Abstr., Vol. 21, p. 1604(A), Dec. 1960

Measurements of the Hall coefficient and magnetoconductivity of holes and electrons trapped in the space charge region adjacent to a thermally oxidized silicon surface were reported. The results are compared with theories for random and specular surface scattering. It is found that p-type samples showed better agreement with random scattering than specular scattering. On an n-type sample, electrons in an accumulation layer indicated random scattering theory, while holes at an inversion layer indicated specular scattering. On samples which were converted from p-type to n-type in the oxidation treatment, better agreement with specular scattering was found for electrons at an n-type surface, while the results for holes at a p-type surface were in better agreement with the random scattering theory.

8294 SIGN REVERSAL OF HALL COEFFICIENTS AT LOW TEMPERATURES IN HEAVILY COMPENSATED p-TYPE GERMANIUM by H. Yonemitsu, H. Maeda, and H. Miyazawa (Toshiba Elect.); J. Phys. Soc. Japan, Vol. 15, pp. 1717-1718(L), Sept. 1960; p. 1907, Oct. 1960

Hall coefficient and resistivity measurements performed on heavily compensated p-type germanium at low temperatures are discussed. Room temperature Hall coefficient and resistivity measurements indicated that the samples were 40 per cent compensated. A maximum in the Hall coefficient was found at 10°K. As the temperature was lowered the Hall coefficient decreased and reversed sign at ~5°K. The Hall coefficient then leveled off and was insensitive to temperature changes below ~5°K. The resistivity measurements indicated impurity conduction below 10°K.

Hall Coefficient Measurements on Bi_2Se_3 at High Temperatures - See 8268

8295 POWER-INDUCED SHIFTS OF CYCLOTRON RESONANCES IN THE VALENCE BAND OF GERMANIUM by B. Levinger and D. R. Frankl (Genl. Tel. Electronics); Phys. Rev. Lett., Vol. 5, pp. 12-13(L), July 1, 1960

Cyclotron resonance absorption measurements made on rod-shaped high-purity Ge samples are discussed. These samples were cut in [100] and [110] orientations at 4.2° and 1.4°K over a range of microwave power levels at 24 kMc. It was found that the light hole absorption shifted to slightly higher magnetic field strengths with increasing power. Shifts were observed in heavy hole absorption near [100] and were absent for orientations around [111]. No shifts were observed in the electron resonances.

8296 CYCLOTRON RESONANCE IN GERMANIUM AND SILICON AND THE EFFECT OF NEGATIVE EFFECTIVE MASSES by Yu. Kagan; Soviet Phys.-JETP, Vol. 11, pp. 1333-1340, Dec. 1960

Cyclotron resonance in semiconductors with degenerate valence bands is discussed. The frequency spectrum for the case where the magnetic field is along the [001] axis is determined. It is shown that there is a branch of negative cyclotron-resonance

frequencies in germanium and silicon. The transport equation is solved to obtain an expression for the absorbed power and the problem of negative absorption is considered.

ESR Determination of Vacancy Interaction in Si - See 8176

ELECTRICAL PROPERTIES OF SURFACES

8297 SKIN EFFECT IN SEMICONDUCTORS by A. H. Frei (RCA Labs.) and M. J. O. Strutt (Swiss Fedl. Inst. Tech.); Proc. IRE, Vol. 48, pp. 1272-1277, July 1960

The theory of skin effect in semiconductor materials including the effect of displacement currents is discussed. In the case of flat plates, formulas are derived for the field distribution, the impedance and the eddy-current power losses, considering symmetrical electric as well as magnetic fields. Impedance as a function of frequency is measured for germanium in the microwave cm-range. The measured values agree with the theoretical results. The equivalent depth of penetration is calculated and compared with the skin depth for metals. All theoretical results are represented in graphs for different values of the ratio γ, i.e., the displacement current divided by the conduction current. The formulas are extended to the case of complex permeability, corresponding to hysteresis.

8298 STANDARDS AND MEASUREMENTS OF MICROWAVE SURFACE IMPEDANCE, SKIN DEPTH, CONDUCTIVITY AND Q by H. E. Bussey (Natl. Bu. Stand.); IRE Trans., Vol. I-9, pp. 171-175, Sept. 1960

Application of a cavity resonator with known Q value as a comparison standard for skin depth measurements is discussed. The metal walls of the resonator become standards of skin depth if the walls are uniform and if contact loss is eliminated, as in the circulator TE_{011} mode. An end plate standardized in this way may be replaced by another flat piece of material and its unknown skin depth easily determined. A copper cavity in use has 94 per cent of theoretical Q. Deoxidization of the surface raises the value to 97 per cent. Surface roughness and mode conversion may account for the remaining Q departure. Accuracy of Q measurement (± 3 per cent) is discussed and preliminary results on several metals are given.

8299 INVESTIGATION OF THE SURFACE ELECTRICAL CONDUCTIVITY OF SINGLE-CRYSTAL GERMANIUM by V. A. Presnov and V. F. Synorov (Siberian Physicotech. Inst.); Soviet Phys.-Solid State, Vol. 2, pp. 357-362, Sept. 1960

The effect of various surface treatments on the surface conductivity of germanium is discussed. The type of bonding between surface germanium atoms and both protons and hydroxyl ions is described. The temperature dependence of the surface resistance of etched, sand-blasted, and lacquer-coated surfaces of both n- and p-type germanium is plotted. Coating with a polar lacquer reduced the surface conductivity of p-type, but increased that of n-type. Treating the surface of n-type with methyl alcohol increased the surface resistance of the germanium.

8300 CHARACTERISTIC ENERGY LOSSES ON REFLECTION OF ELECTRONS FROM MONOCRYSTALS OF ALKALI HALIDES by M. L. Kapitsa, S. A. Fridrikhov, and A. R. Shul'man (Leningrad Polytech. Inst.); Soviet Phys.-Solid State, Vol. 2, pp. 482-488, Sept. 1960

Energy distribution curves of secondary electrons in an alkali halide is discussed. The accuracy of the determination reveals two systems of maxima; one system (right-hand) is related to the characteristic energy losses of the electrons, while the other system (left-hand) requires additional investigation. A similarity between the characteristic loss values below 12ev and optical absorption data is noted. For primary electrons, characteristic losses smaller in value than the forbidden band width are recorded.

MAGNETIC PROPERTIES

GENERAL

Magnetothermal Effect in Si-Fe Alloys - See 8406

8301 EQUATIONS OF STATE DETERMINING THE MAGNETOELASTIC PROPERTIES OF FERROMAGNETIC MONOCRYSTALS by K. B. Vlasov (Inst. Metal Phys.); Soviet Phys.-JETP, Vol. 11, pp. 642-645, Sept. 1960

The equation of state for the small magnetization changes and deformations that determine the magnetomechanical properties of magnetically polarized ferromagnetic single crystals possessing hexagonal symmetry are derived. It is shown that in the case of nonuniform strains the equilibrium values of the mechanical stresses and of the magnetic field intensity are connected by equations of state not only with the magnetization vector and strain tensor, but also with the rotation tensor which determines the orientation of the volume element under consideration. On the basis of the equations obtained, conclusions are made concerning special features of the velocity of propagation and rotation of the plane of polarization of transverse elastic waves in ferromagnets.

8302 UNIFORM AND NONUNIFORM FORM EFFECT IN MAGNETOSTRICTION by R. Gersdorf (U. Amsterdam); Physica, Vol. 26, pp. 553-574, Aug. 1960

A calculation of the form effect observed in magnetostriction is developed. On the assumption that the strains are uniform, a calculation of this effect is made for ellipsoids of rotational symmetry magnetized along a principal axis. This is done for elastically isotropic material and for an elastically anisotropic cubic crystal, with the cube axes in an arbitrary direction. A more accurate investigation showed, however, that in most cases the strains are far from uniform. An exact calculation of the strains as a function of the position could only be made for a sphere, an isotropic sphere and a monocrystalline sphere of cubic crystal symmetry, the magnetization being in a (110) plane. An approximate calculation is made for a few other cases that may be of importance for experiments in which magnetostriction constants are determined.

8303 MAGNETOSTRICTION OF ANTIFERROMAGNETIC NICKEL MONOXIDE by K. P. Belov and R. Z. Levitin (Moscow State U.); Soviet Phys.-JEPT, Vol. 10, pp. 400-401 (L), Feb. 1960

Measurement of the magnetostriction of polycrystalline nickel monoxide NiO is discussed. The measurements were made by the wire probe method by means of a photoelectro-optical

MAGNETIC PROPERTIES (Cont'd)

amplifier. The temperature dependence of the transverse magnetostriction was measured in a field of 14,200 oe. The magnetostriction was found to have a negative sign and decrease monotonically on approaching the Curie point. The field dependence of the transverse magnetostriction was measured at various temperatures and the longitudinal magnetostriction was measured at room temperature. It was found that there is a critical field ($H_c \approx 5000$ oe) below which the magnetostriction is practically zero and above which the magnetostriction increases. It is suggested that the magnetostriction in nickel monoxide is dependent on the existence of a domain structure.

8304 MAGNETOSTRICTION OF YTTRIUM IRON GARNET by T. A. Nakamura and Y. Sugiura (Electrotech. Lab., Tokyo); J. Phys. Soc. Japan, Vol. 15, p. 1704(L), Sept. 1960

Measurements of the magnetostriction of polycrystalline YIG are discussed. The measurements give a value of the saturation magnetostriction constant $\lambda_s = -(3.7 \pm 0.5) \times 10^{-7}$. This small value can be explained by dipolar interaction. The magnetofriction constant was also calculated to be $\lambda_s = 1.1 \times 10^{-7}$. For this calculation the elastic constants of Ni-ferrite were used since those of YIG are not available. The reason for the negative experimental value is discussed.

8305 MAGNETIC TRANSITION IN $TiCl_3$ by S. Ogawa (Hokkaido U.); J. Phys. Soc. Japan, Vol. 15, p. 1901 (L), Oct. 1960

Measurements of the magnetic susceptibility of polycrystalline $TiCl_3$ in the temperature range 77° to 500°K are discussed. Both $\chi_\parallel$ and $\chi_\perp$, the magnetic susceptibilities parallel and perpendicular to the c-axis, drop abruptly at the transition temperature $T_t = 217 \pm 2$°K unlike the behavior of normal antiferromagnetics. Since this anomalous transition suggests the possibility of lattice distortion at T_t, x-ray diffraction measurements were made. The room temperature pattern, except for a slight difference in lattice constants, was found to agree with that reported in the literature. At T_t the lattice symmetry did not change but the lattice spacings changed abruptly. At T_t the lattice contraction in the plane perpendicular to the c-axis is so large that the expansion in the c-direction cannot prevent a volume contraction. The Ti^{3+} ions form a honeycomb lattice in the plane perpendicular to the c-axis with each lattice plane separated from the next plane by two hexagonal lattice planes of Cl^- ions. The observed lattice distortion suggests bonding among Ti^{3+} ions in the plane perpendicular to the c-axis below T_t.

Antiferromagnetic-Paramagnetic Transition in $MnCl_2 \cdot 4H_2O$ - see 8401

FERRO- AND FERRIMAGNETISM

8306 EQUIVALENCE OF THE CRITICAL CONCENTRATIONS IN THE ISING AND HEISENBERG MODELS OF FERROMAGNETISM by R. J. Elliott, B. R. Heap (Clarendon Lab.), D. J. Morgan, and G. S. Rushbrooke (King's Coll.); Phys. Rev. Lett., Vol. 5, pp. 366-367(L), Oct. 15, 1960

The dilution of a magnetic crystal by nonmagnetic atoms randomly arranged in the lattice is discussed. If the crystal is not otherwise changed, the transition temperature drops. Below a critical concentration of magnetic atoms, where the transition temperature is 0°K, the system will not exhibit a transition to magnetic order. It is shown that in ferromagnetic crystals the critical concentration is a topological property of the lattice, is the same as in the Heisenberg and Ising models, and is independent of the value of spin.

8307 SOME MAGNETIC PROPERTIES OF THE ISING MODEL by D. M. Burley (Glasgow U.); Phil. Mag., Vol. 5, pp. 909-919, Sept. 1960

Two properties of the Ising model are considered. First the spontaneous magnetization of a ferromagnet for three-dimensional lattices is obtained by extrapolating the appropriate series expansions. From the results accurate values for the critical temperature are found. Secondly, the high temperature susceptibility of an antiferromagnet is derived from the approximation of Kikuchi. The resulting susceptibility curves show that for loose-packed lattices a maximum value occurs at a temperature slightly above the critical point, while for close-packed lattices no such effect is obtained.

8308 MAGNETIC GRADIENT AT THE SURFACE OF FERROMAGNETIC SUBSTANCES by S. Yamaguchi (Inst. Phys. Chem. Res., Tokyo); J. Electrochem. Soc., Vol. 107, pp. 357-359, Apr. 1960

Measurement of the magnetic gradients at the surfaces of a reduced iron catalyst and the sharp edge of a razor blade of hard steel by means of electron diffraction is discussed. The remanence of the catalyst was about 5000 gauss and that of the razor about 10,000 gauss. The surface of the catalyst was scanned to locate the maximum gradient. The electron beam grazed the sharp edge of the razor blade. The maximum magnetic gradient $\partial H_z / \partial z \cong 6 \times 10^5$ gauss/cm at the surface of the iron catalyst and $\partial H_z / \partial z \cong 9 \times 10^5$ gauss/cm on the razor edge. In studying the magnetic Hedvall effect in catalysis and corrosion of metals, the described electron diffraction technique should be utilized.

8309 MAGNETISM OF THE IRON PARTICLES AS REVEALED BY ELECTRON DIFFRACTION by S. Yamaguchi (Inst. Phys. Chem. Res.); Indian J. Phys., Vol. 34, pp. 535-537, Nov. 1960

The use of electron diffraction to measure the magnetic induction in the interior, B_i, and on the surface, B_s, of iron particles is discussed. The iron particles were held at the sharp edge of a magnetized razor blade. Superimposed electron diffraction patterns of a non-ferromagnetic gold foil and the magnetic sample were obtained with both soft electrons ($\lambda = 0.0479$A) and with hard electrons ($\lambda = 0.0277$A) with the position of the photographic plate and the wave length of the incident beam being kept constant. Eccentric diffraction patterns were obtained at both wave lengths. From the relation $Z_1/Z_2 = \lambda_1 B_s / \lambda_2 B_i$, where Z_1 and Z_2 are the ring eccentricities in the soft electron and the hard electron cases, respectively, and λ_1 and λ_2 are the wave lengths of the soft electrons and hard electrons, respectively, it is found that $B_s/B_i = 0.92$.

8310 MAGNETISM OF THE ELECTRODEPOSITED FILMS AS REVEALED BY ELECTRON DIFFRACTION by S. Yamaguchi (Inst. Phys. Chem. Res., Tokyo); J. Electrochem. Soc., Vol. 107, pp. 55-56, Jan. 1960

The use of the deflection of an electron beam in a magnetic field, as revealed by electron diffraction, to determine the magnetic induction of a ferromagnetic thin film is discussed.

The deflection Δz is determined from the eccentricity of the diffraction pattern of a nonferromagnetic, e.g., a gold foil, superposed on the diffraction pattern of a film of a ferromagnetic such as nickel. The electron wave length and position of the photographic plate are kept fixed while the diffraction patterns are obtained. The magnetic induction is given by $\Delta z = \frac{eL\lambda}{h}\int_0^l Bdl$, where e is the electron charge, m is the electron mass, v is the velocity of the electrons, L is the camera length, λ is the electron wave length, and l is the magnetic field region traversed by the electron beam. The magnetic induction of a nickel film and an iron film have been measured to be $B \cong 7 \times 10^3$ gauss and $B \cong 3 \times 10^4$ gauss, respectively.

8311 DIRECTION OF THE EFFECTIVE MAGNETIC FIELD AT THE NUCLEUS IN FERROMAGNETIC IRON by S. S. Hanna, J. Heberle, G. I. Perlow, R. S. Preston, and D. H. Vincent (Argonne Natl. Labs.); Phys. Rev. Lett., Vol. 4, pp. 513-515(L), May 15, 1960

The correlation in direction between the effective magnetic field at the iron nucleus and the magnetization is discussed. The sense of the correlation has been determined by observing the change in the hyperfine splitting of the nuclear energy levels of Fe^{57} on the application of an external magnetic field. The correlation is negative since shifts to lower energy were observed.

8312 SPONTANEOUS MAGNETIZATION OF MAGNESIUM FERRITE-MANGANITE SYSTEM by K. Muramori and S. Miyahara (Hokkaido U.); J. Phys. Soc. Japan, Vol. 15, p. 2354(L), Dec. 1960

Magnetic moments measured in solid solutions of $MgFe_2O_4$ and $MgMn_2O_4$ are discussed. Powders with the formula $MgFe_{2-a}Mn_aO_4$, with a varying from 0 to 2 in intervals of 0.2 were used. The magnetic moment observed in $MgFe_2O_4$ agrees with the value expected from Néel's theory. When a varied from 0 to ~1 good agreement was also found with Néel's theory. With a >1, however, the measured magnetic moments were smaller than indicated by Néel's theory and decreased with increasing manganese compositions.

Susceptibility of $TiCl_3$ - See 8305

Coercive Force of Fine Powder Hexagonal Fe_2C - See 8220

8313 VARIATION OF THE PERMEABILITY WITH TEMPERATURE IN CERTAIN FERRITES [in French] by Y. Lescroel (Lignes Tel. et Tel.); Solid State Phys. Electronics and Telecommun., Academic Press, 1960, Vol. 3, pp. 142-148

Experimental curves of the initial permeability of manganese ferrite and manganese zinc ferrite as a function of temperature between −200° and 300°C are given. It is shown that this variation depends on the concentration of the ferrite of iron $FeO \cdot Fe_2O_3$ in the material. Practical application to the fabrication of materials shows that the permeability varies very little with temperature.

8314 MAGNETIC SUSCEPTIBILITY OF $CoBr_2 \cdot 6H_2O$ by M. Garber (Michigan State U.); J. Phys. Soc. Japan, Vol. 15, pp. 734-735(L), Apr. 1960

Measurements of the magnetic susceptibility at liquid He temperatures performed on single crystals of $CoBr_2 \cdot 6H_2O$ are discussed. Measurements were made along the b, c, and a' axes. The c-axis is the preferred spin alignment direction. A knee in the X-parallel curve was observed at 3.2°K. This was measured at 1500 oersteds, so that the temperature corresponds to the zero field case. No critical field was observed up to 5000 oersteds. The susceptibilities were also measured at 80°K. In this case $\chi_a = 0.026 \times 10^{-3}$/gm, $\chi_b = 0.123 \times 10^{-3}$/gm, and $\chi_c = 0.118 \times 10^{-3}$/gm. The flat region which extends above the Néel temperature agrees with the large specific heat tail.

8315 PERMEABILITY AND PERMITTIVITY MEASUREMENTS ON MICROWAVE FERRITES USING RESONANT CAVITY TECHNIQUES by J. N. Rogers and J. Watkins (GE Ltd.); Solid State Phys. Electronics and Telecommun., Academic Press, 1960, Vol. 3, pp. 162-168

Resonant cavity techniques for measuring the permeability and permittivity of ferrites at microwave frequencies are discussed. The cavity can support a number of different magnetic and electric field configurations, or modes, at different frequencies. A mode is chosen at the measurement frequency and the specimen is mounted at a position of either zero magnetic or zero electric field for measuring electric or magnetic properties, respectively. From the changes in resonant frequency and Q value on the insertion of the ferrites the permeability or permittivity can be determined. Magnetic and dielectric measurements performed by these techniques on several ferrites are discussed.

8316 THE INFLUENCE OF SUCCESSIVE ASYMMETRICAL MAGNETIZATION REVERSAL ON THE MAGNETIC STATE OF OPEN SAMPLES by V. Hajko and J. Daniel-Szabó (Tech. Coll.); Czech. J. Phys., Vol. 10B, No. 4, pp. 294-298, 1960

A study of the influence of successive asymmetrical magnetization reversal on the magnetic state of open samples, where the macroscopic demagnetization field has a significant effect during magnetization reversal and leads to a sort of rotation of the asymmetrical loops performed one after another is presented. This effect is similar to "reptation," which was studied experimentally by Nguyen van Dang and theoretically explained by Néel. The quantitative expression of the rotation of asymmetrical loops in open samples as a function of the number of loops and amplitude of the disymmetry is similar to that with the "reptation" effect.

8317 THE EFFECT OF CATION VACANCIES ON THE MAGNETIC ANNEALING OF $Co_xFe_{3-x}O_4$ by T. Inoue, H. Mizuta and S. Iida (U. Tokyo); J. Phys. Soc. Japan, Vol. 15, pp. 1899-1900(L), Oct. 1960

Experiments carried out to determine the effect of cation vacancies on the magnitude of anneal-induced uniaxial anisotropy in $Co_xFe_{3-x}O_4$ are discussed. The final magnitude of the anneal-induced anisotropy K_u and the relaxation time $t_{1/2}$ (the time at which K_u becomes one half the initial value) were measured at high temperatures by a torque meter. Special care was taken to control and homogenize the concentration of cation vacancies. It was found that the final magnitude of the uniaxial anisotropy does not depend on the relaxation time. The cation vacancy concentration, therefore, does not affect the final value of the induced anisotropy.

8318 MAGNETIC ANISOTROPY OF THE DISORDERED ALOY Ni_3Mn AT HELIUM TEMPERATURES by N. V. Volkenrein and M. I. Turchinskaya (Metal Phys. Inst.); Soviet Phys.-JETP, Vol. 11, pp. 195-196(L), July 1960

Reversible magnetization curves measured in several crystallographic directions in single crystals of Ni_3Mn at room temperature, liquid nitrogen, hydrogen, and helium temperatures are discussed. At room temperature there is a linear dependence of induction on field in all crystallographic directions and there is no anisotropy. On cooling to liquid nitrogen temperature the curves take the shape of a typical ferromagnet and magnetic anisotropy appears. The anisotropy increases on lowering the temperature to liquid hydrogen temperature but does not change essentially on further cooling to liquid helium temperatures. The difficult, easy, and intermediate directions are the [100], [111], and [110] crystallographic directions, respectively, in the temperature range 77.8° to 4.2°K. The saturation fields at all temperatures are much smaller than the saturation fields obtained previously in polycrystalline specimens. It is suggested that the increase in saturation field with decreasing temperature is due to a transition from a ferromagnetic to an antiferromagnetic state with comparatively low critical fields at which magnetic saturation is obtained.

8319 EXCHANGE ANISOTROPY MEMORY EFFECT by I. S. Jacobs and P. E. Lawrence (GE Res. Labs.); J. Appl. Phys., Vol. 31, pp. 1388-1391, Aug. 1960

A magnetic memory effect in a low Curie point ferrimagnetic spinel ($\sim NiFe_{0.15}Cr_{1.85}O_4$) containing a coherent antiferromagnetic impurity (NiO) with a high Néel point is reported. It is explained in terms of the Meiklejohn-Bean exchange anisotropy coupling the two phases. The past magnetic history is remembered in the spontaneous reacquisition of a fraction of the past remanent state despite prolonged storage at temperatures above the ferrimagnetic Curie point. A feature of the explanation is the condition that antiferromagnetic domains in NiO rotate irreversibly in accessible fields.

8320 POLARIZATION OF NUCLEI IN NONMETALLIC FERROMAGNETIC SUBSTANCES by G. R. Khutsishvili (Inst. Phys., Georgian S.S.R.); Soviet Phys.-JETP, Vol. 2, pp. 1187-1188(L), Nov. 1960

The polarization of the nuclei of ferromagnetic and paramagnetic atoms in ferromagnetic ferrites and garnets is discussed. It is shown that polarization can be achieved by applying a magnetic field to the sample while cooling it to a very low temperature. In the ferrites of Co, Ni, Mn, Ti and Cu considerable polarization of the transition element nuclei is obtained. The limiting degree of polarization is unity. The Fe nuclei will not be polarized, but only aligned. In magnetite, Fe_3O_4, the limiting degree of polarization of the iron nuclei is 1/3. In the garnets both the transition element nuclei and the Fe nuclei will be polarized. The limiting degrees of polarization are unity for the transition element nuclei and -1/5 for the Fe nuclei. The nuclear polarization can be measured by means of nuclear magnetic resonance and, in the case of radioactive nuclei, by studying the angular anisotropy of the γ radiation or the angular asymmetry of the β radiation. The properties of ferrites, garnets, and other nonmetallic ferromagnetics can be studied by means of nuclear polarization.

8321 MAGNETORESISTANCE EFFECT IN THE MAGNETIZATION REVERSAL OF PERMALLOY FILMS by E. Tatsumoto, K. Kuwahara, and M. Goto (Hiroshima U.); J. Phys. Soc. Japan, Vol. 15, p. 1703(L), Sept. 1960

An investigation of the mechanism of magnetization reversal in rectangular 80 Ni permalloy films is discussed. Measurements were made in samples with the length parallel and perpendicular to the easy direction. Magnetoresistance measurements as a function of magnetic field indicate that reversal takes place by the nucleation of reverse domains and their growth in samples with the length parallel to the easy direction and that reversal is due to almost coherent and continuous rotation in samples with the length perpendicular to the easy direction.

8322 MAGNETORESISTANCE AND DOMAIN STRUCTURE IN THIN FERROMAGNETIC FILMS by R. L. Coren (Brooklyn Polytech. Inst.), Diss. Abstr., Vol. 21, p. 1604(A), Dec. 1960

The use of magnetoresistance measurements to determine the magnetic domain structure of nickel films was discussed. Marked differences are found between the measured magnetoresistance and the behavior expected of a single domain film. The nature of the differences indicates that these films must at least contain a distribution of uniaxial magnetic regions in the film plane. A particular model having these properties was developed. The magnetoresistance for this model was computed numerically and found to be in excellent agreement with experimental results.

8323 INVESTIGATION OF THE INTER-DOMAIN BOUNDARIES IN FERROMAGNETS [in Russian] by L. V. Kirenskii and V. V. Veter (Inst. Phys. AN USSR); Izv. VUZ Fiz., No. 4, pp. 183-189, 1960

Investigations of the interdomain partitions in single crystals of silicon iron with a 3 per cent silicon content, using the Kerr magneto-optic effect, are cited. The investigations conducted show that the polarity of the boundaries can be different and that the width of the boundary layers is not stable and fluctuates between 0.6 - 0.9μ for 180° neighbors.

8324 MEASUREMENTS OF OPTIMUM DOMAIN WIDTHS IN SILICON-IRON by R. Carey (U. Nottingham); Proc. Phys. Soc., Vol. 76, pp. 567-569, Oct. 1960

Optimum domain width measurements performed in demagnetized polycrystalline silicon-iron disks with strain-free surfaces are discussed. The mean grain length L of the samples in the [100] direction ranged from 0.04 to 0.3 cm. Good agreement was found between the magnitude of the measured values of the optimum domain width and theoretical values.

8325 DEPENDENCE OF ENERGY AND ORIENTATION OF 90° BLOCH WALL ON STRESS by J. Kaczér and M. Zelený (Czech. Acad. Sci.); Czech. J. Phys., Vol. 10B, No. 8, pp. 561-567, 1960

The energy and orientation of a 90° Bloch wall as functions of the stress are calculated. The relative occurrence of stress in a quenched single crystal of silicon-iron is derived on the basis of the experimental distribution of the zigzag angle.

8326 ELECTROMAGNETIC THEORY OF D-C EFFECTS IN FERROMAGNETIC RESONANCE by H. J. Juretschke (Brook-

lyn Polytech. Inst.); J. Appl. Phys., Vol. 31, pp. 1401-1406, Aug. 1960

Effects of magnetoresistance and extraordinary Hall effect on the propagation of electromagnetic waves through very thin sheets of ferromagnetic conductors are studied. These contributions to the conductivity produce electric fields varying like products of current and magnetization and introduce nonlinear interactions, which are particularly large in the neighborhood of ferromagnetic resonance. Detailed first-order dc electric fields are obtained for the configuration of a very thin ferromagnetic sheet very close to a conducting wall. The results predict signals strictly proportional to incident microwave power, and mostly inversely proportional to film thickness, becoming independent of thickness for the thinnest films. Their magnetic field or frequency dependence gives typical resonance curves modulated by slowly varying amplitudes. The maxima and zeros of these amplitudes are very sensitive to the local field configuration. Once this latter is well-known, however, these effects can be employed to study conveniently the high-frequency conduction and magnetic properties of the thinnest films.

8327 SPIN WAVE RESONANCE IN Ni FILMS by H. Nose (Tokyo Metropolitan U.); J. Phys. Soc. Japan, Vol. 15, pp. 1714-1715(L), Sept. 1960

Measurements of spin wave resonance in thin Ni films are discussed. No spin wave resonance was clearly observed in films prepared by evaporating on mica heated at 320°C. These films exhibited an isotropic stress in the plane of the film, $\sigma = 5.3 \times 10^9$ dyne/cm^2, and a uniaxial stress lying in the film plane at an angle to the direction of the saturization magnetization, $\sigma_u = -1.9 \times 10^3$ dyne/cm^2. These values did not depend on the substrate temperature. In films evaporated on glass the stress values are temperature dependent, decreasing with increasing substrate temperature. These differences are attributed to the differences between the structure of the surfaces of mica and glass. Spin wave resonance was observed in these films. Fiber texture observed by electron diffraction in films evaporated on glass substrates heated below 200°C have no connection with the excitation of spin wave resonance and the magnitude of the stresses.

8328 ELECTRON SPIN RELAXATION IN FERROMAGNETIC INSULATORS by R. C. Fletcher, R. C. LeGraw and E. G. Spencer (Bell Labs.); Phys. Rev., Vol. 117, pp. 955-963, Feb. 15, 1960

A phenomenological description of electron spin relaxation in ferromagnetic insulators is discussed. This work is accomplished by using the rate of energy transfer between the uniform precession, the spin waves, and the lattice. This leads to an equation of motion containing T_{10}, the relaxation time of the uniform precession to the lattice; T_{2k}, the relaxation time of the uniform precession to the kth spin wave; and T_{1k}, the relaxation time of the kth spin wave to the lattice. Experimental measurements at 6200 Mc are made on single crystal spheres of yttrium iron garnet to determine these times. In addition to measurements of resonance line width and high power saturation, these measurements include a frequency modulation method for measuring relaxation times. The theory provides an excellent fit to the experimental data over a range of surface roughness which varies the line width by a factor of 7.5. This enables the volume property, T_{1k}, to be determined experimentally in the presence of large surface scattering. The other volume property, T_{10}, is determined on the smoothest surface and is found to constitute the lower limit for reducing the line width in the present materials at room temperature. The theory and techniques described should facilitate a better understanding of the basic relaxation mechanisms.

8329 MAGNETIC PROPERTIES OF FERROMAGNETIC GARNET SINGLE CRYSTALS by E. R. Czerlinsky and W. G. Field (AF Cambridge Res. Ctr.); Solid State Phys. Electronics and Telecommun., Academic Press, 1960, Vol. 3, pp. 488-499

Microwave resonance field measurements and saturation magnetization measurements made on rare earth iron garnets grown from a lead oxide flux are discussed. The temperature dependence of the saturation magnetization indicates that erbium, holmium, dysprosium, terbium, and gadolinium iron garnets have compensation points ranging from 80° to 290°K. The temperature dependent anisotropy constant K_1 of lutetium iron garnet was found to pass through zero and the anisotropy constant K_2 of some garnets was found to be larger than expected. The origin of anisotropy of some garnets is discussed.

8330 HIGH-PERMEABILITY GARNETS by E. E. Anderson and J. R. Cunningham, Jr. (U.S. Naval Ord. Lab.); J. Appl. Phys., Vol. 31, pp. 1687-1688(L), Sept. 1960

High initial permeability garnets formed by the substitution of indium for iron in polycrystalline yttrium iron garnet (YIG) are discussed. Below 1 Mc the initial permeability in a garnet in which indium replaces 10 per cent of the iron is ~500 while that of YIG is ~100. The initial permeability of a garnet in which 6 per cent of the iron is replaced by indium is ~200 up to 4 Mc. A 14 per cent substitution was attempted but resulted in a mixture of garnet and perovskite phases. The lattice constant and the Curie point of the 10 per cent indium sample are 12.436 ± 0.005A and ~450°K, respectively.

8331 PERTURBATION THEORY OF ANTIFERROMAGNETISM by R. L. Mills, R. P. Kenan, and J. Korringa (Ohio State U.); Physica, Vol. 26, pp. S204-S214, Dec. 1960

An expansion in terms of connected diagrams for the partition function of an antiferromagnetic spin system with isotropic exchange Hamilton is derived. It is shown that the series can be obtained as a perturbation over the Néel theory. A high temperature perturbation expansion which is of similar structure, but with the internal field replaced by a purely imaginary quantity is suggested. The importance of the summation methods is stressed in connection with the fact that the entire formalism is in configuration space. A method in which the thermodynamic energy plays a central role is indicated.

8332 EFFECTS OF DOUBLE EXCHANGE IN MAGNETIC CRYSTALS by P. -G. de Gennes (U. California); Phys. Rev., Vol. 118, pp. 141-154, Apr. 1, 1960

Some effects of mobile electrons in some antiferromagnetic lattices are discussed. It is shown that these electrons (or holes) always give rise to a distortion of the ground state spin arrangement, since electron transfer lowers the energy by a term of first order in the distortion angles. In the most typical cases this results in: (a) a nonzero spontaneous moment in low fields; (b) a lack of saturation in high fields; (c) simultaneous occurrence of "ferromagnetic" and "antiferromagnetic" lines in neutron diffraction patterns; (d) both ferromagnetic and antiferromagnetic branches in the spin wave spectra. Some of these properties have indeed been observed in compounds of

mixed valency such as the manganites with low Mn^{4+} content. Similar considerations apply at finite temperatures, at least for the (most widespread) case where only the bottom of the carrier band is occupied at all temperatures of interest. The free energy is computed by a variational procedure, using simple carrier wave functions and an extension of the molecular field approximation. It is found that the canted arrangements are stable up to a well-defined temperature T_1. Above T_1 the system is either antiferromagnetic or ferromagnetic, depending upon the relative amount of mobile electrons. This behavior is not qualitatively modified when the carriers which are responsible for double exchange fall into bound states around impurity ions of opposite charge. Such bound states, however, will give rise to local inhomogeneities in the spin distortion, and to diffuse magnetic peaks in the neutron diffraction pattern. The possibility of observing these peaks and of eliminating the spurious spin-wave scattering is discussed in an Appendix.

8333 ON THE MAGNETO-ELECTRICAL EFFECT IN ANTIFERROMAGNETS by I. E. Dzyaloshinskii (Inst. Phys. Problems); Soviet Phys.-JETP, Vol. 10, pp. 628-629(L), Mar. 1960

The magnetoelectric effect in antiferromagnetic crystals is discussed. When a crystal is placed in a constant magnetic (or electric) field an electric (or magnetic) moment proportional to the field is produced in the crystal. It is shown that this phenomena cannot occur in paramagnetic materials. It is also shown, from symmetry considerations, that the magnetoelectric effect should occur in antiferromagnetic Cr_2O_3.

8334 THE MAGNETOELECTRIC EFFECT IN ANTIFERROMAGNETICS by D. N. Astrov (Inst. Physico-Tech. and Radiotech. Meas.); Soviet Phys.-JETP, Vol. 11, pp. 708-709(L), Sept. 1960

Measurement of the magnetoelectric effect (i.e., the appearance of a magnetic moment in an applied electric field) in a single crystal of Cr_2O_3 is discussed. The magnetic moment was measured over the temperature range 250°-330°K in fields of 30 v/cm and 230 v/cm. The experimental arrangement is described. The measured curves represent the temperature dependence of the magnetic moment since no ferromagnetic impurities, which could show the same temperature dependence, were observed. The coefficient of proportionality a between the magnetic moment and the applied field was estimated to be 1.2×10^{-5} at 0°C. The antiferromagnetic transition was found to be 312°K.

8335 MAGNETIC PROPERTY OF Cr_2O_5 by E. Hirota and B. Tsubota (Matsushita Elect. Ind.); J. Phys. Soc. Japan, Vol. 15, p. 1715(L), Sept. 1960

Measurement of the magnetic properties of Cr_2O_5 between 77° and 500°K is discussed. The sample was prepared by heating CrO_3 at 305°C in an oxygen pressure of 95 kg/cm² for 12 hrs. The magnetic measurements were made with an automatic recording magnetic balance. At room temperature the paramagnetic susceptibility χ of Cr_2O_5 is $\chi = (19.4 \pm 0.5) \times 10^{-6}$ emu/g. In the high temperature region the $1/\chi - T$ curve obeys the Curie-Weiss law $\chi = C/T + \theta$, where $C = 8.44 \times 10^{-3}$ emu/g-deg and $\theta = 140°K$. It appears that Cr_2O_5 is antiferromagnetic. To be certain of this, however, measurements must be made below 77°K.

8336 WEAK FERROMAGNETISM OF $NaNiF_3$ by S. Ogawa (HokkaidoU.); J. Phys. Soc. Japan, Vol. 15, p. 2361(L), Dec. 1960

The ferromagnetism of $NaNiF_3$ measured in the temperature region 77° to 150°K is discussed. X-ray measurements indicate that the crystal is orthorhombic with lattice constants at 295°K of a = 5.361A, b = 5.524A, and c = 7.688A. The magnetization of polycrystalline $NaNiF_3$ has a field dependence of $\sigma = \sigma_0 + \chi H$ between 77° and 150°K, where σ_0 is the spontaneous magnetization. The magnetic torques, L, of a single crystal in the planes containing the c-axis have an angular dependence of $L = \pm\sigma_0 H \sin\theta$ below 149°K. Typical torque curves are given. Torque measurements indicate that σ_0 appears in the c-direction and is not rotated toward the b-direction but is rotated toward the a-direction by an applied magnetic field of up to 10 koe. σ_0 disappears above the critical temperature $T_c = 149°K$. At 77°K σ_0 is 0.058 μ_B per molecule of $NaNiF_3$ and is only about 3 per cent of the spin magnetic moment of a Ni^{2+} ion. $NaNiF_3$ probably has a G-type spin structure and is believed to be a canted antiferromagnet in which the spins of Ni^{2+} ions are approximately directed along the a-axis and incline slightly toward the c-axis.

PARAMAGNETISM

8337 MAGNETIC PROPERTIES OF Co^{2+} IONS IN TETRAHEDRAL INTERSTICES OF AN OXIDE LATTICE by P. Cossee and A. E. Van Arkel (Rijks-Universiteit); J. Phys. Chem. Solids, Vol. 15, pp. 1-6, Aug. 1960

A discussion of the magnetic properties of Co^{2+} ions in tetrahedral environment in relation to published optical data is presented. It appears that the singlet ground state $^4F(\Gamma_2)$ is responsible for a magnetic moment close to the spin-only value, while the $^4F(\Gamma_5)$ level about 4000 cm^{-1} above this singlet gives rise to a temperature-independent paramagnetic term of $\approx 0.5 \times 10^{-3}$ erg $G^2 \cdot mole^{-1}$. The expected departure from the Curie-Weiss law is demonstrated by susceptibility measurements on mixed crystals of CoO with ZnO, $CoAl_2O_4$ with $ZnAl_2O_4$ and $CoAl_2O_4$ with $MgAl_2O_4$ between 300° and 1200°K. The magnetic properties of Co^{2+} in tetrahedral interstices are compared with those of Co^{2+} ions in octahedral surroundings.

8338 PARAMAGNETIC STUDY OF THE FERRITES OF YTTRIUM AND OF THE RARE EARTHS OF THE FORMULA $5Fe_2O_3 \cdot 3M_2O_3$ [in French] by R. Aléonard (Lab. d'Électrostatique et de Phys. du Métal); J. Phys. Chem. Solids, Vol. 15, pp. 167-182, Aug. 1960

Measurements of the paramagnetic susceptibilities of the ferrites of formula $5Fe_2O_3 \cdot 3(M)_2O_3$ with garnet structure between the Curie point and 1500°K, for M = Y, Gd, Tb, Dy, Ho, Er, Tm, Yb, and Lu are discussed. The experimental results can be interpreted on the basis of Néel's theory of ferrimagnetism. The curve of the reciprocal susceptibility as a function of temperature is of the third or second degree, for magnetic and nonmagnetic M ions, respectively. From these curves, the molecular field coefficients, which are a measure of the interactions between the magnetic ions, can be determined, as well as their temperature coefficient.

8339 INVESTIGATION OF THE LINE WIDTH AND SHAPE IN THE PARAMAGNETIC RESONANCE SPECTRUM OF THE Cr^{+++} ION IN CORUNDUM SINGLE CRYSTALS by A. A. Manenkov

and V. B. Fedorov (Lebedev Phys. Inst., Moscow); Soviet Phys.-JETP, Vol. 11, pp. 751-754, Oct. 1960

The broadening of the fine structure lines in the paramagnetic resonance spectrum of Cr^{+++} in single crystals of Al_2O_3 is discussed. The width and shape of the lines have been investigated for different electronic transitions and for different concentrations of chromium. The experimental results can be qualitatively interpreted on the basis of an assumption of a broadening mechanism and of a local inhomogeneity in the crystalline electric field. However, quantitative comparison of the experimental data with the theory of dipole broadening of paramagnetic resonance lines does not yield satisfactory agreement.

8340 SPIN-PHONON INTERACTION IN PARAMAGNETIC CRYSTALS by R. D. Mattuck and M. W. P. Strandberg (MIT); Phys. Rev., Vol. 119, pp. 1204-1217, Aug. 15, 1960

A general theory of the spin-phonon interaction, which is applicable to any iron group spin not in an S state, is developed. The theory employs a perturbation treatment that has a more direct physical meaning than techniques previously used and that leads to more accurate results. These results are presented in the form of an equivalent spin-phonon interaction Hamiltonian involving sums over products of spin operators and phonon creation-annihilation operators. The interaction between any two spin levels can then be calculated by using the spin wave functions associated with the usual "spin Hamiltonian." It is shown that owing to the dominant role played by the quadratic term in the above interaction, odd half-integer iron group spins ($S>\frac{1}{2}$) obey quadrupole selection rules. A formula for order-of-magnitude calculations of the interaction strength is derived. It is shown that acoustic experiments should provide the ideal way to test this theory in detail, and two methods of checking the quadrupole rule are proposed. Experimental results on observed acoustic saturation in MgO doped with Cr^{+++}, on the absence of saturation between low-field Kramers doublets in ruby, and an apparent saturation effect in F-center quartz are reported.

8341 SPIN-PHONON INTERACTION IN RUBY by E. B. Tucker (GE); Bull. Am. Phys. Soc., Ser. II. Vol. 5, p. 157 (A), Mar. 21, 1960

The experimental observation of the interaction of 9.2 kMc phonons with the Cr^{+++} spins in a piece of ruby bonded to a quartz rod was reported. The bandwidth for the interaction is somewhat smaller than the microwave line width. By determining the law according to which the ultrasonic phonons saturate the spin resonance it is possible to extract the relative matrix elements for the spin-phonon interaction from the experimental data. This data consists of the variation of the spin-phonon interaction with θ (the angle between the dc magnetic field and the axis of symmetry in ruby) for the various lines in the spin resonance spectrum of ruby. The experimental results and comparisons with some of the theoretically predicted transition probabilities were presented.

8342 HARMONIC SPIN COUPLING IN RUBY by J. E. Geusic (Bell Labs.); Phys. Rev., Vol. 118, pp. 129-130, Apr. 1, 1960

Demonstration of a new mode of maser pumping which makes use of harmonic spin coupling in ruby is reported. In addition, higher order harmonic spin coupling effects in ruby have been found experimentally.

Properties of Ruby in Masers - See 8471

8343 SPIN-LATTICE RELAXATION IN CHROMIUM CORUNDUM by A. A. Manenkov and A. M. Prokhorov (Lebedev Phys. Inst., Moscow); Soviet Phys.-JETP, Vol. 11, pp. 527-530, Sept. 1960

Spin-lattice relaxation of Cr^{3+} ions measured in corundum single crystals at 290°, 77°, and 4.2°K and at various magnetic dilutions is discussed. Continuous saturation of paramagnetic resonance absorption at a frequency of 9375 Mc was employed. The spin-lattice relaxation times, determined from the saturation of the lines of various electronic transitions, were found to depend on the degree of magnetic dilution. T_1 varies between 10^{-5} and 10^{-6} sec at 77°K and between 10^{-2} and 10^{-5} sec at 4.2°K when the relative concentration Cr:Al increases from $\sim 5 \times 10^{-4}$ to 6×10^{-3}. For a sample with a large magnetic dilution, the magnitude of T_1 at 4.2°K depends on the saturating power, increasing with increase of the latter. The anomalous character of spin-lattice relaxation in chromium doped corundum is probably connected with energy transfer processes from the spin system to the liquid helium.

8344 ELECTRON SPIN-LATTICE RELAXATION IN DILUTE POTASSIUM CHROMICYANIDE AT HELIUM TEMPERATURES by J. G. Castle, Jr., P. F. Chester, and P. E. Wagner (Westinghouse Res. Labs.); Phys. Rev., Vol. 119, pp. 953-961, Aug. 1, 1960

Measurements made of the electron spin-lattice relaxation of the $-\frac{1}{2}, +\frac{1}{2}$ line of Cr^{+++} in $K_3Co(CN)_6$ at 9 kMc/sec as a function of temperature, chromium concentration, and the proximity of the $-\frac{3}{2}, -\frac{1}{2}$ line are discussed. The experimental procedure, involving inversion of the line, is capable of distinguishing a "bottleneck" relaxation time from a true spin-phonon relaxation time, T_1. At Cr^{+++} concentrations up to 0.5 per cent, the relaxation data are filled well by single exponential functions of time. Between 1.3° and 4.8°K, T_1 varies approximately as $T^{-1.2}$ indicating that the single phonon process is dominant. No phonon-bath bottleneck is observed, in agreement with calculations based on the measured parameters. A "proximity effect" is observed in which the relaxation rate of the $-\frac{1}{2}, +\frac{1}{2}$ line is enhanced when the $-\frac{3}{2}, -\frac{1}{2}$ line is within 20 line widths. At or per cent Cr^{+++}, the relaxation behavior is markedly different; the recovery is considerably faster and can no longer be described by a single time constant. This change and the proximity effect are interpreted qualitatively in terms of spin cross relaxation. The measured line width increases with concentration from 0.03 per cent to 2 per cent Cr^{+++}, even though the line is observed to be inhomogeneous at and below 0.5 per cent Cr^{+++}.

8345 OPTICAL EFFECTS ON F-CENTER SPIN RESONANCE AT LOW TEMPERATURES by J. Lambe and J. Baker (U. Michigan); Quantum Electronics, Columbia U. Press, 1960, pp. 93-99

The effect of F-band light irradiation on the spin resonance of F-centers in KCl at liquid helium temperature is discussed. The light was found to decrease the F-center resonance signal by about 50 per cent and to increase the F-center spin temperature the equivalent of 4°K. The observed effect is of the magnitude expected from theoretical considerations. It is suggested that a local heating effect may contribute to the observed spin temperature effect. A possible application of optical spin heating in maser systems is considered.

8346 NUCLEAR MAGNETIC RESONANCE OF SOLID HYDROGEN (67-86% ORTHO) AND SOLID DEUTERIUM (33% AND

5% PARA) by G. W. Smith and R. M. Housley (Rice Inst.); ys. Rev., Vol. 117, pp. 732-735, Feb. 1, 1960

uclear magnetic resonance studies on solid hydrogen (H_2) of tho concentrations from 67 per cent to 86 per cent and of lid deuterium (D_2) with para concentrations of 33 per cent nd 55 per cent are reported. The method of Cunningham, hapin, and Johnston was used to produce the high concentrations ortho H_2 and para D_2. The temperature (T_λ) of appearnce of side peaks associated with the removal of rotational egeneracy in H_2 was found to shift to 2.18°K for 86 per cent rtho as compared to a value of 1.6°K for the normal concenration. Our T_λ versus concentration data were found to join moothly to the previous lower concentration work of Sugawara t al. In addition an interesting hysteresis phenomenon was bserved for H_2. It was noted that the temperature of appearnce of the side peaks when the H_2 is cooled is some 0.15°K ower than the temperature of their disappearance when the emperature is slowly raised. In the case of deuterium, no eaks were observed for either 33 per cent or 55 per cent para $_2$ at temperatures down to 0.9°K. T_1 was measured roughly or the two concentrations. For n-D_2, T_1 was found to be 7.6 ± sec. This compares well with the theoretical value of 8sec ven by Moriya and Motizuki. For 55 per cent para-D_2, a alue of 3 ± 1 sec was found. The theory of Moriya and Motizuki gives 5 sec.

347 NUCLEAR MAGNETIC RESONANCE IN SCANDIUM ND LANTHANUM METAL by W. E. Blumberg, J. Eisinger, . Jaccarino, and B. T. Matthias (Bell Labs.); Phys. Rev. ett., Vol. 5, pp. 52-53(L), July 15, 1960

Measurements of the nuclear magnetic resonance of Sc^{45} and a^{139} in spectroscopically pure hexagonal Sc and cubic and exagonal La, through temperatures of 1.7° to 300°K and elds extending to 14 koe, are discussed. The magnitudes of e Knight shift were found to have an anomalous dependence n the number of d electrons. It is suggested that this results om an enhanced s-electron polarization produced by the S-d xchange interaction. Both metals exhibit an unexpectedly rge temperature dependence of the Knight shift.

348 FINE STRUCTURE IN THE PARAMAGNETIC RESOIANCE SPECTRUM OF NATURAL SAPPHIRE by V. M. Vinourov, M. M. Zaripov, and N. R. Yafaev (Kazan State U.); oviet Phys.-JETP, Vol. 10, pp. 220-221(L), Jan. 1960

n investigation of the paramagnetic resonance spectrum of veral natural sapphire single crystals at room temperature the range 9600 to 9200 Mc is discussed. Only the effects the Fe^{3+} ions are considered. It was found that the same alues for the constants in the Hamiltonian for natural sapphire so hold for Fe^{3+} ions artificially introduced into Al_2O_3. ese constants are given. A splitting of the atomic Fe^3 lines as observed in natural sapphire crystals for magnetic field rections other than parallel and perpendicular to the trigonal xis of the electric field.

349 THE PARAMAGNETIC RESONANCE SPECTRUM OF $^{3+}$ IN TiO_2 (RUTILE) by A. Okaya, D. Carter, and F. Nash olumbia U.); Quantum Electronics, Columbia U. Press, 1960, . 389-391

e paramagnetic resonance spectrum of Fe^{3+} in TiO_2 single ystals containing 0.04 per cent Fe^{3+} by weight, measured at X and M band frequencies, is discussed. The frequencies between Kramers doublets were measured directly at zero magnetic field. The experimental data can be described by the spin Hamiltonian $H_{op} = g\beta H \cdot S + D[S_z^2 - 1/3\,S(S+1)] + E(S_x^2 - S_y)^2 + a/6[S_x^4 + S_y^4 + S_z^4 - 1/5\,S(S+1)(3S^2 + 3S - 1)]$, with $D = +20.35 \pm 0.20$ kMc, $E = +2.14 \pm 0.06$ kMc, $a = +0.8 \pm 0.4$ kMc, and $g = 2.00 \pm 0.02$. The g factor was found to be isotropic within 1 per cent. The line width varied from approximately 25 Mc to 84 Mc at T = 1.5°K and X-band frequencies.

8350 PARAMAGNETIC RESONANCE OF Cr^{3+} IN YTTRIUM GALLIUM GARNET by S. Geschwind and J. W. Nielsen (Bell Labs.); Bull. Am. Phys. Soc., Ser. II, Vol. 5, p. 252(A), Apr. 25, 1960

Studies of the paramagnetic resonance of a small Cr^{3+} impurity in $3Y_2O_3 \cdot 5Ga_4O_3$ (YGaG) at 24 kMc and room temperature were reported. The Cr^{3+} enters substitutionally for the Ga^{3+} in the octahedral sites only. No evidence of Cr^{3+} in the tetrahedral sites was found. The strength of the resonance signal indicates that the Cr^{3+} is far less soluble than Fe^{3+} in this lattice. The axial crystal field parameter D for Cr^{3+} associated with the axial distortion in the octahedral site was found to be $D = +10,506 \pm 1$ Mc with $g_{\parallel} = 1.9767 \pm 0.002$ and $g_{\perp} = 1.9757 \pm 0.002$. The fact that D for Cr^{3+} is twice as large in YGaG as in Al_2O_3 and opposite in sign will be discussed in terms of the crystal fields in the two lattices.

8351 SPIN RESONANCE OF V^{2+}, V^{3+}, V^{4+} IN a-Al_2O_3 by J. Lambe and C. Kikuchi (U. Michigan); Phys. Rev., Vol. 118, pp. 71-77, Apr. 1, 1960

The electron spin resonance absorption properties of vanadium sapphire are reported. It is shown that normally vanadium is predominantly trivalent with a small amount in the tetravalent state. After x or gamma irradiation, vanadium is converted to the divalent state. The hfs component separations for V^{2+}, V^{3+}, and V^{4+} are about 88, 110, and 140 gauss, respectively. Because of its readily recognizable spin resonance signature, due to its nuclear spin and because of the ease of producing different oxidation states, it is suggested that vanadium may be a suitable probe to study ionization effects in certain solids.

8352 PARAMAGNETIC RESONANCE OF Ni^{++}, V^{++}, AND Cr^{+++} IN ZnF_2 by M. Peter and J. B. Mock (Bell Labs.); Phys. Rev., Vol. 118, p. 137, Apr. 1, 1960

Measurement of the millimeter wave paramagnetic resonance spectra of Ni^{++}, V^{++}, and Cr^{+++} in ZnF_2 is reported. Evidence was found that the extra charge of Cr^{+++} is compensated by an F^- ion, sitting on one of two available nonequivalent neighboring sites. The antiferromagnetic resonance line in NiF_2 which has been postulated by Moriya is now expected to occur at 320 kMc.

8353 PARAMAGNETIC RESONANCE OF IMPURITIES IN $CaWO_4$. I. TWO S-STATE IONS by C. F. Hempstead and K. D. Bowers (Bell Labs.); Phys. Rev., pp. 131-134, Apr. 1, 1960

Paramagnetic resonance measurements on Mn^{2+} and Gd^{3+} ions in single crystals of $CaWO_4$ grown from the melt are reported. In both cases the four different possible substitutional sites in the unit cell lead to identical resonance spectra with tetragonal symmetry. The splitting of the electronic levels in zero magnetic field is much greater for Gd^{3+} than for Mn^{2+}, e.g.,

b_2^0 is 6.7 times greater and b_4^4 is 13 times greater. (b_n^m is the coefficient of an operator function having the same transformation properties as the corresponding spherical harmonic Y_n^m used in expanding the crystalline electric field.) The large value of b_2^0 ($-0.0917\,cm^{-1}$) for Gd^{3+} makes it a potentially useful material for three-level masers. The lines are narrow, and the hfs due to $Gd^{155,157}$ is well resolved: the ratio A^{155}/A^{157} of the hyperfine splitting constants for the two isotopes was determined as 0.763 ± 0.006.

8354 PARAMAGNETIC RESONANCE OF $Mn^{++}-F^-$ PAIR IN SODIUM CHLORIDE by Y. Yokozawa (Hokkaido U.); J. Phys. Soc. Japan, Vol. 15, pp. 1131-1132(L), June 1960

Observations of the paramagnetic resonance spectrum of the $Mn^{++}-F^-$ pair in single crystals of NaCl is discussed. The measurements were made at room temperature in a sample attached to the bottom of a reflection cavity operating in the 10 kMc region with an external magnetic field rotated in the (001) plane of the crystal. The spectrum observed parallel to [100] direction is shown. The doublet structures of each hfs of Mn^{++} indicate the existence of the $Mn^{++}-F^-$ pair in the crystal. These complex structures become obscured as the magnetic field is moved from the [100] direction, except for the case in which the magnetic field is in the [110] direction. The spin Hamiltonian which describes the spectra is discussed. From the value of the spin Hamiltonian constant As, it is estimated that the σ-bond of the $Mn^{++}-F^-$ pair has 0.45 per cent 2s character. It was also found that the $2p\sigma$ character is about 2.4 per cent at the fluorine nucleus.

8355 ELECTRONIC PARAMAGNETIC RESONANCE OF THE Ti^{3+} ION IN CORUNDUM by L. S. Komienko and A. M. Prokhorov (Moscow State U.); Soviet Phys.-JETP, Vol. 2, pp. 1189-1190, Nov. 1960

The electronic paramagnetic resonance of Ti^{3+} measured at liquid helium temperatures in crystals of Al_2O_3 containing Ti^{3+} concentrations of several hundredths atomic per cent is discussed. The electronic paramagnetic resonance line had an unusual shape, with a steeper descent in the direction of increasing magnetic field than in the direction of decreasing magnetic field. The line can be described by the Spin Hamiltonian $\hat{H} = g_{\parallel}\beta H_z \hat{S}'_z + g_{\perp}\beta(H_x \hat{S}'_x + H_y \hat{S}'_y)$, where $g_{\parallel} = 1.067 \pm 0.001$ and $g_{\perp} \leq 0.1$ are the g factors in the direction parallel and perpendicular to the trigonal axis of the crystal field, β is the Bohr magneton, and $\hat{S}'$ is the effective-spin operator, with value $S' = 1/2$. At 4.2°K the width of the EPR line with the external magnetic field in the direction of the trigonal axis of the crystal field was found to be 50 oe. The shape and width of the line did not drop as the temperature was reduced to 1.55°K. The spin lattice relaxation time τ_1 was estimated from the line broadening at ~9°K to be 5×10^{-8} sec at that temperature. By the continuous saturation method τ_1 was found to be 10^{-4} sec at 4.2°K and approximately 10^{-1} sec at 1.55°K.

8356 PARAMAGNETIC RESONANCE OF CdTe:Mn AND CdS:Mn by J. Lambe (Ford) and C. Kikuchi (U. Michigan); Phys. Rev., Vol. 119, pp. 1256-1260, Aug. 15, 1960

Paramagnetic resonance absorption experiments carried out on CdTe and CdS crystals containing manganese are discussed. In CdTe, the lines are found to be very broad at 300°K. At 4.2°K lines narrow sufficiently to measure parameters with the result $g = 2.010$, $A = 0.0055\,cm^{-1}$, and $3a = 0.0084\,cm^{-1}$, where 3a is the zero-field splitting. The superhyperfine splitting is the same as for CdS with components spaced at 1.4 gauss giving $A_{Cd} = 2.6 \times 10^{-4}\,cm^{-1}$. In CdS an interaction with conduction electrons is found which can broaden lines at 300°K. At low temperatures an anomalous spectrum is found in CdS with $D = 0.0295\,cm^{-1}$.

8357 ANOMALOUS PARAMAGNETIC RESONANCE IN $Ni(NH_3)_6Cl_2$ by M. Date (Osaka U.); J. Phys. Soc. Japan, Vol. 15, p. 2115(L), Nov. 1960

An investigation of paramagnetic resonance in single crystals of $Ni(NH_3)_6Cl_2$ is discussed. Above liquid nitrogen temperature isotropic paramagnetic resonance absorption with $g = 2.16$ was observed. The observed line width of 150 oe is independent of the crystal orientation. Below 76°K the resonance line disappears suddenly. The disappearance of the resonance line is independent of the crystal orientation and no line broadening of the paramagnetic resonance is observed near the transition temperature. It is suggested that the observed change may be due to the quenching of the free rotations of the NH_3 groups below 76°K. The disappearance of the paramagnetic resonance does not appear to be magnetic in origin.

8358 SPIN RESONANCE OF ELECTRONS ON DONORS IN p-TYPE SILICON by G. Bemski and B. Szymanski (Bell Labs.) J. Phys.Chem. Solids, Vol. 17, pp. 173-175(L), Dec. 1960

The observation of paramagnetic resonance of donor impurities in B-doped compensated p-type Si at liquid He temperatures is discussed. No resonance is observed when the samples are in the dark. Upon illumination with light of about 1μ wave length electron-hole pairs are produced and resonance absorption typical of the donor is observed. The amplitudes of the lines increase as the absorption of the flux increases, eventually becoming saturated, and remain unchanged for at least several hours after the light is removed. The resonance is due to electrons captured by the donors. Photoconductivity and photo-Hall measurements at He temperatures indicate that the carriers are electrons and that their concentration does not exceed $10^7\,cm^{-3}$. The holes are trapped, probably at the B centers. The latter explains the very long time constants of electrons on donors. The concentration and type of donor impurities in compensated p-type Si can be determined from electron paramagnetic resonance measurements. The lifetime of electrons in p-type Si at He temperatures has been estimated at between 10^{-9} and 10^{-8} sec.

8359 PARAMAGNETIC RESONANCE ABSORPTION FROM ACCEPTORS IN SILICON by G. Feher, J. C. Hensel, and E. A. Gere (Bell Labs.); Phys. Rev. Lett., Vol. 5, pp. 309-311(L), Oct. 1, 1960

The observation of paramagnetic resonance absorption in p-type Si is discussed. The measurements were carried out at 1.3°K and ~9000 Mc with an external compressive stress applied to the Si by means of a calibrated spring whose tension could be varied during the experiment. The stress removes the degeneracy of the valence band. g values obtained on different acceptors in Si subjected to stresses of 700-900 kg/cm^2 in the [100] direction are presented. In B-doped Si with acceptor concentrations between 5×10^{15} and $2 \times 10^{17}\,cm^{-3}$, the g values were found to be concentration independent. For a stress of 800 kg/cm^2 along the [100] direction, g had values of $g_{\perp} = 2.43 \pm 0.01$ and $g_{\parallel} = 1.21 \pm 0.01$. In all samples a small stress dependence of the g value was found. The stress dependence in B-doped samples is $\Delta g_{\perp}/\Delta T = 7 \times 10^{-5}\,cm^2/kg$.

Differences of a few per cent from the [100] values were observed when the g values were measured with stresses applied along the [111] and [110] directions. Experiments are being carried out to evaluate the significance of these differences.

OPTICAL PROPERTIES

ABSORPTION (TRANSMISSION)

8360 LIGHT ABSORPTION BY EXCITONS IN THE Cu_2O CRYSTAL. Part II. ABSENCE OF CONSTANT EXTERNAL FIELDS by S. A. Moskalenko; Optics and Spectrosc., Vol. 9, pp. 192-195, Sept. 1960

P-type hole bands, the exciton spectra based on the mechanism of excitation of the oxygen ions, and the characteristic frequencies of lattice vibrations in Cu_2O are discussed.

8361 THE EXCITON SPECTRUM OF ZINC OXIDE by D. G. Thomas (Bell Labs.); J. Phys. Chem. Solids, Vol. 15, pp. 86-96, Aug. 1960

Observations of the absorption and reflection spectra of ZnO crystals in the near ultraviolet at temperatures between 300° and 4.2°K are discussed. At 77°K three well-marked reflection peaks occur: two for light polarized with $E \perp c$ (c is the hexagonal axis) and one for $E \parallel c$. The reflectance data have been analyzed by means of the Kramers-Kronig relation. The three peaks arise from n = 1 exciton transitions involving holes from each one of the three valence bands. At 4.2°K the n = 2 exciton states become apparent in reflection, allowing estimates to be made of the exciton binding energy and reduced mass. In absorption the lowest energy exciton may be seen in the "wrong" mode of polarization indicating mixing of certain exciton states. Longitudinal excitons and various forbidden transitions are also observed together with a considerable number of "impurity" exciton transitions. At 4.2°K sharp fluorescent lines occur which are associated with the impurity effects. Zeeman effects have been seen in a field of 32,000 G.

8362 OPTICAL TRANSITIONS IN U-CENTERS IN NaCl CRYSTALS by A. A. Kiselev and I. V. Abarenkov; Optics and Spectrosc., Vol. 9, pp. 402-405, Dec. 1960

The U-center in NaCl crystals is considered. Using the polarized point lattice approximation, the energies of the transitions corresponding to the absorption and emission maxima of the U-bands are calculated along with the half width of the U-band. The results obtained agree satisfactorily with the experimental data.

8363 THE INFRARED SPECTRUM OF THE U-CENTER [in German] by G. Schaefer (Tech. Hochschule, Stuttgart); J. Phys. Chem. Solids, Vol. 12, pp. 233-244, Feb. 1960

The measurement of the infrared vibration absorption of a point imperfection in alkali halides (the U-center) is reported. The frequency ν corresponding to the absorption maximum depends upon the lattice spacing and, in a first approximation, is given by the equation $h\nu d^2 = \text{const}$. For the examined crystals the wave length of the absorption maximum lies in the range between 17.75μ (NaCl) and 27.65μ (RbI). The absorption lines show a marked narrowing if the crystal is cooled from room temperature to 57°K. The half width decreases to about one tenth and is then of the order of magnitude 10^{-3} ev. For KCl and KBr at low temperatures, an oscillator strength of about 0.5 could be determined.

8364 INFRARED AND LOW-TEMPERATURE ACOUSTIC ABSORPTION IN SYNTHETIC QUARTZ by J. C. King, D. L. Wood, and D. M. Dodd (Bell Labs.); Phys. Rev. Lett., Vol. 4, pp. 500-501 (L), May 15, 1960

The defect responsible for infrared absorption at 3620 cm^{-1} and for acoustic absorption at 50°K in hydrothermally-grown synthetic quartz crystals is discussed. A crystal grown from a D_2O solution did not show the absorption maximum at 3620 cm^{-1} but did show the other peaks in this spectral region. A peak at 3620 cm^{-1} was also observed in a hydrothermally-grown crystal which was heated at 500°C for 24 hours in an electric field of 1 kv/cm. It was found that the defect responsible for the 50°K absorption was virtually eliminated when a synthetic crystal was given a similar treatment. These results indicate that the 3620 cm^{-1} infrared peak is due to OH while the other peaks are not, and that the 50°K acoustic absorption is not due to an OH defect.

8365 INFRARED ABSORPTION OF ELECTRONS THROUGH PIEZOELECTRIC SCATTERING by T. Tanaka (Tokyo U.); J. Phys. Soc. Japan, Vol. 15, pp. 2110-2111 (L), Nov. 1960

Infrared photon absorption by conduction electrons in wurtzite structure crystals as a result of piezoelectric scattering is discussed. The frequency dependence of the absorption cross section is derived. $\sigma(\omega) \propto T \cdot \omega^{-5/2}$ for $\hbar\omega/2kT \gg 1$ and $\sigma(\omega) \propto T^{1/2}\omega^{-2}$ for $\hbar\omega/2kT \ll 1$. In CdS crystals $\sigma = 1.4 \times 10^{-17}$ cm^2 at T = 300°K and $\lambda = 10\mu$. This value agrees with that derived by the deformation-potential model.

8366 INFRARED ABSORPTION OF FREE CARRIERS IN IONIC CRYSTALS by T. Tanaka (U. Tokyo); J. Phys. Soc. Japan, Vol. 15, p. 2121 (L), Nov. 1960

The magnitude and photon frequency dependence of the infrared absorption of free carriers in ionic crystals are discussed. A relation for the absorption cross section is derived and applied to ZnO. An absorption cross section $\sigma \simeq 1.7 \times 10^{-15} cm^2$ at $\lambda = 10\mu$ and T = 300°K is found. This agrees with Thomas' experimental value $\sigma = 1.2 \times 10^{-15} cm^2$. The dependence of the absorption cross section on photon wave length is shown for $\tau\omega > 1$. The λ^3 dependence in the short wave length region observed in ZnO has not been explained.

8367 OPTICAL PROPERTIES OF IRRADIATED LiF CRYSTALS IN THE EXTREME ULTRAVIOLET REGION by R. Kato, S. Nakashima, K. Nakamura, and Y. Uchida (Kyoto U.); J. Phys. Soc. Japan, Vol. 15, pp. 2111-2112 (L), Nov. 1960

Ultraviolet absorption spectra measured in β- and γ-ray irradiated LiF crystals are discussed. In a specimen irradiated with β-rays at −70°C for 10 sec (specimen 2) a well defined absorption band was found at 11.1 ev. In samples irradiated with β-rays at 350°C for 2 min (specimen 3) and with γ-rays at room temperature for 5 hrs (specimen 4) absorption was observed at 11.75 and 11.1 ev and, faintly, at about 10.7 and 9.5 ev. The latter components became appreciable in specimen 2 when irradiated with F light. The width of the bands observed at 5 ev suggests that specimens 3 and 4 contain 222 mμ and colloid bands which overlap F bands. When specimen 2 was bleached with F light the band at 11.1 ev decreased and the absorption at 11.75 ev increased as the 222 mμ band appeared. Further investigation is required to determine the

nature of the 11.1 ev band. A broad absorption in specimen 2 from 6 to 8.5 ev which disappears with F light irradiation is assumed to be V band.

8368 ULTRAVIOLET ABSORPTION IN THALLOUS HALIDES by S. Tutihasi (U. Rochester); J. Phys. Chem. Solids, Vol. 12, pp. 344-348, Feb. 1960

Measurement of the ultraviolet absorption in TlCl and TlBr on thin films and fused samples as a function of temperature is reported. The effect of excessive Cl or Tl on the optical absorption of TlCl has been studied. The experiments of Vysochanskii are discussed in the light of these observations. The first absorption band in TlCl, which peaks at 3.44ev at −185°C, is absent in films condensed on a cold substrate of KCl and appears after annealing. It seems that the crystal structure of evaporated films of TlCl changes from the NaCl-type to the CsCl-type.

Pressure Dependence of the Absorption Edge of Semiconductors - See 8270

8369 THE PROPERTIES OF THE LONGEST WAVELENGTH LINE IN THE INTRINSIC ABSORPTION OF Cu_2O by I. S. Gorban' and V. B. Timofeev; Optics and Spectrosc., Vol. 9, pp. 250-252, Oct. 1960

A method for measuring the contours of very narrow absorption lines, using a Fabry-Perot interferometer crossed with a spectrograph is described. The properties of the longest wave length line in the intrinsic absorption of Cu_2O are studied over a wide range of low temperatures. It is shown that the line under study is associated with the intrinsic absorption of Cu_2O. Features of the temperature dependence of the line are related to the mechanism of interaction between excitons and crystal lattice vibrations.

8370 QUANTITATIVE STUDIES OF THE ABSORPTION SPECTRUM OF CUPROUS OXIDE by I. S. Gorban'; Optics and Spectrosc., Vol. 9, pp. 398-401, Dec. 1960

A quantitative study of the absorption spectra of CuO_2 crystals, carried out in the visible part of the spectrum, is discussed. The assumption that the hydrogenlike series of bands at the edge of the main band represents the fundamental absorption of the crystal was confirmed. The features of the structure of the edge – the fundamental absorption bands of the CuO_2 spectrum – can be explained theoretically if one assumes that this absorption band is due to transitions between states of equal parity.

8371 INVESTIGATION OF THE X-RAY SPECTRA OF THE SUPERCONDUCTING COMPOUND CuS by I. B. Borovskii and I. A. Ovsyannikova (Inst. Metal., Acad. Sci. USSR); Soviet Phys.-JETP, Vol. 10, pp. 1033-1034(L), May 1960

The results of an investigation of the fine structure of x-ray absorption and emission k spectra of sulfur and copper in the pure elements and in the compound CuS are presented and discussed. It was found that the absorption spectrum of the Cu in the compound changes from that of the free element and approximates that of Zn. This agrees with the theory that in a superconducting compound of non-superconducting elements the x-ray spectra of the metal will change and become closer to the fine structure of a superconducting metal close to it in the periodic table.

RADIATION

8372 INTRINSIC RECOMBINATION RADIATION IN DIAMOND by J. C. Male and J. R. Prior (King's Coll.); Nature, Vol. 186, pp. 1037-1038(L), June 25, 1960

Intrinsic recombination radiation observed in diamond is discussed. The sample was a strongly blue luminescent diamond which showed weak ultraviolet transmission up to 5.50 ev. The luminescence was produced by injecting charge carriers into the diamond. The emitted radiation had a maximum energy of about 5.6 ev, and intensity maxima at 5.278 ± 0.002 ev and 5.125 ± 0.005 ev. The peak intensity at 5.278 ev was of the order of 0.1 per cent of the intensity at the maximum of the blue band at 4400 A. Analysis of the shape of the 5.278 ev peak indicates that the recombination probability for the excitons is proportional to $1/v^n$ where v is the exciton velocity and n lies between 1 and 2.

8373 RADIATIVE RECOMBINATION IN GERMANIUM CRYSTALS BOMBARDED BY FAST ELECTRONS by V. S. Vavilov, A. A. Gippius, M. M. Gorshkov, and B. D. Kopylovskii (Lebedev Phys. Inst., Moscow); Soviet Phys.-JETP, Vol. 10, pp. 15-17, Jan. 1960

Data on the infrared spectrum accompanying the recombination of electrons and holes in Ge single crystals are presented. It is shown that with increasing concentration of Frenkel defects caused by fast electron bombardment the relative intensity of the emission band with a peak at 2.35μ also increases. The emission spectrum gives information about the radiation-induced energy levels.

Color Center Emission in NaCl - See 8362

LUMINESCENCE

8374 THE LIGHT WAVEFORMS EMITTED FROM ELECTROLUMINESCENT CELLS ENERGIZED BY SQUARE WAVES AND PULSES OF VOLTAGE by G. R. Hoffman and D. N. Smith (Manchester U.); J. Electronics Control, Vol. 9, pp. 161-216, Sept. 1960

Light pulses which rise to a maximum in less than 0.2 μsec obtained from electroluminescent cells excited by voltage waveforms with fast edges are discussed. The pulses decay more slowly, taking from 2 to 3 μsec at a pulse repetition frequency of 50 kc and about 100 μsec at 200 cps to decay to one-third of the maximum amplitude. The dependence of this maximum amplitude on the peak value of the voltage obeys a similar law to that already found for the average brightness of a cell. These and other features of the light pulses depend on the time variation of the electric field strength within the phosphor crystal. The waveform of the electric field is quite different from the applied voltage and can be regarded as having two components due respectively to the applied voltage and the internal space charge which is built up during the first few cycles of excitation. The former can be found approximately from a simplified equivalent circuit, and information about the latter can be obtained from a consideration of the part played by electron traps in the mechanism of electroluminescence.

8375 THE MECHANISM OF THE RECOMBINATION LUMINESCENCE OF ACTIVATED ALKALI HALIDE CRYSTALS by C. B. Lushchik, G. G. Liid'ya, I. V. Yaek, and E. S. Tiisler;

Optics and Spectrosc., Vol. 9, pp. 35-39, July 1960

The results of an investigation of recombination luminescence and photochemical transformations in alkali halide crystals are presented. The crystals are activated by the ions Ga^{+}, Ge^{++}, In^{+}, Sn^{++}, Tl^{+}, and Pb^{++}, under excitation by x-rays and light in the exciton and activator absorption band regions, and also in the "zone-zone" bands. The role of electrons, holes, excitons, and sensitization processes in the recombination emission of phosphors of this class is considered.

8376 ELECTROLUMINESCENCE OF CdS SINGLE CRYSTAL by H. Yamashita, S. Ibuki, M. Yoshizawa, and H. Komiya (Mitsubishi Elect.); J. Phys. Soc. Japan, Vol. 15, p. 2366 (L), Dec. 1960

Electroluminescence emission observed in very pure high resistance CdS single crystals near the anode is discussed. Yellow, green, and orange spots were initially observed. When the current exceeded a few hundredths of a microampere green "curtains" about one mm long were observed. The curtains expanded and contracted as they were observed and were found to consist of many stripes perpendicular to the field. The green emission had a very narrow band at about 5300A and the orange emission had a broad band with the maximum at about 6000A. It is believed that the yellow emission is due to mixing of the green and orange emissions. Luminescence measurements as a function of temperature indicate that the emission is caused by a bimolecular mechanism.

8377 MICROSCOPIC OBSERVATIONS ON ELECTROLUMINESCENT ZnS:Cu PHOSPHORS by W. Lehmann (Westinghouse); J. Electrochem. Soc., Vol. 107, pp. 657-658, July 1960

Microscopic observations on electroluminescent ZnS:Cu phosphor particles are discussed. The particles were stuck in a thin plastic layer between two aluminum electrodes evaporated onto a microscope slide and the space between the particles was filled with a highly refracting liquid. Dark segregations of copper sulfide (probably Cu_2S) were observed inside many particles. The segregations were generally thin and elongated. Electroluminescence was observed directly at the ends of the segregations in many cases. Emission which could not be correlated to segregations was observed and in some cases segregations which did not emit emission were observed. Light emission per spot was found to occur only once per cycle of the exciting voltage. The linear dimensions of the segregations approach 5 to 10 per cent of the particle diameter in ordinary phosphor powders. The emitting spots have the same dimensions. The brightness of a single spot does not steadily decrease with time. Irregular fluctuations of the light have been observed.

8378 SPECTRAL COMPOSITION OF THERMOLUMINESCENCE OF COLOURED NaCl CRYSTALS by J. Dolejsi and A. Bohun (Czech. Acad. Sci.); Czech. J. Phys., Vol. 10B, No. 7, pp. 529-535, 1960

Experimental results of a study of the spectral composition of thermoluminescence in the different maxima in photo-chemically colored "pure" NaCl crystals or NaCl crystals containing Cu in different concentrations are discussed.

8379 THERMOLUMINESCENCE OF ZINC SULFIDE PHOSPHORS by K. Osada (Nagoya U.); J. Phys. Soc. Japan, Vol. 15, pp. 145-149, Jan. 1960

Measurement of the glow curves of the thermoluminescence of some zinc sulfide phosphors for two different exponential heating rates is discussed. The values of the depth and frequency factor of their traps are obtained by the Booth method. The value of the frequency factor is not constant for all traps, but becomes larger as the depth increases. Equations which permit the analysis of the glow curves for the exponential heating rate are derived.

8380 ON THE INFRARED FLUORESCENCE OF F-CENTERS AND ITS MECHANISM IN SUBSTRACTIVELY COLORED ALKALI-HALIDE CRYSTALS INVESTIGATED AT HIGH TEMPERATURE [in Russian] by I. I. Ezhik and S. T. Shavlo (Khar'kov Polytech. Inst.); Izv. VUZ Fiz., No. 4, pp. 190-197, 1960

Investigation of the temperature dependence of the intensity of infrared fluorescence, over the 290°-540°K range, in substractively colored crystals of NaCl, KCl and KBr when they are exposed in the F-center absorption band, is discussed. A kinetic scheme is presented which affords the possibility of explaining the mechanism of the origin of infrared fluorescence and of its decay as well as of the maximum on the curves of the temperature dependence of the intensity of infrared fluorescence.

8381 EMISSION SPECTRUM OF TRIVALENT HOLMIUM IN THE SCHEELITE STRUCTURE by L. G. G. van Uitert and R. R. Soden (Bell Labs.); J. Chem. Phys., Vol. 33, pp. 1532-1534, Nov. 1960

Fluorescent emission due to holmium observed in crystals having the scheelite structure and the compositions $Ca_{1-2x}Na_xHo_xWO_4$, where $x = 0.5$, 10^{-1}, 10^{-2}, 10^{-3}, and 10^{-4} under 3660A excitation is discussed. There are at least eight excited states of holmium which fluoresce in the visible range due to transitions to the $^5I_8$ ground state. These emission peaks appear to be due to the development of exchange coupling. A number of emission peaks due to holmium represent transitions which do not correspond to known absorption bands. These peaks are particularly prominent in the emission spectra at high concentrations of holmium.

Phosphorescence in ZnS:P, Al - See 8161

8382 THE LUMINESCENCE PROPERTIES OF SELENIUM-ACTIVATED ZINC OXIDE by L. Ya. Markouskii and N. S. Orshanskaya; Optics and Spectrosc., Vol. 9, pp. 40-42, July 1960

Data on the luminescence properties of Se-activated ZnO are presented. It is shown that the introduction of Se into ZnO causes the appearance in the cathodoluminescence spectrum of a specific band with λ_{max} near 610 mμ. The maximum strength of this band is observed in the two-band luminors containing 0.2 per cent Se and having a band due to a stoichiometric excess of zinc, in addition to the Se band.

8383 PARAMAGNETIC RESONANCE DETECTION OF THE OPTICAL EXCITATION OF AN INFRARED-STIMULATED PHOSPHOR by R. S. Title (IBM); Quantum Electronics, Columbia U. Press, 1960, pp. 100-104

The use of paramagnetic resonance techniques to observe optical excitation in the infrared-stimulated phosphor SrS:Eu, Sm is discussed. The phosphor was irradiated by ultraviolet or blue light, converting Eu^{2+} to Eu^{3+} and Sm^{3+} to Sm^{2+}. The

dimunition of the Eu^{2+} paramagnetic resonance spectrum is indicative of the energy stored in the phosphor. The stored energy determined by the dimunition of the paramagnetic resonance spectrum agrees with the measurements made by observing the intensity of the emitted light when the phosphor is exhausted by 970 mμ radiation.

PHOTOELECTRONIC PROPERTIES

8384 EFFECT OF HEAT-TREATMENT UPON SINTERED CADMIUM SULPHIDE PHOTOCONDUCTIVE FILMS by S. Kitamura (Matsushita Elect. Ind.); J. Phys. Soc. Japan, Vol. 15, p. 1697(L), Sept. 1960

Heat treatment induced effects in sintered CdS photoconductive films are discussed. When the sintered films were heated at a rate of 1°C/min the dark current-temperature relation was found to be reversible below 90°C and irreversible above 90°C. The activation energy of films heat treated at 160°C in vacuum decreased to one twentieth of the original value. Films cooled at liquid air temperature were irradiated with light from an incadescent lamp, a dc voltage was applied in the dark, and the films were heated in a vacuum at a rate of ~1°C/sec. The thermally stimulated current was measured and a peak was found near room temperature. The thermally stimulated current indicates that the sintered films have large trap concentrations.

8385 PHOTOCONDUCTIVITY OF Cu-ACTIVATED CADMIUM SULPHIDE-SELENIDE by S. Asano (Okayama U.); J. Phys. Soc. Japan, Vol. 15, p. 2103(L), Nov. 1960

Measurements of the spectral response of photoconductivity of Cu-activated Cd(S:Se) at room temperature are discussed. The peak due to copper was found to shift toward longer wave lengths as the proportion of CdSe increased. The trough between the fundamental and copper absorption bands became shallower with increasing proportion of CdSe. The value of the forbidden gap in each sample was determined from the position of the absorption edge in the measured reflectance specra. The forbidden gap decreases $\sim 0.69 \times 10^{-2}$ ev/mole per cent of CdSe. The spectral response of the photoconductivity indicates that the energy gap for copper absorption decreases $\sim 0.52 \times 10^{-2}$ ev/mole per cent of CdSe.

8386 PHOTOCONDUCTIVITY IN NICKEL DOPED GERMANIUM by Y. Furukawa (Elect. Commun. Lab.); J. Phys. Soc. Japan, Vol. 15, p. 353(L), Feb. 1960

Measurements of the photoconductivity vs applied voltage in high resistivity nickel doped germanium at 77°K are discussed. Two different contacts made by soldering indium on etched (type 1 contact) and ground surfaces (type 2 contact) were used. A large voltage drop was found with type 2 anodes in both p- and n-type samples, particularly in n-type samples. A detailed explanation for this phenomenon is presented.

Photoconductivity of Semiconductors with Traps - See 8261

Decay Time of PbS Photodetectors - See 8453

8387 SOME ELECTRICAL PROPERTIES OF AMORPHOUS SELENIUM FILMS by R. A. Fotland (Horizons); J. Appl. Phys., Vol. 31, pp. 1558-1565, Sept. 1960

The dark current and photocurrent characteristics of amorphous Se and As-Se alloy films is discussed. One msec after the application of an electric field, the dark current (neglecting capacitance charging) is several orders of magnitude higher than the steady-state dark current. A hysteresis effect is observed in the dark volt-ampere curves with the descending voltage branch exhibiting an exponential volt-ampere relationship. The voltage of a charged Se plate in the dark discharges logarithmically with time as anticipated from the exponential volt-ampere relationship. Upon admitting air to a freshly evaporated Se plate, a negative surface potential of 150 mv is observed. The phenomenon of "fatigue" (i.e., the temporary increase in dark current following an exposure to illumination) obtained with highly absorbed radiation indicates surface barrier effects exert a large measure of control over dark currents. Photogenerated holes and electrons in Se films are trapped with trapping parameters such that the hole range/unit field is on the order of 10^{-8} cm^2/v, and the electron range is less than 10^{-9} cm^3/v. The addition of As to the Se greatly increases the electron effective lifetime. Trapped holes are eliminated in the dark exponentially with time through a process having an activation energy of 0.77 ev. A 40-mv negative surface photovoltage is observed in Se films upon illumination. This voltage may be accounted for by hole diffusion away from the surface. The addition of As to Se extends the spectral response into the red end of the spectrum, results in the initiation of secondary photocurrent effects, intensifies fatigue effects, and increases the softening temperature of the film.

8388 ANOMALOUS PHOTOVOLTAIC EFFECT OF CdS SINGLE CRYSTALS by S. Ibuki, H. Komiya, and H. Yamashita (Mitsubishi Elect.); J. Phys. Soc. Japan, Vol. 15, p. 2356(L), Dec. 1960

Photovoltaic measurements in CdS single crystals are discussed. The crystals were grown by sublimation recrystallization in a N_2 atmosphere containing In vapor. A layer of Cu was evaporated on one half of the crystal. The crystal was then heat treated for several minutes at 600°C and In contacts were soldered to both ends of the crystal. An open circuit voltage of 0.5v with the Cu side positive and a short circuit current of about 1 ma/cm^2 under direct sun light were obtained. At low light levels the polarity of the photovoltage reversed and the Cu side became negative. It was found that the photovoltage is caused by a p-n junction near the boundary of the CdS and the Cu layer and that the negative photovoltage is produced by the electron diffusion current. The negative voltage was not observed when the Cu layer was not heat treated and when there was no Cu layer. The heat-treated Cu layer, then, is important in the electron diffusion process.

8389 THE ANALYSIS OF SPECTRAL YIELD AND ACCELERATING FIELD CHARACTERISTICS OF THE PHOTOELECTRIC EMISSION FROM SEMICONDUCTORS by D. Haneman and E. W. J. Mitchell (The University, Reading); J. Phys. Chem. Solids, Vol. 15, pp. 82-85, Aug. 1960

The relation between yield and accelerating field characteristics of the photoelectric emission from semiconductors is discussed. A comparison of the photoelectric thresholds deduced from these two characteristics is made for germanium, gallium arsenide and indium antimonide.

8390 FIELD INDUCED PHOTOEMISSION AND HOT-ELECTRON EMISSION FROM GERMANIUM by R. E. Simon and W. E. Spicer (RCA Labs.); J. Appl. Phys., Vol. 31, pp. 1505-1506(L), Aug. 1960

Hot electron emission and photoemission induced by an internal

PHOTOELECTRONIC PROPERTIES (Cont'd)

eld observed from a p-n junction in a Ge crystal with a Cs-ated surface are discussed. The thresholds for photoemission ith and without a field applied across the p-n junction were .7 ev and 1.5 ev, respectively. The surface barrier height is out 0.8 ev or 1.5 ev, depending on the energy levels from ich the photoelectrons are excited. At reverse voltages be-w 3 v, the hot electron and field-induced photoemission have most the same voltage dependence. This result indicates at in this voltage range the hot electron emission is propor-ional to the rate of thermal generation of electrons in the -type material. The large field-induced photoemission and e-breakdown hot electron emission suggests that the surface arrier is less than the minimum energy required by an electron produce a hole-electron pair.

391 PHOTOELECTROMAGNETIC EFFECT IN BISMUTH by . Young (IBM); Phys. Rev., Vol. 117, p. 1244, Mar. 1, 1960

bservations of the PEM effect for the first time in bismuth is ported. Evaporated bismuth films as well as bulk material ve been shown to exhibit the effect. The dependence on e wave length of the incident light and on the intensity of gnetic field have been investigated.

ELECTROMAGNETIC PROPERTIES

392 OPTICAL OBSERVATION OF SPIN-ORBIT INTERACTION N GERMANIUM by J. Tauc and E. Antoncik (Inst. Tech. Phys., ague); Phys. Rev. Lett., Vol. 5, pp. 253-254(L), Sept. 15, 960

e reflection spectrum of Ge is discussed. Measurements have own that the peak observed by Philipp and Taft near 2 ev is lit into two peaks, a at 2.1 ev and b at 2.3 ev. The double ak can be explained by the splitting of the L_3' state by spin-bit interaction. This explanation has been verified by meas-ements in Ge-Si alloys in which the splitting diminishes with creasing silicon content. Similar double peaks have been served in the reflection spectra of GaAs, InAs, and InSb. It pointed out that a similar splitting occurs in the absorption ectrum.

393 REFLECTION AND ABSORPTION SPECTRA OF LiF IN HE EXTREME ULTRAVIOLET REGION by R. Kato, K. Naka-ura, A. Matsui, and Y. Uchida (Kyoto U.); J. Phys. Soc. pan, Vol. 15, p. 2105(L), Nov. 1960

sorption and reflection spectra measured in single crystal F at room temperature are discussed. The reflectivity values ere measured with experimental errors of about 10 per cent. peak at 12.7 ev and a valley at 13.8 ev were observed in e reflection spectrum. The peak and valley have been as-gned to the exciton peak and the onset of the band-to-band nsition, respectively. The shape of the reflection spectrum the peak suggests that the exciton band has a multiplet ucture.

394 THE OPTICAL AND PHOTOELECTRIC PROPERTIES OF ETALS IN THE VACUUM ULTRAVIOLET REGION OF THE ECTRUM by O. P. Rustgi (U. Southern California); Diss. str., Vol. 21, p. 1609(A), Dec. 1960

flectivity and transmissivity of thin metallic films in the range om 1600 A to 450 A were discussed. Results on Al, Sn, In, Bi, Te, Au, Ag, Cd, Sb, Ti, and Ge are presented. The general trend of the curves showed a rise in the photoelectric field γ, in the region where the reflectivity declined rapidly. γ showed a maximum near those values of $h\nu$ where the films changed from an absorbing medium to a transmitting one, and then de-creased toward short wave lengths. An attempt was made to observe the temperature variation of reflectivity and transmis-sivity near temperatures of liquid N_2 in the case of Al, Sn, In, and Bi. The observations did not show any difference between the values at room temperature and those at liquid N_2.

Exciton Reflection in ZnO - See 8361

Refractive Indices of Semiconductors - See 8395

8395 THE FARADAY EFFECT IN SEMICONDUCTORS DUE TO FREE CARRIERS IN A STRONG MAGNETIC FIELD by L. E. Gurevich and I. P. Ipatova (Inst. Tech. Phys.); Soviet Phys.-JETP, Vol. 10, pp. 943-946, May 1960

The dielectric constant tensor for semiconductors with electrons with an anisotropic mass in a strong magnetic field is determined. The Faraday effect is considered for the case of hexagonal crystals with an energy minimum in the center of the Brillouin zone and for a cubic crystal with a minimum which does not coincide with the center of the Brillouin zone. The refractive indices evaluated for different directions of the magnetic field relative to the main crystallographic directions in these crystals are found to depend strongly on the magnetic field direction. This permits the determination of the effective mass tensor by measuring the angle of rotation of the plane of polarization.

8396 FARADAY EFFECT IN YTTRIUM GARNET AT INFRARED FREQUENCIES by G. S. Krinchik and M. V. Chetkin (Moscow State U.); Soviet Phys.-JETP, Vol. 2, p. 1184(L), Nov. 1960

Measurements of the Faraday effect in $Y_3Fe_5O_{12}$ in the wave length region 0.94 to 9μ are discussed. The single crystal plate of $Y_3Fe_5O_{12}$ 75 microns thick was magnetized in a field of 3500 oe. Near the edge of the electronic absorption band, at $\lambda \sim 1\mu$, the rotation of the plane of polarization drops off sharply. In the region of maximum transparency and in the region in which the phonon absorption begins the rotation re-mains approximately constant. Mechanisms which can explain the observations are discussed. The intensity of the transmitted light at $\lambda \sim 1\mu$ was changed by the Faraday effect by approxi-mately 30 per cent when the specimen magnetization was re-versed. It is suggested that this phenomenon can be used in controllable-gyrator or in light-modulator type devices.

8397 INFRA-RED FARADAY ROTATION AND FREE CARRIER ABSORPTION IN Bi_2Te_3 by I. G. Austin (GE Ltd.); Proc. Phys. Soc., Vol. 76, pp. 169-179, Aug. 1960

The Faraday rotation at wave lengths in the range 8-15μ meas-ured on several n- and p-type single crystals of Bi_2Te_3 using a magnetic field of 17 koersteds is discussed. The results are in-terpreted as the sum of rotations arising from free carriers and interband transitions. The latter appear to be sensitive to the impurity content. An attempt has been made to separate the components and use the free carrier rotation to estimate the effective mass parameters. Free carrier absorption measure-ments in the range 8-20μ are also reported. These lead to an independent estimate of the same effective mass parameters which shows fair agreement with the Faraday measurements. The results are discussed in the light of recent galvanomagnetic measurements on some of the crystals.

8398 SURFACE SPECIFIC HEAT OF AN ISOTROPIC SOLID AT LOW TEMPERATURES by M. Dupuis, R. Mazo, and L. Onsager (Yale U.); J. Chem. Phys., Vol. 33, pp. 1452-1461, Nov. 1960

The effect of realistic boundary conditions on the computation of the specific heat of an isotropic solid at low temperatures is investigated. Two cases are considered: the surface free of stress and the surface rigidly clamped. The first of these is the one of physical interest. For both cases a term in the specific heat arises which is proportional to the specific area and to T^2 and appreciably higher than Montroll's result in the case of the free solid. The effect of approximations introduced during the computation is estimated. Available experimental data are not adequate for a critical test of the theory.

8399 DIFFERENCES IN LATTICE SPECIFIC HEATS IN THE NORMAL AND SUPERCONDUCTING PHASES by H. A. Boorse, A. T. Hirshfeld, and H. Leupold (Columbia U.); Phys. Rev. Lett., Vol. 5, pp. 246-248(L), Sept. 15, 1960

Measurements which indicate that the lattice specific heat in superconducting Nb is different from that of normal Nb is discussed. At 1.7°K the total superconducting specific heat was found to be less than the corresponding lattice heat in the normal state. The specific heat capacities of both the normal and superconducting Nb were measured below $T^2 = 5$. These measurements agreed with previous measurements and showed that C_s, the specific heat in the superconducting phase, at the lowest temperatures is smaller than the normal lattice heat in the same range.

8400 DEBYE Θ OF SOME CRYSTALS by S. K. Joshi and S. S. Mitra (Allahabad U.); Indian J. Phys., Vol. 34, pp. 532-534(L), Nov. 1960

The Debye temperatures θ for a number of crystals belonging to the cubic, hexagonal, and trigonal systems, including cadmium sulfide, are presented. The values were calculated from elastic constants recently measured at temperatures other than 0°K. For CdS the Debye $\theta = 214$°K.

8401 HEAT CAPACITY OF A SINGLE CRYSTAL OF $MnCl_2 \cdot 4H_2O$ by H. Forstat, G. O. Taylor, and B. R. King (Michigan State U.); J. Phys. Soc. Japan, Vol. 15, p. 528(L), Mar. 1960

Heat capacity measurements performed on a single crystal of $MnCl_2 \cdot 4H_2O$ in the temperature range 1.17°–4.43°K are discussed. The single crystal, which weighed 2.58 gm and was approximately 2x1.0x1.5cm in size, was grown from an aqueous solution at room temperature. A λ-type anomaly, characteristic of a phase transition ordering process, was observed at 1.60° ± 0.01°K. This transition has been identified as an antiferromagnetic-paramagnetic transition. This result agrees with the observation of Friedberg and Wasscher that an antiferromagnetic-paramagnetic transition takes place at 1.622°K. Friedberg and Wasscher used a sample which weighed approximately 88 gm and consisted of a large number of small crystals. The entropy change which occurs as the crystal cools through the transition temperature is estimated to be 3.50 cal/mole-deg.

8402 THE THERMAL CONDUCTIVITY OF SILICON AT LOW TEMPERATURES by B. T. Sandlin (U. Texas); Diss. Abstr., Vol. 21, p. 1609(A), Dec. 1960

Measurements of the thermal conductivity, k, between 2.5° and 10°K for three silicon samples with room-temperature resistivities of 2 - 7, 20 - 40, and 1200 - 1250 ohm-cm and between 2.5° and 150°K for two p-type silicon samples with room temperature resistivities of 14 - 35 and 1200 - 1250 ohm cm are reported. The thermal potentiometer technique was used for the measurements. At liquid-He temperatures, k was proportional to a power of the mean sample temperature, and this power was 1.1, 2.6, 2.9, 2.2, and 2.7 for the five samples respectively. Maximum values of k of 16 and 26 watts/c degree K occurred at 22° and 28°K for the last two samples. Each of these samples exhibited the Umklapp behavior in k for temperatures above these associated with its maximum value o k and below about 100°K. Between 100° and 150°K, k varie inversely as the temperature.

8403 THERMAL TRANSPORT IN DILUTE ALLOYS by G. K. White (CSIRO); Austl. J. Phys., Vol. 13, pp. 255-259, July 1960

Experimental values of the thermal resistivity for a number of elements, including Cu, Ag, Au, Ge, Si, Sb, and Bi are compared with theoretical values deduced from the anharmonic coupling between lattice vibrations. For Cu-, Ag-, and Au-rich alloys experimental and theoretical data for scattering of lattice waves by point defects are compared.

8404 THE THERMAL CONDUCTIVITY OF SUPERCONDUCTORS IN THE INTERMEDIATE STATE by N. V. Zavaritskii (Inst. Phys. Problems); Soviet Phys.-JETP, Vol. 11, pp. 1207-1214, Dec. 1960

The thermal conductivities of Pb, Sn, and Ga in the intermediate state measured between 0.15° and 3.7°K are discussed. It was found that the transition to the intermediate state is, for heat transport due to phonons, accompanied by an increase in thermal resistivity ΔW_{gi} which is proportional to T^{-3} over the whole temperature range. The magnitude of ΔW_{gi} is close to that calculated on the assumption that the phonons are scattered by conduction electrons in the normal state domains. For heat transport by electrons the increase in thermal resistivity ΔW_{ei} depends weakly on the impurity content of the specimen. Only the dependence of $\Delta W_{ei}/W_{es}$ on T/T_c is similar for all metals. This ratio decreases approximately 30 times between $0.4T_c$ and $0.9T_c$. At temperatures below $\sim 0.4T_c$ the value of ΔW_{ei} is close to that calculated on the assumption that the electron mean free path is limited by the boundaries of the intermediate state domains.

8405 RADIATION ENERGY TRANSFER AND THERMAL CONDUCTIVITY OF CERAMIC OXIDES by D. W. Lee and W. D. Kingery (MIT); J. Am. Ceram. Soc., Vol. 43, pp. 594-607, Nov. 1960

The heat transfer mechanisms in several ceramic oxides investigated from room temperature to 1250°C are discussed. The conductivity of normal sintered porous polycrystalline oxides results from phonon conduction, and results agree with theoretical expectations for the effect of impurities, structure, and temperature dependence. Single crystals, glasses, and low porosity aggregates show deviations from the expected phonon conduction which are attributed to a second mechanism of heat transfer, namely photon conduction. Measurements of photon conduction are related to infrared transmission, structure, and conditions of the measurements. Photon conduction can be a significant portion of the total heat conduction at high

emperatures; however, for normal polycrystalline ceramic ox-
es of porosities greater than 2 per cent, this contribution is
mall.

06 MAGNETOTHERMAL EFFECTS IN SILICON-IRON AL-OYS by N. N. Saunders and R. S. Tebble (U. Sheffield); oc. Phys. Soc., Vol. 76, pp. 282-294, Aug. 1960

Measurements of the reversible magnetothermal effect in two loys of silicon-iron are discussed. Analysis of the measure-nts by the method of Stoner and Rhodes, though hindered by e absence of reliable data on the basic magnetic constants of he materials, shows that over the field range studied the perimental coefficient b" is nowhere constant but tends to he 'rotational' value $b = (T/K_1)(\partial K_1/\partial T)$ as the field in-reases. The possibility that the variation is associated with anges in a 'spike' domain center is considered. It is con-uded that such a structure may be involved but cannot by it-elf account for the details of the observations.

407 THERMOELECTRIC POWER OF DILUTE COPPER AND ILVER ALLOYS by F. J. Blatt, M. Garber, R. H. Kropschot, nd B. Scott (Michigan State U.); Austl. J. Phys., Vol. 13, p. 223-237, July 1960

Measurements of the thermoelectric power of several dilute Cu nd Ag alloys are reported. The thermoelectric powers of the lloys were measured between ~8° and 350°K. The results ave been analyzed using the Mott-Fridel relation. Good greement between the calculated and measured thermoelectric owers can be obtained only if it is assumed that the absolute hermoelectric power of pure Cu and pure Ag consists of two ontributions: one, the usual free-electron contribution and nother, which is believed to be due to phonon drag. This honon drag contribution is of the correct magnitude and shows he expected temperature dependence. Moreover, the effect f alloying on the phonon drag contribution is in agreement ith theoretical estimates.

408 THEORETICAL BOUND ON THE THERMOELECTRIC IGURE OF MERIT by F. J. Donahoe (Franklin Inst.); Elect. ngrg., Vol. 79, pp. 488-490, June 1960

he upper limit for the figure of merit Z of thermoelectric ma-erials is discussed. It is pointed out that because of the de-endence of thermal conductivity K on electrical conductivity σ and of the dependence of the Seebeck coefficient S on σ n an extrinsic semiconductor there exists a value of S at which Z is a maximum. Three cases are considered. When the lat-ice thermal conductivity K_g is much greater than the thermal onductivity of the free charge carriers, Z has a maximum when $= \pm 172\,\mu v$ per degree; when K_g is comparable with the ther-al conductivity of the free carriers, Z has a maximum when $= \pm 172\,(K/K_g)\mu v$ per degree. This equation holds only for he charge carrier density $n_c \approx 2(2\pi m^* kT/h^2)^{3/2}$ where m^* is he density of states effective mass of the free charge carriers. When the lattice thermal conductivity is so small that it is egligible in comparison with the free charge carrier thermal onductivity, it is shown that the maximum figure of merit $Z_m = 1/8T\{\alpha^{1/2}(\alpha-2)^{1/2} - \ln[\alpha - 1 + \alpha^{1/2}(\alpha-2)^{1/2}]\}^2$ where α s the energy transported in units of kT.

Thermoelectric Properties of Semiconductors - See 8458

Thermoelectric Properties of Semiconductor Alloys and Ternary Compounds - See 8459

Coefficient of Thermal Expansion of BiPt - See 8288

MECHANICAL PROPERTIES

8409 THE TEMPERATURE DEPENDENCE OF THE ELASTIC CONSTANTS OF POTASSIUM BROMIDE SINGLE CRYSTALS by S. P. Nikanorov and A. V. Stepanov (Leningrad Physico-Tech. Inst.); Soviet Phys.-JETP, Vol. 10, pp. 1280-1281 (L), June 1960

Measurements of the temperature dependence of the elastic constants of potassium bromide single crystals in the temperature range from room temperature to the melting point are discussed. Using the composite oscillator method, measurements of Young's modulus and the shear modulus were made on specimens cut along the [100] and [110] directions. The experimental details and the accuracy of the measurements are discussed. By extrapolating the experimental data to absolute zero, the following values for the elastic constants at T = 0°K were obtained: $S_{11} = 24.0 \times 10^{-13}$, $S_{44} = 180 \times 10^{-13}$, and $S_{12} = -2.8 \times 10^{-13}\,cm^2/dyne$.

8410 ELASTIC MODULI OF SINGLE-CRYSTAL RUTILE (TiO_2) by G. L. Vick, L. E. Hollander, and A. E. Brown (Lockheed); Bull. Am. Phys. Soc., Ser. II, Vol. 4, p. 463 (A), Dec. 28, 1959

Elastic moduli measured in rutile were discussed. By means of a 10 Mc ultrasonic pulse technique the moduli C_{11}, C_{33}, C_{44}, and C_{66} were found to have the following values (in units of 10^{12}dynes/cm^2), respectively: 2.8 ± 0.3, 4.6 ± 0.4, 1.2 ± 0.1, and 1.6 ± 0.2 and by combining ultrasonic pulse data and Bridgman's compressibility data the moduli C_{12} and C_{13} were found to have the values 1.8 ± 0.2 and 1.4 ± 0.2, respectively. Good agreement was obtained with previously computed values except in the case of C_{33}. However, only nearest-neighbor interactions were considered in this analysis. C_{33} was also measured in oxygen-deficient rutile having a resistivity of 10^{-1} ohm-cm. No change within the limits indicated was observed, but the acoustic attenuation was greatly increased. The attenuation is also much greater in the [100] than in the [001] crystal direction in both reduced and oxidized rutile.

8411 ELASTIC CONSTANTS OF YTTRIUM SINGLE CRYSTALS IN THE TEMPERATURE RANGE 4.2°-400°K by J. F. Smith and J. A. Gjevre (Iowa State U.); J. Appl. Phys., Vol. 31, pp. 645-647, Apr. 1960

Determination of the five independent elastic constants for yttrium single crystals by the pulse-echo technique over the temperature range, 4.2°-400°K is reported. The experimental values extrapolated to 0°K are: $C_{11} = 8.34 \pm 0.02$, $C_{33} = 8.01 \pm 0.02$, $C_{44} = 2.690 \pm 0.006$, $C_{12} = 2.91 \pm 0.03$, and $C_{13} = 1.9 \pm 0.4$ in units of 10^{11} d/cm^2. The degree of elastic anisotropy is

low throughout the entire temperature range. The curves illustrating the temperature dependence of the elastic constants show several inflections, and the curve for C_{11} crosses that for C_{33} near 390°K. The behavior is somewhat unusual, and is probably explicable on the basis that the degree of band overlap in yttrium is quite sensitive to interatomic spacing. Such a sensitivity has previously been postulated to explain the temperature dependence of the Hall coefficient.

8412 THE INFLUENCE OF TEMPERATURE AND STRAIN RATE ON THE FLOW STRESS OF MAGNESIUM SINGLE CRYSTALS by Z. S. Basinski (Natl. Res. Counc., Ottawa); Austl. J. Phys., Vol. 13, pp. 284-298, July 1960

The temperature and strain-rate dependence of the flow stress of Mg single crystals in the temperature range 1.45°-248°K are measured. Some incidental observations were also made on the form of the stress-strain curves and the appearance of slip lines. The deformation characteristics show close similarity with those of the fcc metals.

8413 MAGNETIC-FIELD DEPENDENCE OF THE ULTRASONIC ATTENUATION IN METALS by M. H. Cohen and M. J. Harrison (U. Chicago); Phys. Rev., Vol. 117, pp. 937-952, Feb. 15, 1960

A self-consistent, semiclassical treatment for the attenuation of a sound wave by a free-electron gas in a positive background which supports the sound wave is given. Emphasis is placed upon the kinds of magnetic-field dependence which can be found under a wide range of values for the magnetic field, frequency, and mean free path. Applications of the general formalism include propagation parallel and perpendicular to the magnetic field. The special phenomena studied include geometric resonances, cyclotron resonances, and magneto-plasma resonance. A qualitative physical interpretation of the various effects found in the detailed calculations is also presented.

Ultrasonic Absorption in Synthetic Quartz - See 8364

8414 DEPENDENCE OF MECHANICAL Q AND YOUNG'S MODULUS OF FERROELECTRIC CERAMICS ON STRESS AMPLITUDE by R. Gerson (Clevite); J. Acoust. Soc. Am., Vol. 32, pp. 1297-1301, Oct. 1960

The effects of stress amplitude on the mechanical properties of several barium-titanate and lead-titanate-zirconate compositions are discussed. The mechanical Q was found to decrease to about 1/3 of its low signal value at a dynamic stress of about 1500 psi. No further decrease occurred with stress up to about 4000 psi, the limit of these tests. Young's modulus decreased by about 5 per cent in materials used in power transducers, and by about 25 per cent in special compositions having low coersive force. It is concluded that the mechanical quality at the highest stress amplitude is still sufficiently high so that it will not seriously affect the efficiency of a well-matched acoustic transducer.

RESISTORS

8415 VACUUM-DEPOSITED METAL-FILM RESISTORS: APPLICATION TO POTENTIOMETER TRACKS [in French] by J. Vermandé (Lab. Cent. de Res.); Onde Elect., Vol. 40, pp. 466-473, June 1960

The fabrication of thin metallic film resistors and their applications in the field of high temperature components are described. Oxide films and vacuum deposited films are discussed. Manufacture of the latter is described in more detail, including support, contacts, nature of the film, technique of evaporation, stabilization of the film, finishing and appearance. Comparative properties of metal film resistors and other types of resistors available on the market are discussed, along with stability, temperature coefficient, voltage coefficient noise, HF properties, performance at high temperatures and under climatic conditions. The possible extension to potentiometer tracks is mentioned.

8416 RESISTORS OF DIFFERENT NONLINEARITY FORMED FROM OXIDE SEMICONDUCTORS [in Russian] by M. M. Nekrasov (Kiev Polytech. Inst.); Izv. VUZ Fiz., No. 1, pp. 191-196, 1960

The characteristics of oxide semiconductor resistors are discussed. Resistance as a function of capacitance and temperature is described and the nonlinearity is cited. Resistors of type R_U, where voltage remains constant for current variations, and of type R_i, where current remains constant for voltage variations, are discussed.

DIODES

8417 SEMICONDUCTOR CAPACITOR by E. I. Doucette and C. J. Spector (Bell Labs.); U.S. Pat. 2,964,648, Issued Dec. 13, 1960

A variable capacitance diode having a very abrupt step or change in capacitance at a particular bias voltage is described. A semiconductor p-n junction diode in the form of a thin circular wafer, having a p-n junction parallel to the major faces of the wafer, contains a concentric annular trench with a depth that approaches the junction. Application of a reverse bias at low voltages provides a capacitance due to the entire cross-sectional area of the wafer. At a higher voltage the depletion layer boundary intersects the boundaries of the trench decreasing the area of the effective capacitance and providing, from that voltage on, a smaller area capacitor.

8418 TUNNELING PROBABILITY IN GERMANIUM p-n JUNCTIONS by Y. Furukawa (Elect. Commun. Lab.); J. Phys. Soc. Japan, Vol. 15, p. 730(L), Apr. 1960

Measurements of the tunnel current in Esaki diodes made by

alloying pellets of 0.5 per cent Ga, 99.5 per cent In on As- or Sb-doped Ge are discussed. The log I_{max} per cm^2 versus $(1/n + 1/p)^{1/2}$ curves obtained from these measurements have slopes of -2.72×10^{10} for Sb-doped Ge and -3.16×10^{10} for As-doped Ge. These values are very close to -3.2×10^{10} the value determined by means of a theoretical expression for the tunneling probability in step junctions. It is suggested that the dependence of I_{max} per cm^2 on donor impurity is due to the change of state density or the change of the effective mass with impurity.

8419 PLANAR FUSED GaAs-DIODES by Yu. M. Burdukov, A. N. Imenkov, D.N. Nasledov and B.V. Tsarenkov (Phys.-Tech. Inst., Leningrad); Sov. Phys.-Solid State, Vol. 3, pp. 721-723(L), Sept. 1961

Properties of planar fused GaAs diodes are described. P-n junctions were formed by fusing either Zn or a Zn-Au alloy into GaAs discs formed from single crystal material. Oscillograms of static current-voltage characteristics of the diodes were made at 25° and 300°C. The forward branch of the characteristics could be represented by an empirical formula and the temperature dependence of coefficients in the formula is discussed. The appearance of two exponential sections in the forward branch of the characteristics is explained in terms of surface properties. The cutoff voltage of the forward branch is less than the contact potential difference and diminishes with temperature rise. The incremental resistance at zero voltage is determined by the generation recombination process. The reverse branch can also be described by an empirical formula and breakdown voltage increases with temperature.

8420 MEASUREMENTS ON POWER CONVERSION GAIN AND NOISE RATIO OF THE 1N26 CRYSTAL RECTIFIERS by A.Dymanus and A. Bouwknegt (Rijksuniversiteit, Utrecht); Physicia, Vol. 26, pp. 115-126, Feb. 1960

Measurements of the power conversion gain G and noise ratio of a number of 1N26 Si rectifiers are discussed. The noise ratio was investigated both with microwave excitation (10^{-6} - 10^{-3}w at 24 kMc) and with dc excitation by currents up to 100 μa in the forward direction and up to 20 μa in the reverse direction. The results confirm the reverse frequency dependence of n in the frequency region from 100 to 455 kMc and the independence of G (~ 0.2 for sensitive rectifiers) of microwave power at powers higher than about 3×10^{-4}w. There is, however, a considerable discrepancy between the present results and the results of other investigators on G at powers below ~ 3×10^{-4}w, and on the power and dc current dependence of n for microwave and dc excitation, respectively. A possible explanation for the discrepancy of the power dependence of n is suggested. However, no explanation can be given of the saturation of n at dc excitation by currents in the forward direction through sensitive rectifiers. No n-saturation was observed at microwave excitation.

8421 GERMANIUM-GALLIUM ARSENIDE CONTACTS by R. L. Anderson (Syracuse U.); Diss. Abstr., Vol. 21, p. 1603(A), Dec. 1960

A method of producing an epitaxial contact between Ge and GaAs was described. The junction between these semiconductors was abrupt. An energy band model of the junction region was proposed and measurements on diodes made from this material were interpreted in accordance with the model. Measurement on n-n junctions and n-p junctions agreed well with the proposed theory. A method was developed to use transition capacity measurements to determine the net ionized impurity density as a function of distance from the junction. It was found that n-type GaAs tended toward p-type near the surface as a result of the treatment used in producing the junction.

8422 P-N JUNCTIONS BETWEEN SEMICONDUCTORS HAVING DIFFERENT ENERGY GAPS by T.K. Lakshmanan (Daystrom); Proc. IRE, Vol. 48, pp. 1646-1647(L), Sept. 1960

P-n junctions formed between quite dissimilar semiconductors such as selenium and nondegenerate semiconducting cadmium oxide are discussed. The Se-CdO junction can be formed by the reactive sputtering of a thin layer of CdO on a layer of selenium. Selenium is a p-type semiconductor with an energy gap of 1.6 ev; CdO is an n-type semiconductor with an energy gap of about 2 ev. Conductivity and Hall constant measurements performed on CdO films are discussed. The general equations for current flow in these junctions, under dark conditions, are $J_h = e\mu_h pE^{(h)} - eD_h \nabla p$ and $J_e = e\mu_e nE^{(e)} + eD_e \nabla_n$ where the superscript and subscript e and h refer to electrons and holes, respectively.

Microplasma Phenomena in Si Junctions - See 8445

8423 SILICON POWER DIODES [in French] by F. Weil (Philips); Acta Electronica, Vol. 4, No. 4, pp. 533-548, 1960

The practical and theoretical aspects of Si rectifiers are discussed. For diodes of good direct characteristic and high breakdown voltage, the p-i-n and p-π-n structures are found superior. Fabrication features of the diodes are discussed and practical considerations, i.e., thermal and electrical stability, overload protection, security margin and cooling, are surveyed for "in circuit" conditions.

8424 MANUFACTURE OF SEMICONDUCTOR RECTIFIER DEVICES by L.J.C. Connell (GE Ltd.); U.S. Pat. 2,965,818, Issued Dec. 20, 1960

The fabrication of Ge p-n junction rectifiers is described. A Ge wafer is soldered to a hollow Cu block which is cooled by means of an internal flowing liquid, and a p-n junction is formed on the upper surface of the wafer by alloying an In pellet. An electrode with a flexible lead attached to it is cold-pressure welded to the In contact with the junction. A metallic envelope is then placed over the device so that the flexible lead makes contact with a thimble-like terminal which is insulated from the rest of the device. The device is sealed by resistance seam welding, ring welding, argon arc welding, or cold welding the envelope to a flange brazed to the Cu block.

8425 SEMICONDUCTOR DEVICE by P.J.W. Jochems (Philips); U.S. Pat. 2,926,290, Issued Feb. 23, 1960

A one step technique for forming alloyed junctions of known dimensions in a semiconductor and making contact to the junction is described. An electrode consisting of a low melting point metal and a high melting point metal is heated in contact with the semiconductor surface. The only pressure between the two is the weight of the electrode itself. The low melting component may be the core of the electrode, a coating on a high melting point core, or the filler for pores in the electrode. Electrodes can be formed simultaneously on the opposite surfaces of the wafer by clamping the wafer between a bent electrode wire and heating the assembly. When the assembly is cooled, the electrode loop is cut.

Low Resistivity Ge for Esaki Diodes - See 8200

8426 DIODE by J.A. Herbst (Bogue); U.S. Pat. 2,956,214, Issued Oct. 11,1960

Improved diode thermal dissipating characteristics, achieved by use of spring members that resiliently force the surfaces of a semiconductor diode into intimate contact with heat-conducting discs, are discussed. The diode housing consists of a ring shaped ceramic insulating material sealed at the ends to metal discs by annular strips of solder. Maximum semiconductor surface contact to the metal discs is provided by a set of metal spring members in bowed form, arranged at right angles to a second set of similar spring members and interleaved. The intersecting mid-portions of the spring members are formed with registering openings for receiving the diode assembly.

Heat Sinks for Diodes - See 8446

8427 SEMICONDUCTOR RECTIFIER ASSEMBLIES by P.M. Tipple (English Elect. Valve); U.S. Pat. 2,960,639, Issued Nov. 15, 1960

The use of a ring of solid dessicant to maintain the dryness of the gas in a hermetically sealed rectifier is described. The solid dessicant eliminates the difficulties encountered when powdered dessicants are used. The dessicator ring may be made, for example, of molecular sieved aluminum sodium silicate. The ring also prevents the vapors produced during the final brazing of the envolope from reaching the p-n junction.

TRANSISTORS

8428 AUTOMATIC INSTRUMENT FOR THE MEASUREMENT OF TRANSISTORS [in French] by M. Guemene and L. Caille (Soc. Lignes Tel. and Tel.); Onde Elect., Vol. 40, pp. 772-781, Oct. 1960

The principle and design of an automatic instrument for the measurement of transistor properties is described. The instrument consists of a measuring device which provides in analogue form the results of a series of measurements made of the various characteristics of the transistor, and a reading and recording device which reproduces these results on a punched card. A numerical analogue converter associated with a card punch is also described.

8429 HIGH GAIN SEMI-CONDUCTOR DEVICES by L.E. Barton (RCA); U.S. Pat. 2,965,820, Issued Dec. 20, 1960

A semiconductor device having an improved gain due in part to the fact that the emitter and collector electrodes are of different metals is described. An example of an n-type Ge crystal, having the emitter and collector electrodes in high-resistance, rectifying, point-contact with the Ge is presented. The collector electrode consists of an alloy of the donor type to enhance electron injection into the n-type Ge. The emitter may consist of steel, copper, beryllium copper, duralumin, brass, etc. but not an alloy of the donor type. No definite theory of operation of the device is advanced.

8430 THEORETICAL ASPECTS OF THE POWER TRANSISTOR [in French] by J. Revuz (Labs. d' Electronique et de Phys. Appl.); Acta Electronica, Vol. 4, No. 4, pp. 549-559, 1960

The measurement of electrical and thermal characteristics of power transistors is discussed. A method which employs certain hypotheses to simplify the computation is described. The elements of semiconductors, junctions, and transistors are also discussed.

8431 AN ALLOYED SILICON POWER TRANSISTOR [in French] by F. Desvignes, J.J. Brissot, and J. Revuz (Labs. d' Electronique et de Phys. Appl.); Acta Electronics, Vol. 4, No. 4, pp. 561-593, 1960

A study of transistor design methods and construction processes in order to determine their ability to produce transistors of given characteristics is presented. Examples are given which compare design characteristics, performance and actual structural data (geometry, electric properties of the semiconducting regions of the transistor, etc.) for nine transistors.

8432 SEMI-CONDUCTOR DEVICES by R.C. Hibberd (Brit. Thomson-Houston); U.S. Pat. 2,966,434, Issued Dec. 27, 1960

A method of fabricating a multi p-n junction device is described. A two step process is used in which one or more p-n junctions are formed by alloying n-type Ge with p-type Si, then fusing In to the Ge to form a further p-n junction. As the latter step requires a much lower temperature than is used in forming the Ge-Si junction, the Ge-Si junction will not be damaged or affected by the formation of the In-Ge junction.

8433 SEMICONDUCTOR DEVICES by R.J. Zelinka (Minn.-Honeywell); U.S. Pat. 2,923,870, Issued Feb. 2, 1960

A composite tetrode transistor consisting of two concentric, interconnected tetrode junction transistors on one semiconductor wafer is described. The wafer is cut from a crystal which has

igh resistivity inner region and a low resistivity outer region. e transistor fabricated on the high resistivity inner region is input stage of the device, while that fabricated on the ter part of the crystal is the output stage of the composite evice. The high resistivity material results in low leakage urrent and the low resistivity material in the output section rmits a large current density.

34 LOW-FREQUENCY PARAMETERS OF AN AMPLIFYING PACISTOR-TRIODE [in Russian] by A.L. Zakharov (Radio lectronics Ministry, USSR); Izv. VUZ Radiotek., Vol. 3, o. 2, pp. 233-246, 1960

investigation of the dependence of the low frequency rameters of a three electrode spacistor on its geometry and erating region is reported. The parameters, transconduct-nce, and voltage gain coefficient are calculated on the basis f a practical spacistor model.

35 ON THE FREQUENCY PROPERTIES OF A SPACISTOR-IODE [in Russian] by A.L. Zakharov (Radio Electronics inistry, USSR); Izv. VUZ Radiotek., Vol. 3, No. 4, pp. 31-440, 1960

n analysis of properties of an amplifying spacistor-triode at evated frequencies is presented. The maximum operating equency of a spacistor is computed. Frequency properties of ansistors and spacistors are compared and certain recommen-tions for the construction of high-frequency spacistors are ven.

436 AN n-p-n FUSION ALLOY SILICON TRANSISTOR FOR AVALANCHE MODE" OPERATION by R.C. Wonson and W. . McCarthy (Raytheon); 1960 IRE Intl. Conv. Rec., Part 3, . 10-16

peration of an n-p-n Si transistor in the "avalanche mode" described. Normally, the transistor has a very low frequen-limitation, having switching times of approximately two icroseconds. When operated in the "avalanche mode," the ansistor exhibits switching times of two millimicroseconds or etter. Its high temperature performance has been examined detail. Measurement techniques are described as well as expensive methods of determining performance. Practical rcuit applications are discussed with particular emphasis on completely designed pulse generator.

437 LUMPED-MODEL ANALYSIS OF SPACE-CHARGE IDENING by J.F. Gibbons and D.A. Linden (Stanford U.); roc. IRE, Vol. 48, p. 1920(L), Nov. 1960

pace-charge layer widening effects in transistors are analyzed. tilizing a lumped model of a transistor, two equivalent tech-iques are used to determine the collector conductance and e voltage feedback factor which result from a small change collector voltage. In both cases the results agree with those btained by Early.

8438 REVERSION OF BASE CURRENTS IN THE DIPPING GROWN DIFFUSED TRANSISTORS by M. Yasufuku and T. Kawamura (Fuji Denki); J. Electrochem. Soc. Japan, Vol. 28, No. 4-6, pp. E-74 - E-76, 1960

Measurements made on dip grown diffused Ge transistors with two types of collector contacts are discussed. Contacts were made by soldering a Ni wire with an alloy of Pb and Sn at 300°-400°C and by alloying with In at 500°-550°C. It was found that the drop in base current in the grounded base configuration and the negative resistance in the grounded emitter configuration which occur in devices utilizing Pb-Sn contacts is due to electron injection from the collector contact. These effects can be eliminated by using alloyed In collector contacts.

8439 AVALANCHE CARRIER MULTIPLICATION IN JUNCTION TRANSISTORS AND ITS IMPLICATIONS IN CIRCUIT DESIGN by M.L.N. Forrest (Intl. Comp. and Tab. Ltd., England); J. Brit. IRE, Vol. 20, pp. 429-439, June 1960

Theories of junction breakdown and transistor action necessary to account for the observed characteristics of avalanche carrier multiplication are surveyed. The implications of these characteristics in circuit design are discussed and certain special techniques for avoidance of anomalous operation in conventional circuits are described. Avalanche multiplication may be used to obtain useful device characteristics, and circuits for exploitation of these are surveyed. Methods of measurement of avalanche characteristics are outlined.

8440 LARGE SIGNAL OPERATION OF A SEMICONDUCTOR TRIODE [in Russian] by T.M. Agakhanian (Engrg.-Phys. Inst., Moscow); Izv. VUZ Radiotek., Vol. 3, No. 1, pp. 87-93, 1960

The fundamentals of a method of analyzing the large signal operation of a semiconducting triode are presented. The influence of the electric field existing in the base is discussed and an equivalent circuit of the triode is given.

8441 A CONTROLLED DIFFUSION PROCESS FOR INDIUM IN n-TYPE GERMANIUM by F. Barson, M.J. Dyett, C. Karan, and W.E. Mutter (IBM); J. Electrochem. Soc., Vol. 107, pp. 459-461, May 1960

The fabrication of n-p-n diffused base Ge transistors is discussed. The p-type diffused layer is produced by heating a Ge wafer containing a thin evaporated film of In on one surface in a forming gas atmosphere at 875°C. The film of In serves both as a getter for Cu impurities in the Ge, thus preventing thermal conversion, and as a source of the diffusant. The evaporated layer is lapped off following the completion of the diffusion operation. When a film of tin-indium is used as the getter source, the concentration of In in the film is reduced. Since the vapor pressure of the solute is proportional to its mole fraction in the solution, the vapor pressure of the In at the diffusion temperatures and C_0 decrease. This reduction in C_0 simplifies the emitter alloying process.

8442 POWER TRANSISTORS by A. Herlet (Siemens AG); U.S. Pat. 2,924, 760, Issued Feb. 9, 1960

A technique for increasing the power handling capacity of alloyed junction power transistors is described. The efficiency of these devices is improved by employing emitter strips $2\sqrt{2}\,L_p$ wide, where L_p is the diffusion length in the base region at high injection levels. The strips may be circular, straight, or comb-shaped. In each case base strips, also $2\sqrt{2}\,L_p$ wide, are employed between the emitter strips.

8443 SEMICONDUCTOR DEVICES AND THEIR MANUFACTURE by E. Paskell (McGraw-Edison); U.S. Pat. 2,964,435, Issued Dec. 13, 1960

A method of providing a large area junction type semiconductor device having particular application in the field of overvoltage protection of electric circuits is described. A single crystal semiconductor material having high resistivity is masked with flat quartz plates leaving the outer edges of the crystal exposed. The uncovered areas of the semiconductor are diffused with an impurity-converting dopant. The edges of the slice are trimmed, following diffusion, resulting in a concentration of impurities which are highest at the surface, decreasing toward the interior, so that breakdown will occur within the body of the slice rather than at the surface.

8444 LOCATION OF DIFFUSED p-n JUNCTIONS ON GERMANIUM BY ELECTRODEPOSITION OF COPPER by R. Glang (Diamond Ord. Fuze Labs.); J. Electrochem. Soc., Vol. 107, pp. 356-357, Apr. 1960

A technique for delineating diffused Ge p-n junctions is described. A small piece of a wafer is angle lapped to expose the junction and the surface is cleaned. A drop of a plating solution prepared by dissolving approximately 20 gm of $CuSO_4 \cdot 5H_2O$ in 80 ml of water and adding about 1 ml of concentrated (49 per cent) HF is placed carefully on the beveled surface where the junction is believed to be located. A small dc voltage determined by the sample dimensions and sheet resistivity is then applied between two adjustable metal probes, one of which is in contact with the beveled p-region and the other with the nonbeveled n-region, at 20 sec intervals for about 1 sec. The p-region is the cathode and the Cu is plated on the p-side of the junction. Photographs of delineated junctions are presented.

8445 VISIBLE LIGHT EMISSION AND MICROPLASMA PHENOMENA IN SILICON p-n JUNCTION. Part II. CLASSIFICATION OF WEAK SPOTS IN DIFFUSED p-n JUNCTIONS by M. Kikuchi (Electrotech. Lab., Tokyo); J. Phys. Soc. Japan, Vol. 15, pp. 1822-1831, Oct. 1960

The identification of weaknesses in diffused Si p-n junctions is discussed. The weaknesses were uncovered during study of the visible light emission and plastic phenomena of the junctions. The weaknesses can be roughly classified into two groups, one including tiny weak spots which reveal microplasma current pulses at certain characteristic bias voltages, and the other including tiny spots which contribute "soft" components to the reverse current without accompanying microplasma pulses. The latter type of spots could be produced by scratching the surface of the junction with a tungsten needle; the former type could not. Typical experimental results are given and the correlation between those weak spots and the current voltage characteristics is discussed. The defects described do exist in real diffused junctions.

8446 HEAT DISSIPATING ELECTRONIC MOUNTING APPARATUS by J. Rosenbaum; U.S. Pat. 2,965,819, Issued Dec. 20, 1960

A heat sink for use with transistors and diodes is discussed. The unit consists of a metal plate and integral, parallel fins extending from one side of the plate. Metals such as Cu, Al, or Ag can be used. The semiconductor device is mounted on the plate and the heat sink is mounted on an electronic chassis. A convention current, produced by heating the air between the fins, cools the semiconductor device. The heat sinks may be interleaved for high efficiency.

8447 HEAT DISSIPATORS FOR TRANSISTORS by J.C. McAdam (Intl. Electronic Res.); U.S. Pat. 2,964,688, Issued Dec. 13, 1960

Heat dissipators, adapted to cooling transistors, together with a method of applying to the dissipators a coating to give a highly desirable dielectric characteristic, are discussed. The dissipator comprises an end which is circumferentially continuous and an end which is made up of a multiple number of spring fingers, directed obliquely inward toward the transistor. A series of tabs are stamped from the wall of the dissipator and bent inwardly to form openings which aid convection currents. The coating, 0.0005 to 0.001-in thick, consists of a composite filled plastic material made up of a synthetic plastic polymerized resin in which is mixed finely powdered molybdenum disulfide.

FUNCTIONAL UNITS

Design of Functional Units - See 8487

8448 PRINTED-CIRCUIT BOARDS: A GUIDE TO FABRICATING TECHNIQUES by W.J. Prise (Lockheed); Electronic Design, Vol. 9, pp. 42-45, Nov. 22, 1959

A tabular presentation of step-by-step procedures involved in each of four basic printed-circuit processes is given. At each step, potential problem areas are pointed out. The four methods are: Method A, boards are photo-etched, conductive pattern is solder-coated and eyelets are placed in holes drilled through the solder-coated foil; Method B, board is photo-etched using gold plating as an etching resist. Conductive pattern of the board is gold-plated and gold-plated through-holes are employed; Method C, board is photo-etched in the same manner as in process B. Conductive pattern is gold-plated with gold-plated through-holes. Eyelets are installed after gold-plating, and Method D, similar to process A except in the method of installing the eyelets. In this process, eyelets are resistance-

used to the conductive pattern of the board. Characteristics which a well manufactured printed circuit board should have are outlined.

MAGNETOELECTRIC DEVICES

8449 HALL EFFECT MEMORY DEVICE by H.L. Barney and E.P. Burns (Bell Labs.); U.S. Pat. 2,964,738, Issued Dec. 13, 1960

Electrical circuits with the ability to store electrical pulse signal information within a magnetic core by establishing either of two alternative magnetic conditions and to recover that information rapidly and unequivocally but without any destruction of the stored information are described. This ability is achieved by the employment of a rectangular core constructed of material having a rectangular hysteresis loop and having a magnetic gap into which a Hall effect plate is inserted.

8450 HALL EFFECT AMPLIFIER by H.K. Henisch (Sylvania); U.S. Pat. 2,877,309, Issued Mar. 10, 1959

An improved Hall effect amplifier possessing increased sensitivity and amplification is described. The circuit comprises an H-shaped structure composed of p- or n-type semiconductor material. The crossbar of the H contains a reverse biased p-n junction. An input signal applied to the side members of the structure causes current flow in these members. Hall effect is achieved through the imposition of a magnetic field perpendicular to the current flow. The displacement voltage generated will create current flow in the p-n junction. This current flow represents , in amplified form, the input signal. Additional amplification is obtained by placing two additional p-n junctions in the carrier deficient region of each leg and adding the signals created therein to the crossbar signal.

8451 THE POSSIBILITY OF A SELF-SUSTAINING CORBINO DISK by D. Midgley (U. St. Andrews); Nature, Vol. 186, p. 377(L), Apr. 30, 1960

Devices which utilize a Corbino disk are discussed. Without the impressed axial field a disk can serve as a two-state digital computer element in which the two states are self-sustaining current vortices of opposite spin. A magnetic power amplifier which utilizes the increase in total flux with a ring of given width towards the center of the disk and a bistable trigger circuit constructed by adding a magnetic feedback path to the power amplifier are also described.

8452 SEMICONDUCTOR AMPLIFIERS AND GENERATORS WITH CARRIERS HAVING NEGATIVE EFFECTIVE MASS by N.G. Basov, O.N. Krokhin, and Yu. M. Popov (Lebedev Phys. Inst.); Soviet Phys.-JETP, Vol. 11, pp. 720-721(L), Sept. 1960

Amplification and generation of electromagnetic waves in semiconductors by means of the negative effective mass of carriers is discussed. It is shown that amplification is possible only if in some energy interval $\epsilon_2 - \epsilon_1$ there are states such that $\delta F(\epsilon)/\delta\epsilon > 0$. The condition $\delta F(\epsilon)/\delta\epsilon > 0$ cannot be attained by means of a constant electric field. Such states can, however, be obtained by means of monochromatic radiation or of a pulsed electric field.

PHOTODEVICES

8453 ON THE TEMPERATURE DEPENDENCE OF THE PHOTOCONDUCTIVE DECAY TIME OF FILMS OF THE LEAD SALTS by F.M. Klaassen, J. Blok, H.C. Booy, and F.J. deHoog (Vrije U., Amsterdam); Physica, Vol. 26, pp. 623-628, Aug. 1960

Measurements performed on the temperature dependence of the relaxation time of PbS photodetectors are discussed. The results were compared with a theoretical expression for this time, following the kinetics of carrier transitions in semiconductors with trapping of minority carriers. Good agreement was found. From the results we found for the value of the energy depth of the trapping centers 0.165 ev. Moreover, it is concluded that the minority carriers are retrapped many times before recombination takes place.

Photovoltaic Effect in CdS - See 8388

8454 ELECTROLUMINESCENT DEVICES by S. Yando (Sylvania); U.S. Pat. 2,922,923, Issued Jan. 26, 1960

An electroluminescent device for observing the interaction between three pulses is described. One pulse train is applied to a pair of electrodes on the opposite faces of one end of a piezoelectric strip, and a second pulse train is applied to a pair of contacts on opposite faces at the other end of the strip. A third pulse train is applied between an electrode on one surface of the piezoelectric strip, between the end contacts, and a transparent electrode of the same surface area applied to an electroluminescent layer on the other surface of the piezoelectric strip. The electric fields associated with the elastic waves produced by the first two pulse trains and the electric field of the third pulse train produce a spot of light on the electroluminescent layer. The position of the spot depends on the relative timing of the pulses. By continuously varying the relative timing, the spot of light will scan the strip at a velocity dependent on the rate of timing variation. The light intensity of the spot can be modulated by varying the pulse amplitude.

8455 COLD CATHODE LIGHT SOURCE by L. Thorington (Duro-Test); U.S. Pat. 2,955,221, Issued Oct. 4, 1960

A light source using a cold cathode and employing cathode-luminescence as the source of light is described. Use is made of the phenomenon of electro-luminescence for initiating the operation of cathode-luminescent light sources, thus eliminating the need of a starting element. The electro-luminescent and cathode-luminescent materials take the form of a mechanically-mixed coating or of a single phosphor which exhibits both electro-luminescent and cathode-luminescent properties. When a potential of from 200 - 300 v is applied across the electrodes, the electro-luminescent particles are caused to luminesce, thereby sensitizing a magnesium oxide coating (cathode) which then starts emitting electrons. These electrons bombard the cathode-luminescent layer resulting in the efficient generation of light.

8456 EXPERIMENTAL STUDY OF LIGHT AMPLIFICATION IN A "PHOTOCONDUCTOR-FERROELECTRIC-ELECTROLUMINOR" ELEMENT by I.N. Orlov and N.I. Taborko; Optics and Spectrosc., Vol. 9, pp. 329-331, Nov. 1960

A circuit for an electroluminescent image amplifier element in which a photoconductor and a ferroelectric material are

used is described. A qualitative basis is given for choosing the parameters of this circuit. Experimental characterisitcs are listed for a single-element light amplifier. It is shown that using a zinc sulfide electroluminor with green luminescence, a photoconductive cadmium sulfide powder and a single crystal of triglycin sulfate, it is possible to obtain a light flux amplification coefficient of about 50,000 at low input illumination (of the order of 0.01 flux).

THERMAL DEVICES

8457 SEMICONDUCTING DIAMONDS AS THERMISTORS by G.B. Rodgers and F.A. Raal (Diamond Res. Lab.); Rev. Sci. Instr., Vol. 31, pp. 663-664, June 1960

The fabrication and properties of semiconducting diamond thermistors are discussed. The thermistors are made of small cylinders drilled out of the semiconducting parent stone. Platinum leads are attached to the diamond by heating the leads together with a silver-copper eutectic at 1200°C for ~1 min in an argon atmsophere and allowing the device to cool in the gas. Semiconducting diamond is extremely resistant to corrosion and abrasion, making it suitable for use under severe ambient conditions, has excellent thermal conductivity, low specific heat, can withstand high pressures, and has a negative temperature coefficient of resistance α below ~ 350°C. Over the same temperature range, diamond thermistors do not have as large an α as oxide thermistors and α decreases more rapidly with increasing temperature up to 350°C but is still greater than for platinum resistance thermometers up to 250°C.

8458 SEMICONDUCTOR THERMOELECTRIC ELEMENTS AND THEIR APPLICATIONS [in French] by N. Thien Chi and J. Vergnolle (Ctr. de Recherches Phys. Chem., Comp. Gén. T.S.F.); Onde Elect., Vol. 40, pp. 450-465, June 1960

Model theories about thermoelectric properties of semiconductors which make them clearly superior to metals are discussed. A detailed account is given of the thermocouple as a current generator (Seebeck effect) or as a heating and cooling element (Peltier effect); the theory and the practical performance are compared.

8459 SEMICONDUCTOR MATERIALS FOR THERMOELECTRIC POWER GENERATION UP TO 700°C by F.D. Rosi, J.P. Dismukes, and E.F. Hockings (RCA); Elect. Engrg., Vol. 79, pp. 450-459, June 1960

Experimental studies of the thermoelectric properties of Bi_2Te_3 alloys, ternary semiconductor compounds, and InAs-GaAs alloys over the temperature range 25° to 700°C are discussed. A power-generating thermocouple has been constructed with n-type Bi_2Te_3 - 25 per cent Bi_2Se_3 and p-type Bi_2Te_3 - 40 per cent Sb_2Te_3 - 10 per cent Sb_2Se_3 alloys. The power generator exhibited a maximum efficiency of 6.5 per cent with a temperature difference between the hot and cold junctions of 300°C. The p-type ternary compound $AgSbTe_2$ and the p-type alloy $AgSbTe_2$ - 90 per cent GeTe were found to be very promising materials for use in thermoelectric power generation. An average figure of merit of ~ 1.75×10^{-3} per degree was obtained with $AgSbTe_2$ over the temperature range 175° to 525°C. N-type InAs-GaAs alloys have shown figures of merit up to 1×10^{-3} per degree at 700°C.

8460 PELTIER COOLING OF HOTSPOTS by D.S. Gage (Northwestern U.); Proc. Natl. Electronics Conf., Vol. 16, pp. 134-138, 1960

Utilization of the Peltier effect to move heat "downhill" (i.e., from a higher to a lower temperature) is discussed. The figure of merit is shown to be α^2/ρ. When moving heat downhill, the Peltier cooling obtained from reported materials is small when compared to the heat-conduction cooling obtained from Cu. The possible existence of other materials which will make practical the Peltier cooling of hotspots is mentioned.

FERRITE DEVICES

Dielectric and Magnetic Loss Mechanisms in Ferrites - See 8221

8461 K-BAND RECIPROCAL FERRITE PHASE MODULATOR by F. Reggia (Diamond Ord. Fuze Labs.); IRE Trans., Vol. MTT-9, pp. 269-270(L), May 1960

Design data of a K-band (23,640 to 25,000 Mc) rectangular waveguide reciprocal phase modulator are given. Some experimental results connected with the design are also presented. The device is similar in principle to the X-band phase modulator of the author and Spencer. The figure of merit is over 3000.

8462 FINAL ENGINEERING REPORT by T.N. Anderson (Airtron); U.S. Gov. Res. Rep., Vol.33, p. 494(A), May 13, 1960 PB 137 649

A high powered ferrite circulator, developed for duplexing in radar systems in conjunction with conventional TR's, is described. The final version of the duplexer showed the following low-level characteristics: a 33.8 to 35.9 kmc range, less than 0.7 db insertion loss (of which the ferrite losses were only a small part), more than 20 db of isolation between all arms, and a maximum input VSWR of 1.30. The device has inherent load-to-magnetron isolation and it removes the bulk of the power from the TR. No breakdown occurred during high-power tests at 70 kw peak power pressurized with 2 atmospheres and at 100 kw peak power with a 2:1 mismatch on 4 atmospheres.

8463 STRIP-LINE Y CIRCULATOR by S. Yoshida (Tokyo Shibaura); Proc. IRE, Vol. 48, pp. 1337-1338(L), July 1960

A Y-junction stripline circulator designed for use with masers and parametric amplifiers at L-band is described. The circulator utilizes disks of yttrium iron garnet placed on the inside walls of the ground plates at the center of the junction. Circulator action is obtained by applying, by means of an external electromagnet, a magnetic field of about 1400 oersteds of either polarity in the direction transverse to the plane of the stripline junction. Typical characteristics of the device are 0.3 db insertion loss, over 23 db isolation with VSWR less than 0.5 db over or 100 Mc bandwidth in the L-band and is 0.2_2 to 37 db with VSWR 0.1_5 db at the center of the band. Better performance can be obtained when the circulator is used without coaxial connectors and coaxial stripline junctions. The stripline circulator with permanent magnet and coaxial connectors occupies a volume less than 4.5 inches in diameter and 2 inches in height.

Hall Effect Memory Device Employing Rectangular Hysteresis Core - See 8449

8464 MAGNETIC MEMORY DEVICE by J.L. Rogers (Bell Labs.); U.S. Pat. 2,926,342, Issued Feb. 23, 1960

Coincident current storage cores which exhibit high speed switching without limitation on the value of the drive current are discussed. The cores consist of a rectangular piece of rectangular hysteresis material containing three equally-spaced holes. A main drive lead passes through the center aperture, an auxiliary drive lead passes through one of the other apertures, and an output lead passes through the third aperture. A "zero" is stored by the simultaneous application of pulses to the main drive lead and to the auxiliary drive lead and a "one" by application of a pulse of a particular polarity to the main drive lead only. A "one" is read out by applying a pulse of opposite polarity. A word organized matrix which employs the cores is described.

8465 SWITCHING DEVICES. THE LOGIMAG [in French] by J. Brard (Soc. Electronique et Auto.); Onde Elect., Vol. 40, pp. 647-656, Oct. 1960

The Logimag, a device intended to replace conventional relays in their switching function with improved reliability, is described. Its operation is related to the use of materials having rectangular hysteresis characteristics; the two turnover points are equivalent at the output to the closed or open condition of relay contacts. The Logimag finds application in industrial automation sequences, being capable of directly-related operations.

8466 FEATURES OF CYLINDRICAL WAVEGUIDES CONTAINING GYROMAGNETIC MEDIA by R.A. Waldron (Marconi Wireless); J. Brit. IRE, Vol. 20, pp. 695-706, Sept. 1960

The electromagnetic field components and density of energy flow, as functions of position in the transverse plane, for the H_{11} mode in a cylindrical waveguide of radius a containing a concentric ferrite rod of radius b are computed. Typical values are chosen for the ferrite properties, and three values of a (normalized with respect to wavelength) that are likely to be found in practice. Values of b/a ranging from 0 to 1 are taken. The field components and power distribution values for given values of a and b, and for variation in a and b, are presented. The results are discussed in relation to each other and to phase constant curves previously obtained. It is concluded that the behavior of these cylindrical systems is mainly dependent on b alone, and not on the ratio b/a.

8467 THEORY OF A NEGATIVE-RESISTANCE TRANSMISSION LINE AMPLIFIER WITH DISTRIBUTED NOISE GENERATORS by K.K.N. Chang (RCA Labs.); J. Appl. Phys., Vol. 31, pp. 871-875, May 1960

A transmission line with distributed positive and negative resistances such as tunnel diodes or parametric diodes, as well as with distributed noise generators, is discussed. Gain and noise factor as a function of boundary conditions, matching conditions, and distributed noise are derived. It is found that low-noise amplification can be achieved on such a line provided that the line is characterized by high gain per unit length, high total gain, good matching, and low distributed noise. A distortionless active line for such low-noise amplifiers appears attractive.

MASERS AND LASERS

8468 SOME OBSERVATIONS ON "STAIRCASE" INVERSION by P.E. Wagner, J.G. Castle, Jr., and P.F. Chester (Westinghouse); Quantum Electronics, Columbia U. Press, 1960, pp. 509-514

The use of simultaneous passage to invert the spin populations between the 1-2 and 2-3 levels in a 3-level spin system is discussed. A "turnover efficiency" parameter

$$\alpha_{ij} = \frac{(n_i - n_j) \text{ after passage}}{(n_j - n_i) \text{ before passage}},$$

where n_i and n_j are the spin populations in levels i and j, respectively, is introduced. It is shown that spin populations $n_3 \geq n_1$ can be obtained by sequential passage if $\alpha < 0$. Spin-spin coupling between the superposed lines keeps them at the same spin temperature throughout passage. In the case of sequential inversion, cross relaxation during the time interval between inversion of the 1-2 and 2-3 lines reduces the final value of $n_3 - n_1$. Experimental evidence of simultaneous inversion is presented.

8469 MASERS by K.W.H. Stevens (U. Nottingham); Contemp. Phys., Vol. 2, pp. 1-13, Oct. 1960

The problem of microwave amplification and a description of the properties of the populations of energy levels in thermal and other kinds of equilibrium are presented. Basic physics is stressed. Particular attention is paid to the way in which a population reversal can be used for amplification, the basis of the maser. The performance characteristics to be anticipated and descriptions of the ammonia maser and the ruby 3-level maser, are included. The 2-level maser is also discussed.

8470 QUANTUM-MECHANICAL SEMICONDUCTOR GENERATORS AND AMPLIFIERS OF ELECTROMAGNETIC OSCILLATIONS by N.G. Basov, B.M. Vul, and Yu.M. Popov (Lebedev Phys. Inst.); Soviet Phys.-JETP, Vol. 10, p. 416(L), Feb. 1960

The attainment of negative temperature in a semiconductor, thus permitting its use as a maser amplifier or generator, is discussed. Negative temperatures can be achieved by means of impurity ionization when a pulsed electric field is applied to the semiconductor at a low temperature. The frequency of the device is determined by the separation of the impurity levels from the valence or conduction band.

8471 INDUCED MICROWAVE EMISSION IN RUBY by G. Makhov, C. Kikuchi, J. Lambe, and R.W. Terhune (U. Michigan); Solid State Phys. Electronics and Telecommun., Academic Press, 1960, Vol. 4, pp. 571-581

The feasibility of using ruby in maser amplifiers and oscillators is examined. Experimental results for devices which utilized a ruby crystal containing 0.1 per cent Cr and measuring 0.6 x 0.6 x 1.0 cm are given. This crystal had a line width at room temperature of 23.5 gauss, a dielectric constant of approximately 11, and a filling factor of almost 0.01. With a magnetic field of 4250 gauss and a pump frequency of 24 kMc, the emitted frequency was 9.06 kMc. For K-band power input to the cavity of 53 mw, the CW power output of the oscillator was 4 μw. The mode of operation of an oscillator was dependent on the amount of pumping power. Gain of 37 db was observed in a maser amplifier with an input power of 0.1 μw, an input frequency of 9.06 kMc, and a K-band pump.

8472 RECENT DEVELOPMENTS ON SOLID STATE MASERS by J.W. Meyer (Lincoln Lab.); Solid State Phys. Electronics and Telecommun., Academic Press, 1960, Vol. 4, pp. 565-570

Some experimental investigations of 10, 20, and 100 cm reflection cavity type masers utilizing cobalt: potassium cyanide containing 1/2 to 1 per cent Cr are discussed. The 10 cm maser, which had a relatively low effective filling factor at the signal frequency, and the 20 cm maser, which had an improved filling factor as a result of utilizing a re-entrant cavity, had pumping frequencies and gain-bandwidth products of near 9000 Mc and about 2×10^6 per sec, respectively. In the 100 cm maser a very large filling factor was obtained by using a superconducting loop as the UHF resonator. A gain-bandwidth product of about 10^6 per sec was measured in this device. Noise measurements are also discussed.

8473 TRAVELING-WAVE SOLID STATE MASERS by A.E. Siegman, J. Cromack, W.S.C. Chang (Stanford U.); Solid State Phys. Electronics and Telecommun., Academic Press, 1960, Vol. 4, pp. 559-564

Traveling wave masers, which exhibit greatly increased amplification bandwidth over cavity masers, are discussed. In the traveling wave maser a series of crystals are connected into a transmission line circuit. The circuit has a negative attenuation and propagates waves which amplify as they travel. It is shown that stability can be achieved in transmission type traveling wave masers by both (a) using the nonreciprocal nature of the magnetic interaction in the paramagnetic crystal itself and (b) putting nonreciprocal ferrite elements into the maser. The "easitron" and helix-type traveling wave maser structures are discussed.

8474 OPERATION OF A CHROMIUM-DOPED TITANIA MASER AT X- AND K-BAND by H.J. Gerritsen and H.R. Lewis (RCA Labs.); Quantum Electronics, Columbia U. Press, 1960, pp. 385-388

The operation of a maser utilizing titania (TiO_2) in which 0.12 per cent of the Ti ions were replaced by Cr ions is described. Because of its high dielectric constant the TiO_2 crystal was used as a resonant cavity. X-band amplification and oscillation were obtained with two different modes of operation. In one mode the pump was applied between levels 1 and 3, the signal between levels 1 and 2, and the magnetic field of 5600 gauss made an angle of 12° with the c-axis. At a signal frequency of 10.3 kMc, pump frequency of 35.3 kMc, and pump power above 25 mw, oscillations with a frequency of 10.3 kMc were observed. In the second mode (pump applied between levels 2 and 4 and the signal applied between levels 3 and 4) amplification and oscillation were observed at several frequencies between 8.2 and 10.6 kMc. At K-band some amplification was obtained with a pump power of only about 2 mw. All measurements were performed at 4.2°K. It is suggested that signal frequencies up to about 40 kMc are possible and that the large dielectric constant of the material makes it suitable for use in traveling wave masers.

8475 RESONANT MODES IN AN OPTICAL MASER by A.G. Fox and T. Li (Bell Labs.); Proc. IRE, Vol. 48, pp. 1904-1905(L), Nov. 1960

A digital computer study of reflections of a uniform plane wave in a Fabry-Pérot interferometer filled with a maser material is discussed. It was found that after hundreds of reflections, diffraction losses cause the wave to grow weaker with successive transits and the amplitude at the edges drops to a small fraction of the center valve. After a number of transits a steady state was reached. These results indicate that uniform plane waves cannot be considered as stable modes for a Fabry-Pérot interferometer. The loss per transit for plane and confocal paraboloidal mirrors is compared.

SUPERCONDUCTIVE DEVICES

8476 MULTIPLE-CHARACTERISTIC SUPERCONDUCTIVE WIRE by H.O. McMahon (A.D.Little); U.S. Pat. 2,958,836, Issued Nov. 1, 1960

A composite cryotron conductor comprising a Ta wire having niobium-coated portions with the uncoated portions serving as gate segments and the coated ones, which have a substantially greater quenching field, serving as control segments is described. This composite cryotron, which can be used in all types of cryotron circuits, will enable the elimination of many of the welded connections between gate and control elements. A circuit for using it as a flip-flop is included.

8477 THE VARIATION OF CRYOTRON CURRENT AMPLIFICATION FACTOR WITH TEMPERATURE by A.E. Brennemann (IBM); IBM J. Res. and Dev., Vol. 4, p. 197(L), Apr. 1960

The current amplification factor of a shielded, thin film cryotron as a function of temperature below the critical temperature of the gate is discussed. At the critical temperature of the gate, the amplification factor is zero. As the temperature is lowered from the critical temperature, and the depth of penetration decreases, the amplification factor rises rapidly. The current amplification factors in all cryotrons tested were found to be less than one tenth the gate film width to control film width ratio when the helium bath temperature was near the critical temperature of the gate.

ELECTROMECHANICAL DEVICES

8478 PIEZO-ELECTRIC QUARTZ CRYSTAL OF ELONGATED SHAPE by C. Frank (Philips); U.S. Pat. 2,925,502, Issued Feb. 16, 1960

A technique for reducing transverse oscillations in a longitudinally oscillating X-cut quartz crystal is described. These oscillations can be eliminated by using a parallelogram-shaped quartz crystal. The angles between the sides of the parallelogram are determined from the orientation of the long side of the crystal with respect to the Y-axis. Some measurements showing the effectiveness of the technique are presented. The technique can also be used with other than X-cut crystals and its use is illustrated in the case of MT-cut crystals.

8479 PIEZOELECTRIC RESONATORS OF SYNTHETIC QUARTZ by J. Zelenka (Tesla, Lanshkroun); Slabproudy Obzor, Vol. 21, pp. 638-641, Nov. 1960

The electrical qualities of piezoelectric resonators composed of synthetic quartz monocrystals are discussed. Resonators of the AT, BT, CT, Dt, and XYt-ϕ cuts are reviewed, with special attention to the temperature dependence of frequency as well as to the parameters of the electrical equivalent circuit. The qualities of resonators containing either synthetic or natural quartz are compared.

BASIC SOLID STATE DEVICE CIRCUITS

GENERAL

1480 ACTIVE RC SYNTHESIS WITH PRESCRIBED SENSITIVITIES by L.P. Huelsman (U. Arizona); Proc. Natl. Electronics Conf., Vol. 16, pp. 412-426, 1960

From a mathematical viewpoint, the basic theory of negative-impedance converter RC synthesis is considered. The conditions are determined under which an arbitrary polynomial representing the numerator or denominator of a given transfer function can be equated to the difference of two polynomials. Root-locus techniques are used to determine the most advantageous choice of these polynomials from the standpoint of sensitivity to changes in the gain of the negative-impedance converter. Application of these results can be made to the development of a method of synthesis in which control of the sensitivities of both the numerator and denominator polynomial of a given transfer function is possible.

1481 ON MINIMAL REALIZATION OF RC TWO-PORTS by M.L. Hakimi and J.B. Cruz, Jr. (U. Illinois); Proc. Natl. Electronics Conf., Vol. 16, pp. 258-267, 1960

From a given RC-realizable voltage transfer function, some lower bounds for the minimum possible number of elements in the network are derived. For the case of bilinear and biquadratic functions, minimal network realizations are tabulated although not all realizable biquadratic functions are covered. The table, together with the corresponding design formulas, may be useful for routinely synthesizing low order minimal compensating networks. For the special case of an n-pole transfer function with symmetrically clustered zeros, a realization involving at most two elements more than the lower bound is obtained using Guillemin's parallel ladder procedure. The class of transfer functions covered is enlarged by considering the effect of interchanging the input terminals as well as the effect of a special RC to CR transformation.

1482 SYNTHESIS OF ACTIVE RC NETWORKS by B.K. Kinariwala (Bell Labs.); Bell Sys. Tech. J., Vol. 38, pp. 1269-1316, Sept. 1959

A basic theorem is derived for RC networks containing active elements. It is shown that no more than one active element, embedded in a passive RC network, is needed to realize any driving-point function. Sufficiency of only one active element is shown by developing a synthesis method. A synthesis technique for n-port passive RC networks is developed in order to establish the sufficiency proof of the basic theorem. A more practical method of realizing driving-point functions, using active RC networks, termed the "cascade" method, is also presented. This method is applied to the design of a tenth-order Tchebycheff parameter filer.

1483 AN APPROACH TO THE SYNTHESIS OF LINEAR NETWORKS THROUGH USE OF NORMAL COORDINATE TRANSFORMATION LEADING TO MORE GENERAL TOPOLOGICAL CONFIGURATIONS by E.A. Gullemin (MIT); IRE Intl. Conv. Rec., Part 2, pp. 171-179, 1960

A more general and potentially useful approach to network synthesis is presented. The proposed procedure includes a method of determining parameter matrices from given impedance functions through use of normal coordinate transformations and realizes the pertinent network by identical tree configurations in single-element-kind networks having a general topological structure. Essentially the same procedure is applicable to passive bilateral networks and to nonpassive and/or nonbilateral ones. The availability of modern computers overcomes the tedious computations involved.

8484 ON POLES AND ZEROS OF A RANDOM PROCESS IN LINEAR AND NONLINEAR SYSTEMS by A.A. Wolf (Stromberg-Carlson); Proc. Natl. Electronics Conf., Vol. 16, pp. 268-278, 1960

A systamatic means of uniquely describing a random process by means of its poles and zeros in a complex plane, under certain conditions, is presented. The method is based on an extension of the transform-ensemble theorem of Ku and Wolf and three new theorems which are developed in detail. The first theorem allows expansion of a given probability density function as a linear combination of all the moments of the density function and the derivatives of the Dirac delta function. Justification of the theorem, an example of its use and various necessary lemmas are given. The second theorem deals with the synthesis of a nonstationary random process and a certain class of deterministic processes. The third theorem develops the relation that the residue of the (n-1)st convolution of the ensemble average of the transform of a random process is equal to the ensemble of the mean n-th value of the given random process itself.

8485 A SIMPLIFIED DERIVATION OF THE MANLEY AND ROWE POWER RELATIONSHIP by J.E. Carroll (Cambridge U.); J. Electronics Control, Vol. 6, pp. 359-361, Apr. 1959

A simplified analysis of power flow in inductive elements is performed. The same analysis applies also to capacitive elements. The same relationships obtained by Manley and Rowe are derived. Hysteresis and an extension of the analysis to any number of incommensurate frequencies are considered.

8486 NEW IN INTEGRATED CIRCUITS: TRANSISTOR-COUPLED LOGIC by T.E. Mount (Electronic Design); Electronic Design, Vol. 9, pp. 8-9, Nov. 22, 1959

The technique of employing transistors, instead of resistors or ultrafast diodes to couple input-transistor switches to the output fan-outs in digital circuits is reported. With coupling transistors, logic modules could be produced in high-yield batches since manufacture is simplified. Other advantages include wider design and production, level shifting so the integrated circuits can communicate with other types of logic schemes, and fast coupling. The coupling transistor is in the "always-saturated" state. In switching, the only internal effect is a redistribution of excess carriers in the base region. A schematic diagram and some circuit details are given. The transistor-coupled logic circuits show promise for inexpensive, fast, integrated-circuit modules.

8487 OPTIMUM STABILIZATION NETWORKS FOR FUNCTIONAL ELECTRONIC BLOCKS by J.D. Meindl and O. Pitzalis (USASRDL); Proc. Natl. Electronics Conf., Vol. 16, pp. 576-583, 1960

The problem of optimizing the design of the stabilization network of a functional block capable of performing as an audio, tuned or video amplifier, harmonic oscillator, modulator, mixer, detector, etc., is discussed. The active element may be either a single bipolar transistor or a group of several connected directly in tandem. The functional device-design

procedure differs widely from the conventional and utilizes, as the broad optimizing criterion, the minimization of power dissipation in the functional block. With optimum designs, 3 to 1 reductions in power dissipation are common and 10 to 1 or better possible. The design procedure includes the important effects in semiconductor blocks of temperature variation for all passive elements, as well as the supply voltage. The results show that well-stabilized transistor operation is possible for resistive networks whose temperature variation is 50 per cent over a 130°C range. Both transistor and resistor manufacturing tolerances are quantitatively considered. Experimental data support the design theory.

AMPLIFIERS

AGC in Transistor Radio Receivers - See 8523, 8524

8488 DISTORTION IN CLASS A-B PUSH-PULL AMPLIFIERS by I.S. Docherty and R.E. Aitchison (U. Sidney); Proc. IRE Austl., Vol. 20, pp. 737-741, Dec. 1959

The Fourier coefficients of the current waveform for a single vacuum tube or transistor operating under various bias conditions are evaluated as a function of the angle of flow of the output current. Consideration is given to Class A, various degrees of Class AB, and Class B operations. From these results the harmonic distortion is determined for a balanced push-pull system. Modifications of these results for imperfectly balanced systems are evaluated. The effect of departure of the transfer characteristic from an ideal linear relationship is outlined. The importance of these results in practical push-pull vacuum tube and transistor amplifiers is discussed.

8489 LOCAL FEEDBACK IN TRANSISTOR AMPLIFIERS by H. Pfyffer (GE Ltd.); Electronic Engrg., Vol. 31, pp. 550-555, Sept. 1959

The effects of negative feedback on the gain, impedance, and cutoff frequency in the common emitter amplifier stage are discussed. Design equations are derived for both series-current and parallel-voltage feedback, and the results are simplified by standard approximations useful in amplifier design. The variation of overall current and voltage gain with frequency is shown for various values of feedback resistance. A single stage amplifier is designed for both current and voltage feedback; the measured results are then plotted with the calculated results, showing excellent agreement over a wide range of frequencies (10 kc to 5 Mc).

8490 ON THE THEORY OF TWO-WIRE AMPLIFIERS [in German] by T. Greive (Stand. Elekt. Lorenz); Arch. Elekt. Uebertragung, Vol. 13, pp. 243-252, June 1959; pp. 287-302, July 1959

An expansion of the Bartlett and Brune transformation of a symmetrical quadripole into its equivalent bridge circuit to include quadripoles with transfer-asymmetrical halves is presented. If the expanded transformation is used for the two wire repeater with one amplifier for the go and one for the return direction, a two wire repeater with two negative impedances in a bridge circuit is obtained. These negative impedances are each generated by an amplifier that is made regenerative by means of a bridge circuit. The general relationships derived for this basic circuit can also be applied to degenerative amplifiers and oscillators. The scatter matrix is used for stating the linear sets of equations. The stability problem existing with two wire lines with several amplifiers is solved by a new method in which the overall circuit is broken down into individual unstable sections.

8491 TRANSISTORIZED RELAY AMPLIFIER by R.A. Bruns and J.H. Wilcher (Calif. Inst. Tech.); U.S. Gov. Res. Rep., Vol 33, p. 379(A), Apr. 15, 1960 PB 144 715

The development of a transistorized relay amplifier with performance superior to that of vacuum-tube amplifiers is described. The circuit was designed from an analytic approach utilizing matrices amenable to digital computer solution. The digital computer permits a thorough survey of parameter studies and illustrates a powerful design method extendable to circuits of greater complexity. Performance tests of the transistorized relay amplifier with the analog computer showed it to be superior to the vacuum-tube type in lower noise level, smaller inactive zone, and much faster time response.

8492 TEMPERATURE COMPENSATED TRANSISTOR AMPLIFIER by S. Darlington and J.H. Felker (Bell Labs.); U.S. Pat. 2,885,494, Issued May 5, 1959

A multistage transistor amplifier with transmission characteristics fixed by the characteristics of an external feedback circuit is described. Internal feedback through a series of stages decreases exponentially with the number of stages and with three stages it becomes entirely negligible. An odd number of n-p-n junction transistor stages are dc coupled and provided with a feedback resistor between the output and the input stages. Negative feedback is insured by the odd number of stages since each stage has a phase inverting grounded emitter configuration. It is shown that the voltage gain is relatively independent of μ and of the load resistance. This amplifier is stable with variations in α. Auxiliary circuits which provide additional stability are discussed.

8493 TEMPERATURE COMPENSATED FEEDBACK TRANSISTOR CIRCUITS by A.N. DeSautels (Minn.-Honeywell); U.S. Pat. 2,925,559, Issued Feb. 16, 1960

A method of temperature compensation by the use of temperature sensitive components in a feedback loop is described. The temperature sensitive elements are resistances with positive and negative temperature coefficients. These are used in a feedback loop from collector to base in a conventional single transistor amplifier or from third collector to first base in a three stage amplifier. The elements are chosen to have a minimum resistance in the mid-temperature range, with increasing resistance outside this range, thus effecting a temperature-dependent degenerative feedback proportional to the magnitude of the resistance. The result is a temperature-stabilized amplifier whose gain varies less than 1/2 per cent (0.5 per cent) over a temperature range from -30° to +160°F.

Low Noise Transmission Line Amplifiers - See 8467

8494 TRANSIENT RESPONSE AS A DESIGN CRITERION FOR STABILIZATION OF FEEDBACK AMPLIFIERS by J.H. Mulligan, Jr. (N.Y.U.); Proc. Natl. Electronics Conf., Vol. 15, pp. 747-760, Oct. 12-14, 1959

A design criterion for use in the stabilization of feedback amplifiers which is concerned directly with pole locations and with a feature of the transient response is discussed. The

terion is the relative damping of the amplifier step-function sponse, i.e., the ratio of the deviations from unity in the rmalized time response at two successive extreme values. e of the proposed criterion in conjunction with a dominant m approximation to the transient response to formulate de- n equations for representative transistor and vacuum tube plifier stages is demonstrated. Transient response curves r a particular design, using various values of mid-band loop in, illustrate the effect of parameter changes on the stabi- ation design parameter.

495 MEASURING THE STABILITY OF FEEDBACK TRANSIS- OR REPEATERS [in Czech] by M. Pajgrt; Slaboproudy Obzor, l. 20, pp. 542-548, Sept. 1959

e calculation of the equivalent impedance at the "cut" of e feedback loop of feedback transistor repeaters is discussed. measurement for the exact determination of this impedance suggested and the possibility of substituting for the compli- ted repeater circuit a simple four terminal network for which tability measurement technique has been devised is indi- ted. A method of measurement which does not necessitate connecting the feedback loop is also discussed.

496 FEEDBACK WITH HALF WAVE CIRCUIT by H. F. AcKenney (Sperry Rand); U.S. Pat. 2,923,877, Issued Feb. , 1960

two-stage half-wave bridge type magnetic amplifier is de- ribed. Only one additional winding is connected so as to ffect combination bias and feedback characteristics. The econd stage bridge network currents bias the magnetic cir- its of the first stage to a constant and selected flux level uring each off-half-cycle of the first stage. Each stage is djusted to fire at 90° with the second stage phase angle dis- laced 180° from the first. A signal impressed on the first age differentially presets the flux level unbalancing the ridge network; similarly the second stage will be unbalanced. owever, currents flowing in the second stage also flow rough the feedback-bias winding of the first and thus effect negative feedback. A reversal of polarity of these windings ill produce a positive signal feedback characteristic.

497 MAGNETIC FILM PARAMETRIC AMPLIFIERS by A.A. ead and A.V. Pohm (Iowa State U.); Proc. Natl. Electronics onf., Vol. 15, pp. 65-78, 1959

he use of inductive elements made from thin ferromagnetic ilms (similar to those being used for computer memories) as arametric amplifiers is discussed. An experimental para- etric amplifier has been constructed having a pump frequency n the 20 to 30 Mc range. Signal gains in the 30 db range as ell as superregenerative detection of very low level signals ave been obtained. Thin-film parametric amplification is iscussed both graphically and analytically in terms of a uasi-static model. At frequencies below VHF this is satis- actory; at higher frequencies a model with losses must be onsidered. Such a model indicates that operation up to 1000 Mc or higher should be feasible with moderate pumping powers.

498 TRANSDUCER CHARACTERISTICS OF VARACTOR AM- LIFIERS [in German] by V.W. Dahlka, R. Maurer, and J. chubert (Telefunken); Arch. Elekt. Uebertragung, Vol. 13, p. 321-340, Aug. 1959

he quadripole equations and simple equivalent circuits for variable-reactance amplifiers which consist of two parallel resonant circuits coupled by a diode are derived. These are used to investigate the transducer characteristics of variable-reactance amplifiers, which are classified as inverting and noninverting frequency mixers and straight amplifiers. Transducer gain, amplifier bandwidth, stability, noise figure and efficiency are calculated from the given data. Design rules are determined for amplifiers with minimum noise figure, which furnish the required data of the diode and circuits as a function of the required amplifier performance data. The principal transducer and design parameters of the three amplifier types are tabulated and compared and the characteristic parameters required for the assessment of diodes are explained. Because of the negative diode conductances appearing in the circuits of the frequency inverters, the circuits allow a remarkable reduction of the contribution of the following amplifier to the overall noise figure.

Conditions for Amplification by Negative Mass Amplifiers - See 8452

8499 INSTABILITY IN A SEMICONDUCTOR AMPLIFIER WITH NEGATIVE EFFECTIVE CARRIER MASS by A. L. Zakharov; Soviet Phys.-JETP, Vol. 11, pp. 478-479(L), Aug. 1960

Some difficulties involved in the negative effective mass amplifier proposed by Krömer are discussed. It is shown that the specific negative conductivity of the device implies that it will be unstable in operation and that the device will probably be extremely noisy. It is suggested that it be used as a noise generator. A possible method for overcoming the inherent instability of the device is proposed.

Magnetic Power Amplifiers Employing Corbino Disks - See 8451

Analysis of Magnetic Amplifiers - See 8536

OSCILLATORS

8500 ON THE THEORY OF A GENERATOR WITH A POINT CONTACT TRANSISTOR [in Russian] by N.I. Ashbel' (NIFTI, Gorkii U.); Izv. VUZ Radiofiz., Vol. 3, No. 5, pp. 866-871, 1960

Investigation of a generator using a point contact transistor with feedback between collector and emitter through a series LC loop is cited. The work was done on the basis of a piecewise-linear approximation of the static characteristics. The self-excitation condition for self-oscillations is obtained and the boundaries of the linearity domain on the phase plane are determined for the equilibrium state located in the operating region of the transistor. The possibility of the existence of a stable limit cycle in the system is shown.

8501 A TRANSISTOR OSCILLATOR WITH LIMITING IN THE SATURATION REGION by A.N. Bazhan and L.N. Kaptsov (Moscow State U.); Radio Engrg. Electronics, Vol. 4, pp. 215-227, 1959

A study of the build-up process of stationary regenerative oscillations in an almost harmonic oscillator using a transistor is made. The limiting of the oscillations in the saturation region is examined. Formulae are deduced for an oscillator of this type.

8502 ON THE BUILD-UP OF OSCILLATIONS IN TRANSISTOR OSCILLATORS by L.N. Kaptsov, K.Ya. Senatorov, and O.I. Poplavskaya (Moscow State U.); Radio Engrg. Electronics, Vol. 4, pp. 228-236, 1959

A linear and nonlinear analysis of an almost sinusoidal transistor oscillator is given. It is shown that stationary oscillations can be obtained as a result of the nonlinear input impedance of the transistor.

8503 TRANSISTOR POWER OSCILLATOR by J.H. Guyton and K.S. Vogt (Genl. Motors); U.S. Pat. 2,925,560, Issued Feb. 16, 1960

A single transistor relaxation oscillator is described. The circuit uses inductive feedback through the primary of a transformer to establish and maintain the oscillations. The transformer secondary may be connected to the load either directly or through a rectifying and filtering system which provides direct current. The circuit is designed to work from a source of low potential, not exceeding sixteen volts.

8504 PARAMETRIC OSCILLATIONS WITH POINT CONTACT DIODES AT FREQUENCIES HIGHER THAN PUMPING FREQUENCY by L.U. Kibler (Bell Labs.); Proc. IRE, Vol. 48, pp. 239-240(L), Feb. 1960

Oscillations observed in gallium arsenide point contact diodes at frequencies higher than the pumping frequency are discussed. The signal and idler frequency were located symmetrically with respect to "m" times the pumping frequency. Diodes having two different capacitance-bias voltage curves were utilized. One diode produced oscillation at 11.63 kMc when pumped at 11.03 kMc. The corresponding symmetrical lower sideband was observed at 10.430 kMc. Approximately 10 mw of pump power was used. This diode also oscillated at 530 Mc when pumped at 480 Mc. The symmetrical signal was observed at 430 Mc and the pump power into a matched load was about 20 mw. The actual power absorbed by the diode was not determined. Another diode produced oscillation at 530 Mc when pumped at 470, 460, and 450 Mc. Pump power was approximately 30 mw and again the actual power absorbed by the diode was not determined. These results are shown to be consistent with the Manley-Rowe relations.

8505 EFFECT OF COLLECTOR p-n JUNCTION THICKNESS MODULATION ON THE OPERATION OF A TRANSISTOR OSCILLATOR by L.N. Kaptsov (Lomonosov State U., USSR); Radio Engrg. Electronics, Vol. 5, No. 7, pp. 202-213, 1960

It is shown that collector junction capacitance averaged with respect to the first harmonic voltage component increases with an increase of signal amplitude. For certain conditions this ensures a weak operating condition of the oscillator at most harmonic oscillation frequencies in the common-base circuit in the ultrasonic and higher frequency band.

SWITCHING CIRCUITS

Bistable Trigger Circuits Employing Corbino Disks - See 8451

8506 BISTABLE TRANSISTOR CIRCUIT by R.K. Richards (IBM); U.S. Pat. 2,923,836, Issued Feb. 2, 1960

A high output power bistable thyratron transistor circuit which can be triggered by small magnitude pulses of short duration or by light pulses directed against the base regions of the transistors is described. Circuit operation is improved by use of a common emitter resistor input or by use of a common emitter input clamp capacitor and resistor.

Flip-Flop Cryotron Circuit - See 8476

8507 CRYSTAL GATING CIRCUIT by W.F. Schreiber (Sylvania); U.S. Pat. 2,923, 819, Issued Feb. 2, 1960

A simplified signal coincidence circuit requiring only one nonlinear element is described. Two input signals are supplied at the two-terminal input. Each terminal is connected through an isolation resistor to the third terminal. An asymmetrically conductive element such as a crystal diode is connected between the third terminal and a point of biasing potential. The biasing potential is chosen with respect to the polarity and magnitude of the two incoming signals such that the diode is made nonconductive at coincidence. This results in an output signal at the third terminal. In all other situations the diode remains heavily conductive clamping the third terminal to the bias potential point. Two modifications of the basic three element circuit are given.

8508 LOW VOLTAGE LEVEL TRANSISTOR GATES by E.J. Slobodzinski and H.S. Yourke (IBM); U.S. Pat. 2,923,838, Issued Feb. 2, 1960

A low voltage level binary switching gate employing surface barrier transistors which provides minimum loading of a bistables circuit and permits operation at a pulse repetition rate of 10 Mc is described. Current switching transistor gates are connected to each binary input with one gate also connected to one of the binary outputs. An input transistor, turned on by the trigger pulse, switches one of the gates (determined by the state of the bistable unit) to provide the binary switching pulse. The switching network provides its own loads and does not impede the switching speed of the bistable circuit.

8509 SWITCHING CIRCUITS AND METHODS by R.K. Willardson and A.C. Beer (Battelle); U.S. Pat. 2,889,492, Issued June 2, 1959

A method of opening and closing electrical connections with a minimum of arcing is described. The method comprises shunting the switch to be opened with a magnetoresistance element, opening the switch, increasing the resistance of the magnetoresistance element through application of a magnetic field, and removing the shunt. Current load on a switch prior to opening can be reduced to any desired degree by applying the technique with cascaded magnetoresistance elements.

SIGNAL CONVERTERS

8510 LINEAR VOLTAGE-TO-FREQUENCY CONVERTER by J. Maurushat, Jr. (Bell Labs.); U.S. Pat. 2,924,788, Issued Feb. 9, 1960

A variable frequency generator whose output frequency is determined by the amplitude of the input signal is described. The generator consists of a bistable multivibrator, diode switches, RC timing circuits, and transistor reset gates. The input signal charged the timing capacitor to a predetermined voltage level. Upon reaching this level, the capacitor discharges through the associated diode switch which it has

rward biased. This discharge changes the state of the multi-ibrator, and an output signal is obtained simultaneously with e reset signal which restores the timing capacitor to its ini-ial condition. Since the amplitude of the input signal deter-nes the charging rate of the timing capacitor and thus the witching rate, the frequency of the output signal is effectively measure of the amplitude of the input signal.

511 PHASE-SENSITIVE AMPLIFIER by D.K. Schaeve (Barber-oleman); U.S. Pat. 2,924,757, Issued Feb. 9, 1960

phase-sensitive amplifier which provides a pulsating direct rrent output whose amplitude and polarity are dependent on e amplitude and polarity of the input signal is described. he amplifier employs two transistors in a push-pull configura-ion, using a signal source in the emitter circuit and a refer-nce source together with the load in the collector circuit. he circuit may be employed both as a phase-sensitive detec-or and as a frequency detector; in the latter case, the fre-uency of the pulsating output is equal to the difference in requency between the signal and reference sources.

512 PHASE DIFFERENCE DETECTOR OR FREQUENCY DE-MODULATOR by A.J.W.M. van Overbeek (Philips); U.S. at. 2,924,723, Issued Feb. 9, 1960

A phase difference detector or frequency demodulator employ-ng two crystal diodes and a transistor is described. The theory f operation is given using an equivalent three diode circuit. ach output of two voltage generators of same frequency but ifferent phase is connected through a diode to one side of the hird diode. This diode is held nonconductive at all times xcept when both generator voltages are positive. During this nterval the third diode conducts through the load. The dura-ion of output current is proportional to the relative phase dif-erence between the two generators. A practical circuit is iven which includes: two critically coupled tuned circuits hich provide two signals of the same frequency but with a requency dependent phase difference, and a transistor ampli-ier output in which the emitter base junction also serves as he third diode element. The circuit is suitable for connection o an amplifier having a low input impedance.

513 DISCRIMINATOR CIRCUIT by C.R. DeWeese, J.W. acey, and R.R. Webster (Texas Instr.); U.S. Pat. 2,925,501, ssued Feb. 16, 1960

A discriminator circuit utilizing a compound transistor of the lotted type is described. The transistor is in the form of an rch, with each lag of the arch forming a collector electrode, apped by a base layer, and the span of the arch forming an mitter common to both collectors. This type of transistor is articularly suited to discriminator circuits since shift of the ero-signal characteristics of a two-transistor unit due to un-qual heating of the transistors is avoided by incorporating oth transistors in a common unit. The common emitter will eat both collector units when either one conducts, thereby educing the temperature difference between them.

514 NEW PHASE- AND FREQUENCY-COMPARISON CIR-UITS [in German] by G.G. Gassmann (Stand. Elekt. Lorenz); rch. Elekt. Uebertragung, Vol. 15, pp. 359-376, Aug. 1961

A new method for producing a rectified voltage that is a func-ion of the phase and frequency difference of two alternating voltages is discussed. It is well suited to the comparison of pulsed alternating voltages and is quite accurate despite its simplicity. The application of follow-up synchronization in phase and frequency comparison circuits allows wide pull-in range with relative freedom from interference. A theoretical discussion of well-known phase comparison circuits is given and an analysis of the circuit requirement criteria which lead to the new design is presented.

Time to Amplitude Converter - See 8575

WAVE GENERATORS
(See also Oscillators)

Pulse Generator Design Using Avalanche Mode Transistors - See 8436

8515 MAGNETIC AMPLIFIER PULSE GENERATORS by H.A. Miller and H. Eisler (Raytheon); U.S. Pat. 2,873,422, Issued Feb. 10, 1959

A magnetic amplifier which produces a dc output pulse from an ac source is described. Its advantage over similar devices is the use of only one saturable core to produce a single output pulse on either of the half cycles of the input signal. The circuit exhibits "single cycle response" whereby any change in input voltage is reflected in the output within one half to one cycle of the input voltage. It can be used to control a wide range of power outputs. A typical application is in a reversible, variable speed motor drive dircuit, which is shown schematically and described in detail.

8516 SOLID STATE GENERATOR FOR 2×10^{-10} SECOND PULSES by A.F. Dietrich and W.M. Goodall (Bell Labs.); Proc. IRE, Vol. 48, pp. 791-792(L), Apr. 1960

A pulse generator which can produce pulses as short as 2×10^{-10} sec is described. A diffused silicon mesa diode is mounted in shunt of a 50 Ω coaxial line and is biased in the forward direction. The diode is driven by a 20 Mc generator and a sharp step is produced on the trailing edge of the generator pulses by the shunt diode at about the time the diode stops conducting. A differentiating stub then translates the step voltage into 2×10^{-10} sec pulses. Either the sharp steps or short pulses can be produced at any repetition rate from one to several hundred million per sec.

8517 TRANSISTOR CIRCUIT FOR PRODUCING CURRENT PULSES THROUGH A VARIABLE IMPEDANCE by T.J. Tulp and H.A. Rodrigues de Miranda (Philips); U.S. Pat. 2,956,174, Issued Oct. 11, 1960

A transistor circuit applicable as a constant amplitude pulse source for variable impedance loads, such as ferromagnetic memory cores, is described. A controllable impedance comprising an inductance is coupled to the load and the control circuit to provide a low or a high impedance below or above a predetermined current level.

PULSE CIRCUITS

8518 A COMPARISON OF METHODS FOR THE ANALYSIS OF PULSED LINEAR SYSTEMS by H. Freeman (MIT); Proc. NEC, Vol. 15, pp. 1032-1043, Oct. 12-14, 1959

A thorough study of the properties of both "wide-pulse" and

"narrow-pulse" types of pulsed linear systems is made. Mathematical models are presented. It is shown that the signals can be expressed in terms of a generalized solution based on an extension of the Laplace transform.

8519 SIGNAL PULSE CONVERTER by S.E. Gluck (Burroughs); U.S. Pat. 2,957,166, Issued Oct. 18, 1960

A circuit utilizing magnetic core elements which converts microsecond duration pulses to unidirectional voltage for actuating a relay or other slow switching device is described. Duration of output voltage level is dependent upon a predetermined number of cycles of "ping-pong" circuit operation during which the binary state "1" is shifted back and forth between two magnetic cores comprising the "ping-pong." Application of the converter in computers as an error detector or teletype actuater is cited.

8520 NOISE DISCRIMINATION CIRCUIT by E.S. Wilson (IBM); U.S. Pat. 2,923,821, Issued Feb. 2, 1960

A magnetic circuit, capable of discriminating between noise and signal pulses, which functions on an energy level basis, is described. Pulses below a selected voltage-time integral level are blocked; pulses above are passed. Cores with the proper loop characteristics, whereby only pulses having greater than a critical voltage-time integral will effect switching, are employed. Using an Othonal core of cross section 0.0935 square inch and a pulse height of 35, switching times between 10 and 100 microseconds have been measured. A core of smaller cross section covers the same range of switching time at a 15 level. A bias winding on the core determines the critical switching energy level and also the signal polarity to which the device will respond.

OTHER CIRCUITS

Diode Rectifying Circuits - See 8526

8521 SEMI-CONDUCTOR FILTER CIRCUITS by H.J. Woll (RCA); U.S. Pat. 2,892,164, Issued June 23, 1959

A filter circuit utilizing opposite conductivity transistors for removing alternating current components from a direct current voltage is described. A pair of opposite conductivity transistors are connected in parallel to form a two-terminal device having a high dc resistance and a low ac impedance. The transistors are so connected that the ripple voltage which is applied to the terminals of the circuit is amplified. A current is fed back in such a manner that the ripple voltage is effectively cancelled. The input impedance Z of the entire filter circuit is given by $Z = R/(a_{cb_1})(a_{cb_2})$. R is the base input resistance of one transistor and a_{cb} is the current gain between collector and base electrodes. Efficient and reliable ripple attenuation is accomplished by the circuit which occupies a minimum of space.

Negative Mass Amplifier as Noise Generator - See 8499

8522 TRANSISTOR TIME DELAY CIRCUIT by R.L. Bright (Westinghouse); U.S. Pat. 2,892,101, Issued June 23, 1959

A time delay circuit which uses an RC charging network to initiate breakdown of a Zener diode is described. The sharp surge of current occurring at breakdown of the diode is used to trigger a transistor switch which then establishes the desired output voltage of known delay. Using this method, the time delay of the circuit has been found to be accurate to within 3 to 5 per cent over a range of temperatures from -60° to +60°C. Variation in the characteristics of the circuit components, other than the Zener diode, has no appreciable affect on the operation of the circuit.

APPLICATIONS OF SOLID STATE DEVICES

RADIO AND TELEVISION

8523 AUTOMATIC GAIN CONTROL WITH VARIABLE RESISTANCE DEVICE IN ANTENNA CIRCUIT by J.B. Schultz (RCA); U.S. Pat. 2,923,816, Issued Feb. 2, 1960

A method for providing automatic gain control for a transistor radio receiver by shunting the receiver antenna with a variable resistance element is described. A crystal diode is employed as the variable resistance device. It is connected in series with a winding on a ferrite rod which functions as a core for a loop-type antenna. When the received signal reaches a predetermined level the diode is automatically forward biased to decrease its resistance and lower the Q of the antenna tuned circuit. The receiver will operate satisfactorily at 10 to 20 times the signal strength which would normally cause overload.

8524 AUTOMATIC GAIN CONTROL FOR TRANSISTOR RECEIVER CIRCUITS by R.L. Layburn and B.R. Stachiewicz (Genl. Dynamics); U.S. Pat. 2,892,932, Issued June 30, 1959

A forward acting gain control circuit which does not require a dc amplifier is described. Variations in the rectified signal current at the detector output are used to vary the load impedance of the detector and a preceding amplifier. Two thermistors are connected in series between the amplifier output and the detector output with the junction point of the thermistors returned to ground through a capacitor. The first thermistor serves as an ac load for the amplifier, with the detector operating potential supplied through the series-connected thermistors. Since the thermistor impedance varies inversely with the rectified carrier current output of the detector, regulation is achieved with no effect on the operating characteristics of the transistors. Because of the slow response of the thermistors, the AGC circuit does not respond to the audio variations in the detector output. The circuit is particularly adapted for use in telephone carrier circuits.

8525 THE APPLICATION OF TRANSISTOR DC CONVERTORS TO PORTABLE TRANSRECEIVERS by M.V. Joshi and M.A. Narayanan (Natl. Phys. Lab., India); Electro-Tech., Vol. 4, pp. 3-13, Jan.-Feb. 1960

The design of transistor dc convertors for application of two portable transceivers is discussed. The various performance requirements and limitations due to the use of readily available batteries are stated. The performance of a transceiver when operated through the transistor dc convertor is compared with

...s normal ac performance and it is shown that satisfactory ...eration is obtained when transistor dc convertors are used. ...rcuit and design details and performance figures for the ...ansistor dc convertors are made available. Probable power ...ources for operation of dc convertors are studied. Test data ...n batteries are included and it is suggested that batteries of ...ype 6G and type 286 may find use in this application.

...26 H.T. SUPPLY UNITS FOR TELEVISION RECEIVERS ...QUIPPED WITH SILICON DIODES by J.F. vanDam, L.A.L. ...sseling, A.M.H. Schellekens, and A.P. Tanis (Philips); ...lectronic Applic., Vol. 21, No. 1, pp. 1-24, 1960-1961

...gh voltage power supply units for TV receivers are discussed. ...survey of the development of semiconductor rectifiers and ...he manufacture, operation and characteristics of Si diodes is ...lso presented. The fundamental Si diode rectifier parameters ...pplicable to single-phase half-wave rectification, two-phase ...alf-wave rectification and voltage doubler circuits are dis-...ussed. Smoothing by means of RC networks is exhaustively ...nvestigated and is illustrated by a detailed example. The ...onsequences of the fact that the waveform of the ac supply is ...ot purely sinusoidal are investigated.

...527 SAWTOOTH WAVE GENERATOR by M.B. Finkelstein ...nd H.C. Goodrich (RCA); U.S. Pat. 2,926,284, Issued Feb. ...3, 1960

...A transistor sawtooth wave generator for use in the deflection ...circuits of television receiving systems is described. The gen-...erator includes a transistor which is coupled to an inductive ...oad circuit. A connection is made from the load circuit to ...he base electrode of the transistor to compensate for variations ...n the rate of change of current in the load by altering the ...ransistor emitter bias. A transformer secondary winding and a ...liode are connected in series between the base and the load ...circuit. The secondary winding provides a feedback voltage of ...polarity and magnitude to provide regenerative operation of ...he sawtooth generator, while the diode provides an open ...circuit between the second secondary winding and the load ...circuit to permit rapid cutoff of the transistor. The circuit ...rovides a substantially linear sawtooth wave output with ...ommercially available transistors and deflection transformers.

MICROWAVE AND TELEMETRY

...3528 DUPLEXING SYSTEMS AT MICROWAVE FREQUENCIES ...y A.F. Harvey (Roy. Radar Estab.); IRE Trans., Vol. MTT-8, ...p. 415-431, July 1960

...The various methods of duplexing at microwave frequencies ...are reviewed. General principles, including the use of pas-...ive and solid state devices, are discussed. The characteristics ...f gaseous discharge duplexing tubes of both self- and exter-...nally-excited types are examined and data for typical examples ...given. The various arrangements of discharge tube duplexers ...nd methods of measuring their performance are described. A ...ibliography is included.

...3529 A TELEMETERING SYSTEM FOR STOMACH PRESSURE ...F ANIMALS by R.W. Allington (U. Nebraska); Elect. ...ngrg., Vol. 79, pp. 590-593, July 1960

...A telemetering system for measuring rumen pressure in animals ...uch as cattle and sheep is described. The transmitter uses a 2N35 n-p-n junction transistor in a modified Hartley oscillator circuit and is packaged in a 1-1/4 by 7 inch tube constructed of methacrylic resin plastic. The transmitter operates at 90 kc, has a power input of 15 milliwatts (and therefore a battery life of 9 days) and a radiated power output of 2 milliwatts. The transmitter is frequency modulated by a condenser microphone shunted across the oscillator coil which also serves as the radiating antenna coil.

8530 MULTIPLEX MODULATION COMMUNICATION SYSTEM by S. Metzger (RCA); U.S. Pat. 2,925,469, Issued Feb. 16, 1960

A time division multiplex communication system in which the commutating, modulating, and demodulating functions at the transmitting and receiving ends are performed by circuits containing a transistor and a magnetic core is described. The transistors act as switches for the associated cores, the latter being connected to operate as a ring counter. This provides a pulse position modulation system, whereby the time of each of the modulated signals produced at the transmitter end is varied according to the amplitude of the modulating signal energy during the sampling interval. Each cycle of operation of the ring counter is begun by the production of a synchronizing signal in the first channel, providing an identification marker for the modulated signals of the succeeding channels. At the receiving end, each demodulator stage includes a transistor bistable multivibrator and a low pass filter. The multivibrators each function in response to the pulse position modulated signals to produce a pulse corresponding to the received signal. This is then applied to the proper utilization circuit through a low-pass filter.

OTHER COMMUNICATION-TYPE APPLICATIONS

8531 PORTABLE TRANSISTOR AMPLIFIER FOR NEWS RECORDING APPLICATIONS by E.M. Tink (WLAC-TV); J. Soc. Mot. Pict. TV Engrs., Vol. 68, pp. 83-86, Feb. 1959

A lightweight sound-on-film recording system which utilizes a portable power supply and a miniature transistor amplifier mounted directly on the side of an Auricon 16mm camera is described. The power supply is housed in a standard camera gadget bag and supplies both ac power to the camera drive motor and dc power to the amplifier and exposure lamp. Battery replacement is kept to a minimum through the use of nickel-cadmium cells and a built-in charger.

COMPUTERS

8532 COMPONENTS AND BASIC CIRCUITS by N.H. Taylor (Itek); Handbook Automn. Computatn. and Control, Vol. 2, J. Wiley and Sons, 1959, pp. 14-01 to 14-54

Design philosophy and practical techniques for achieving digital system reliability are discussed. The system design project is described in terms of three steps. The capabilities of each individual component to be used in the system is analyzed. Data from the first step are employed to evaluate applications of these components that avoid their worst limitations. The final phase is the electronic circuit design, based upon component analyses and application notes derived earlier, with the objective of the achievement of high reliability. The thorough design method developed by Lincoln Laboratory is

described in detail. This method provides reasonable component tolerances and adequate safety margins, and incorporates marginal checking throughout the design process. The method is described in a detailed example of a high-speed vacuum tube flip-flop. Additional tube and transistor basic building-block circuits are described and discussed with the aid of transfer characteristics and circuit diagrams. These basic circuits have been employed in the assembly of large data processing systems. A section on components, characteristics and application notes deals with tubes, semiconductor diodes, relays, connectors, resistors, capacitors, transformers, and transistors.

8533 "POWER-LOGIC" WITH SCRs by T.P. Sylvan (GE); Electronic Design, Vol. 9, pp. 46-49, Nov. 22, 1959

The utility of SCRs (silicon-controlled rectifier) as a means of handling power and logic simultaneously and efficiently is described. Three classes of circuits are described: ring counter and shift register, time delay circuits, and high-speed fault switching circuits. Each example circuit is described in detail and some applications are given. The SCR may be switched on within a few microseconds after being triggered and its high surge rating permits it to carry momentary currents as high as 2000 amp for 2 msec without damage.

8534 TRANSISTOR CIRCUITS by I.L. Auerbach (Auerbach Electronics); Handbook Automn. Computatn. and Control, Vol. 2, J. Wiley and Sons, 1959, pp. 16-01 to 16-30

A design approach and basic circuits for three techniques of transistor digital computer design are discussed. The techniques are direct coupled transistor logic (DCTL) or switching circuits, point-contact transistor pulse amplifiers with diode gates, and transistor circuitry connected by dc paths with diode clamping. In each case a computer based on the technique is described. They are, respectively, Transac (Philco), Tradic Phase I (Bell Labs.), and IBM 608. Essential features of the machines are summarized in a table. Particular attention is given to the logic and control circuit techniques. Detailed characteristics of the transistors and the circuits in which they are employed are given. As a logical element the transistor has the following advantages: its life span is several orders of magnitude that of vacuum tubes, transistors may be dc coupled, they may be connected in parallel and series (by using n-p-n's and p-n-p's together in circuits possessing complementary symmetry), great design flexibility can be obtained, high efficiency is possible in switching, and the transistor provides considerable economics in size, weight, and power requirements.

8535 MAGNETIC CORE CIRCUITS by I.L. Auerbach (Auerbach Electronics); Handbook Automn. Computatn. and Control, Vol. 2, J. Wiley and Sons, 1959, pp. 15-01 to 15-25

A detailed discussion of magnetic cores and magnetic core circuits is given. Circuits employing bistable magnetic cores are characterized by compactness, low power consumption, and long life with reliable operation. They are capable of performing most of the functions of digital data processing systems, including storage, delay, control, and logical operations. Fundamental concepts and logical representation of core circuits are discussed. A description is given of magnetic core materials in regard to their size and construction, and technical data for circuit design are provided in graphic form. Basic theory of transfer loops, which are circuits connecting two or more cores for the purpose of information transfer, is given. Improved, practical transfer loop circuits are also discussed. Applications of magnetic cores in shift registers, logical function circuits, magnetic core storages, timing control circuits, arithmetic and miscellaneous or nondigital applications are described. A short discussion is presented on drivers for magnetic core circuits.

8536 ANALYSIS OF MAGNETIC AMPLIFIER CIRCUITS by T.H. Bonn (Rem. Rand); Ann. Comp. Lab. Harvard U., Vol. 30, pp. 149-160, 1959

Magnetic amplifier and transistor logic circuits are discussed. It is concluded that the only serious disadvantage of magnetic circuitry is the inherent delay associated with the magnetic amplifier. The basic magnetic amplifier circuits are catalogued and means for reducing delay are discussed. Coil gating circuits competitive with transistor circuits are presented and an analogy with relay networks is drawn.

8537 BALANCED LOGICAL MAGNETIC CIRCUITS by A.J. Meyerhoff (Burroughs); U.S. Pat. 2,925,500, Issued Feb. 16, 1960

A technique of improving the reliability of logical magnetic circuits by the use of balanced circuit techniques in bistable magnetic circuits is described. The use of balanced circuits obviates the need for noise reduction circuitry, since any tendency for one element to produce a different noise impulse amplitude or shape than any other element is immediately opposed by the inherent balancing action of the circuits. The application of balancing techniques in performing various logical functions is shown; among these functions are logical inhibit, EXCLUSIVE OR, and binary counting.

8538 MAGNETIC SWITCHING DEVICE by H. van der Heide (Philips); U.S. Pat. 2,960,685, Issued Nov. 15, 1960

A magnetic switching device which employs two or more separated plate shaped parts of ferromagnetic material is described. Each plate is furnished with a hole through which input and output windings are connected. The windings may consist of single conductors. The ferromagnetic plates are shown to be electrically equivalent to commonly used ring cores. By suitable choice of material, dimensions, and numbers of turns it is possible to obtain a magnetic circuit which in given cases may have better properties than the corresponding ring core arrangement. Circuits for a memory switch and a memory matrix employing ferromagnetic plates are given. Magnetic devices with plate shaped materials are more easily handled and less fragile than corresponding annular core devices.

8539 FERRITE-DIODE IMPEDANCE CIRCUITS FOR LOGICAL OPERATIONS AND THEIR SYNTHESIS [in Russian] by A.M. Nechaev (Moscow U.); Izv. VUZ Radiofiz., Vol. 3, No. 5, pp. 892-900, 1960

An analysis of a ferrite-diode element with at least 500 kc speed which can be used to construct any logic circuit is presented. The operation of a circuit of any complexity is executed in two cycles. A regular method is developed for the synthesis of ferrite-diode circuits based on such an element. Examples of the synthesis of the most useful circuits in computers are analyzed.

Two-State Digital Computer Elements Employing Corbino Disks - See 8451

Hall Effect Memory Device Circuits - See 8449

8540 STORAGE by D.R. Brown (Mitre) and J.I. Raffel (MIT); Handbook Automn. Computatn. and Control, Vol. 2, J. Wiley and Sons, 1959, pp. 19-01 to 19-35

Basic concepts of storage and storage techniques including magnetic drum and magnetic core storage are discussed. Principal parts of a typical storage unit are: the address register, the selection circuits, the storage medium, the storage (or buffer) register, and the storage control. The principle of operation of storage units and important characteristics such as capacity, speed, and reliability are discussed. A simplified block diagram of a magnetic drum storage unit is shown. The principle of operation, construction, writing, and reading circuits are discussed in some detail for magnetic drum storage. Similarly, magnetic core storage characteristics are discussed employing numerous diagrams (waveform, block, schematic and pictorial) to supplement the description. Other storage techniques discussed are: nondestructive readout techniques, thin magnetic films, ferrite plates, multiaperture cores, acoustic delay line storage, mercury delay lines, cathode-ray storage tubes, capacitor-diode storage, ferroelectric storage, cryogenic films, the twistor (which makes use of helical strain anisotropy of magnetic wires), and the parametron (information storage is possible with two phases of oscillation of a pumped resonant circuit).

8541 DRUM INDEXING SYSTEM by J.A. Blickensderfer (GE); U.S. Pat. 2,923,922, Issued Feb. 2, 1960

An improved magnetic drum indexing system applicable in information handling machines is described. A single track on a magnetic drum is employed wherein pulses are placed to indicate where incoming data should be written in a particular sector on the drum which is assigned for the storage of that data. A complete description is given on the drum-indexing system in connection with a buffer store. The buffer store receives its data from an input keyboard and may also employ other input sources. The system is less wasteful of drum space and in many instances less time-consuming than systems used in the past.

8542 MAGNETIC DRUM MEMORY FOR ELECTRONIC COMPUTERS by R. Thorensen, W.R. Arsenault, and B.F. Ambrosio (Sec. of Commerce); U.S. Pat. 2,925,587, Issued Feb. 16, 1960

A magnetic drum memory unit and associated control circuitry that greatly reduces the over-all access time to the drum memory is described. A number of diagrams for the complete system and its components, and a detailed description of the operation of the system is given. Means are provided to transfer information in sizeable blocks from the magnetic drum memory to the electrostatic memory of a computer. Access time to the drum memory is held to a minimum. The address of the particular word passing under the reading and writing heads is known at all times and is available to the control circuitry of the computer immediately upon the receipt of the drum operation signal. Information recorded on the drum is grouped in words. There is an equality between the number of words in a single channel of the drum and a predetermined number of complete lines of the electrostatic memory. The coder may choose the particular consecutive lines of the electrostatic memory to be communicated with, while the drum system controls the particular location in those lines at which the transfer of information is to start.

Coincident Current Core Memories - See 8464

8543 TRANSISTOR CIRCUITS FOR MAGNETIC MATRIX STORES by G.C. Padwick (Mullard); Electronic Applic., Vol. 21, No. 2, pp. 76-87, 1960-1961

A transistorized coincident-current magnetic matrix store is described. A detailed circuit description of the drive and output circuitry is given. The clock frequency, a 100 kc square wave, controls the read and write pulse generators. The pulses are routed by gating matrices and pass through the planes of the store in series. Addresses are set up in staticisors which operate gating matrices by using decoders and transistor switches. The output of each plane is separately amplified and shaped, with the inhibit current for each plane generated separately. The extracted information is immediately rewritten. To permit current flow in both directions, the switching transistors are mounted in diode bridges. Half of a 10 μsec cycle is used for driving the memory cores with the remaining 5 μsec used for opening gates and selecting new addresses.

8544 INTELLIGENCE STORAGE DEVICES WITH COMPENSATION FOR UNWANTED OUTPUT CURRENT by D.S. Ridler and R. Grimmond (Intl. Stand. Elect.); U.S. Pat. 2,958,853, Issued Nov. 1, 1960

A method for compensating unwanted output current from magnet storage reading circuits is given. To read stored information, pulses are applied which reset all elements to one stable state, "0." A large voltage output signal is obtained from each element which stores "1" and a small output known as a sneak is obtained from each element which stores "0." The sneak is eliminated by application of a second toroid associated with each storage element. A reading pulse produces an output in the second toroid which is opposite and cancels out the sneak reading of the first when the element is in the "0" state. When the first element is in the "1" state the two outputs do not cancel and a large output is available to indicate presence of the "1" state. Applications of the basic circuit given are storage matrix, shifting register, and a multistable register.

8545 ELECTRICAL CIRCUITS EMPLOYING FERROELECTRIC CAPACITORS by J.R. Anderson (Bell Labs.); U.S. Pat. 2,876,436, Issued Mar. 3, 1959

Use of a double-anode saturation diode in series with a ferroelectric capacitor to improve the signal storage characteristics of the latter is discussed. The squareness of the hysteresis loop, and thereby the SNR, is considerably increased. The double-anode diode, or two saturation diodes in series opposition, negates the effects of space charge buildup, internal bias, nonsquare hysteresis loops, and disturbing pulses. The technique is applied to signal-storage matrices.

8546 INFORMATION HANDLING DEVICE by E.J. Schmitt (RCA); U.S. Pat. 2,925,589, Issued Feb. 16, 1960

A system for transferring information between a cyclical memory and a high-speed random access memory is described. A block diagram and detailed description of the system is given. Information may be transferred between a cyclical storage device and a random access storage device in either direction. The system provides for preswitching to select the desired cyclic memory channels and for continuing with other computing

operations while such switching takes place. In addition, a means for modifying individual instructions in the storage devices is provided. The system may be employed to economize computer time.

Error Detector or Teletype Actuator for Computers - See 8519

8547 NONLINEAR ELECTRONIC COMPUTER ELEMENTS by G.A. Bekey (Space Tech. Labs.); Handbook Automn. Computatn. and Control, Vol. 2, J. Wiley and Sons, 1959, pp. 23-01 to 23-40

Nonlinear electronic computer elements such as function multipliers, function generators, switching devices, trigonometric devices, and time delay simulators are discussed. The electronic time division multiplier, the "quarter squares" multiplier, and the electromechanical servo multiplier are treated in detail; other types of multipliers are surveyed more briefly. Function generators such as curve follower devices, biased diode function generators, servo-driven tapped potentiometers and photoformers are discussed. Several techniques for obtaining trigonometric functions to express angular variations or to perform coordinate transformations are described. Simulation of a true time delay of the form $f(t-\tau)$ involving the use of a device to store information is cited.

8548 PULSE SHAPING WITH VARIABLE-CAPACITANCE DIODES by D.P. Schulz (Hughes); Proc. IRE, Vol. 48, p. 1918 (L), Nov. 1960

Integrating and differentiating circuits which utilize variable capacitance diodes are analyzed. It is found that diode integrators produce an output proportionan to $[\int f(e)]^{1/(1-n)}$ and that diode differentiators produce an output proportional to

$$\frac{1}{[f(e)]^n}\ \frac{1}{dt}\ f(e),$$

where f(e) is the input pulse. The output voltage of integrators and differentiators using both conventional capacitors and semiconductor capacitors for various input wave shapes are presented.

8549 OPERATIONAL DIGITAL TECHNIQUES by B.M Gordon and J.F. LaFontaine (Epsco); Handbook Automn. Computatn. and Control, Vol. 2, J. Wiley and Sons, 1959, pp. 29-01 to 29-29

Operational digital techniques, called hybrid systems, are discussed. Essentially, in the hybrid system, digital techniques are used in functional units that are laid out in operational form. Objectives of the hybrid system are: greater precision that can be attained with analog techniques and at lower cost, greater speed and control than is possible with programmed digital units, less complexity than is involved when programmed digital units alone are used, and the ability to accept input data in the analog form in which they usually occur. Basic devices such as a binary rate multiplier, magnetic core transistor multiplier, and a dynamic rate multiplier are described in detail. Other devices which perform typical mathematical operations are also briefly treated. Machine tool control and information averaging are discussed to illustrate the application of operational digital techniques. A hybrid computer which is composed essentially of digital computer circuitry (therefore achieving the high accuracy of a digital computer) is discussed in great detail. It operates in nearly real time, by means of incremental computation techniques, and therefore possesses one of the salient characteristics of the analog computer.

8550 SEMICONDUCTING CONVERTER OF ANALOG QUANTITIES INTO DIGITAL EQUIVALENTS [in Russian] by V. Z. Naiderov (L'vov Polytech. Inst.); Izv. VUZ Radiotek., Vol. 3, No. 5, pp. 463-473, 1960

The construction of semiconductor circuits that may be employed to convert analog quantities into digital is discussed. A linear voltage generator and a comparator are described and the necessary design relationships are given. The possibility of obtaining a conversion accuracy not worse than 0.1 per cent is shown.

POWER APPLICATIONS

8551 HOME GENERATION OF POWER BY PHOTOVOLTAIC CONVERSION OF SOLAR ENERGY by J.F. Elliott (GE); Elect. Engrg., Vol. 79, pp. 735-738, Sept. 1960

An economic and technological investigation of the feasibility of individual homeowners in certain parts of the U.S.A. generating their own electric power by means of photovoltaic conversion of solar energy is discussed. A high reliability power plant can be provided using a tilted flat collector converter and a storage system having a capacity of 1-1/2 days. The energy supplied by this plant can compete economically with power from a conventional central station delivered to the home by transmission lines if the photovoltaic cell is sold to the consumer for less than $0.61 per square foot. These arguments hold in locations where the daily insolation during the winter is at least 0.3 kw per square foot.

8552 TRANSISTOR POWER SUPPLY by W.H. Manning (U.S. Army); U.S. Pat. 2,924,727, Issued Feb. 9, 1960

A point contact oscillator which can supply both ac and dc voltages to separate loads is described. Starting under load conditions is achieved by means of current controlled regenerative feedback. After the oscillations begin the current controlled feedback is reduced to a low value. A tank circuit transformer coupled to the oscillator determines the frequency of the oscillator. An ac voltage is supplied to an inductance in the tank circuit. A dc voltage is provided by filtering the output voltage which appears across another secondary winding of the transformer coupled to the oscillator. The dc and ac voltages are regulated by a peak-clipping voltage regulator.

Power Supply for Photomultiplier - See 8564

8553 BATTERY POWERED CONVERTER RUNS MULTIPLIER PHOTOTUBE by R.P. Rufer (U. California); Electronics, Vol. 33, p. 51, July 8, 1960

A high voltage power supply for use with photomultiplier tubes is described. A low dc voltage is converted to ac by means of a conventional flip-flop and the individual dynode voltages are obtained by multiplying the input ac voltage through a string of Cockroft-Walton voltage doublers utilizing silicon diodes. A nine-stage photomultiplier requires ten doubler stages. The supply provides a more constant dynode voltage than a supply which employs a bleeder resistance chain and does not suffer from the quiescent power loss inherent in bleeder resistance chains. The unit has also been operated in daylight with colar cells.

POWER APPLICATIONS (Cont'd)

dc to ac Converters - See 8525

8554 DESIGN OF A SATURABLE CORE POWER INVERTER by C.M. Bailey, Jr. (Bell Labs.); Proc. NEC, Vol. 15, pp. 656-665, Oct. 12-14, 1959

The design of a 100 watt, 2800 cps dc to ac transistor core inverter power supply is discussed. A brief review of the simple inverter circuit and various modifications thereof, and a detailed discussion of the operation of the circuit selected for the application concerned with particular emphasis on achieving a reliable circuit design which is simplified and feasible for mass production are included. While the treatment of the subject is for a specific application, the information contained is of general interest to designers.

8555 CONTROLLED DC TO DC VOLTAGE STEP-UP WITH A SINGLE TRANSISTOR by R.E. Morgan (GE); Proc. NEC, Vol. 15, pp. 674-678, Oct. 12-14, 1959

A dc inverter that provides an output voltage greater than the input voltage is described. The output voltage is controllable and can be varied over a 10-to-1 voltage ratio. A single transistor and a saturable current transformer oscillate and control by a time ratio control method. A single transistor can step up and control over 100 watts.

CONTROL APPLICATIONS

Motor Speed Control Employing Magnetic Pulse Generator - See 8515

8556 REVERSING MOTOR CONTROL SYSTEM by C.A. Cibelius, Jr. (Barber-Coleman); U.S. Pat. 2,924,763, Issued Feb. 9, 1960

A system for controlling the direction of rotation and torque of a shaded pole motor is described. An error signal supplied by any suitable electromechanical pickup is fed to a conventional two-stage transistor amplifier and thence to a motor supply circuit. This circuit consists of a single transistor operating in class C and supplying half wave pulses of voltage to the shading windings of the motor. The motor connections are modified such that adjacent pairs of shading windings are oppositely poled and connected in series, resulting in substantially zero induced voltage; the pairs are then connected in parallel. With this arrangement, induced voltages are self-cancelling and are not applied to the transistor; in addition, low power transistors can be used. Thus a transistor rated at one watt is capable of controlling a motor rated at four watts. The result is a lightweight, low cost control system.

8557 A SYSTEM OF STATIC RELAYS FOR INDUSTRY [in French] by M. Cambornac (Soc. Servos. Electroniques); Onde Elect., Vol. 40, pp. 665-672, Oct. 1960

A system of static relays operating at industrial frequencies and using transistors and magnetic amplifiers simultaneously is described. Starting from a single base function there have been developed: (1) simple relay elements, (2) measuring elements, (3) power elements, and (4) conversion elements. These are plug-in relays and each has its own signal-handling arrangements.

8558 STATIC RELAYS USING LOGISTOR TRANSISTORS [in French] by M. Gauvin (Bur. Pilote Auto., Soc. Alsthom); Onde Elect., Vol. 40, pp. 673-683, Oct. 1960

A static relay using Logistor transistors, which operates in an on-off manner in the same way as a conventional electromagnetic relay which it is designed to replace in complex automatic devices or in heavily loaded service, is described. The information delivered at the output of an element is directly related to the information supplied at the input terminals. Resolving circuits constructed with Logistor relays are logically based (i.e., made up of directly related functions). These are built up from a single basic element which is a NOR element with three inputs. A few other standard elements make possible the connection of the logical section to other stages of the equipment. A prime application of the Logistor transistor is in control programs for numerical instructions.

Magnetic Bridge Amplifiers - See 8496

Thyratron Transistor Circuit - See 8506

INSTRUMENTATION

8559 TRANSISTOR MULTIRANGE DC MILLIVOLTMETER by K. Holford (Mullard); Electronic Applic., Vol. 21, No. 3, pp. 107-113, 1960-1961

A transistorized portable dc millivoltmeter having a maximum sensitivity of 10 mv full-scale and an input resistance of one megohm/v is described. To reduce the transistor temperature dependence, a long-tailed-pair circuit, in which the signal is applied differentially between the base terminals of two similar common-emitter transistors, is used. Using BCZ 11 transistors, a temperature compensation of better than 99 per cent is obtained over a 20°C range. The zero stability is less than 5 per cent of full scale over this range, with an increase in the calibration error of one per cent. The meter will operate to 75°C ambient.

8560 PORTABLE ELECTROMETER VOLTMETER by W.E.K. Gibbs (Austl. Def. Sci. Service); J. Sci. Instr., Vol. 37, p. 296, Aug. 1960

A portable high impedance voltmeter for measurements up to two volts is described. Using a Mullard ME 1401 electrometer with a three transistor amplifier, the device has an input impedance of about 10^{10} ohms. Measurement accuracy and short term zero drift are both approximately 2 per cent of full scale.

8561 APPLICATION OF TRANSISTORS TO FREQUENCY METER FR-67/U AND MANUFACTURE OF EXPERIMENTAL MODELS by H. Chisholm, R. Ellsworth, and R. Evans (Beckman Instr.); U.S. Gov. Res. Rep., Vol. 33, p. 497(A), May 13, 1960 PB 145 260

The manufacture and testing of two complete frequency meters which comply with all electrical specifications are described. Most of the final report deals with the circuitry of the resultant units. The theory and characteristics of each major function is given, followed by a section on operating techniques and a section of maintenance procedures. Photographs, sketches, and complete schematics are given.

8562 FLUX PATTERN INSTRUMENTATION USING HALL PROBES by H. Hollitscher (Canadian GE); Elect. Engrg., Vol. 79, p. 996, Dec. 1960

Equipment which utilizes Hall probes to measure the magnetic flux density in the air gap of rotating machines is discussed. Auxiliary equipment such as power supplies for the probes, calibrating milliammeter, shunts, selector switches, etc. are built into a portable unit. A dual-beam oscilloscope and a multichannel recorder are used for the display and recording of the flux traces. The equipment has the following advantages over more conventional methods of exploring magnetic fields: (1) Pointwise measurement of flux is possible. (2) The flux density at several points, even in different directions, can be measured simultaneously. (3) Results are obtained directly in flux density and no integration is necessary. (4) Any stationary or alternating field can be measured as well as fields in which the dc and ac components are superimposed.

8563 PULSING HALL PROBES FOR GREATER OUTPUT by D. L. Shirer (Argonne Natl. Lab.); Rev. Sci. Instr., Vol. 31, pp. 1000-1001, Sept. 1960

The use of a pulsed control current to increase the output of a Hall probe 10 to 20 times its normal value is discussed. The average dissipation of the semiconductor must be kept well below its rated value. The block diagram of a circuit used to pulse the control current is presented and discussed. A Siemens FC 33 probe which has a continuous control current rating of 0.1 amp has been pulsed at 1 and 2 amp at a duty cycle of less than 1 per cent with no apparent harm. The control current pulses had widths 5 - 50 msec and repetition periods ~ 5 sec. With a 1 amp pulsed control current, the output of the FC 33 probe is repeatable to within better than 0.03 per cent in a magnetic field of 400 gauss which changes at a rate of 30 kgauss/sec. The pulsed probe is particularly suited to applications where the instant at which a rapidly-changing magnetic field passes through a chosen value must be known with a high degree of precision, e.g., the determination of the injection time of protons into a synchrotron.

8564 TRANSISTOR CIRCUITRY FOR A VERY SENSITIVE PHOTOMULTIPLIER by J.R. Groves (Weapons Res. Establ., Austl.); Proc. IRE, Austl., Vol. 21, pp. 142-147, Mar. 1960

Completely transistorized circuits for a photomultiplier which is to be used in an investigation of upper atmosphere phenomena are described. Details of the high voltage regulated power supply, the chopping oscillator and the narrow bandwidth tuned amplifier are given. The equipment is designed for convenient operation in the field or laboratory.

8565 THRESHOLD SENSITIVITY OF RADIATION RECEIVERS by E.S. Ratner; Optics and Spectrosc., Vol. 9, pp. 52-55, July 1960

The threshold sensitivity of radiation receivers is discussed. The customary criterion in the case of an electrical output indicator is usually of the form $U_s/U_n = m$ where U_s is the signal voltage at the output of the system from the detected radiation, U_n is the noise output voltage in absence of signal, and m is a coefficient determined by the required magnitude of the probability of detection by means of a single observation. In a number of cases this criterion is not correct. One such system is discussed which is assumed to be free from self-generated noise. In the absence of extraneous irradiation ($U_n = 0$) this leads to an absurd result. Equations are developed, based on statistical analysis of the fluctuations in the effectively absorbed quanta, which consider the relationship of the sensitivity threshold of radiation receivers to the magnitude of the steady background and certain properties of the receiver-amplifier-indicator system.

8566 EXTENDED RANGE PIRANI GAUGE by A.W. Smith (Union Carbide); Rev. Sci. Instr., Vol. 30, pp. 485-486, June 1959

A Pirani gauge which is useful from atmospheric pressure to 10^{-5} mm Hg is described. The gauge has two elements, a platinum ribbon active in the low-pressure region and a thermistor bead active in the high-pressure region. By a simple but unique electrical circuit, the high-level sensitivity in the intermediate region is maintained. In any pressure region, the gauge has the optimum characteristics possible with a Pirani-type gauge.

8567 SWEEP VOLTAGE GENERATOR by G.E. Edens (Tektronix); U.S. Pat. 2,924,712, Issued Feb. 9, 1960

A transistorized apparatus for generating a voltage which is proportional to the displacement of a movable member from a predetermined position is described. The device is useful in a rotation analyzer for producing a sweep voltage for an oscilloscope. Quantitites such as pressure, velocity, torque, or vibration can thus be displayed (by use of suitable transducers) as functions of instantaneous position of the element regardless of the speed of the internal combustion engine or variations of such speed. The principle can be also applied to analyzing devices involving reciprocating motion. Equally spaced markers are positioned on an element attached to a movable member of the machine to be analyzed. A voltage pulse is produced by the passing of each market past the pickup. Such pulses are amplified, shaped to a constant amplitude and integrated to produce the output sweep voltage. A trigger marker is employed to reset and synchronize the sweep output. A detailed discussion of the theory of operation of the circuit is presented.

8568 MAGNETIC PULSE COUNTING AND FORMING CIRCUITS by C. Neitzert (Genl. Time); U.S. Pat. 2,897,380, Issued July 28, 1959

A circuit for pulse counting and forming, using automatically reset saturable cores, with the input-output pulse ratio adjustable, is described. With the application of input pulses, the core is driven beyond the knee of the hysteresis loop; the flux abruptly decreases after the last pulse in the train to be counted, and falls to the knee of the hysteresis loop. This operates the reset switch and produces an output pulse. The reset switch consists of a junction transistor connected as a blocking oscillator type of relaxation oscillator which is held cutoff by the supply voltage. A voltage, induced by the flux decreases after the last pulse in the counting train, switches the transistor on. The transistor current saturates the core in the reverse direction before arrival of the next input pulse. During reset current flow, the induced voltage holds the transistor on. When the core reaches reverse saturation, the induced voltage decreases to zero and the transistor cuts off. The output pulse is induced by the core flux excursion during reset operation. The pulse count ratio is determined by turns selection.

8569 FURTHER CHARACTERISTICS OF THE SOLID-STATE IONIZATION CHAMBER by R.J. Grainger, J.W. Mayer, J.S. Wiggins, and S.S. Friedland (Hughes Aircraft); Bull. Am. Phys. Soc., Ser. II, Vol. 5, p. 265(A), Apr. 25, 1960

The response of high resistivity shallow diffused Si diodes to charged particles was discussed. When operated at $\cong$ 200 v reverse bias, units whose resistivity is 6×10^3 ohm-cm had a response proportional to proton energy up to 9 Mev. These same units responded linearly to electrons from the internal conversion lines of Cs^{137}, Cs^{134}, and others. The data indicate that, within experimental limits, the detectors respond linearly to the energy of particles whose mass varied from electron mass to the mass of carbon ions and fission fragments. Using a detector with area of $2 mm^2$, the width of the pulse-height distribution at half-maximum was measured to be 17.5 kev for natural alpha particles. The scattering of protons from Al and Be yielded resolutions of approximately 1 per cent, sufficient to resolve the nuclear levels. The resolution of large area units was discussed.

8570 PERFORMANCE OF p-n JUNCTION PARTICLE DETECTORS UNDER GAMMA IRRADIATION by C.T. Raymo, J.W. Mayer, J.S. Wiggins, and S.S. Friedland (Hughes Aircraft); Bull. Am. Phys. Soc., Ser. II, Vol. 5, pp. 354-355(A), June 15, 1960

The use of shallow-diffused silicon p-n junctions as neutron detectors was discussed. The noise level and resolution were measured under γ irradiation. In a γ flux of 4×10^5 r/hr, the noise level of 300 ohm-cm 2 x 2 mm detectors increased to an equivalent noise level of 2.3 Mev with a subsequent deterioration of resolution for 4.5 Mev α particles with 1 to 25 per cent. With units of higher base resistivity and/or larger surface area the equivalent noise level increased. For example 10^4 ohm-cm 5 x 5 mm units had an equivalent noise level of 20 Mev. These effects could not be attributed solely to the increased dc current but are apparently caused in part by "pile-up" effects in the detector of pulses caused by γ-generated Compton electrons. The results indicate that low resistivity devices are useful as fission fragment and/or neutron detectors in high γ fluxes, but their application as spectrometers is restricted. Under lower fluxes, the detrimental effects of the γ rays are reduced.

8571 PERFORMANCE OF LARGE AREA p-n JUNCTION PARTICLE SPECTROMETERS by J.W. Mayer, R.J. Grainger, J.W. Oliver, J.S. Wiggins, and S.S. Friedland (Hughes Aircraft); Bull. Am. Phys. Soc., Ser. II, Vol. 5, p. 355(A), June 15, 1960

The response of devices five millimeters square of larger to alpha particles, fission fragments, protons, and electrons was discussed. Studies of the width of the pulse height distribution as related to the noise level and reverse current were presented and the question whether the major component of the current is contributed by carriers generated in the space-charge region was considered. Deterioration of the performance of the detectors at elevated temperatures were indicated.

8572 APPLICATION OF THICK-DEPLETION-LAYER SILICON p-n JUNCTIONS TO PROPORTIONAL DETECTIONS OF GAMMA RADIATION AND PENETRATING NUCLEAR PARTICLES by P.F. Donovan (Bell Labs.), G.L. Miller (Bell Labs. and Brookhaven Natl. Lab.), and M.B. Foreman, Jr. (Brookhaven Natl. Lab.); Bull. Am. Phys. Soc., Ser. II, Vol. 5, p. 355(A), June 15, 1960

The preparation of Si p-n junction particle detectors which have depletion layers about 0.8 mm thick was discussed. Conversion electrons and γ-rays which give photoelectrons with ranges less than this distance have been detected with good energy resolution. The γ-ray line widths are about 6.5 kev. This width appears to be limited by electronic noise. These counters also have been used to detect cylotron-produced helium ions up to 40 Mev and protons up to 12 Mev. The pulse heights were proportional to the particle energy, and the energy resolution was apparently limited by the cyclotron beam spread. Proton and α-particle groups with energies up to about 12.5 Mev were observed with good linearity and energy resolution from the reactions $B^{10}(d,p)B^{11}$ and $B^{10}(d,\alpha)Be_\alpha$ with 1.5 Mev incident deutrons. Resolution appears to have been limited by target thickness and angular spread to about 70 kev. Elastic scattering experiments with helium ions and protons at energies up to 3 Mev gave line widths as low as 20 kev. Minimum ionizing particles have been detected with good signal-to-noise ratio.

8573 GALLIUM ARSENIDE FOR γ-RAY SPECTROSCOPY by W.R. Harding, C. Hilsum, M.E. Moncaster, D.C. Northrop, and O. Simpson (SERL); Nature, Vol. 187, p. 405(L), July 30, 1960

The use of gallium arsenide as a γ-ray detector is discussed. The resistivity of the material should be greater than 10^6 Ωcm at room temperature. Pulses of 0.5 mv across an MΩ load with a rise time of about 5 μsec have been observed in both n- and p-type GaAs with an applied field of 200 v/cm. The samples used were 1 cm x 0.2 cm x 0.1 cm.

8574 MULTICHANNEL UNIT OF JUNCTION COUNTERS FOR NUCLEAR SPECTROSCOPY by O.M. Bilaniuk and B.B. Marsh (U. Rochester); Bull. Am. Phys. Soc., Ser. II, Vol. 5, p. 226(A), Apr. 25, 1960

A matrix of twenty 2 mm x 12 mm surface junction counters for use in the image plane of a magnetic spectrometer was described. The outputs of individual crystals are displayed in predetermined channels of a 100-channel pulse height analyzer. This is done by connecting separate crystals to successive sections of a delay line and converting the time difference between signals arriving at the ends of the line into pulse heights. Typical results obtained with this unit were presented. Simple procedures for producing reliable Ge-Au surface junctions, and contacts and properties of such counters were discussed.

8575 TIME-TO-AMPLITUDE CONVERTER by J. Brotzman (U.S. Naval Res. Lab.); Rev. Sci. Instr., Vol. 31, p. 467, Apr. 1960

A simple time-to-amplitude converter which utilizes three resistors, a diode, and an oscilloscope is described. A first event triggers an oscilloscope to produce a positive sweep voltage. This voltage is fed from a divider to a diode which conducts through a low resistance resistor to ground. The diode is biased in the reverse direction by a positive gate generated by a second event. The output rises to a value proportional to the sweep voltage at that time and then returns to ground at the trailing edge of the gate pulse.

OTHER APPLICATIONS

8576 A THERMOELECTRIC REFRIGERATING SYSTEM FOR SUBMARINES by R.G. Sickert (Whirlpool); Elect. Engrg., Vol. 79, pp. 364-371, May 1960

An investigation of the feasibility of a thermoelectric refrigerating system for submarines is discussed. A design method is outlined and is employed in the design of a practical system. The expected performance of the system is considered. It is concluded that with the thermoelectric materials presently available such a system is feasible.

8577 THERMOELECTRIC REFRIGERATION by W.L. Wright (Westinghouse); Elect. Engrg., Vol. 79, pp. 380-384, May 1960

Several applications of thermoelectric coolers utilizing semiconductor thermoelements are described. Coolers for cooling infrared detectors and other semiconductor devices such as transistors are described. Laboratory applications of thermoelectric cooling such as cooling beakers and controlling the temperature of a biological temperature chamber are pointed out and devices developed for these applications are shown. An experimental thermoelectric air conditioner-heater-refrigerator unit and a thermoelectrically air-conditioned suit, being developed for the navy, are discussed.

8578 THERMOELECTRIC AIR CONDITIONING OF TOTALLY ENCLOSED ENVIRONMENTS by G.D. Hudelson (Carrier); Elect. Engrg., Vol. 79, pp. 460-468, June 1960

The design of a thermoelectric air conditioning system for use in a closed environment such as a submarine or an earth satellite is discussed. Two systems, one incorporating a thermoelectric water chiller with conventional air cooling coils and the other utilizing a conventional water-to-water heat exchanger with thermoelectric air coolers are analyzed. The emphasis is on the temperature and humidity control sections of the air conditioning system. It was found that a considerable improvement in the performance of the thermoelectric system can be obtained by reducing the load. In one system, for example, a reduction in the load of only 5% reduced the power requirement 48% and increased the efficiency 71%.

8579 ALTERNATING CURRENT SYSTEM by J.F. Reuther (Westinghouse); U.S. Pat. 2,924,726, Issued Feb. 9, 1960

A device for obtaining from a high voltage alternating current circuit a relatively small electrical output quantity proportional to the circuit voltage is described. A multi-layered condenser bushing provides input coupling to the system which includes a push-pull p-n-p transistor amplifier utilized to drive the output translators. In a particular application involving a 46 kilovolt bushing device the input voltage applied to the amplifier was approximately 25 v at 3 ma. This voltage value is many times smaller than those encountered in potential devices of previous design. The device may be employed to energize a protective circuit breaker or the output may be connected to a measuring instrument.

SUBJECT INDEX

A

Absorption:
- in Alkali Halides 8244
- in Cu_2O 8369, 8370
- in Cu_2O, Exciton 8360
- Edge, Pressure Dependence of 8270
- in Halide Crystals, Infrared 8363
- in Ionic Crystals, Infrared 8366
- in LiF 8367, 8393
- in NaCl, Color Center 8362
- in Synthetic Quartz 8364
- in Thallous Halides, Ultraviolet 8368
- in Wurtzite Structure Crystals 8365
- in ZnO, Exciton 8361

Acceptor Levels in Si, γ-Irradiated 8237
Acoustic:
- Absorption in Synthetic Quartz 8364
- Attenuation in TiO_2 8410

Activation Energy of Diffusion, Evaluation of 8196
Adsorption of O_2 on:
- Ge Surfaces 8231
- Si Surfaces 8230

Alkali Halide Color Centers, Radiation Required to Produce 8179
Alkali Halides,
- Dielectric Absorption in 8244
- Infrared Fluorescence of F-Centers in 8380
- Recombination Luminescence in 8375
- Reflection of 8300

Alloyed Junctions, Formation of 8425
Alloys,
- Sensitive Determination of Transition Metal Content in 8156
- Thermal Resistivity of 8403
- Thermoelectric Power of Cu- and As- 8407
- Thermoelectric Properties of 8459

Aluminum,
- Effect of Pressure on the Critical Field of Superconducting 8283
- Zone Refining of 8194

Aluminum in Si, Precipitation of Impurity 8202
Aluminum Oxide,
- ESR of V in α- 8351
- Flash Etching Technique for Grain Boundaries in 8189

Aluminum Phosphide in ZnS, Solid Solubility of 8161
Amplifiers,
- Bridge 8496
- Computer Design of 8491
- Distortion in Class A-B Push-Pull 8488
- Feedback 8494
- Feedback in 8489
- Hall Effect 8450
- Light: Electroluminescent 8456
- Negative Mass: Conditions for Amplification 8452
- Parametric:
  - Magnetic Film 8497
  - Transducer Characteristics of 8498
- Ruby Maser 8471
- Stability of Negative Mass 8499
- Temperature Compensated 8492, 8493
- Theory of Two-Wire 8490
- Transmission Line 8467

nalog:
Computer Arithmetic Units, Diode 8548
Computers, Nonlinear Electronic Elements in 8547
nalog-Digital Converters 8550
nalysis of Alloys, X-Ray Fluorescent 8156
nisotropy of Magnetization in $Co_xFe_{3-x}O_4$, Effect of Cation Vacancies on Uniaxial 8317
nthracene, Drift Mobility and Carrier Production in 8262
nthracene Single Crystals, Growth of 8219
ntiferromagnetic:
Cr_2O_3, Magnetoelectric Effect in 8334
Metals, Existence of Superconductivity in 8290
Transition Temperature of Cr_2O_3 8334
ntiferromagnetism,
Double Exchange Effects in Magnetic Crystals Exhibiting 8332
Perturbation Theory of 8331
ntimony in Pb, Determination of 8192
rithmetic Units, Diode 8548
rsenic-Selenium Films, Photoelectric and Electrical Properties of 8387
tomic Scattering Factor of Ge 8242
utomatic Gain Control in Radio Receivers 8523, 8524
valanche:
Breakdown in Junction Transistors 8439
Mode Operation of Si Transistors 8436

B

arium Fluoride-Barium Titanate System, Phase Diagram of 8224
arium Strontium Titanate, Temperature Dependence of Piezoresistivity in 8255
arium Titanate,
Domain Wall Motions in 8249, 8250
Factors Effecting Switching in 8251
Mechanical Properties of 8414
Ohmic Contacts to 8235
Resonance Quality Factor (Q) of 8248
arium Titanate Single Crystals, Growth of 8224
arium Titanate-Strontium Titanate Solid Solution Single Crystals, Growth and Properties of 8225
arium Zirconium Metaniobite, Ferroelectric Properties of 8252
artlett-Brune Transformation in Degenerative Amplifiers and Oscillators 8490
inary:
Gates, Low Voltage 8508
Semiconductors, Stability Limits of 8168
ismuth, Photoelectromagnetic Effect in 8391
ismuth Crystal Structure at Low Temperatures 8171
ismuth Platinum,
Crystal Structure of 8288
Thermal Expansion of 8288
Transition Temperature of 8288
ismuth Selenide at High Temperatures, Electrical Properties of 8268
ismuth Telluride,
Effective Mass Parameters of 8397
Faraday Rotation in 8397
Infrared Absorption in 8397
Ohmic Contacts to 8235
istable:
Switching Circuits, High Power 8506
Trigger Circuits Employing Corbino Disks 8451
loch Walls in Si-Fe, Energy and Orientation of 8325
onding Scheme for CdI_2-Type Compounds 8169
oron, Preparation of 8226
reakdown in:
Semiconductors, Circuit Protection Employing 8443
Transistors, Avalanche 8439
ridge Amplifiers, Magnetic 8496

C

Cadmium Antimonide, Dissociation Pressure and Heat of Dissociation of 8159
Cadmium Iodide-Type Compounds, Bonding Scheme for 8169
Cadmium Selenide, Mechanism for Electrical Conduction in 8276
Cadmium Sulfide,
Absorption in 8365
Debye Temperature of 8400
Electroluminescence in 8376
Etch Pits in 8182
Growth of 8213, 8214
Photovoltaic Effect in and Preparation of 8388
Piezoelectric Constants of 8257
Cadmium Sulfide Photoconductive Films, Effect of Heat Treatment on Sintered 8384
Cadmium Sulfide:Manganese, PRM Absorption in 8356
Cadmium Sulfide-Selenide, Photoconductive Spectral Response of Cu-Activated 8385
Cadmium Telluride:Manganese, PMR Absorption in 8356
Calcium in NaCl, Measurement of Concentration of 8244
Calcium Tungstate, PMR of Mn^{2+} and Gd^{3+} in 8353
Calcium Tungstate Crystals Containing Paramagnetic Ions, Growth of 8222
Capacitors, Storage Circuits Employing Ferroelectric 8545
Carrier:
Production in Anthracene 8262
Properties of Semiconductors with Traps, Theory of 8261
Catalysis, Studies of Surface 8232
Cavity Masers, Characteristics of Reflection 8472
Ceramic Oxides, Heat Transfer Mechanisms in 8405
Ceramics, Effects of Stress on the Mechanical Properties of Ferroelectric 8414
Cesium Bromide, Ionic Conductivity and Diffusion in 8245
Cesium Chloride, Cohesive Energy of 8236
Cesium Iodide, Ionic Conductivity and Diffusion in 8245
Characteristics of:
Epitaxial Junctions Formed between Ge and GaAs 8421
GaAs Diodes 8419
Power Transistors, Measurement of 8430
Chlorine in InAs, Solubility of 8203
Chromic Oxide,
Antiferromagnetic Transition Temperature of 8334
Magnetoelectric Effect in Antiferromagnetic 8334
Chromium^{3+}:
in Al_2O_3, PMR Line Width Broadening of 8339
Doped Corundum, Spin-Lattice Relaxation in 8343
in $K_3Co(CN)_6$, Electron Spin-Lattice Relaxation of 8344
Spin-Phonon Interaction in Ruby 8341
in YGaG, PMR of 8350
in ZnF_2, PMR of 8352
Chromium-Doped Titania Maser, Operation of a 8474
Chromium Pentoxide, Magnetic Properties of 8335
Circuit:
Analysis 8485
Breakers, Energizer for 8579
Protection, Semiconductor Breakdown Device for 8443
Circulators,
Ferrite 8462
Y-Junction Stripline 8463
Class A-B Amplifiers, Distortion in 8488
Cleavage Whiskers in Crystals 8206
Cobalt^{2+} Ions in Mixed Paramagnetic Crystals 8337
Cobalt Dichloride Hexahydrate, Crystal Structure of 8172
Cobalt Iron Oxide, Effect of Cation Vacancies on Uniaxial Anisotropy in 8317
Cobaltous Bromide, Susceptibility of 8314
Coercive Force of Fe_2C 8220
Cohesive Energies of CsCl and KCl 8236
Coincidence Circuit Using a Diode 8507
Cold Cathode Light Sources, Fabrication and Properties of 8455
Collector Contact Effects on Parameters of Dip Grown Diffused Ge Junction Transistors 8438
Color:
Center:
Absorption and Emission in NaCl 8362
Spin Resonance at Low Temperatures, Optical Effects on 8345
Centers in:
Alkali Halides 8178
Alkali Halides,
Infrared Fluorescence of 8380
Radiation Energy Required to Produce 8179
NaCl, Formation by γ-Irradiation of 8177
Common Emitter Amplifier Stage, Design of 8489
Composition of Binary Semiconductor Compounds, Stability Limits of 8168
Compound Junction Transistor 8513
Computer:
Circuits - See Specific Circuit
Components, Reliability of 8532
Design of Amplifiers 8491
Computers, Hybrid 8549
Computers - See also Analog Computers and Digital Computers
Conductivity,
Measurement of Microwave Surface 8298
Pressure Dependence of 8270
Conductivity:
- See also Resistivity
of α-Fe_2O_3 8275
of CdSe, Mechanism for 8276
of CsBr and CsI 8245
of Films Produced by Electrostatic Charging, Changes in Normal-State 8282
in GaAs, Thermal Conversion Due to Cu of 8273
Contacts to Semiconductors, Ohmic 8235
Control Relays 8557, 8558
Controlled Rectifier Logic Circuits 8533
Controls, Motor 8556
Converters,
Analog-Digital 8550
Phase and Frequency 8514
Time to Amplitude 8575
Transceiver Application of 8525
Voltage to Frequency 8510
Copper:
Alloys, Thermoelectric Power of 8407
in GaAs, Thermal Conductivity Conversion Due to 8273
Core Memory Units 8464
Corundum,
Etching of Dislocations in 8183
PMR:
Line Width Broadening of Cr^{3+} in 8339
of Ti^{3+} in 8355
Spin-Lattice Relaxation in Cr^{3+} Doped 8343
Counters for Nuclear Spectroscopy, Multi-Channel Junction 8574
Counting Circuits, Magnetic: 8537
Pulse 8568
Critical:
Currents in Superconducting Tin Films 8286
Field of Superconducting:
Aluminum and Zinc 8283
Mercury 8284
Tin 8285

Cryostat for Electrical Measurements on Semiconductors 8267
Cryotrons,
  Fabrication of Multiple-Characteristic 8476
  Temperature Dependence of Current Amplification Factor of Thin Film 8477
Crystallographic Polarity on the Perfection of GaAs Crystals, Effect of 8209
Crystals,
  Measurement of Lattice Constants of 8170
  Plastic Resistance in 8186
  Surface States of Ionic and Valence 8238
Cupric Sulfide, X-Ray Spectra of Superconducting 8371
Cuprous Oxide,
  Absorption in 8369, 8370
  Exciton Absorption in 8360
Current Flow in Junctions between Semiconductors Having Different Energy Gaps 8422
Cyclotron:
  Resonance in Ge and Si 8296
  Resonances in the Valence Band of Ge, Power-Induced Shifts of 8295

D

dc to:
  ac:
    Converters 8525
    Inverters 8554
  dc Inverters 8555
Debye Temperature of CdS 8400
Decay Time of PbS Photodetectors 8453
Defect Structure of FeO 8204
Defects in:
  Si, X-Ray Transmission Technique for Observing 8174
  Si Junctions 8445
Deflection Circuit, TV 8527
Delineation of:
  Diffused p-n Junctions 8444
  Junction Defects 8445
Design of Junction Transistors 8431
Desorption of H_2 from Ge Surfaces 8231
Dessicants in Hermetically Sealed Gas Filled Semiconductor Rectifiers, Solid 8427
Detectors,
  GaAs Gamma-Ray 8573
  Junction Particle 8569, 8570, 8572
  Phase: 8513
    and Frequency 8511
Deuterium, NMR of Solid 8346
Diamond, Intrinsic Recombination Radiation in 8372
Diamond Thermistors, Fabrication and Properties of Semiconducting 8457
Dielectric:
  Absorption in Alkali Halides 8244
  Properties, Theory of Lattice Effects on 8243
  Properties of:
    Ga-Sr and Ba-Pb Titanates 8225
    Lead Titanite Zirconate 8258
    Pb-Ba Niobates 8254
Diffusion:
  Coefficients in Crystals, Evaluation of 8196
  in Crystals, Statistical Dynamics of Atomic 8195
  in CsBr and CsI, Ionic 8245
  of Hg in Se, Rate of 8198
  of Li in Si 8199
  of an n-p-n Ge Transistor Base 8441
Diffusion-Controlled Process in InSb Oxidation 8229
Digital Computer Storage 8540
Diodes,
  Design and Properties of Variable Capacitance 8417
  Heat Sinks for 8446
  Method for Increasing Thermal Dissipation of 8426
  Power - See Rectifiers 8423
  Survey of 8526
Discriminator Circuit 8513
Discriminators, Pulse 8520
Dislocation:
  Motion, Plastic Resistance of Crystals to 8186
  Velocities in Ge and Si, Stress Dependent 8187
Dislocations, Edge 8184
Dislocations in:
  Ag, Method for Detecting Edge and Screw 8180
  CdS, Etch Pits of 8182
  Corundum, Etching of 8183
  Ge Crystals Pulled with Varying Velocity 8208
  LiF 8185
  Si, Etch Pits Due to 8181
Dissociation Pressure of CdSb 8159
Distortion in Class A-B Push-Pull Amplifiers 8488
Distribution Coefficient of:
  In in Ge, Temperature Dependence of 8165
  Zn in GaAs 8166
Domain:
  Structure of Ni Films 8322
  Wall Motions in $BaTiO_3$ 8249, 8250
  Walls in Si-Fe 8323, 8324, 8325
Domains in X-Ray Damaged Rochelle Salts 8247
Donors in Compensated Si, EPR of 8358
Doping of Group III-V Compounds with Group IV Elements 8197
Drift Mobilities of Anthracene 8262
Duplexers, Ferrite 8462
Duplexing Systems, Microwave 8528

E

Edge Dislocations 8184
Effective Mass:
  of Bi_2Te_3 8397
  Tensor of Electrons in Semiconductors 8395
Elastic:
  Constants of:
    KBr Single Crystals, Temperature Dependence of the 8409
    Yttrium 8411
  Moduli of TiO_2 8410
Electric Power Generators, Photovoltaic 8551
Electrical Properties of:
  Bi_2Se_3 at High Temperatures 8268
  Se and AsSe Films 8387
Electrodes for Semiconductor Devices 8425
Electroluminescence in:
  CdS 8376
  ZnS:Cu Phosphors, Microscopic Observations on 8377
Electroluminescent:
  Cells, Light Waveforms Emitted from 8374
  Device for Observing Pulse Trains 8454
  Light Amplifier 8456
Electrolysis, Production of Boron by 8226
Electrometer Voltmeters 8560
Electron:
  Density Distribution in Ge 8242
  Diffraction Measurement of the Magnetic Induction at the Surface and Interior of Fe Particles 8309
  Microscopy in Surface Structure Determination 8205
  Paramagnetic Resonance of Donors in Compensated Si 8358
  Spin:
    Relaxation in Ferromagnetic Insulators 8328
    Resonance:
      Spectra of Si 8176
      of V in α-Al_2O_3 8351
  Spin-Lattice Relaxation in $K_3Co(CN)_6$ 8344
Electron-Phonon Scattering in Normal Metals 8266
Emission:
  Band of Electron Bombarded Ge, Radiative Recombination 8373
  in NaCl, Color Center 8362
Energy:
  Gap:
    of Bi_2Se_3 at High Temperatures 8268
    Width of CdI_2-Type Compounds 8169
  Levels:
    in Ge, Electron Irradiation Induced 8373
    of InSb-GaSb Alloy 8262
Epitaxial:
  Ge Layers on Ge, Perfection of 8215
  Junctions between Ge and GaAs 8421
  Si Layers on Si, Growth of 8201, 8216
Equivalent Circuit of Transistor Triode 8440
Error Detectors, Magnetic Core 8519
Etching:
  of Dislocations in:
    Cadmium Sulfide 8182
    Corundum 8183
    Silicon 8181
    Silver 8180
  of Grain Boundaries in Al_2O_3, Flash 8189
  Growth Patterns of Quartz 8190
  of Twin Boundaries 8188
Europium, Resistivity of 8274
Exciton:
  Absorption in Cu_2O 8360
  Spectra of ZnO 8361

F

Fabrication of:
  Cold Cathode Light Sources 8455
  Ge p-n Junction Rectifiers 8424
  Hall Effect Memory Devices 8449
  Junction Transistors 8431
  Semiconducting Diamond Thermistors 8457
  Si Power Rectifiers 8423
  Tetrode Transistors 8433
Fabry-Pérot Interferometer 8475
Faraday:
  Effect in $Y_3Fe_5O_{12}$, Infrared 8396
  Rotation in:
    Bi_2Te_3 8397
    Cerium Phosphate Glass, Measurement of the Intermediate State in Superconductors by 8287
Feedback:
  Amplifiers, Stabilization of 8494
  Repeaters, Stability of 8495
  in Transistor Amplifiers 8489
Ferric Oxide, Conductivity of 8275
Ferrite:
  Circulator 8462
  Phase Modulator 8461
Ferrite-Diode Logic Circuits, Synthesis of 8539
Ferrites,
  Measurement of the Permeability and Permittivity of 8315
  Paramagnetic Susceptibilities of Iron-Yttrium and Iron-Rare Earth 8338
  Temperature Variation of the Initial Permeability in 8313
Ferrites for Microwave Devices, Preparation and Properties of 8221
Ferroelectric:
  Ceramics, Effects of Stress on the Mechanical Properties of 8414
  $LiH_3(SeO_3)_2$, Crystal Structure of 8173
  Properties of:
    Barium Zirconium Metaniobate 8252
    Tetramethylammonium-Trichloro-Mercurate ($[N(CH_3)_4]\cdot HgCl_3$) 8253
  Storage Units 8545
Ferroelectrics, Resonance Quality Factor (Q) of 8248
Ferromagnetic:
  Insulators, Electron Spin Relaxation in 8328
  Iron, Correlation between the Magnetization and the Effective Magnetic Field in 8311
  Properties of Garnets 8163, 8329
  Resonance of Thin Ferromagnetic Sheets 8326
  Sheets, Ferromagnetic Resonance of 8326
  Single Crystals, Magnetoelastic Properties of 8301

Thin Films, Measurement of the Magnetic Induction of 8310
romagnetics,
Electron Diffraction Measurement of the Magnetic Gradient at Surfaces of 8308
Polarization of Nuclei in Nonmetallic 8320
rromagnetism, Equivalence of the Critical Concentrations in the Ising and Heisenberg Models of 8306
rromagnetism in $NaNiF_3$ 8336
errous Oxide, Defect Structure of 8204
ield Effects on Mobility of Surfaces 8264
im Resistors, Fabrication and Applications of Deposited 8415
ims,
Electron Microscopy Determination of Surface Structure of 8205
Measurement of the Magnetic Induction of Ferromagnetic Thin 8310
Mechanisms for Si Oxide 8227
ter Circuits 8521
ission Fragment Detectors 8570
lash Etching Technique for Al_2O_3 8189
ip-Flop Cryotron Circuit 8476
ow Stress of Mg, Parameters Influencing 8412
uorescence of:
Color Centers in Alkali Halides 8380
Ho in Crystals with the Scheelite Structure 8381
ZnO 8361
orming Circuits, Magnetic Pulse 8568
our-Layer Semiconductor Device Fabrication of 8432
ree Energy of Formation of PbSe, Standard 8158
requency:
Converters 8514
Detectors 8511
Inverters, Parametric 8498
Meters 8561
unctional Units, Design of 8487

G

adolinium^{3+} in $CaWO_4$, Paramagnetic Resonance of 8353
allium Antimonide, Reflection Spectrum of 8392
allium Arsenide,
Distribution Coefficient of Zn in 8166
Effect of Crystallographic Polarity on the Perfection of 8209
Growth Mechanism of 8207
Ohmic Contacts to 8235
Photoemission from 8389
Reflection Spectrum of 8392
Thermal Conductivity Conversion Due to Cu in 8273
allium Arsenide:
Diodes, Characteristics of 8419
γ-Ray Detector 8573
allium Phosphide, I Impurities in 8203
amma-Ray Detectors 8570, 8573
arnets,
Ferromagnetic Properties of 8329
Preparation of High Permeability 8330
Solid Solutions in 8163
ates, Binary 8508
ating Circuits, Diode 8507
enerators - See also Oscillators 8500
enerators,
Pulse 8515, 8516, 8517
Sawtooth 8527
ermanium,
Atomic Scattering Factor of 8242
Cyclotron Resonance in 8296
Delineation of Diffused p-n Junctions in 8444
Detection of Growth Striations in 8191
Distribution Coefficient of In in 8165
Effects of Surface Treatments upon Surface Conductivity of 8299
Electron Density Distribution in 8242
Hollow Cylindrical Seeds Used in Growth of 8210
Hot Electron Emission and Field Induced Photoemission from 8390
Ion Radius of 8242
Perfection of Epitaxial Ge Layers on 8215
Photoconductivity in 8386
Photoemission from 8389
Power-Induced Shifts of Cyclotron Resonances in the Valence Band of 8295
Production of 8155
Radiative Recombination in Electron Bombarded 8373
Recombination Mechanisms on Photoconductivity of 8259
Reflection Spectrum of 8392
Scattering in 8265
Stress Dependent Dislocation Velocities in 8187
Temperature Dependence of the:
Hall Coefficient of Compensated 8294
Surface Tension of 8160
Tunneling Probability in 8418
Twin Boundaries in 8188
Germanium:
Crystals, Solvent Evaporation Technique for Growing Low Resistivity 8200
Crystals:
by the Pedestal Method, Growth of 8211
Pulled with Varying Velocity, Dislocations in 8208
Junction Transistors, Fabrication of Diffused n-p-n 8441
p-n Junction Rectifiers, Fabrication of 8424
Saturated with Group III-V Compounds, Preparation of 8162
Surfaces, Properties of 8233
Germanium-Silicon, Reflection Spectrum of 8392
Gettering in Fabrication of Diffused n-p-n Ge Junction Transistors 8441
Glow Curves of Thermoluminescence of ZnS 8379
Gold, Zone Refining of 8194
Grain Boundaries in:
Al_2O_3, Etching of 8189
CdS, Etch Pits of 8182
Graphite, Magnetoresistance and Hall Coefficient of 8291
Group:
III-V:
Compound Surfaces, Damaged Layers and Crystalline Perfection in 8234
Compounds,
Preparation of Ge Saturated with 8162
Techniques for Revealing Twin Boundaries in 8188
Compounds with Group IV Elements, Doping of 8197
Growth:
Patterns of Quartz 8190
Striations in Ge, Detection of 8191
Growth of:
Anthracene Single Crystals 8219
$BaTiO_3$ Single Crystals 8224
$BaTiO_3$-$PbTiO_3$ Solid Solution Single Crystals 8225
$BaTiO_3$-$SrTiO_3$ Solid Solution Single Crystals 8225
Cadmium Sulfide 8213, 8214
Calcium Tungstate Crystals Containing Paramagnetic Ions 8222
Epitaxial Si Layers on Si 8201, 8216
Ge, Use of Hollow Cylindrical Seeds in 8210
Germanium:
Saturated with Group III-V Compounds 8162 and Si Crystals by the Pedestal Method 8211
Large Single Crystals of ZnO 8218
Lead Sulfide 8214
Low Resistivity Ge Crystals by Solvent Evaporation Technique 8200
Quartz Single Crystals 8223
Si by Thermal Decomposition of $SiCl_4$ 8212
ZnF_2:Mn Single Crystals by the Moving Crucible Technique 8217
Zinc Sulfide 8213, 8214
Gyromagnetic Media, Characteristics of Wave Guides with 8466

H

Hall:
Coefficient, Cryostat for the Measurement of 8267
Coefficient:
of Bi_2Se_3 at High Temperatures 8268
in Compensated Ge, Temperature Dependence of the 8294
of γ-Irradiated Si 8237
Graphite 8291
of Si 8293
Effect:
Amplifier 8450
Memory Devices, Fabrication and Properties of 8449
in PbTe 8292
Probes:
with Large Outputs 8563
for Measuring Magnetic Flux Density in the Air Gap of Rotating Machines 8562
Heat:
Capacity of $MnCl_2 \cdot 4H_2O$ 8401
Dissipators for Transistors 8447
of Dissociation of CdSb 8159
Pumps, Peltier 8460
Sinks for:
Diodes 8426
Transistors and Diodes 8446
Transfer Mechanisms in Ceramic Oxides 8405
Treatment Effects on CdS Films 8384
Hexamminenickel Chloride, PMR in 8357
High Voltage Power Supplies 8553, 8564
Holmium in Crystals with the Scheelite Structure, Fluorescence of 8381
Hot Electron Emission from Ge 8390
Hybrid Computers 8549
Hydrogen, NMR of Solid 8346
Hydrogen on Ge Surfaces, Desorption Processes of 8231
Hydrothermal Crystal Growth of ZnO 8218
Hysteresis in X-Ray Damaged Rochelle Salts 8247

I

Indium in Ge, Temperature Dependence of Solid Solubility of 8165
Indium Antimonide,
Oxidation Kinetics of 8228, 8229
Photoemission from 8389
Pressure Dependence of the Resistivity and Melting Point of 8271
Reflection Spectrum of 8392
Tunneling in Narrow Junctions Formed in 8278
Indium Antimonide-Gallium Antimonide, Mobilities and Energy Levels of 8262
Indium Arsenide,
Cl Impurities in 8203
Reflection Spectrum of 8392
Solubility of Al in 8203
Infrared:
Absorption in:
Bi_2Te_3 8397
Halide Crystals 8363
Ionic Crystals 8366
Synthetic Quartz 8364
Wurtzite Structure Crystals 8365
Faraday Effect in $Y_3Fe_5O_{12}$ 8396
Fluorescence of F-Centers in Alkali Halides 8380
Injection of Electrons from Collector, Effects of Contact Material on 8438
Integrated Circuits, Transistor Coupled Logic 8486
Intermetallic Compounds, Conditions Governing Formation of 8164

Inversion of Spin Populations by Simultaneous Passage 8468
Inverters, dc to:
  ac 8554
  dc 8555
Iodine in GaP, Solubility of 8203
Ion Radius of Ge 8242
Ionic:
  Conductivity of CsBr and CsI 8245
  Crystals,
    Infrared Absorption in 8366
    Surface States of 8238
  Diffusion in CsBr and CsI 8245
Ionization:
  Chambers, Solid State 8569
  Potential of Atoms 8164
Iron Particles by Electron Diffraction, Measurement of the Magnetic Induction at the Surface and Interior of 8309
Iron^{3+} in:
  Sapphire, PMR of 8348
  TiO_2, PMR of 8349
Iron-Rare Earth Ferrites, Paramagnetic Susceptibility of 8338
Iron Carbide, Preparation and Coercive Force of Fine Powder Hexagonal 8220
Iron Oxide-Lanthanum Oxide System in Air, Phase Equilibria of 8157
Iron-Yttrium Ferrites, Paramagnetic Susceptibility of 8338
Irradiation Produced Color Centers in NaCl 8177
Ising:
  Model, Magnetic Properties of the 8307
  Model of Ferromagnetism 8306

J

Junction:
  Counters for Nuclear Spectroscopy, Multi-Channel 8574
  Fabrication by Masking 8443
  Particle Detectors 8570, 8572
Junctions,
  Breakdown in: Avalanche 8439
  Defects and Weaknesses in Si 8445
  Tunneling in Narrow InSb 8278
Junctions:
  in Ge, Delineation of Diffused p-n 8444
  between Ge and GaAs, Epitaxial 8421
  between Se-CdO, Current Flow Equations of 8422
  between Semiconductors Having Different Energy Gaps 8422

L

Lanthanum, NMR of La^{139} in 8347
Lanthanum Oxide-Iron Oxide System in Air, Phase Equilibria of 8157
Large-Signal Parameters of Transistor Triodes 8440
Lattice:
  Constants of Single Crystals, Measurement of 8170
  Defects in Si Crystals, Observation of 8174
  Effects on Dielectric Properties 8243
  Parameters of:
    Bi at Low Temperatures 8171
    $CoCl_2 \cdot 6H_2O$ 8172
    $LiH_3(SeO_3)_2$ 8173
  Specific Heats of Superconducting and Normal Nb 8399
  Vibrational Modes 8241
  Wave Scattering by Point Defects 8403
Lead, Determination of Sb and Tl in 8192
Lead-Barium Niobates, Dielectric Properties of 8254
Lead Fluoride-Zinc Oxide System, Eutectic Point and Composition in 8218
Lead Selenide, Standard Free Energy of Formation of 8158
Lead Sulfide, Growth of 8214
Lead Sulfide Photodetectors, Relaxation Time of 8453
Lead Telluride,
  Hall Effect and Magnetoresistance in 8292
  Piezoresistivity of 8256
Lead-Titanate-Zirconate,
  Dielectric Properties of 8258
  Properties of 8414
  Resonance Quality Factor (Q) of 8248
Lifetime - See also Recombination
Lifetime, Microwave Absorption Technique for Measurement of 8260
Light:
  Amplifier, Electroluminescent 8456
  Emission in Si Junctions, Visible 8445
Linear Networks,
  Random Process in 8484
  Synthesis of 8483
Lithium in Si, Diffusion of 8199
Lithium Fluoride,
  Absorption and Reflection Spectra of 8393
  Dislocations in 8185
  Ultraviolet Absorption in 8367
Logic Circuits,
  Comparison of Magnetic and Transistor 8536
  Ferrite-Diode: Synthesis of 8539
  Magnetic 8535, 8537, 8538
  Si Controlled Rectifier 8533
  Transistor: 8534
    Coupled: Integrated 8486
Logimag Ferromagnetic Switching Device 8465
Logistor Relays 8558
Loss Mechanisms in Ferrites, Dielectric and Magnetic 8221
Luminescence of Se Activated ZnO 8382
Luminescent Light Source, Cold Cathode 8455

M

Magnesium, Parameters Influencing Flow-Stress of 8412
Magnesium Film, Surface Structure of 8205
Magnesium-Ferrite-Manganite System, Magnetization of the 8312
Magnetic:
  Amplifiers 8496, 8536
  Anisotropy in:
    Ferrimagnetic Spinel 8319
    Ni_3Mn 8318
  Core Signal Pulse Converters 8519
  Cores 8464
  Crystals, Double Exchange Effects in 8332
  Drum:
    Memory 8542
    Memory, Indexing System for 8541
  Field:
    at the Iron Nucleus, Correlation between the Magnetization and the Effective 8311
    Meters 8562, 8563
  Gradient at Surfaces of Ferromagnetics by Electron Diffraction, Measurement of the 8308
  Induction:
    of Ferromagnetic Thin Films, Measurement of the 8310
    at the Surface and Interior of Iron Particles, Electron Diffraction Measurement of the 8309
  Logic Circuits 8535, 8537
  Matrix Store 8543
  Power Amplifiers Employing Corbino Disks 8451
  Properties of:
    Cr_2O_5 8335
    the Ising Model 8307
  Pulse Counting and Forming Circuits 8568
  State, Effect of Magnetization Reversal on 8316
  Storage Units 8544
  Switching Circuits 8538
  Transition in $TiCl_3$ 8305
Magnetization:
  and Effective Magnetic Field in Ferromagnetic Iron, Correlation between 8311
  of the Magnesium-Ferrite-Manganite System 8312
  Reversal Effect on the Magnetic State 8316
  Reversal of Permalloy Films 8321
  of Single Crystals of Ni_3Mn 8318
Magnetoelastic Properties of Ferromagnetic Single Crystals 8301
Magnetoelectric Effect in Antiferromagnetic Cr_2O_3 8333, 8334
Magnetoresistivity of:
  Graphite 8291
  Lead Telluride 8292
  Silicon 8293
Magnetostriction:
  in NiO 8303
  Strains, Calculations of 8302
  of YIG 8304
Magnetothermal Effects in Si-Fe Alloys 8406
Manganese^{2+} in $CaWO_4$, PMR of 8353
Manganese Dichloride, Antiferromagnetic-Paramagnetic Transition in 8401
Manganese^{2+}-Fluorine^{1-} in NaCl, PMR of 8354
Masers,
  Characteristics of:
    Reflection Cavity 8472
    Traveling Wave 8473
  Harmonic Spin Coupling Mode in Ruby 8342
  Negative Temperature in Semiconductor 8470
  Operation of Chromium-Doped Titania 8474
  Resonant Modes in Optical 8475
  Theory of 8469
  Use of Ruby in 8471
Measurement of:
  Electrical Properties of Semiconductors, Cryostat for 8267
  the Temperature Dependence of the Surface Tension of Ge by the Maximum Gas Bubble Pressure Method 8160
  Transistor Properties, Automatic Instrument for 8428
Mechanical:
  Properties of Ceramics, Effects of Stress on 8414
  Rate Meters 8567
Medical Electronics: Telemetering System for Stomach Pressure 8529
Melting Point of InSb, Pressure Dependence of 8271
Memories, Coincident Current Core 8464
Memory,
  Indexing System for Magnetic Drum 8541
  Magnetic 8543
Memory:
  Devices, Hall Effect 8449
  Transfer Circuits 8546
  Units - See also Storage Units
Mercury, Critical Field of Superconducting 8284
Mercury in Se, Diffusion Rate of 8198
Metallic:
  Alloys, Resistivity of 8272
  Films, Vacuum Deposited 8415
Metals,
  Mutual Solubility of 8164
  Superconductivity in Antiferromagnetic 8290
  Thermal Resistivity of 8403
  Ultrasonic Attenuation in 8413
Meters,
  Frequency 8561
  Magnetic Field 8562, 8563
  Mechanical Rate 8567
Microplasma Phenomena in Si Junctions 8445
Microwave:
  Duplexing Systems 8528
  Maser Amplifier 8474
Military Electronics: Thermoelectric Refrigerating System for Submarines 8576
Millivoltmeter, dc 8559
Mobility, Effects of Electric and Magnetic Fields on Surface 8264

Mobility of:
Anthracene, Drift 8262
an Electron in Donor Band of Compensated Semiconductors 8263
γ-Irradiated Si 8237
InSb-GaSb Alloy 8262
Modulator,
dc to ac 8510
Reciprocal Ferrite Phase 8461
Motor Controls 8556
Multi-Layer Semiconductor Device, Fabrication of 8432
Multiplexer, Transistor - Magnetic Core 8530

N

Negative:
Mass:
Amplifiers,
Conditions for Amplification by 8452
Stability of 8499
Amplifiers as Noise Generators 8499
Temperature in Semiconductor Masers 8470
Network Synthesis,
Active RC 8482
Linear 8483
RC 8480, 8481
Neutron Detectors 8570
Nickel, Zone Refining of 8194
Nickel^{2+} in ZnF_2, PMR of 8352
Nickel Films,
Magnetic Domain Structure of 8322
Magnetoresistance in 8322
Spin Wave Resonance in 8327
Nickel Ferrite, Electrical Resistivity of 8269
Nickel Manganese,
Magnetic Anisotropy in 8318
Magnetization of 8318
Volume Changes on Ordering in 8167
Nickel Monoxide, Magnetostriction in 8303
Niobium, Lattice Specific Heats of Superconducting and Normal 8399
Noise:
Generators, Negative Mass Amplifiers as 8499
Ratio of Si Crystal Rectifiers 8420
Nonequilibrium Superconductive Phase in Cu-Bi Alloys 8289
Nonlinear:
Electronic Computer Elements for Analog Computers 8547
Networks, Random Process in 8484
Nuclear:
Magnetic Resonance of:
La^{139} in La and of Sc^{45} in Sc 8347
Solid Hydrogen and Deuterium 8346
Spectroscopy, Multi-Channel Junction Counters for 8574
Nuclei in Nonmetallic Ferromagnetics, Polarization of 8320

O

Optical:
Effects on F-Center Spin Resonance at Low Temperatures 8345
Masers, Resonant Modes in 8475
Properties of Metallic Films 8394
Tape Sound Recording System, Transistorized 8531
Order-Disorder in Ni_3Mn Alloy 8167
Oscillations in Quartz Crystals 8478
Oscillators - See also Generators 8500
Oscillators,
Degenerative 8490
Parametric 8504
Relaxation 8503
Transistor:
Effect of Collector Junction Thickness on 8505
Limiting in Saturation Region of 8501
Oscillation Build Up in 8502
Theory and Design of 8500
Use of Ruby in Maser 8471
Oxidation Kinetics of InSb 8228, 8229
Oxide Films on Si, Mechanism for 8227
Oxygen on:
Ge Surfaces, Adsorption of 8231
Si Surfaces, Adsorption of 8230

P

Packaging of:
Diodes,
Dessicants Used in 8427
Heat Sink Configuration for 8426
Transistors, Heat Dissipators for 8447
Paramagnetic:
Crystals, Spin-Phonon Interaction in 8340
FeO, Defect Structure of 8204
Ions, Growth of $CaWO_4$ Crystals Containing 8222
Resonance:
Absorption, Observation of Energy Storage in Phosphors by 8383
Absorption in:
CdTe:Mn and CdS:Mn 8356
Silicon 8359
of Color Centers in KCl, Optical Effects on 8345
of Cr^{3+} in YGaG 8350
of Fe^{3+} in TiO_2 8349
Line Width Broadening of Cr^{3+} in Al_2O_3 8339
of Mn^{2+} and Gd^{3+} in $CaWO_4$ 8353
in $Ni(NH_3)_6Cl_2$ 8357
of Ni^{2+}, V^{2+} and Cr^{3+} in ZnF_2 8352
of Sapphire 8348
of Ti^{3+} in Al_2O_3 8355
Susceptibility of:
Iron-Yttrium and Iron-Rare Earth Ferrites 8338
Mixed Paramagnetic Crystals 8337
Parametric:
Amplifiers,
Magnetic Film 8497
Transducer Characteristics of 8498
Oscillators 8504
Particle Detectors 8569, 8570, 8572
Pedestal Method for Growing Ge and Si Crystals 8211
Peltier Coolers, Properties of 8460
Permalloy Films, Magnetization Reversal of 8321
Permeability, Temperature Variation of 8313
Permeability:
- See also Susceptibility
of Ferrites, Measurement by Resonant Cavity Techniques of 8315
Perturbation Theory of Antiferromagnetism 8331
Phase:
Converters 8514
Detectors 8511, 8512, 8513
Equilibria of La_2O_3-Iron Oxide Systems in Air 8157
Modulator, Reciprocal Ferrite 8461
Phosphors,
Charge Compensation Theory in 8161
Electroluminescence in ZnS:Cu 8377
PMR Absorption Observation of Energy Storage in 8383
Photoconductive Films, Effect of Heat Treatment on Sintered CdS 8384
Photoconductivity:
of Cu-Activated Cd(S:Se), Spectral Response of the 8385
in Ge,
Effects of Contacts on the 8386
Temperature Variation of 8259
of Semiconductors with Traps, Theory of 8261
Photodetectors, Relaxation Time of PbS 8453
Photoelectric Properties of:
Metallic Films 8394
Se and AsSe Films 8387
Photoelectromagnetic Effect in Bi 8391
Photoemission from:
Ge, Field Induced 8390
Semiconductors 8389
Photometric Determination of Sb and Tl in Pb 8192
Photomultipliers,
Power Supply for 8553
Transistor 8564
Photovoltaic Electric Power Generators 8551
Piezoelectric:
Constants of CdS, Measurement of 8257
Quartz Crystals, Reduction of Transverse Oscillations in 8478
Resonators, Properties of Synthetic Quartz 8479
Piezoresistivity of:
$(Ba\cdot Sr)TiO_3$, Temperature Dependence of 8255
Indium Antimonide 8271
Lead Telluride 8256
Pirani Gauge Utilizing Thermistors 8566
Plastic Resistance to Dislocation Motion in Crystals 8186
Plasticity of Mg, Parameters Influencing 8412
Point:
Contact Transistors, Fabrication and Properties of 8429
Defects in NaCl, K^+ 8175
Polarization of:
Nuclei in Nonmetallic Ferromagnetics 8320
Triglycine Sulfate, Spontaneous: Pyroelectric Technique for Determination of 8246
Potassium$^+$ Point Defects in NaCl 8175
Potassium Bromide,
Infrared Absorption in 8363
Temperature Dependence of the Elastic Constants of 8409
Potassium Chloride,
Cohesive Energy of 8236
Infrared Absorption in 8363
Measurement of Sr Concentration in 8244
Potassium Chromicyanide, Electron Spin-Lattice Relaxation in 8344
Potentiometer Tracks, Application of Deposited Film Resistors to 8415
Power:
Conversion Gain of Si Crystal Rectifiers 8420
Dissipation of Diodes, Method for Increasing 8426
Flow in Reactive Elements 8485
Generators,
Photovoltaic Electric 8551
Semiconductors for Thermoelectric 8459
Supplies,
dc and ac Voltage Output 8552
Photomultiplier 8553, 8564
TV Receiver 8526
Switching Circuits 8506, 8509
Transistors,
Increasing Power Handling Capacity of 8442
Measurement of Characteristics of 8430
Precipitation of Impurities in Si by Annealing 8202
Preparation of:
Boron 8226
Ferrites 8221
Fine Powder Hexagonal Fe_2C 8220
High Permeability Garnets 8330
Pressure Gauge, Pirani 8566
Printed Circuits, Fabrication of 8448
Production of Ge by Titration 8155
Properties of:
CdI_2-Type Compounds, Predicted 8169
Transistors, Automatic Instrument for Measurement of 8428
Pulse:
Converters, Magnetic Core 8519
Counting and Forming Circuits, Magnetic 8568
Discriminators 8520
Generators 8516
Generators,
Constant Amplitude 8517
Magnetic 8515
Si Avalanche Mode Transistors in 8436
Shaping with Variable Capacitance Diodes 8548
Systems, Analysis of 8518

Trains, Electroluminescent Device for Observing 8454
Purification of Si by Zone Refining 8193
Push-Pull Amplifiers, Distortion in 8488
Pyroelectric Technique for Determination of Spontaneous Polarization of Triglycine Sulfate 8246

Q

Q Value, Measurement of Microwave 8298
Quartz,
Acoustic Absorption in Synthetic 8364
Growth Patterns of 8190
Infrared Absorption in Synthetic 8364
Reduction of Transverse Oscillations in Piezoelectric 8478
Quartz:
Crystals, Growth of 8223
Piezoelectric Resonators, Properties of Synthetic 8479

R

Radar Duplexer, Ferrite 8462
Radiation:
Energies Required to Produce Color Centers in Alkali Halides 8179
from Phosphors, PMR Absorption Observations of 8383
Receivers, Threshold Sensitivity of 8565
Radiative Recombination in:
Diamond 8372
Electron Bombarded Ge 8373
Random Process in Linear and Nonlinear Systems, Poles and Zeros of 8484
Rare Earth Ions, Growth of $CaWO_4$ Crystals Containing 8222
RC Network Synthesis 8480, 8481, 8482
Reactive Elements, Power Flow in 8485
Receivers,
AGC in 8523, 8524
Radiation: Threshold Sensitivity of 8565
Recombination:
- See also Lifetime 8260
in Ge, Radiative Electron Bombardment Induced 8373
Luminescence in Alkali Halides 8375
Mechanisms in Ge 8259
Radiation in Diamond, Intrinsic 8372
Recording System, Optical Tape Sound 8531
Rectifiers,
Fabrication:
and Characteristics of Si Power 8423
of Ge p-n Junction 8424
Noise Ratio and Power Conversion Gain of Si Crystal 8420
Solid Dessicants in Hermetically Sealed Gas Filled Semiconductor 8427
Rectifying Circuits 8526
Reflection:
of Electrons from Alkali Halides 8300
Spectrum of:
Germanium 8392
Lithium Fluoride 8393
in ZnO, Exciton 8361
Reflectivity Properties of Metallic Films 8394
Refrigeration Units, Thermoelectric 8576, 8577, 8578
Relaxation:
Oscillators 8503
Time of PbS Photodetectors 8453
Relay Amplifiers, Computer Design of 8491
Relays,
Control 8557
Logistor 8558
Reliability of Computer Components 8532
Repeater Circuit, Equivalent Circuit for 8495
Repeaters, Stability of Feedback 8495
Resistivity - See also Conductivity 8269
Resistivity of:
AgAuCd Ternaries 8277
Bi_2Se_3 at High Temperatures 8268
Eu and Yb 8274
γ-Irradiated Si 8237
InSb, Pressure Dependence of the 8271
Metallic Alloys, Order and Temperature Effects on 8272
Nickel Ferrite 8269
Semiconductors, Cryostat for the Measurement of 8267
Resistors,
Current-Voltage Characteristics of Semiconductor 8416
Fabrication and Applications of Deposited Film 8415
Resonance Quality Factor (Q) of Ferroelectrics 8248
Resonant Modes in Optical Masers 8475
Resonators, Quartz 8479
Rochelle Salts, Hysteresis and Domains in X-Ray Damaged 8247
Rubidium Iodide, Infrared Absorption in 8363
Ruby,
Spin Coupling in 8342
Spin-Phonon Interaction in 8341
Ruby in Masers, Use of 8471

S

Sapphire, PMR of Fe^{3+} in 8348
Sawtooth Generators, TV Deflection 8527
Scandium, NMR of Sc^{45} in 8347
Scattering in:
Normal Metals, Electron-Phonon 8266
Semiconductors, Group Theory of 8265
Scheelite Structure, Fluorescence of Holmium in Crystals with the 8381
Seebeck Effect 8408
Selenium, Diffusion Rate of Hg in 8198
Selenium Films, Photoelectric and Electrical Properties of 8387
Selenium-Cadmium Oxide Junctions, Current Flow Equations of 8422
Semiconductor:
Devices,
Electrodes for 8425
Fabrication of Four-Layer 8432
Masers, Negative Temperature in 8470
Resistors, Current-Voltage Characteristics of 8416
Thermoelectric Elements 8458
Semiconductors,
Carrier Properties and Photoconductivity of 8261
Cryostat for Electrical Measurements on 8267
Effective Mass Tensor and Dielectric Constant Tensor of 8395
Lifetime Measurements by Microwave Absorption Technique of 8260
Mobility of: 8264
Electrons in Compensated 8263
Photoemission from 8389
Pressure Dependence of Properties of 8270
Theory of Skin Effect in 8297
Semiconductors Having Different Energy Gaps, Junctions between 8422
Shift Registers, Magnetic 8537
Signal Pulse Converters, Magnetic Core 8519
Silicon,
Cyclotron Resonance in 8296
Diffusion of Li in 8199
Electrical Properties of 8193
EPR of Donors in Compensated 8358
Etch Patterns of Dislocations in Single Crystal 8181
γ-Irradiation Effects on Acceptor Levels and Electrical Properties of 8237
Growth of Epitaxial:
Layers of Doped Si on 8201
Si Layers on 8216
Hall Coefficient and Magnetoresistivity of 8293
PMR Absorption in 8359
Precipitation of Impurities in Al Doped 8202
Scattering in 8265
Stress Dependent Dislocation Velocities in 8187
Techniques for Revealing Twin Boundaries in 8188
Thermal Conductivity of 8402
Vacancy Interaction in 8176
X-Ray Transmission Technique for Observing Lattice Defects in 8174
Zone Refining Purification of 8193
Silicon:
Crystal Growth by:
the Pedestal Method 8211
Thermal Decomposition of $SiCl_4$ 8212
Junctions, Defects and Weaknesses in 8445
Oxidation in Steam and Oxygen, Mechanisms for 8227
Power Rectifiers, Fabrication and Characteristics of 8423
Surfaces,
Adsorption of Oxygen on Clean 8230
Properties of 8233
Silicon-Iron,
Domain Walls in 8323
Optimum Domain Width of 8324
Magnetothermal Effects in 8406
Silicon-Iron Bloch Walls, Energy and Orientation of 8325
Silver, Method for Detecting Edge and Screw Dislocations in 8180
Silver Alloys, Thermoelectric Power of 8407
Silver-Gold-Cadmium Ternaries, Resistivity of 8277
Skin:
Depth, Standards of Microwave 8298
Effect in:
Semiconductors 8297
Superconductors 8279
Sodium Chloride,
Color Center Absorption and Emission in 8362
Infrared Absorption in 8363
K^+ Point Defects in 8175
Measurement of Ca Concentration in 8244
Thermoluminescence in 8378
Sodium Chloride Color Centers, Formation by γ-Irradiation of 8177
Sodium Fluonickelate, Ferromagnetism in 8336
Solid:
Solutions, Conditions Governing Formation of 8164
Solutions in Garnets 8163
Solids, Specific Heat of Isotropic 8398
Solubility:
of In in Ge, Temperature Dependence of Solid 8165
of Metals, Mutual 8164
in the ZnS-AlP System, Solid 8161
Solvent Evaporation Technique for Growing Low Resistivity Ge Crystals 8200
Space-Charge Layer Widening in Junction Transistors, Analysis of 8437
Spacistors,
Fabrication and Properties of High-Frequency 8435
Low-Frequency Parameters of 8434
Specific Heat of Isotropic Solids 8398
Spectroscopy, Multi-Channel Junction Counters for 8574
Spin:
Coupling in Ruby 8342
Inversion in Masers 8468
Populations by Simultaneous Passage, Inversion of 8468
Wave Resonance in Ni Films 8327
Spin-Lattice Relaxation in Cr^{3+} Doped Corundum 8343
Spin-Phonon Interaction in:
Paramagnetic Crystals 8340
Ruby 8341

Spinel, Magnetic Anisotropy in Ferrimagnetic 8319
Spirals on GaAs (111) Surfaces 8207
Stability Limits of Binary Semiconductor Compounds, Composition 8168
Stark Splitting Observation by Means of Tunneling Transitions 8278
Stomach Pressure of Animals, Telemetering System for 8529
Storage, Digital Computer 8540
Storage:
Transfer Circuits 8546
Units - See also Memory Units
Units,
Ferroelectric Capacitor 8545
Magnetic: 8544
Drum 8542
Strains, Calculation of Magnetostriction 8302
Stress Dependent Dislocation Velocities in Ge and Si 8187
Striations in Ge, Detection of 8191
Strontium in KaCl, Measurement of Concentration of 8244
Structure of:
Bi at Low Temperatures 8171
BiPt 8288
$CoCl_2$-$6H_2O$ 8172
$LiH_3(SeO_3)_2$ 8173
Superconducting:
Al, Effect of Pressure on the Critical Field of 8283
CuS, X-Ray Spectra of 8371
Ground States 8280
Hg, Critical Field of 8284
Nb, Lattice Specific Heat of 8399
Normal Transition in Sn Films 8281
Tin Films, Critical Currents in 8286
Transition Temperature Produced by Electrostatic Charging, Changes in 8282
Zn, Effect of Pressure on the Critical Field of 8283
Superconductive Wires, Fabrication of Multiple-Characteristic 8476
Superconductivity in:
Antiferromagnetic Metals, Existence of 8290
Sn Films, Critical Magnetic Fields and Currents for the Destruction of 8285
Superconductors, Measurement of the Intermediate State by Faraday Rotation in Cerium Phosphate Glass 8287
Superconductors in:
the Intermediate State, Thermal Conductivity of 8404
a Magnetic Field, Surface Impedance of 8279
Surface:
Catalysis, Studies of 8232
Conductivity of Ge, Effects of Surface Treatments on 8299
Impedance, Measurement of Microwave 8298
Levels 8239
Mobility, Effects of Electric and Magnetic Fields on 8264
States: 8239
of Ionic and Valence Crystals 8238
of ZnO 8240
Structure Determination by Electron Microscope 8205
Tension of Ge, Temperature Dependence of the 8160
Treatments for Ge 8299
Surfaces,
Adsorption of Oxygen on Clean Si 8230
Damaged Layers and Crystalline Perfection in Group III-V Compounds 8234
Displacement Processes on Ge 8231
Mechanisms for Steam and Oxygen Oxidation of Si 8227
Properties of Ge and Si 8233
Spirals on GaAs (111) 8207
Susceptibility:
- See also Permeability 8313
of $CoBr_2 \cdot 6H_2O$ 8314
of Iron-Yttrium and Iron-Rare Earth Paramagnetic Ferrites 8338
of Mixed Paramagnetic Crystals 8337
of $TiCl_3$ 8305
Switching, Ferromagnetic 8465
Switching:
in $BaTiO_3$, Factors Effecting 8251
Circuits,
Binary 8508
Diode 8507
Magnetic 8538
Power 8509
Thyratron 8506
Transistor 8534
Synthesis of:
Active RC Networks 8482
Linear Networks 8483
RC Networks 8480, 8481

T

Tamm Surface States 8239
Tantalum, Measurement of Intermediate Superconducting State in 8287
Telemetering:
System, Multiplex 8530
System for Stomach Pressure of Animals 8529
Teletype Actuators, Magnetic Core 8519
Television:
Deflection Circuit 8527
Receivers, Power Supplies for 8526
Temperature:
Compensated Amplifiers 8492, 8493
Dependence of Current Amplification Factor of Thin Film Cryotrons 8477
Tetramethylammonium-Trichloro-Mercurate, Ferroelectric Properties of 8253
Tetrode Junction Transistors, Fabrication of 8433
Thallium in Pb, Determination of 8192
Thallium Bromide, Ultraviolet Absorption in 8368
Thallium Chloride, Ultraviolet Absorption in 8368
Thermal:
Conductivity: 8408
of Ceramic Oxides 8405
of Silicon 8402
of Superconductors in the Intermediate State 8404
Etching of Ag to Detect Dislocations 8180
Expansion of BiPt 8288
Resistivity of Metals and Alloys 8403
Thermistor AGC Circuit 8524
Thermistors,
Fabrication and Properties of Semiconducting Diamond 8457
Pirani Gauge Utilizing 8566
Thermoelectric:
Air Conditioning Systems for Totally Enclosed Environments 8578
Elements, Semiconductor 8458
Figure of Merit 8408
Power:
of Cu- and Ag-Alloys 8407
Generators, Semiconductors for 8459
Refrigerating System for Submarines 8576
Refrigeration, Applications of 8577
Thermoluminescence of:
NaCl 8378
ZnS, Glow Curves of 8379
Thin Film Cryotrons, Temperature Dependence of Current Amplification Factor of 8477
Thin Films, Measurements of Reflectivity and Transmissivity of Metallic 8394
Threshold Sensitivity of Radiation Receivers 8565
Thyratron Transistor Circuit, High Power Bistable 8506
Time:
to Amplitude Converters 8575
Delay Circuit, Transistorized 8522
Tin, Measurement of Intermediate Superconducting State in 8287
Tin Films,
Critical:
Currents in Superconducting 8286
Magnetic Fields and Currents for the Destruction of Superconductivity in 8285
Superconducting-Normal Transition in 8281
Titania Maser, Operation of a Chromium-Doped 8474
Titanium, Zone Refining of 8194
Titanium^{3+} in Al_2O_3, PMR of 8355
Titanium Chloride, Magnetic Transition and Susceptibility of 8305
Titanium Dioxide,
Elastic Moduli and Acoustic Attenuation in 8410
Paramagnetic Resonance Spectrum of Fe^{3+} in 8349
Transceivers, Application of dc Converters to 8525
Transistor:
Coupled Logic Integrated Circuits 8486
Properties, Automatic Instrument for Measurement of 8428
Transistors,
Avalanche Breakdown in 8439
Heat:
Dissipators for 8447
Sinks for 8446
Junction:
Analysis of Space-Charge Layer Widening in 8437
Avalanche Mode Operation of Si 8436
Compound 8513
Design and Fabrication of 8431
Fabrication:
of Diffused n-p-n Ge 8441
and Properties of High-Frequency Spacistor 8435
of Tetrode 8433
Increasing Power Handling Capacity of 8442
Large-Signal Parameters of Triode 8440
Low-Frequency Parameters of Spacistor 8434
Measurement of Electrical and Thermal Characteristics of Power 8430
Parameters of Dip Grown Diffused Ge 8438
Point Contact: Fabrication and Properties of 8429
Transition:
Metal Content in Alloys, Sensitive Determination of 8156
Temperature of BiPt 8288
Transmission Line Amplifiers, Theory of Negative Resistance 8467
Transmissivity Properties of Metallic Films 8394
Traps:
Induced by γ-Irradiation in Si 8237
in Semiconductors, Theory of 8261
Traveling Wave Masers, Characteristics of 8473
Triglycine Sulfate, Spontaneous Polarization of 8246
Tunnel Diodes,
Low Resistivity Ge for Fabricating 8200
Tunneling in 8418
Tunneling:
in Narrow InSb Junctions 8278
Probability in Ge 8418
Twin Boundaries, Techniques for Revealing 8188
Two-State Digital Computer Elements Employing Corbino Disks 8451

U

Ultrasonic Attenuation in Metals 8413
Ultraviolet Absorption in:
Irradiated LiF Crystals 8367
Thallous Halides 8368

V

Vacancies in Uniaxial Anisotropy in $Co_x Fe_{3-x} O_4$, Effect of Cation 8317

Vacancy Interaction in Si, ESR Determination of 8176
Valence Crystals, Surface States of 8238
Vanadium, Zone Refining of 8194
Vanadium in α-Al_2O_3, ESR of 8351
Vanadium^{2+} in ZnF_2, PMR of 8352
Vanadium Sapphire, ESR of V in 8351
Varactors, Design and Properties of 8417
Variable Capacitance Diodes, Design and Properties of 8417
Veterinary Applications: Telemetering System for Stomach Pressure of Animals 8529
Vibrations, Modes of Lattice 8241
Voltage to Frequency Converter 8510
Voltmeters,
  dc Milli- 8559
  Electrometer 8560
Volume Changes in Ni_3Mn on Ordering 8167

W

Wave Guides with Gyromagnetic Media, Characteristics of 8466
Whiskers on Cleavage Steps in Crystals 8206
Wurtzite Structure Crystals, Infrared Absorption in 8365

X

X-Ray Spectra of Superconducting CuS 8371

Y

Ytterbium, Resistivity of 8274
Yttrium, Elastic Constants of 8411
Yttrium Gallium Garnet, PMR of Cr^{3+} in 8350
Yttrium Indium Garnets, Permeability and Preparation of 8330
Yttrium Iron Garnet,
  ESR in 8328
  Infrared Faraday Effect in 8396
  Magnetostriction of 8304
Yttrium Iron Garnet Circulators 8463

Z

Zinc, Effect of Pressure on the Critical Field of Superconducting 8283
Zinc in GaAs, Distribution Coefficient of 8166
Zinc Fluoride, PMR of Ni^{2+}, V^{2+} and Cr^{3+} in 835
Zinc Fluoride:Manganese Single Crystals, Moving Crucible Growth of 8217
Zinc Oxide,
  Absorption in 8366
  Luminescence of Se Activated 8382
  Optical Properties of 8361
  Surface States of 8240
Zinc Oxide Crystals, Growth of Large 8218
Zinc Sulfide,
  Growth of 8213, 8214
  Solid Solubility of AlP in 8161
  Thermoluminescence in 8379
Zinc Sulfide:Copper Phosphors, Electroluminescence in 8377
Zone Refining of:
  Metals 8194
  Silicon 8193

AUTHOR INDEX

Abarenkov, I.V. 8362
Abel, Jr., G.J. 8155
Addamiano, A. 8161
Aerts, A.E. 8238, 8264
Agakhanian, T.M. 8440
Aitchison, R.E. 8488
Akimchencko, I.P. 8199
Alekseevskii, N.E. 8286, 8289
Aléonard, R. 8338
Alger, R.S. 8179
Allington, R.W. 8529
Ambrosio, B.F. 8542
Anderson, E.E. 8330
Anderson, J.R. 8545
Anderson, R.L. 8421
Anderson, T.N. 8462
Antell, G.R. 8203
Antoncik, E. 8392
Arsenault, W.R. 8542
Asano, S. 8385
Ashbel', N.I. 8500
Astrov, D.N. 8334
Auerbach, I.L. 8534, 8535
Augustine, F. 8190
Austin, I.G. 8271, 8397

Bachmann, L. 8205
Bailey, Jr., C.M. 8554
Bailyn, M. 8266
Baker, J. 8345
Barney, H.L. 8449
Barrett, C.S. 8171
Barson, F. 8441
Barton, L.E. 8429
Basinski, Z.S. 8412
Basov, N.G. 8452, 8470
Baxter, P. 8254
Bazhan, A.N. 8501
Beal, M.T. 8272
Beauchamp, E.K. 8189
Beer, A.C. 8509
Bekey, G.A. 8547
Belov, K.P. 8303
Bemski, G. 8358
Berlincourt, D.A. 8258
Bilaniuk, O.M. 8574
Blatt, F.J. 8407
Blickensderfer, J.A. 8541
Blok, J. 8453
Blumberg, W.E. 8347
Bogachev, I.N. 8167
Bohun, A. 8378
Bond, W.L. 8170
Bondar, V.V. 8289
Bonn, T.H. 8536
Boorse, H.A. 8399
Booy, H.C. 8453
Borovskii, I.B. 8371
Bouwknegt, A. 8420
Bowers, K.D. 8353
Bozorth, R.M. 8163
Brand, F.A. 8260
Brard, P. 8465
Brebrick, R.F. 8168
Brennemann, A.E. 8477
Bright, R.L. 8522
Brissot, J.J. 8431
Brochocki, A. 8208
Brotzman, J. 8575
Brown, A.E. 8410
Brown, D.R. 8540
Brown, P.J. 8156
Bruns, R.A. 8491
Bullough, R. 8202
Burdukov, Yu.M. 8419
Burley, D.M. 8307
Burns, F.P. 8449
Bussey, H.E. 8298
Byrnes, J.J. 8194

Caille, L. 8428
Cambornac, M. 8557
Carey, R. 8324
Carroll, J.E. 8485
Carter, D. 8349
Castel, Jr., J.G. 8344, 8468
Chang, K.K.N. 8467
Chang, W.S.C. 8473
Chaudhuri, A.R. 8187
Chester, P.F. 8344, 8468
Chetkin, M.V. 8396
Chisholm, H. 8561
Chynoweth, A.G. 8246, 8278
Cibelius, Jr., C.A. 8556
Cmolik, C. 8258
Cohen, M.H. 8413
Colwell, J.F. 8236
Connell, L.J.C. 8424
Cook, J.S. 8244
Coovert, R.E. 8293
Coren, R.L. 8322
Cossee, P. 8337
Crawford, Jr., J.N. 8177
Cromack, J. 8473
Cruz, Jr., J.B. 8481
Cunningham, Jr., J.R. 8330
Curry, M.A. 8274
Czerlinsky, E.R. 8329

Dahlka, V.W. 8498
Daniel-Szabó, J. 8316
Danilov, V.N. 8180
Darlington, S. 8492
Dash, W.C. 8211
Date, M. 8357
Davis, D.D. 8163
Dearborn, E.F. 8218
de Gennes, P.-G. 8332
de Hoog, F.J. 8453
De Sautels, A.N. 8493
De Sorbo, W. 8287
Desvignes, F. 8431
Dewald, J.F. 8240
Diesel, T.J. 8256
Dietrich, A.F. 8516
Dismukes, J.P. 8459
Docherty, I.S. 8488
Dodd, D.M. 8364
Dolce, A. 8259
Dolejsi, J. 8378
Donahoe, F.J. 8408
Donovan, P.F. 8572
Dorsi, D. 8194
Doucette, E.I. 8417
Dresselhaus, G. 8279
Dresselhaus, M.S. 8279
Drougard, M.E. 8251
Dryden, J.S. 8244
Dupuis, M. 8398
Dyett, M.J. 8441
Dymanus, A. 8420
Dzyaloshinskii, I.E. 8333

Edens, G.E. 8567
Eisinger, J. 8347
Eisler, H. 8515
Elliott, J.F. 8551
Elliott, R.J. 8265, 8306
Ellsworth, R. 8561
English, A.C. 8191
Esseling, L.A.L. 8526
Evans, R. 8561
Ezhik, I.I. 8380

Falk, D.S. 8243
Fatuzzo, E. 8253
Faust, Jr., J.W. 8188
Feber, G. 8359
Fedorov, V.B. 8339
Felker, J.H. 8492
Field, W.G. 8329
Finch, C.B. 8158
Finkelstein, M.B. 8527
Finnemore, D.K. 8284
Fisher, J.C. 8280
Fletcher, R.C. 8328
Foreman, Jr., M.B. 8572
Forrest, M.L.N. 8439
Forstat, H. 8401
Fotland, R.A. 8387
Fox, A.G. 8475
Frank, C. 8478
Frank, R.C. 8210
Frankl, D.R. 8295
Freeman, H. 8518
Frei, A.H. 8297
Fridrikhov, S.A. 8300
Friedland, S.S. 8569, 8570, 8571
Furukawa, Y. 8386, 8418

Gage, D.S. 8460
Garber, M. 8314, 8407
Gassmann, G.G. 8514
Gatos, H.C. 8209, 8234
Gauvin, M. 8558
Gebbie, H.A. 8271
Gel', E.P. 8178
Geller, S. 8163
Gere, E.A. 8359
Gerritsen, H.J. 8474
Gersdorf, R. 8302
Gerson, R. 8414
Geschwind, S. 8350
Geusic, J.E. 8342
Gibbons, J.F. 8437
Gibbs, P. 8183
Gibbs, W.E.K. 8560
Gilman, J.J. 8185, 8186
Ginzburg, N.I. 8285
Gippius, A.A. 8373
Gjevre, J.A. 8411
Glang, R. 8201, 8444
Glover, III, R.E. 8282
Gluck, S.E. 8519
Goodall, W.M. 8516
Goodman, C.H.L. 8169
Goodman, G. 8252
Goodrich, H.C. 8527
Goorissen, J. 8193
Gorban', I.S. 8370
Gordon, B.M.
Gorshkov, M.M.
Goto, M.
Gourary, B.S.
Grainger, R.J. 8571
Green, M. 8230,
8233
Greive, T.
Grimmond, R.
Gross, D.
Groves, J.R.
Guemene, M.
Gullemin, E.A.
Gurevich, L.E.
Guyton, J.H.

Hajko, V.
Hakimi, S.L.
Hale, D.R.
Haneman, D.
Hanlet, J.M.N.
Hanna, S.S.
Harada, R.
Harding, W.R.
Hardy, J.R.
Harrison, M.J.
Harvey, A.F.
Heap, B.R.
Heberle, J.
Heikes, R.R.
Hellicar, N.J.
Hempstead, C.F.
Henisch, H.K.
Hensel, J.C.
Hepburn, W.D.
Herbst, J.A.
Herlet, A.
Hibberd, R.C.
Hilsum, C.
Hirakawa, K.
Hirota, E.
Hirshfeld, A.T.

AUTHOR INDEX *(Continued)*

ockings, E.F. 8459
offman, G.R. 8374
olford, K. 8559
ollander, L.E. 8256, 8410
ollitscher, H. 8562
ousley, R.M. 8346
udelson, G.D. 8578
uelsman, L.P. 8480
ughes, F.L. 8217
usimi, K. 8249

uki, S. 8376, 8388
ua, S. 8317
enkov, A.N. 8419
gham, Jr., H.S. 8215
ue, T. 8317
otova, I.P. 8395
anov-Omskii, V.I. 8262

accarino, V. 8347
acobs, H. 8260
acobs, I.S. 8319
affe, H. 8258
affe, M. 8223
achems, P.J.W. 8425
ahn, H.F. 8188
ahnston, W.D. 8220
ahnston, W.G. 8185
ordan, R.D. 8179
oshi, M.V. 8525
oshi, S.K. 8400
uretschke, H.J. 8326

aczér, J. 8325
agan, Yu. 8296
anai, Y. 8292
apitsa, M.L. 8300
aptsov, L.N. 8501, 8502, 8505
aran, C. 8441
arpenko, B.V. 8290
ato, R. 8367, 8393
awamura, T. 8438
enan, R.P. 8331
epler, R.G. 8262
hutsishvili, G.R. 8320
ibler, L.U. 8504
ikuchi, C. 8351, 8356, 8471
ikuchi, M. 8445
ikuchi, R. 8195
inariwala, B.K. 8482
ing, B.R. 8401
ing, J.C. 8364
ing, J.H. 8271
ingery, W.D. 8405
ippenhan, B.W. 8201
irenskii, L.V. 8323
irk, E.S. 8268
iselev, A.A. 8362
itamura, S. 8384
laassen, F.M. 8453
lick, C.C. 8241
obus, A. 8208
ohra, K. 8174
okes, R.J. 8232
olomiets, B.T. 8262
omienko, L.S. 8355
omiya, H. 8376, 8388
opylovskii, B.D. 8373
orringa, J. 8331
orsunskii, M.I. 8198
outecky, J. 8239
inchik, G.S. 8396
okhin, O.N. 8452
opschot, R.H. 8407
oupa, F. 8184

Kubota, B. 8335
Kuwahara, K. 8321

Lacey, J.W. 8513
LaFontaine, J.F. 8549
Lakshmanan, T.K. 8422
Lambe, J. 8345, 8351, 8356, 8471
Lavine, M.C. 8209, 8228, 8234
Lawrence, P.E. 8319
Layburn, R.L. 8524
Lazarev, V.B. 8160
Lee, D.W. 8405
Lee, M.A. 8165
Le Graw, R.C. 8328
Legvold, S. 8274
Lehmann, W. 8377
Lescroel, Y. 8313
Leupold, H. 8399
Levinger, B. 8295
Levitin, R.Z. 8303
Lewis, H.R. 8474
Li, T. 8475
Ligenza, J.R. 8227
Liid'ya, G.G. 8375
Linares, R.C. 8224
Linden, D.A. 8437
Little, W.J. 8207
Logan, R.A. 8278
Lord, H. 8269
Loudon, R. 8265
Ludwig, G.W. 8176
Luke, C.L. 8192
Lushchik, C.B. 8375
Lynch, D.W. 8245

Maeda, H. 8294
Makhov, G. 8471
Male, J.C. 8372
Manenkov, A.A. 8339, 8343
Manley, O.P. 8196
Manning, W.H. 8552
Mapother, D.E. 8284
Maradudin, A.A. 8263
Mark, A. 8216
Markouskii, L.Ya. 8382
Marsh, B.B. 8574
Matarrese, L.M. 8217
Matsui, A. 8393
Matthias, B.T. 8347
Mattuck, R.D. 8340
Maurer, R. 8498
Maurushat, Jr., J. 8510
Maxwell, K.H. 8230, 8231
Mayer, J.W. 8569, 8571
Mazo, R. 8398
McAdam, J.C. 8447
McCaldin, J.O. 8162, 8197
McCarthy, K.A. 8207
McCarthy, W.A. 8436
McDade, P.J. 8215
McKenney, H.F. 8496
McMahon, H.O. 8476
Meindl, J.D. 8487
Mel'nikova, V.I. 8167
Mesnard, G. 8259
Metzger, S. 8530
Meyer, J.W. 8472
Meyerhoff, A.J. 8537
Midgley, D. 8451
Mikheeva, M.N. 8286
Miller, C.E. 8163
Miller, G.L. 8572
Miller, G.T. 8226
Miller, H.A. 8515
Miller, R.C. 8250
Mills, J.R. 8267
Mills, R.L. 8331
Mitchell, E.W.J. 8389
Mitra, S.S. 8400
Miyahara, S. 8312
Miyazawa, H. 8294
Mizuno, J. 8172
Mizuta, H. 8317
Mock, J.B. 8352
Moncaster, M.E. 8573
Moody, P.L. 8209
Morgan, D.J. 8306
Morgan, R.E. 8555
Moruzzi, V.L. 8157
Moskalenko, S.A. 8360
Mount, T.E. 8486
Mulligan, Jr., J.H. 8494
Muramori, K. 8312
Mutter, W.E. 8441

Naiderov, V.Z. 8550
Nakamura, A. 8304
Nakamura, K. 8367, 8393
Nakashima, S. 8367
Nakau, T. 8275
Narayanan, M.A. 8525
Nash, F. 8349
Nasledov, D.N. 8419
Nassau, K. 8222
Nechaev, A.M. 8539
Negishi, K. 8248
Neitzert, C. 8568
Nekrasov, M.M. 8416
Newman, R.C. 8202
Nielsen, J.W. 8218, 8350
Nii, R. 8292
Nikanorov, S.P. 8409
Nishimura, J. 8182, 8213
Nitsche, R. 8253
Northrop, D.C. 8573
Nose, H. 8327

Ogawa, S. 8305, 8336
Okada, K. 8247
Okaya, A. 8173, 8349
Okkerse, B. 8193
Oliver, D.J. 8281
Oliver, J.W. 8571
Olsen, J.L. 8283
Onsager, L. 8398
Orlov, I.N. 8456
Orr, W.H. 8205
Orshanskaya, N.S. 8382
Osada, K. 8379
Ovsyannikova, I.A. 8371

Padwick, G.C. 8543
Pajgrt, M. 8495
Paskell, E. 8443
Patel, J.R. 8187
Pepinsky, R. 8173
Perlow, G.I. 8311
Peter, M. 8352
Petrolo, J. 8220
Pfyffer, H. 8489
Pitzalis, O. 8487
Pohm, A.V. 8497
Polukarov, Yu.M. 8289
Poplavskaya, O.I. 8502
Popov, Yu.M. 8452, 8470
Porbansky, E.M. 8200
Presnov, V.A. 8299
Preston, R.S. 8311
Pringle, D.H. 8221
Prior, J.R. 8372
Prise, W.J. 8448
Prokhorov, A.M. 8343, 8355
Pugachevich, P.P. 8160

Raal, F.A. 8457
Raffel, J.I. 8540
Ramsa, A.P. 8260
Ratner, E.S. 8565
Ravich, L.E. 8214
Raymo, C.T. 8570
Rayner, M.J. 8281
Read, A.A. 8497
Reggia, F. 8461
Reuther, J.F. 8579
Revuz, J. 8430, 8431
Reznik, M.V. 8198
Rhoderick, E.N. 8281
Rhodin, T.N. 8205
Richards, R.K. 8506
Ridler, D.S. 8544
Robin, J. 8270
Rodgers, G.B. 8457
Rodrigues de Miranda, H.A. 8517
Rogers, J.L. 8464
Rogers, J.N. 8315
Rollin, B.V. 8267
Rosenbaum, J. 8446
Rosenberg, A.J. 8228, 8229
Rosenstock, H.B. 8241
Rosi, F.D. 8459
Roth, W.L. 8204
Rothwarf, F. 8277
Rubin, L.G. 8187
Rufer, R.P. 8553
Rushbrooke, G.S. 8306
Russel, J.P. 8267
Rustgi, O.P. 8394

Saburi, O. 8255
Sakudo, T. 8225
Sandlin, B.T. 8402
Sauer, H.A. 8235
Saunders, N.N. 8406
Savage, A. 8250
Savintsev, P.A. 8164
Schaefer, G. 8363
Schaeve, D.K. 8511
Schellekens, A.M.H. 8526
Scheuplein, R. 8183
Schmitt, E.J. 8546
Schreiber, W.F. 8507
Schubert, J. 8498
Schultz, J.B. 8523
Schulz, D.P. 8548
Scott, B. 8407
Senatorov, K.Ya. 8502
Shafer, M.W. 8157
Shal'nikov, A.I. 8285
Shashkov, Yu.M. 8199
Shavlo, S.T. 8380
Shaw, R.W. 8284
Sheleg, A.U. 8242
Sherrill, M.D. 8282
Sherwood, J.N. 8219
Shibata, A. 8166
Shirer, D.L. 8563
Shul'man, A.R. 8178, 8300
Sickert, R.G. 8576
Siegel, B.M. 8205
Siegman, A.E. 8473
Silvestri, V.J. 8159
Simon, R.E. 8390
Simpson, O. 8573
Sirota, N.N. 8181, 8242
Slavikovskii, G.F. 8180
Slobodzinski, E.J. 8508
Smith, A.W. 8566
Smith, D.N. 8374
Smith, G.W. 8346
Smith, J.F. 8411
Smith, M.J. 8268
Smith, P.L. 8271
Soden, R.R. 8381
Sonder, E. 8237
Spector, C.J. 8417
Spedding, F.H. 8274
Spencer, C.W. 8268
Spencer, E.G. 8328
Spicer, W.E. 8390
Spitzer, W.G. 8227
Spry, W.J. 8291
Stachiewicz, B.R. 8524
Stepanov, A.V. 8409
Stepanova, A.A. 8288
Stevens, K.W.H. 8469
Strandberg, M.W.P. 8340
Strutt, M.J.O. 8297
Sugiura, Y. 8304
Suzuki, N. 8276
Sylvan, T.P. 8533
Synorov, V.F. 8299
Szymanski, B. 8358

Taborko, N.I. 8456
Tanabe, Y. 8213
Tanaka, S. 8257
Tanaka, T. 8257, 8365, 8366
Tanis, A.P. 8526
Tatsumoto, E. 8321
Tauc, J. 8392
Taylor, G.O. 8401
Taylor, N.H. 8532
Tebble, R.S. 8406
Templeton, L.C. 8237
Terhune, R.W. 8471
Thien Chi, N. 8458
Thomas, D.E. 8278
Thomas, D.G. 8361
Thomas, Jr., J.E. 8210
Thomson, S.J. 8219
Thorensen, R. 8542
Thorington, L. 8455
Tiisler, E.S. 8375
Timofeev, V.B. 8369
Tink, E.M. 8531
Tipple, P.M. 8427
Title, R.S. 8383
Tomasek, M. 8239
Tonoyan, A.A. 8181
Trumbore, F.A. 8200
Tsarenkov, B.V. 8419
Tubota, H. 8276
Tucker, E.B. 8341
Tulp, T.J. 8517
Turchinskaya, M.I. 8318
Turner, D.R. 8235
Turobinski, T.J. 8223
Tutihasi, S. 8368

Uchida, Y. 8367, 8393
Ufimtsev, B.F. 8164

Van Arkel, A.E. 8337
van Dam, J.F. 8526
van der Heide, H. 8538
van Overbeek, A.J.W.M. 8512
Van Roosbroeck, W. 8261
van Uitert, L.G.G. 8222, 8381
Vavilov, V.S. 8373
Vedam, K. 8173
Venables, J.D. 8206
Vergnolle, J. 8458
Vermandé, J. 8415
Veter, V.V. 8323
Vick, G.L. 8410
Vincent, D.H. 8311
Vinokurov, V.M. 8348
Vlasov, K.B. 8301
Vogt, K.S. 8503
Volkenshtein, N.V. 8318
Vorob'ev, A.A. 8164
Vul, B.M. 8470

Wagner, Jr., J.B. 8158
Wagner, P.E. 8344, 8468
Wakefield, J. 8202
Waldron, R.A. 8466
Wannier, G.H. 8278
Warekois, E.P. 8234
Watanabe, N. 8292
Watkins, J. 8315
Webster, R.R. 8513
Weil, F. 8423
Wernick, J.H. 8194
White, G.K. 8403
Wiggins, J.S. 8569, 8571
Wilcher, J.H. 8491
Willardson, R.K. 8509
Willis, J.B. 8202
Wilson, E.S. 8520
Wolf, A.A. 8484
Woll, H.J. 8521
Wonson, R.C. 8436
Wood, D.L. 8364
Woodbury, H.H. 8176
Wright, W.L. 8577
Wysock, J.J. 8273

Yaek, I.V. 8375
Yafaev, N.R. 8348
Yamaguchi, S. 8308, 8309, 8310
Yamashita, H. 8376, 8388
Yando, S. 8454
Yasufuku, M. 8438
Yokozawa, Y. 8354
Yonemitsu, H. 8294
Yoshida, S. 8463
Yoshimatsu, M. 8174
Yoshizawa, M. 8376
Young, Jr., F.W. 8177
Young, T. 8391
Yourke, H.S. 8508

Zakharov, A.L. 8434, 8435, 8499
Zaripov, M.M. 8348
Zavaritskii, N.V. 8404
Zelenka, J. 8479
Zelený, M. 8325
Zelinka, R.J. 8433
Zhuravlev, N.N. 8288
Zyuzin, N.I. 8288

in'for·ma'tion re·triev'al, *n.* **1.** rapid location of technical information on specific topics.

information retrieval system for the solid state:

SOLID STATE ABSTRACTS ON CARDS

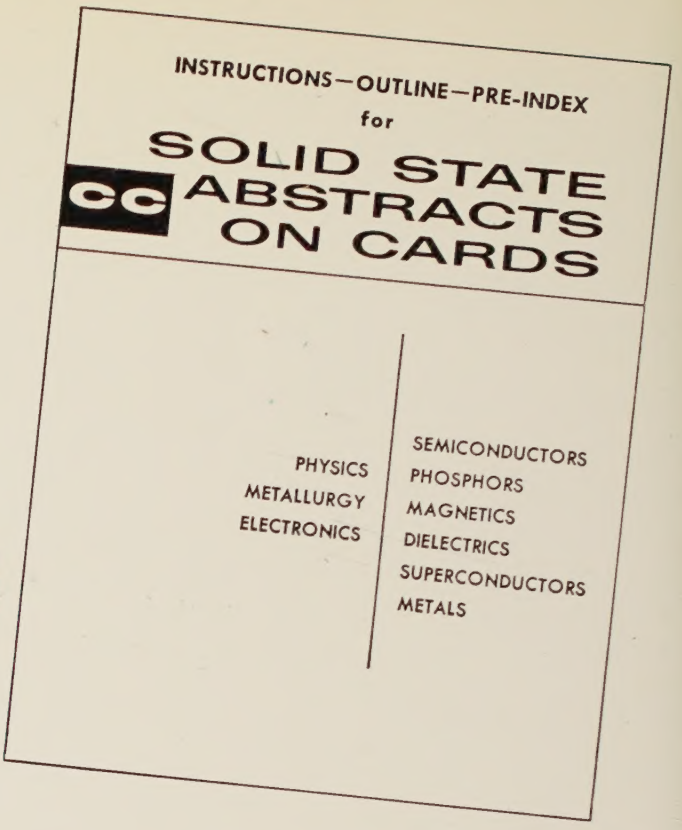

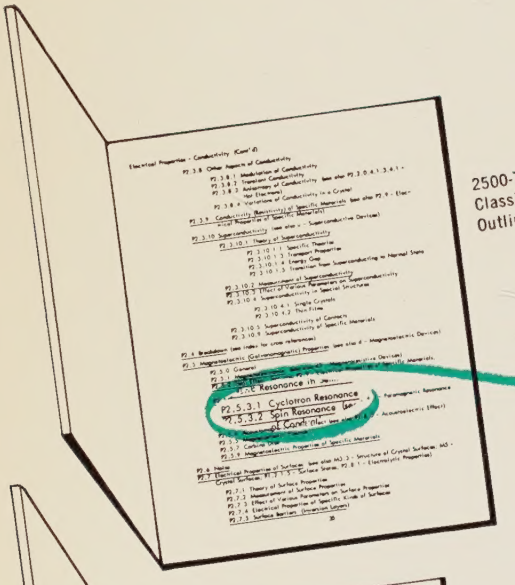

2500-Topic Classification Outline

Send for your free copy of our new 120 page book describing this unique system which is now being used in more than 300 solid state laboratories throughout the world.

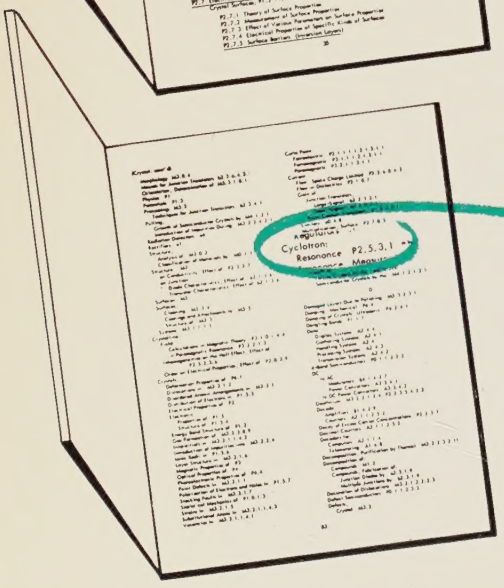

4000-Entry Alphabetical Pre-Index

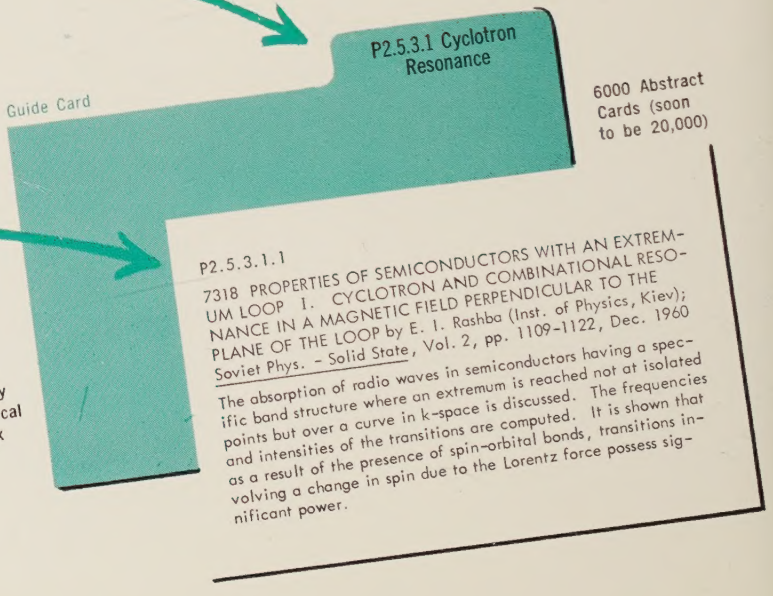
P2.5.3.1 Cyclotron Resonance
Guide Card
6000 Abstract Cards (soon to be 20,000)
P2.5.3.1.1
7318 PROPERTIES OF SEMICONDUCTORS WITH AN EXTREMUM LOOP I. CYCLOTRON AND COMBINATIONAL RESONANCE IN A MAGNETIC FIELD PERPENDICULAR TO THE PLANE OF THE LOOP by E. I. Rashba (Inst. of Physics, Kiev); Soviet Phys. - Solid State, Vol. 2, pp. 1109-1122, Dec. 1960
The absorption of radio waves in semiconductors having a specific band structure where an extremum is reached not at isolated points but over a curve in k-space is discussed. The frequencies and intensities of the transitions are computed. It is shown that as a result of the presence of spin-orbital bonds, transitions involving a change in spin due to the Lorentz force possess significant power.

CAMBRIDGE COMMUNICATIONS CORPORATION

236 MAIN STREET • CAMBRIDGE 42, MASSACHUSETTS • **Tel. 491-0710**